

University of Alberta

**Novel polymeric micellar drug conjugates and
nanocontainers for drug delivery applications**

By

Abdullah Al Mahmud 

A thesis submitted to the Faculty of Graduate Studies and Research in
partial fulfillment of the requirements for the degree of

DOCTOR OF PHILOSOPHY
IN
PHARMACEUTICAL SCIENCES

Faculty of Pharmacy and Pharmaceutical Sciences

Edmonton, Alberta

Fall 2008



Library and
Archives Canada

Published Heritage
Branch

395 Wellington Street
Ottawa ON K1A 0N4
Canada

Bibliothèque et
Archives Canada

Direction du
Patrimoine de l'édition

395, rue Wellington
Ottawa ON K1A 0N4
Canada

Your file *Votre référence*

ISBN: 978-0-494-46376-5

Our file *Notre référence*

ISBN: 978-0-494-46376-5

NOTICE:

The author has granted a non-exclusive license allowing Library and Archives Canada to reproduce, publish, archive, preserve, conserve, communicate to the public by telecommunication or on the Internet, loan, distribute and sell theses worldwide, for commercial or non-commercial purposes, in microform, paper, electronic and/or any other formats.

The author retains copyright ownership and moral rights in this thesis. Neither the thesis nor substantial extracts from it may be printed or otherwise reproduced without the author's permission.

AVIS:

L'auteur a accordé une licence non exclusive permettant à la Bibliothèque et Archives Canada de reproduire, publier, archiver, sauvegarder, conserver, transmettre au public par télécommunication ou par l'Internet, prêter, distribuer et vendre des thèses partout dans le monde, à des fins commerciales ou autres, sur support microforme, papier, électronique et/ou autres formats.

L'auteur conserve la propriété du droit d'auteur et des droits moraux qui protègent cette thèse. Ni la thèse ni des extraits substantiels de celle-ci ne doivent être imprimés ou autrement reproduits sans son autorisation.

In compliance with the Canadian Privacy Act some supporting forms may have been removed from this thesis.

Conformément à la loi canadienne sur la protection de la vie privée, quelques formulaires secondaires ont été enlevés de cette thèse.

While these forms may be included in the document page count, their removal does not represent any loss of content from the thesis.

Bien que ces formulaires aient inclus dans la pagination, il n'y aura aucun contenu manquant.


Canada

Dedications

This thesis is dedicated to

My dearest parents, with love and thanks, who dedicated their life for the education of their children;

My wife, Salma, who has presented me a lovely family and has been with me all the way as a support and encouragement;

And,

My son, Saajid, whose lovely smile was the source of my all motivation and inspiration towards completing this research.

Abstract

Self associating poly(ethylene oxide)-*block*-poly(ester) (PEO-*b*-poly(ester)) block copolymers are of increasing interest in drug delivery application. However, the application of this class of block copolymers has been limited due to the lack of functional groups on the poly(ester) block. The aim of this study was to develop novel micelle-forming PEO-*b*-poly(ester) block copolymers, such as methoxy PEO-*b*-poly(ϵ -caprolactone) (MePEO-*b*-PCL), bearing functional side groups on the poly(ester) block and investigate their potential for the delivery of model anticancer drugs. Towards this goal, functionalized ϵ -caprolactone monomer, i.e., α -benzylcarboxylate- ϵ -caprolactone, was synthesized by anionic activation of ϵ -caprolactone and used in a ring opening polymerization initiated with MePEO to prepare MePEO-*b*-poly(α -benzylcarboxylate ϵ -caprolactone) (MePEO-*b*-PBCL). Further catalytic debenzylation of MePEO-*b*-PBCL produced MePEO-*b*-poly(α -carboxyl ϵ -caprolactone) (MePEO-*b*-PCCL) and used to attach a model anticancer drug, doxorubicin (DOX) covalently to prepare MePEO-*b*-P(CL-DOX) conjugate. DOX loaded micellar nanocontainers were prepared from MePEO-*b*-PBCL, MePEO-*b*-PCCL and MePEO-*b*-P(CL-DOX) and evaluated for the level of DOX encapsulation, release and cytotoxicity against mouse melanoma B16F10 cells. Among different nanocontainers, a core of PBCL provided the maximum DOX encapsulation and control over the rate of DOX release, while maintaining sufficient DOX cytotoxicity. Micellar DOX conjugate did not show any sign of DOX release, but was still cytotoxic. In further studies, substitution of cholesteryl side chains on the PCL block was pursued to increase the encapsulation of a chemically compatible drug, i.e., cucurbitacin I (CuI), in polymeric micelles. Compared to MePEO-*b*-PCL, MePEO-*b*-

poly(α -cholesteryl carboxylate ϵ -caprolactone) (MePEO-*b*-PChCL) micelles demonstrated increased solubilization of CuI, but their efficiency in controlling the rate of CuI release from micellar carrier was not superior to that of MePEO-*b*-PCL. Finally, the effect of block copolymer structure on the rate, extent, and mechanism of cellular internalization of MePEO-*b*-PCL micelles was assessed revealing the involvement of energy dependant process in the internalization mechanism. Although the internalization was found to be affected by both core and shell structure, polymeric micellar delivery was found to reduce the internalization of incorporated drug. The results of this study revealed a tremendous potential for novel PEO-*b*-poly(ester) block copolymers with reactive side groups on the poly(ester) block in the design of optimized carriers for the delivery of various therapeutic agents.

Acknowledgements

This research work has been fulfilled due to the collaboration and support of a group of people and organizations. I would like to thank some of them in particular:

- ❖ My supervisor, Dr. Afsaneh Lavasanifar, for her support, guidance, and insight without which it wouldn't be possible to accomplish this research. Specially, I would like to acknowledge for her caring attitude, excellent teaching, strong guidance in research and wonderful motivation capacity that made me possible to win this journey. I would like to thank Dr. Lavasanifar for giving me the opportunity to participate in five international conferences, her financial assistance and overall for being beside me all the way.
- ❖ Dr. John Samuel for his excellent insights in different aspects of my research as a member of my supervision committee and providing his cell culture lab and other instrumental facilities.
- ❖ Dr. Ayman El-Kadi for his thoughtful comment as my supervisory committee member, and granting me access to his UV and fluorescent spectrophotometer facilities. Specially, his friendly attitude and kindness was really supportive for me.
- ❖ Dr. Kamaljit Kaur for her thoughtful questions, and suggestive comments as a part of my supervisory committee members.
- ❖ Dr. Raimar Löbenberg with whom I was working as a graduate teaching assistant for last 4 years.
- ❖ Dr. Hasan Uludag for expressing his interest to be a member of my examinee committee in his busy schedule.
- ❖ Dr. Jashim Uddin and Dr. Praveen Rao for helping me in chemical synthesis.
- ❖ Staff of the faculty, in particular, Ms. Joyce Johnson for her very cooperative role in all aspects of my graduate program, Mr. Don White for technical assistance, Jeff Turchinsky whose care for the graduate students is beyond explanation, Gordon McRae for computer facilities and Dr. Somyaji for NMR analysis.
- ❖ My all lab colleagues, Dr. Xioa-bing Xiong, Dr. Hamid Montazeri Aliabadi, Kamyar Sarkhosh, Sara Elhasi, Ziyad Bin Khatlan, Mostafa Shahin, Nazila Safaei-Nikouei and Arash Falamarzian for their friendly presence in the lab and constructive critics in group meeting.
- ❖ All the graduate students in the faculty of Pharmacy and Pharmaceutical sciences.
- ❖ Rx &D HRF/CIHR graduate scholarship, Walter H. Johns Graduate fellowship and J Gordin Kaplan Graduate student Award of University of Alberta, Dr. Leonard Wiebe Graduate Award in Pharmaceutical Science, Antonie Nujaim Graduate Scholarship in pharmacy, GSA professional development award that enabled me to complete this program.
- ❖ And last but not least, faculty members from whom I have learned during the Ph. D program

Table of contents

1. INTRODUCTION.....	1
1.1. Introduction	2
1.2. Amphiphilic block copolymers and polymeric micellar delivery system	4
1.2.1 Definitions	4
1.2.2. Self assembly of amphiphilic block copolymers	5
1.2.3. Most commonly used block copolymers for drug delivery	8
1.2.4. Different designs of polymeric micellar systems for drug delivery	13
1.2.4.1. Micelle forming polymer-drug conjugates	13
1.2.4.2. Micellar nanocontainers	15
1.2.4.3. Polion complex micelles	16
1.3. The physicochemical characteristics of polymeric micellar delivery systems	18
1.3.1. Thermodynamic and kinetic stability	18
1.3.2. Micellar size	20
1.3.3. Morphology	20
1.3.4. Drug loading	21
1.3.5. Drug release	22
1.4. The biological characteristic of polymeric micellar delivery systems	25
1.4.1. Biodistribution and pharmacokinetic properties	25
1.4.2. Cellular internalization and intracellular distribution	29
1.5. Polymeric micelles for drug targeting	33
1.5.1. Physiological properties of tumor vasculature and enhanced permeability and retention (EPR) effect	33
1.5.2. Polymeric micelles for passive drug targeting	37
1.5.3. Polymeric micelles for active drug targeting	41
1.5.3.1. Ligand mediated targeting by polymeric micelle	41
1.5.3.2. pH responsive polymeric micelles for drug targeting	43
1.5.4. Multifunctional polymeric micelles for drug targeting	46
1.6. Model anticancer drugs under current study	47
1.6.1. Doxorubicin	47
1.6.1.1. Commercial formulations of doxorubicin	49
1.6.1.2. Polymer conjugates of doxorubicin in clinical trials	50
1.6.1.3. Polymeric micellar formulations of doxorubicin in clinical trials	51
1.6.2. Cucurbitacin I	52
1.7. Thesis proposal	55
1.7.1. Rationale	55
1.7.2. Hypothesis	56

1.7.3. Objective	56
1.7.4. Specific aims	56
1.8. References	58

2. PREPARATION AND CHARACTERIZATION OF METHOXY POLY (ETHYLENE OXIDE)-*b*-POLY(ϵ -CAPROLACTONE) BLOCK COPOLYMER MICELLES 67

2.1. Introduction	68
2.2. Experimental section	69
2.2.1 Materials	69
2.2.2. Synthesis and characterization of MePEO- <i>b</i> -PCL block copolymers	69
2.2.3. Assembly of MePEO- <i>b</i> -PCL and Cremophor EL and characterization of associated structures	71
2.2.4. Statistical analysis	73
2.3. Results	74
2.4. Discussion	83
2.5. Conclusion	87
2.6. References	88

3. SYNTHESIS AND CHARACTERIZATION OF NOVEL SELF ASSOCIATING METHOXY POLY(ETHYLENE OXIDE)-*b*-POLY(ϵ -CAPROLACTONE) BLOCK COPOLYMERS WITH FUNCTIONAL SIDE GROUPS ON THE POLYESTER BLOCK FOR DRUG DELIVERY 90

3.1. Introduction	91
3.2. Experimental section	92
3.2.1. Materials	92
3.2.2. Synthesis of α -benzylcarboxylate ϵ -caprolactone	92
3.2.3. Synthesis of MePEO- <i>b</i> -PBCL	95
3.2.4. Reduction of α -benzylcarboxylate bearing block copolymer to α - carboxyl bearing block copolymer	95
3.2.5. Characterization of synthesized block copolymers	96
3.2.6. Assembly of block copolymers and characterization of the assembled structures.....	98
3.2.7. Assessing the biocompatibility of prepared block copolymers	99
3.2.8. Statistical analysis	100
3.3. Results and discussion	101

3.3.1. Preparation of MePEO- <i>b</i> -PCL block copolymers with aromatic side groups on the PCL block	101
3.3.2. Synthesis and characterization of MePEO- <i>b</i> -PCCL block copolymers	109
3.3.3. Synthesis and characterization of MePEO- <i>b</i> -PCL- <i>co</i> -PCCL block copolymer	110
3.3.4. Assembly of block copolymers and characterization of self-assembled structure.....	115
3.3.5. Assessing the biocompatibility of prepared block copolymers	124
3.4. Conclusion	126
3.5. References	127
4. DEVELOPMENT OF NOVEL POLYMERIC MICELLAR DRUG CONJUGATES AND NANOCONTAINERS WITH HYDROLYSABLE CORE STRUCTURE FOR DOXORUBICIN DELIVERY	129
4.1. Introduction	130
4.2. Experimental section	132
4.2.1. Materials	132
4.2.2. Synthesis of MePEO- <i>b</i> -P(CL-DOX) and its characterization	132
4.2.3. Measurement of DOX conjugated levels	135
4.2.4. Self assembly of block copolymers and physical encapsulation of DOX in the assembled structures	136
4.2.5. Characterization of polymeric micelles	136
4.2.6. Release of DOX from polymeric micelles	137
4.2.7. Assessing the hydrolysis of poly(ester) core in MePEO- <i>b</i> -P(CL-DOX) micelles	138
4.2.8. <i>In-vitro</i> cytotoxicity of polymeric micellar DOX nanocontainers and drug conjugate against mouse melanoma cells	138
4.2.9. Statistical analysis.....	139
4.3. Results	140
4.3.1. Synthesis of MePEO- <i>b</i> -P(CL-DOX) and its characterization.....	140
4.3.2. Self assembly of MePEO- <i>b</i> -P(CL-DOX) and characterization of micellar structures	143
4.3.3. Preparation of DOX loaded micelles and their characterization	145
4.3.4. Release of DOX from polymeric micelles	147

4.3.5. Hydrolysis of poly(ester) core of MePEO- <i>b</i> -P(CL-DOX) micelles	149
4.3.6. <i>In vitro</i> cytotoxicity study.....	151
4.4. Discussion	154
4.5. Conclusion	158
4.6. Reference	160

5. CHEMICAL TAILORING OF MICELLE FORMING POLY(ETHYLENE OXIDE)-*b*-POLY (ϵ -CAPROLACTONE) BLOCK COPOLYMERS FOR THE SOLUBILIZATION AND CONTROLLED DELIVERY OF STAT-3 INHIBITOR CUCURBITACIN I

5.1. Introduction	163
5.2. Experimental section	164
5.2.1. Materials	164
5.2.2. Calculation of the compatibility between micellar core and CuI	164
5.2.3. Synthesis of α -cholesteryl carboxylate ϵ -caprolactone monomer	165
5.2.4. Synthesis of MePEO- <i>b</i> -PChCL block copolymer	169
5.2.5. Characterization of MePEO- <i>b</i> -PChCL block copolymer	169
5.2.6. Assembly of block copolymers and characterization of self assembled structures	170
5.2.7. Encapsulation of CuI in polymeric micelles	170
5.2.8. Release of CuI from polymeric micelles	172
5.2.9. Statistical analysis	172
5.3. Results	173
5.3.1. Calculation of the compatibility between micellar core and CuI	173
5.3.2. Preparation of MePEO- <i>b</i> -PCL block copolymers with cholesteryl side groups on the PCL block	173
5.3.3. Assembly of MePEO- <i>b</i> -PChCL block copolymers and characterization of self-assembled structures	180
5.3.4. Encapsulation of CuI in polymeric micelles	182
5.3.5. <i>In vitro</i> release of CuI from different block copolymer nanocarriers	185
5.4. Discussion	186
5.5. Conclusion	189
5.6. References	190

6. THE EFFECT OF BLOCK COPOLYMER STRUCTURE ON THE INTERNALIZATION OF POLYMERIC MICELLES BY HUMAN BREAST CANCER CELLS	192
6.1. Introduction	193
6.2. Experimental section	194
6.2.1. Synthesis, characterization and self assembly of block copolymers	194
6.2.2. Assembly of MePEO- <i>b</i> -PCL block copolymers and characterization of self-assembled structures	194
6.2.3. Preparation and characterization of fluorescent dye loaded MePEO- <i>b</i> -PCL micelles	195
6.2.4. Cellular uptake studies	196
6.2.5. Confocal microscopy studies	197
6.2.6. Statistical analysis	198
6.3. Results	198
6.3.1. Synthesis, characterization and micellization of MePEO- <i>b</i> -PCL block copolymers	198
6.3.2. Preparation and characterization of DiI loaded MePEO- <i>b</i> -PCL micelles	199
6.3.3. The effect of block copolymer structure on the extent, rate and mechanism of MePEO- <i>b</i> -PCL micellar uptake by MCF-7 cells	201
6.4. Discussion	211
6.5. Conclusion.....	214
6.6. References	215
7. GENERAL DISCUSSION AND CONCLUSIONS	217
7.1. General discussion	218
7.2. Conclusions	225
7.3. Future perspective	226
7.4. References	229

List of Tables

Table 1.1. Polymeric micellar delivery systems in clinical trials	39
Table 2.1. Characteristics of the prepared MePEO- <i>b</i> -PCL block copolymers	78
Table 2.2. Characteristics of Cremophor EL and MePEO- <i>b</i> -PCL micelles with different PCL molecular weights	79
Table 3.1. Characteristics of substituted and unsubstituted MePEO- <i>b</i> -PCL block copolymers	108
Table 3.2. Characteristics of substituted and unsubstituted MePEO- <i>b</i> -PCL block copolymer micelles (n=3)	117
Table 4.1. Characteristics of empty block copolymer micelles (n=3)	144
Table 4.2. Characteristics of DOX loaded nanocontainers (n=3)	146
Table 5.1. Characteristics of synthesized block copolymers	178
Table 5.2. Characteristics of empty block copolymer nanocarriers (n=3)	182
Table 5.3. Characteristics of CuI loaded block copolymer nanocarriers (n=3)	184
Table 6.1. Characteristics of the prepared MePEO- <i>b</i> -PCL block copolymers	200
Table 6.2. Characteristics of the prepared MePEO- <i>b</i> -PCL block copolymer micelles. .	202

List of Figures

- Figure 1.1.** The architecture of different types of copolymers (**A** and **B** are hydrophilic and hydrophobic monomer units, respectively)5
- Figure 1.2.** Schematic representation of the micellization process 7
- Figure 1.3.** Chemical structures of the most commonly used poly(ester) and poly(amino acid) core forming blocks in polymeric micelles 12
- Figure 1.4.** Different designs and models for micelle-forming drug-block copolymer conjugates. 14
- Figure 1.5.** Modes of drug release from polymeric micelles 24
- Figure 1.6.** Itinerary of block copolymer micelles after i.v. administration 27
- Figure 1.7.** A proposed model for the cellular internalization of free fluorescent dye and dye incorporated in micelles. (**A**) Free dye diffuses first through the cell membrane and then enters the cytosol. (**B**) Dye loaded micelle enters the cytoplasmic compartment by endocytosis. (**C**) Trafficking of dye loaded micelles into endosome. (**D**) Localization of the dye loaded micelles into the acidic lysosomal compartment. (**E**) Drug/Dye molecule eventually diffuse out from the micelle and distribute through the cytoplasm 31
- Figure 1.8.** The vascular network in normal and tumor tissue: **A**) Normal tissues have relatively uniform and well- ordered blood vessels that are sufficiently close together to oxygenate all of the tissue, **B**) Blood vessels in tumors are tortuous, have incomplete vessel walls, have sluggish and irregular blood flow and have regions of hypoxia between the vessels, **C**) Structure of normal blood vessel, **D**) Structure of fenestrated, discontinuous vessels in tumor area 35
- Figure 1.9.** **A**) PEO-*b*-PLLA-DOX conjugate via hydrazone linkage and *cis*-aconityl linkage **B**) PEO-*b*-p(Asp-Hyd-DOX) conjugates with hydrazone acid liable bonds 45
- Figure 1.10.** Chemical structure of doxorubicin 48
- Figure 1.11.** Chemical structure of cucurbitacin I 53
- Figure 2.1.** ¹H NMR spectrum and peak assignments of **A**) MePEO-*b*-PCL block copolymer and **B**) ε-Caprolactone monomer. The ¹H NMR spectra were obtained in CDCl₃. **C**) IR spectrum of MePEO-*b*-PCL block copolymer. The IR spectrum was obtained by preparing a thin film of block copolymer on sodium chloride disc using a FT-IR spectrometer (Nicolet Magna-IR[®] 550, USA)75-76

- Figure 2.2.** A) The effect of temperature on the percentage of ϵ -caprolactone conversion to PCL in the synthesis of MePEO-*b*-PCL di-block copolymers at a catalyst to monomer molar ratio of 0.002. B) The effect of catalyst concentration on the percentage of ϵ -caprolactone conversion to PCL in the synthesis of MePEO-*b*-PCL di block copolymer at 140 °C after 4 hours of reaction77
- Figure 2.3.** TEM pictures of colloidal particles assembled from MePEO-*b*-PCL block copolymers: A) 5000-5000, B) 5000-13000, C) 5000-24000 (magnification of 18000 \times 6.1). The bar in the image represents 100 nm. 80
- Figure 2.4.** A) Intensity ratio (337 nm/333 nm) of pyrene (6×10^{-7} M) from excitation spectrum as a function of block copolymer concentration. B) Fluorescence emission spectrum of 1,3-(1,1'-dipyrenyl)propane in micellar solutions of MePEO-*b*-PCL (different PCL chain lengths) in comparison to Cremophor EL as an indication of micellar core viscosity. No significant change in I_e/I_m ratios of dipyrene probe was detected between micelles of 5000-13000 and 5000-24000 ($p > 0.05$, unpaired student's t test). 82
- Figure 3.1.** A) ^1H NMR; B) ^{13}C NMR; C) IR; and D) Mass spectra of α -benzylcarboxylate- ϵ -caprolactone and peak assignments 104-105
- Figure 3.2.** ^1H NMR spectrum and peak assignments for A) MePEO-*b*-PBCL in CDCl_3 ; B) MePEO-*b*-PCCL in DMSO-d_6 ; and C) MePEO-*b*-PCL-*co*-PCCL in CDCl_3 111-113
- Figure 3.3.** - IR spectrum of A) MePEO-*b*-PBCL ($M_n=9700 \text{ g.mol}^{-1}$) and B) MePEO-*b*-PCCL ($M_n=7530 \text{ g.mol}^{-1}$). Arrow indicates the presence of broad peak caused by OH of pendant COOH group. The IR samples were prepared using sodium chloride disc method. 114
- Figure 3.4.** GPC chromatogram for A) MePEO, $M_n= 5000 \text{ g.mol}^{-1}$, $M_w/M_n=1.62$; B) MePEO-*b*-PBCL, $M_n=9700 \text{ g.mol}^{-1}$, $M_w/M_n=1.74$; and C) MePEO-*b*-PCCL, $M_n=7530 \text{ g.mol}^{-1}$, $M_w/M_n= 1.52$ 115
- Figure 3.5.** TEM picture of micelles prepared from A) MePEO-*b*-PBCL ($M_n=9700 \text{ g.mol}^{-1}$) and B) MePEO-*b*-PCCL ($M_n=7530 \text{ g.mol}^{-1}$) block copolymers (magnification 18000 \times 6.1). The bar on the images represents 200 nm. 118
- Figure 3.6.** The intensity ratio (339 nm/334 nm) of pyrene ($6 \times 10^{-7} \text{ M}$) from excitation spectrum as a function of log concentration of different block copolymers. Each point represent average \pm SD ($n=3$) 120
- Figure 3.7.** ^1H NMR spectrum of A) MePEO-*b*-PBCL and B) MePEO-*b*-PCCL block copolymer micelles in D_2O . Limited mobility of the core forming block has been demonstrated from the reduced ϵ -caprolactone peaks in the ^1H NMR spectrum.123

Figure 3.8. *In vitro* biocompatibility assessment of MePEO-*b*-PCL, MePEO-*b*-PBCL, MePEO-*b*-PCCL, MePEO-*b*-PCL_{25-co}-PCCL₅ and MePEO-*b*-PCL_{16-co}-PCCL₁₀ block copolymers: **A)** cytotoxicity study against human fibroblast cells; and **B)** hemolysis study against RBCs. The cell viabilities are expressed as a function of the logarithm of the copolymer concentrations. Each experiment was performed in triplicate, and results are plotted as the mean \pm SD 125

Figure 4.1. ¹H NMR spectrum and peak assignments of **A)** MePEO-*b*-P(CL-DOX) block copolymer in DMSO-d₆ and in CDCl₃ (Figure 4.1A, window); **B)** free DOX in DMSO-d₆.....141

Figure 4.2. Typical HPCL chromatogram of **A)** free DOX; and **B)** MePEO-*b*-P(CL-DOX) polymer. Reversed phase chromatography was carried out with a Waters 10 μ m C18-125 Å column (3.9 \times 300 mm) in a gradient elution using 0.05% trifluoroacetic acid aqueous solution and acetonitrile. 142

Figure 4.3. TLC chromatogram showing the spot of **A)** free DOX at R_f value of 0.68 and **B)** MePEO-*b*-P(CL-DOX) at the base line after running with butan-1-ol:acetic acid: water (4:1:4) as mobile phase142

Figure 4.4. *In vitro* DOX release profile from polymeric micelles at **A)** pH: 5.0, and **B)** pH: 7.4 at 37 °C. Each point represent mean \pm SD (n=3) 148

Figure 4.5. Gel permeation chromatogram of MePEO-*b*-P(CL-DOX) before and after incubation at pH 5.0 for 72 hrs 150

Figure 4.6. *In vitro* cytotoxicity of free and polymeric micellar DOX formulations against B16.F10 mouse melanoma carcinoma cells after **A and C) 24 h**, and **B and D) 48 h** incubation. **A and B)** The cell viabilities are expressed as a function of the logarithm of the DOX concentration. Each point represent mean \pm SD (n=3). For DOX loaded in MePEO-*b*-P(CL-DOX) micelles, the concentration of total DOX in the micelle (physically encapsulated + chemically conjugated DOX) is calculated and used in the graph. **C and D)** IC₅₀ values of free DOX and DOX loaded polymeric micellar DOX formulations against B16.F10 cells were calculated from the plots of *in vitro* cytotoxicity (plot A and B). Discontinuation of the line under the bars indicates the significant difference of the IC₅₀ values among different formulations (P < 0.05). Differences between means (n=3) of IC₅₀ were assessed using one way ANOVA followed by *post hoc* analysis using Dunnett T3 test (SSPS for Windows v.13, Cary, NC). The level of significance was set at $\alpha=0.05$ 152-153

Figure 5.1. Chemical structure of Cucurbitacin I168

Figure 5.2. A) ^1H NMR in CDCl_3 ; B) IR; and C) Mass spectra of α -cholesteryl carboxylate- ϵ -caprolactone (substituted monomer) and peak assignments	174-176
Figure 5.3. ^1H NMR spectrum and peak assignments of MePEO- <i>b</i> -PChCL block copolymer	179
Figure 5.4. TEM picture of nanoassemblies prepared from MePEO- <i>b</i> -PChCL block copolymer (magnification 18000×6.1). The bar on the images represents 500 nm	181
Figure 5.5. <i>In vitro</i> CuI release profile from polymeric nanocarriers at 37 °C. Each point represent mean \pm SD (n=3). * Shows significant difference in release profile from MePEO- <i>b</i> -PCL and MePEO- <i>b</i> -PChCL ($P < 0.05$, One way ANOVA). † Shows significant difference from MePEO- <i>b</i> -PCL at 1 hour ($P < 0.05$, One way ANOVA)	186
Figure 6.1. Release of free and encapsulated fluorescent probe, DiI, to lipid vesicles. Each point represents the mean of three samples \pm S.D	203
Figure 6.2. Comparative uptake of free and MePEO- <i>b</i> -PCL block copolymer micelle loaded DiI by MCF-7 human breast cancer cells after 6 and 12 h incubation. Each bar represents the mean of three samples \pm S.D.....	204
Figure 6.3. The effect of A) MePEO and B) PCL molecular weights on the uptake of MePEO- <i>b</i> -PCL micelles by MCF-7 cells. Each bar represents the mean of three experiments \pm S.D. (Symbols of * and ** correspond to a significance of difference at $P < 0.05$ and $P < 0.01$, respectively)	206
Figure 6.4. The effect of A) reduced temperature (incubation at 4°C); B) pretreatment with chlorpromazine and C) pretreatment with cytochalasin B on the internalization of MePEO- <i>b</i> -PCL micelles by MCF-7 cells. Uptake was quantified by fluorescence concentration analyzer after 6 h incubation. Each bar represents the mean of three samples \pm S.D. (Symbols of * and ** correspond to a significance of difference between normal uptake and inhibitor treated groups at $P < 0.05$, $P < 0.01$, respectively. NS corresponds to no significance in difference at $P > 0.05$)	208-209
Figure 6.5. Confocal microscopy images of MCF-7 cells incubated in different conditions: A) MCF-7 cells stained with Con-A Alexa fluor 488 conjugate; B) MCF-7 cells incubated with free DiI at 37°C; C) MCF-7 cells incubated with DiI labeled 5000-5000 MePEO- <i>b</i> -PCL micelles at 37°C; D) MCF-7 cells incubated with free DiI at 4°C; E) MCF-7 cells incubated with 5000-5000 DiI labeled MePEO- <i>b</i> -PCL micelles at 4°C	210

List of Synthetic schemes

- Scheme 2.1.** General reaction scheme for the synthesis of MePEO-*b*-PCL block copolymers through ring opening polymerization of ϵ -caprolactone by MePEO in the presence of stannous octoate 71
- Scheme 3.1.** Synthetic scheme for the preparation of α -benzylcarboxylate- ϵ -caprolactone (α -carbon substituted monomer) 94
- Scheme 3.2.** General synthesis scheme for the preparation of MePEO-*b*-PBCL, MePEO-*b*-PCCL, MePEO-*b*-PCL-*co*-PBCL and MePEO-*b*-PCL-*co*-PCCL block copolymers97
- Scheme 3.3.A)** Intramolecular transesterification and **B)** Intermolecular transesterification of MePEO-*b*-PCL 102
- Scheme 4.1.** Synthetic scheme for the preparation of MePEO-*b*-P(CL-DOX) block copolymer 134
- Scheme 5.1.** Synthetic scheme for the preparation of α -cholesteryl carboxylate- ϵ -caprolactone.....167
- Scheme 5.2.** Synthetic scheme for the preparation of MePEO-*b*-PChCL block copolymers 168

List of abbreviations

AFM	Atomic force microscopy
AmB	Amphotericin B
Ang 1	Angiopoietin 1
Ang 2	Angiopoietin 2
ASGP	asialoglycoprotein
ATP	Adenosine triphosphate
BCL	α -benzylcarboxylate- ϵ -caprolactone
bFGF	basic fibroblast growth factors
BSA	bovine serum albumin
Bu-Li	butyl lithium
CDCl ₃	deuterated chloroform
CDDP	Cisplatin
CL	Clearance
ϵ CL	ϵ Caprolactone
CMC	Critical micellar concentration
CP	cyclophosphamide
CsA	cyclosporin A
CuI	cucurbitacin I
D ₂ O	deuterium oxide
Da	dalton
DAF	5-dodecanoylamino fluorescein
DCC	dicyclocarbodiimide

DLS	dynamic light scattering
DNA	Deoxyribonucleic acid
DMSO	dimethyl sulfoxide
DMSO-d ₆	deuterated dimethyl sulfoxide
DOX	doxorubicin
DP	degree of polymerization
DSPC	1,2-Distearoyl-sn-glycero-3-phosphocholine
DSPE	1,2-distearoyl-sn-glycero-3-phosphoethanolamine
EDTA	ethylene diamine tetracetic acid
EPC	egg phosphatidylcholine
EPR	enhanced permeability and retention effect
FBP	folate-binding proteins
FT-IR	Fourier transform infra red spectroscopy
GCM	group contribution method
GPC	gel permeation chromatography
GRGDS	Gly-Arg-Gly-Asp-Ser
h	Hour
HLB	hydrophilic lipophilic balance
HPMA	N-(2-hydroxypropyl) methacrylamide)
HSPC	hydrogenated soy phosphatidylcholine
IC ₅₀	inhibitory concentration for 50%
I _e /I _m	Intensity ratio of excimer to monomer
IL-8	interleukin 8

I.S	internal standard
i.v.	intravenous
KDa	kilodalton
KV	kilovolt
LDA	lithium diisopropylamide
LLC	lewis lung carcinoma
mAb	monoclonal antibody
MDCK	Madin-Darby Canine Kidney epithelial cells
MDR	multi-drug resistant
MePEO	methoxy poly(ethylene oxide)
MHz	megahertz
MePEO- <i>b</i> -PBCL	methoxy poly(ethylene oxide)- <i>block</i> -poly(α -benzyl carboxylate- ϵ -caprolactone)
MePEO- <i>b</i> -PCL- <i>co</i> -PBCL	methoxy poly(ethylene oxide)- <i>block</i> -poly(ϵ -caprolactone)- <i>co</i> -poly(α -benzylcarboxylate- ϵ -caprolactone)
MePEO- <i>b</i> -PCL- <i>co</i> -PCCL	methoxy poly(ethylene oxide)- <i>block</i> -poly(ϵ -caprolactone)- <i>co</i> -poly(α -carboxyl- ϵ -caprolactone)
MePEO- <i>b</i> -PCCL	methoxy poly(ethylene oxide)- <i>block</i> - poly(α -carboxyl- ϵ -caprolactone)
MePEO- <i>b</i> -PCL	methoxy poly(ethylene oxide)- <i>block</i> -poly(ϵ -caprolactone)
M/I	monomer/initiator
MLV	multilamellar vesicle
MMPs	matrix metalloproteinases
M_n	number average molecular weight

M _w	weight average molecular weight
MTD	maximum tolerable dose
MTT	3-(4,5-dimethylthiazol-2-yl)-2,5-diphenyltetrazolium bromide
MTX	methotrexate
NHS	N hydroxy succinamide
NMR	nuclear magnetic resonance
NSCLC	non-small-cell lung cancer
o/w	oil in water
P(Asp)	poly(aspartic acid)
PBCL	poly(α benzylcarboxylate ϵ -caprolactone)
PBLA	poly(β -benzyl L-aspartic acid)
PBS	phosphate buffer solution
PCCL	poly(α -carboxyl ϵ -caprolactone)
PDI	polydispersity index
PChCL	poly(α -cholesteryl carboxylate ϵ -caprolactone)
PCL	poly(ϵ -caprolactone)
PDLLA	poly(D, L lactic acid)
PEO	poly(ethylene oxide)
PEO- <i>b</i> -P(Asp)	poly(ethylene oxide)- <i>block</i> -poly(L-aspartic acid)
PEO- <i>b</i> -PBLA	poly(ethylene oxide)- <i>block</i> -poly(β -benzyl L-aspartic acid)
PEO- <i>b</i> -PCL	poly(ethylene oxide)- <i>block</i> -poly(ϵ caprolactone)
PEO- <i>b</i> -PDLLA	poly(ethylene oxide)- <i>block</i> -poly(D, L lactic acid)
PEO- <i>b</i> -PLAA	poly(ethylene oxide)- <i>block</i> - poly(L-amino acids)

PEO- <i>b</i> -PLGA	poly(ethylene oxide)- <i>block</i> -poly(lactic- <i>co</i> -glycolic acid)
PEO- <i>b</i> -PLLA-DOX	poly(ethylene oxide)- <i>block</i> poly(L-lactic acid) doxorubicin
P(Asp-Hyd-DOX)	poly(aspartic acid-hydrazone-doxorubicin)
PEO- <i>b</i> -P(His)	PEO- <i>b</i> -poly(L-histidine)
PEG	poly(ethylene glycol)
PECAM	platelet-endothelial cell-adhesion molecule
PEI	polyethyleneimine
P(Glu)	poly(L-glutamic acid)
PGA	poly(glycolic acid)
PGs	prostaglandins
PIC	polyion complex
PLA	poly(lactic acid)
PLGA	poly(lactic- <i>co</i> -glycolic acid)
PLLA	poly (L-lactic acid)
PLL	poly(L-lysine)
ppm	parts per million
PPO	poly(propylene oxide)
PTX	paclitaxel
pNP-PEO-PE	p-nitrophenylcarbonyl-polyethylene oxide – phosphatidylethanolamine
RBC	red blood cells
RNA	ribonucleic acid
rpm	revolutions per minute
S.D	standard deviation

SDS	sodium dodecyl sulfate
STAT3	signal transducer and activator of transcription-3
TAT	<i>trans</i> activating transcriptional activator
TEM	transmission electron microscopy
TMRCA	tetramethylrhodamine-5-carbonyl azide
T _g	glass transition temperature
THF	tetrahydrofuran
TLC	thin layer chromatography
TNF- α	tumor necrosis factor- α
UV	ultraviolet
VE	vascular endothelial
V _d	volume of distribution
V _{d_{ss}}	volume of distribution at steady state
VEGF	vascular endothelial growth factor
VEGFR	vascular endothelial growth factor receptor
VEC	vascular endothelial cell

Chapter 1

Introduction

1. 1. Introduction

The idea of selective delivery of drugs to their site of action was first introduced by Paul Ehrlich in 1890, who proposed the need for the development of “magic bullets” to improve drug performance, about a century ago. The systemic attempts to materialize this concept were started in the mid 1960’s. Since then a better understanding of mechanisms underlying drug action and disposition in the body as well as advances in nanotechnology have resulted in the development of a number of creatively designed targeted dosage forms such as microparticles [1], microcapsules [2], lipoproteins [3], liposomes [4], nanoparticles [5], polymer-drug conjugates [6] and polymeric micelles [7]. However, development of true targeted nanocarriers that can solubilize therapeutic agents efficiently, protect them against destabilizing biological environment and direct them towards diseased site of action will be a major step towards finding the ideal magic bullet.

Recently, polymeric micelles, have gained considerable attention as versatile nano-medicine platforms that can fulfill the requirements of an ideal drug carrier for target specific drug delivery [8-14]. Polymeric micelles are formed through self-assembly of amphiphilic block copolymers in an aqueous environment. They have a nanoscopic, usually spherical, core/shell structure in which the hydrophobic core acts as a nanoreservoir for the encapsulation of hydrophobic drugs, proteins or DNA and the hydrophilic shell interfaces the biological environment. Due to the presence of hydrophilic shell polymeric micelles can escape opsonization and further uptake by mononuclear phagocytic system (MPS) and circulate for longer periods of time in the blood and eventually accumulate in tissues bearing leaky vasculature, a behavior that is not unique to polymeric micelles and can be achieved by other stealth nano-carriers such as stealth liposomes [15-17]. The unique feature that has made polymeric micelles superior to other colloidal delivery systems; however, is the

chemical flexibility of the core/shell structure, which allows for the development of custom-made nano-carriers individually designed with respect to the physicochemical properties of the incorporated drug, individual requirements for various modes of drug release, responsiveness to internal or external stimuli and interaction with specific molecular targets [18-21]. In this context, polymeric micelles formed through self assembly of poly (ethylene oxide)-*block*- poly(L-amino acids) (PEO-*b*-PLAA) are of special interest. This is due to the presence of free functional groups on the PLAA section of the block copolymers, which allows conjugation of drugs [21, 22], drug compatible moieties [23, 24] and stimuli responsive groups [25] to the core structure. Despite, great potential for chemical tailoring, the biodegradability of PLAA structures is still not established [26]. In contrast, poly(ester)s have long been used as biodegradable surgical materials in human but do not contain any functional groups in their structure which makes them less flexible for chemical modification [26, 27]. The purpose of this research was to synthesize a family of novel self-associating PEO-*b*-poly(ester) block copolymers bearing functional side groups on their poly(ester) block and investigate the potential of prepared structures for the formation of polymeric micellar drug conjugates and nanocontainers suitable for anticancer drug delivery. The PEO-*b*-poly(ester) block copolymers with functionalized poly(ester) block can overcome the limitations of PEO-*b*-PLAAs in terms of biodegradability, and at the same time be engineered chemically for optimum properties in targeted drug delivery, opening a new chapter in the development of polymer based systems for various drug delivery applications.

1.2. Amphiphilic block copolymers and polymeric micellar delivery systems

1.2.1. Definition- Copolymers are defined as polymers composed of several different monomer units in a polymeric chain. Physical properties of polymers such as glass transition temperature (T_g), melting temperature, and crystallinity can be modified by copolymerization [28]. Copolymers can be classified into three categories according to the arrangement of the repeating units along the polymer chain: random copolymers, alternating copolymers, and block copolymers (Figure 1.1). Random copolymers are characterized by the disorganized placement of co-monomers along the polymeric backbone where the distribution of the repeat units is truly random. Alternating copolymers have only two different types of repeat unit and these are arranged alternately along the polymer chain. Block copolymers are linear copolymer in which the repeat units exist only in long sequences, or blocks, of the same type [29, 30]. Block copolymers themselves can be classified to di, tri, multi-block and graft copolymers based on the number of blocks in the polymeric chain. Block copolymers have been extensively utilized for drug delivery applications. The simplest type of block copolymer is diblock structure, commonly referred to as an AB-type block copolymer, which is composed of one segment of A units and one segment of B units. When the B segment is connected with two A segment at both terminals, this polymer is commonly referred to as an ABA- triblock copolymer. The third type alternately repeats A and B segments many times in one polymer chain and referred to as $(AB)_n$ multi-block copolymer. When more than two blocks originate from the same point in a star shape arrangement instead of linear architecture the polymer is termed as star $(AB)_n$ block copolymer. Graft copolymers are branched polymers in which the branches have different chemical structure to that of the main chain and resemble a comb (Figure 1.1).

Amphiphilic molecules have dual affinity for two different types of environments. This dual affiliation is built into the molecule by the covalent attachment of parts (blocks) of different chemical character and polarity. Surfactants and lipids are representative examples of low molecular weight amphiphiles with distinct hydrophilic and hydrophobic parts. Amphiphilic block copolymers, on the other hand, are macromolecules in which different blocks forming the copolymer differ from one another in terms of polarity.

Random copolymer: A-A-B-A-C-A-C-C-C-B-B-A-B-B-B-A-AA-B-AA

Alternating copolymer: A-B-A-B-A-B-A-B-A-B-A-B-A-B-A-B-A-B-A

Block copolymer:

i) Di block type A-A-A-A-A-A-A-A-A-A-B-B-B-B-B-B-B-B-B-B-B

ii) Tri block type A-A-A-A-A-A-A-B-B-B-B-B-B-B-B-A-A-A-A-A-A-A

iii) Multi block type (A-A-A-A-A-A-A-A-A-A-B-B-B-B-B-B-B-B-B-B-B)n

iv) Graft copolymer A-A
 B B B
 B B B
 B B B
 B B B
 B B B

Figure 1.1- The architecture of different types of copolymers (A and B are hydrophilic and hydrophobic monomer units, respectively).

1.2.2. Self-assembly of amphiphilic block copolymers- Similar to low molecular weight surfactants, amphiphilic block copolymers self-associate when placed in a solvent that is selective for either the hydrophilic or hydrophobic block. At very low concentrations, block

copolymers only exist as single chains with a collapsed insoluble block. As the concentration increases to critical micelle concentration (CMC), the collapsed block of each polymer chain begin to associate in such a way that the insoluble part of the copolymer will avoid contact with the media in which the polymer is dissolved (Figure 1.2). The core/shell structure formed from self assembly of block copolymers is called “micelle”. At concentrations right above CMC, a significant amount of solvent is trapped inside the micellar core and micelles are described as loose aggregates which exhibit larger size than micelles formed at higher polymer concentrations. At this concentration, the equilibrium will favor micelle formation; micelles will adopt their low energy state configuration and the remaining solvent will gradually be released from the hydrophobic core resulting in a decrease in micellar size [31]. Formation of multi-molecular polymeric micelles with core-shell architecture was first verified by Plestil and Baldrian through small angle X-ray scattering (SAXS) measurement of poly(styrene)-*b*-poly(butadiene)-*b*-poly(styrene) ABA tri-block copolymer in ethyl methyl ketone, which is a selective solvent for poly(styrene) [32].

Micellization is a spontaneous process leading to a net decrease in the total free energy of the system. The amount of change in the free energy, ΔG , is dependant on changes in the enthalpy, ΔH and the entropy, ΔS , of the system (Eq 1.1).

$$\Delta G = \Delta H - T\Delta S \quad (\text{Eq 1.1})$$

In organic solvents, micellization is an exothermic (enthalpy-driven) process while the micelle formation is often endothermic (entropy driven) in aqueous solvent. Therefore, elevated temperatures would stimulate micelle formation in an aqueous environment while causing the solubilization of micelles in an organic solvent [33]. The key to understanding the entropy driven micellization in an aqueous environment is the hydrogen bonding of water. Hydrogen bonds between water molecules are broken at the edge of the hydrocarbon

chain of an amphiphile, leading to a positive enthalpy contribution. Because of surface tension, water molecules become more ordered around the hydrocarbon chain with an attendant decrease in entropy. Formation of micelles from individual amphiphiles allows the cavity to revert to the structure of pure liquid water and an increase in entropy [34]. The entropy driven micellization process may proceed further by a combination of hydrophobic interaction, electrostatic interaction, metal complexation and hydrogen binding of block copolymers [8].

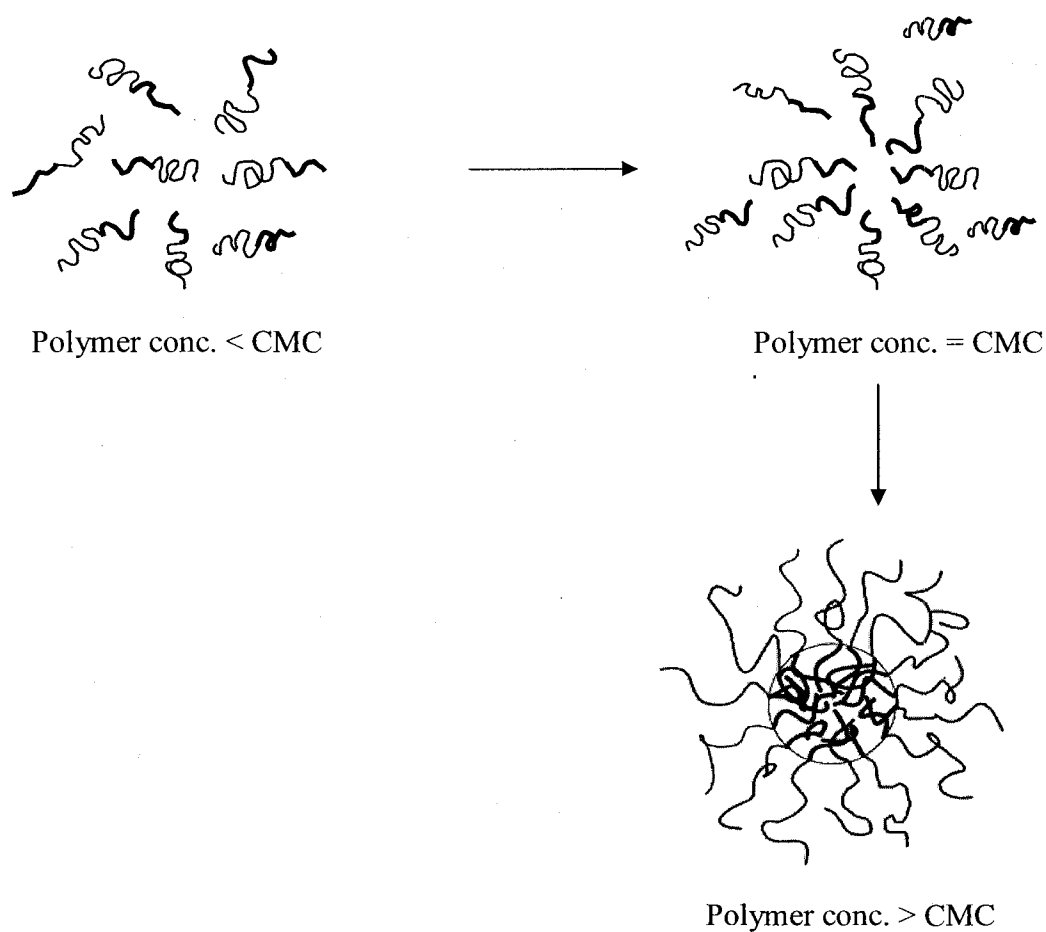


Figure 1.2- Schematic representation of the micellization process.

Although the self assembly of block copolymers and surfactants are very similar, a number of differences also exist between them. The tendency for micellization is overall much higher in block copolymers in comparison to surfactants since the exposure of long hydrophobic block to water is unfavorable to a greater extent. Therefore, block copolymers exhibit a much lower CMC than low molecular weight surfactants. Evidence points to a closed association for micellization of block copolymers, where sufficient cohesive forces in the micellar core exist, which is unlike surfactant micelles [35]. An estimate for the changes in standard free energy of micellization, ΔG° , by closed association is given by Eq. 1.2 [31].

$$\Delta G^\circ = RT \ln [\text{CMC}] \quad (\text{Eq. 1.2})$$

Where R is the gas constant and T is the absolute temperature. The thermodynamic tendency for micellization is represented by a negative value of ΔG° and low CMC.

1.2.3. Most commonly used block copolymers for drug delivery- Recently, there has been increasing interest in the application of polymeric micelles as drug delivery systems [9, 10, 12, 14, 36]. Efforts have led to the preparation of micellar carriers that can be safely administered to humans and adequately solubilize drugs. The hydrophilic block in these systems is usually PEO with a molecular weight ranging from 1000 to 20000 g.mol⁻¹. PEO has been used safely in humans and is approved by regulatory agencies for administration. The use of other hydrophilic polymers as shell-forming blocks has been reported for bioadhesive or thermoresponsive properties [37, 38]. Unlike the shell-forming block, the choice for a core-forming block is relatively diverse. The length of the core-forming block is usually equal or shorter than the PEO block to maintain water solubility and form spherical core/shell micelle structures.

Most of the studies on block copolymers have been conducted on Pluronic[®] (PEO-*b*-poly(propylene oxide)-*b*-PEO). Like low molecular weight surfactants, Pluronic[®] demonstrate solubilizing effects for parenteral drug administration [39, 40]. Pluronic[®] have been used to solubilize haloperidol [41], indomethacin [42], doxorubicin (DOX) [43], epirubicin [43] and Amphotericin B (AmB) [44]. Overall, many Pluronic[®] used for drug solubilization have high ratios of PEO to poly(propylene oxide) (PPO) and are non-toxic relative to many low molecular weight surfactants, e.g. Tween 80, especially in terms of cell membrane lysis, e.g. hemolysis [45]. Relatively hydrophobic Pluronic[®], on the other hand, have been used to induce immune responses and act as adjuvants [46]. Pluronic[®] have shown other important biological effects, e.g., inhibiting P-glycoprotein, which is believed to be at least partly responsible for multi-drug resistance (MDR) in cancer cells [43, 47]. Lastly, Pluronic[®] have been used to increase the transport of drugs across membrane barriers [48].

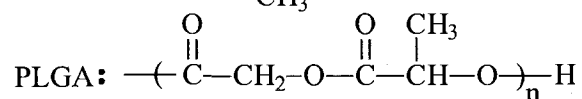
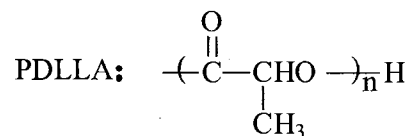
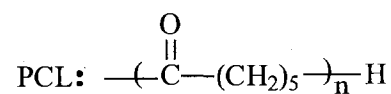
Block copolymers based on PEO-*b*-PLAA are unique among amphiphilic block copolymers owing to the chemical flexibility of core-forming PLAA block. The presence of free functional groups (e.g. amine or carboxylic acid) in the PLAA block provides extra advantage for the chemical attachment of drugs, drug compatible moieties, genes or intelligent vectors to the micellar core. Existence of free amine or carboxylic groups has been used for the electrostatic complexation of charged chemotherapeutic agent or nucleic acid based drugs, as well. For instance, core forming poly(L-aspartic acid) (P(Asp)) and poly(L-glutamic acid) (P(Glu)) that have free carboxylic side groups have been used to encapsulate cisplatin (CDDP) [49, 50]. A core of poly(L-lysine) (PLL) that has pendant amine groups, on the other hand, was used to incorporate plasmid DNA [51, 52]. In addition, the presence of functional groups provides opportunity for systemic alteration in the structure of the core-forming block. This strategy may be used to fine tune the micellar

delivery system for better control over the extent of drug loading, release or activation. For example, enhancement in the encapsulation level of DOX [53] was achieved in PEO-*b*-poly(benzyl L-aspartic acid) (PEO-*b*-PBLA) due to the enhanced interaction of DOX with benzyl side chain in PBLA core. Replacement of benzyl side chain in PBLA core with saturated fatty acid ester or cetyl ester resulted in increased encapsulation of aliphatic antifungal agent AmB [54] and antineoplastic agent, KRN-5500 [24], respectively .

To avoid long-term toxicities, biodegradable block copolymers with poly(ester) core-forming structures such as poly(lactic acid) (PLA), poly(glycolic acid) (PGA), poly(ϵ -caprolactone) (PCL) and their copolymers have been developed and used for drug delivery (Figure 1.3). Poly(ester)s have a history of safe use in humans as biodegradable surgical sutures, bone fracture fixture devices and controlled drug delivery systems. In 1994, Gref *et al* prepared block copolymers of PEO-*b*-poly(lactic-*co*-glycolic acid) (PEO-*b*-PLGA). Following self-assembly by an O/W emulsion process, nanospheres with an average diameter of 140 nm were formed from PEO-*b*-PLGA, showing an enhanced blood circulation particularly at a high PEO content. The carrier was used successfully to encapsulate lidocaine and prednisolone (45% w/w drug to polymer) [55]. Micelles from PEO-*b*-poly(D, L lactic acid) (PEO-*b*-PDLLA) were also developed and shown to form micelles (50 nm in size) capable of solubilizing high level of hydrophobic drugs such as paclitaxel (PTX) at 25% w/w drug to polymer [56]. This higher level of loading for PTX is in contrast to low loading levels of 0.5% for this drug in Pluronic[®] micelles. High solubility was attributed to higher hydrophobicity and T_g of the PDLLA block. PCL is a semicrystalline polymer with a T_g of -60 °C which is known for its biodegradability and biocompatibility. In 1997, Kim *et al* prepared PEO-*b*-PCL block copolymer micelles for the purpose of drug delivery and investigated the *in vivo* biocompatibility after intravenous (i.v.)

administration to mice. The study showed survival of most of the test animals showing normal weight gain after receiving six times of single dose by 1 h period. [57]. Later, Lee *et al* prepared indomethacin loaded PEO-*b*-PCL micelles by dialysis method with a high drug loading (42% w/w drug to polymer ratio) [58]. Further investigation with dihydrotestosterone [59], cyclosporin A (CsA) [60], DOX [61], PTX [62] and FK 506 [63] demonstrated the potential of PEO-*b*-PCL in drug delivery applications. Also, there are reports on the use of PGA [64], PLGA [65] and poly (L-lactic acid) (PLLA) [66] as core-forming blocks for the encapsulation different therapeutic agents. Despite great potential in drug delivery, poly(ester)s are less suitable for chemical engineering due to the lack of functional groups on the polymer backbone. Functionalization of the poly(ester) is mostly carried out through activation of their terminal hydroxyl group only. Hence, unlike PLAA block, poly(ester)s cannot easily be tailored for hydrophobic interactions, ionic association, and chemical conjugation of drugs or drug compatible moieties for the development of smart micellar delivery system.

Poly(ester)s:



Poly(amino acid)s:

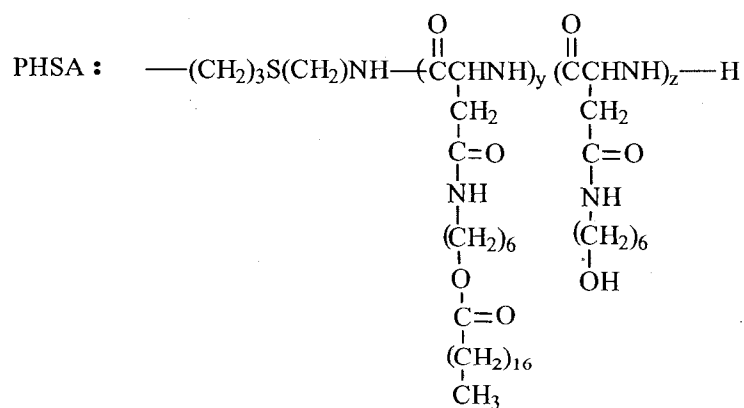
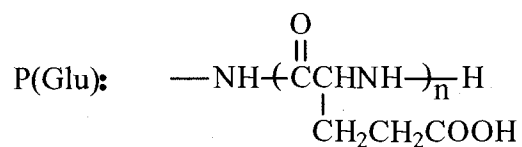
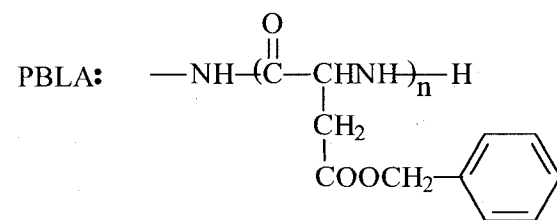
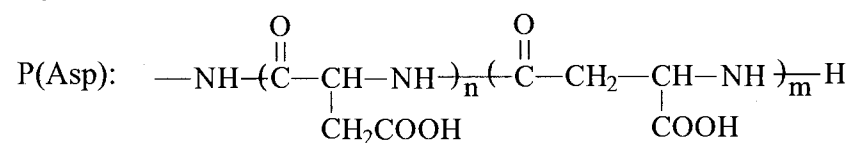


Figure 1.3- Chemical structures of the most commonly used poly(ester) and poly(amino acid) core-forming blocks in polymeric micelles

1.2.4. Different designs of polymeric micellar systems for drug delivery

1.2.4.1. Micelle forming polymer-drug conjugates- In this approach the incorporation and stabilization of drug within the micellar carrier is achieved through the formation of chemical bonds between the functional group(s) of the polymeric backbone and the drug (Figure 1.4 A-D). Drug conjugation to PEO-*b*-poly(ester)s is mostly carried out through the formation of covalent bonds between the activated terminal hydroxyl group of the poly(ester) section and reactive groups on the drug molecule (Figure 1.4 A) [66-68]. On the other hand, PLAA segments bear several functional groups (Figure 1.3) providing several sites for the conjugation of a number of drug molecules to one polymer chain (Figure 1.4 B-D).

The first report on the preparation of micelle forming block copolymer conjugates was published by Ringsdorf's group [69]. They attached antineoplastic drug, cyclophosphamide to PEO-*b*-PLL block copolymer. The idea was further advanced by Yokoyama *et al* who conjugated DOX to PEO-*b*-P(Asp) by an amide linkage to provide a delayed mode of DOX cleavage from the PEO-*b*-P(Asp-DOX) micelles. Indeed, the formulation showed sufficient micellar stability evidenced by a slow rate of dissociation even in the presence of rabbit serum, *in vitro* [70]. However, the amide linkage formed between the carboxyl group of the aspartic acid and the amino group of the glycosidyl residue on DOX was found too stable for any drug release *in vivo*. With the same goal, Yoo *et al* studied the chemical conjugation of DOX to PEO-*b*-PLGA block copolymer forming a carbamate linkage between the primary amine group in DOX and the terminal hydroxyl group in *p*-nitrophenyl chloroformate-activated PLGA [71]. In PBS (phosphate buffer saline), PEO-*b*-PLGA micelles released 50% of their drug content in a sustained manner over 2 weeks, whereas release from physically encapsulated DOX in PEO-*b*-PLGA only lasted for 3 days.

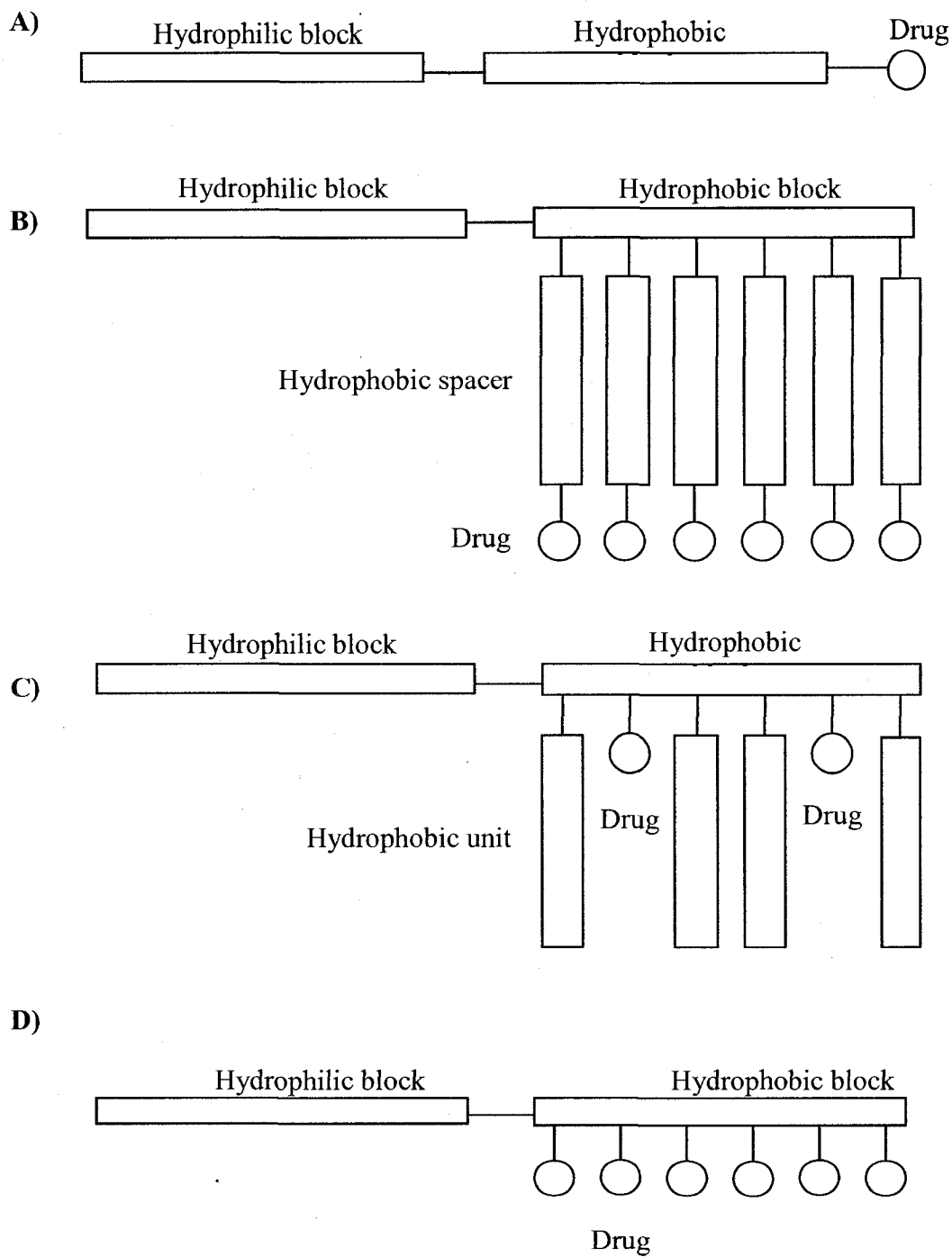


Figure 1.4- Different designs and models for micelle-forming drug-block copolymer conjugates.

To overcome the excessive stability of an amide linkage between a drug and core forming block, Kwon *et al* reported the formation of ester bond between the carboxylic acid groups of another chemotherapeutic agent, methotrexate (MTX) and hydroxyl group of PEO-*b*-poly(hydroxyl alkyl-L-aspartamide) (PEO-*b*-PHAA) block copolymers [22, 72]. The result of release studies showed a 5-20% of MTX release from the polymeric micellar carrier within 21 days in PBS. It was concluded that MTX esters of PEO-*b*-PHAA can be structurally modified by varying the degree of drug substitution, which in turn changed the overall hydrophobicity of the block copolymer, thereby, influencing micelle stability and controlling drug release.

1.2.4.2. Micellar nanocontainers- Several amphiphilic block copolymers have been used to noncovalently incorporate drug molecules. In this system, the formation of hydrophobic interactions or hydrogen bonds between the micelle forming block copolymer and drug provides the basis for the solubilization and stabilization of drugs in the polymeric micelles. The physical encapsulation of drugs within polymeric micelles is generally a more attractive approach than micelle-forming polymer-drug conjugates since many polymers as well as drug molecules do not bear reactive functional groups or the free functional group may be required for the pharmacological effectiveness of the drug.

The physical encapsulation of drugs in polymeric micelles may be accomplished by direct addition and incubation of drug with block copolymers in an aqueous environment, only if the block copolymer and drug are water soluble [73-75]. However, most of the block copolymers are not soluble in water and produced poor drug loading in direct mixing method. Therefore, physical incorporation of hydrophobic drugs into polymeric micelles is usually achieved by dialysis, oil in water (o/w) emulsion, solvent evaporation or co-solvent

evaporation methods depending on the block polymer and drug characteristics. In *dialysis* method [76, 77], the drug and block copolymers are dissolved in a good solvent and then dialyzed against a selective solvent. As polymeric micelles form during the dialysis process, the drug is incorporated into the cores of the micelles. Excess drug is also removed during the dialysis process. In *oil in water emulsion* method [53, 78], a drug dissolved in a water-immiscible organic solvent (such as, dichloromethane) is added drop-wise to water under vigorous stirring. The polymer may be dissolved in either organic or aqueous phase. The organic solvent is then removed by evaporation. The *solvent evaporation* method [56, 79] is based on dissolving the drug and polymer in a volatile organic solvent and complete evaporation of the organic solvent leading to the formation of polymer/drug film. This film is then solvated in aqueous phase by gradual shaking to facilitate slow detachment of block copolymer and formation of micelle. *Co-solvent evaporation* method [60, 62] involves the drug and polymer being dissolved in a volatile water-miscible organic solvent (co-solvent). Micellization and drug entrapment is then triggered by the addition of aqueous phase (non-solvent for the core forming block) to the organic phase (or vice versa), followed by the evaporation of the organic co-solvent.

The drug loading capacity of micelles depends to a high extent on the interaction between core-forming blocks and incorporated drug. If the type, length and chemistry of the hydrophobic block are properly chosen, drug solubility may be increased thousand times compared to saturation solubility of drug in water [24, 56, 80-83].

1.2.4.3. Polyion complex micelles- Polyion complex micelles (PIC)s can incorporate and deliver different therapeutic moieties that carry charge; i.e., small drugs [50, 84], peptides [85] or DNA [52, 86, 87]. In this approach, drug incorporation is promoted through electrostatic

interactions between oppositely charged polymer/drug combinations. Neutralization of the charge on the core-forming segment of the block copolymer will trigger the self-assembly of the PICs and further stabilization of the complex within the hydrophobic environment of the micelle core. The physicochemical properties of PIC micelles are significantly affected by the molecular weights, charge densities, the pKa value, the bulkiness and mobility of the charged groups. In particular, it is known that the PIC micelles are destabilized with increase in ionic strength of the medium due to electrostatic shielding [88]. The incorporation of peptides or DNA into the core of the PIC micelles may lead to the stabilization against digestive enzymes such as nuclease and facilitate their long circulation in blood. Cisplatin (CDDP) is an example of a charged drug, which has been extensively studied for the formation of PIC micelles. Kataoka *et al* reported the complexation of CDDP with PEO-*b*-P(Asp) block copolymer in an aqueous medium [84]. In *in vitro* release study, a sustained mode of CDDP release was obtained at physiological temperature, exhibiting 50% of drug release for more than 20 h. However, the PEO-*b*-P(Asp) micellar CDDP did not show any significant benefit over beyond 4 days after i.v. administration to the lewis lung carcinoma (LLC) tumor bearing C57BL mice. Dissociation of the micellar structure and premature release of CDDP was speculated as possible reason for the lower accumulation of micellar drug inside the tumor. The P(Asp) core was later replaced with P(Glu), which is more hydrophobic, to improve micellar stability. PEO-*b*-P(Glu) micelle released CDDP over a period of >150 h in a sustained manner, with no initial burst release at physiological condition. The modified formulation demonstrated superior biodistribution and higher antitumor activity compared to free CDDP. This formulation is now in phase I clinical trials. [89]. PIC micelles can also be used for gene delivery applications [51, 90-92].

1.3. The physicochemical characteristics of polymeric micellar delivery systems

1.3.1. Thermodynamic and kinetic stability- Block copolymer micelles loaded with therapeutic agents should be stable enough in the blood circulation to provide a sufficient time for accumulation in the target site and simultaneously be able to slowly dissociate into unimers so that they can easily be eliminated through kidney and do not accumulate in the body. The stability of polymeric micelles includes two different concepts: thermodynamic stability and kinetic stability. The thermodynamic stability of micelles or tendency of block copolymers towards micellization is characterized by their CMC, which is the minimum concentration of amphiphile required for micelle formation. In polymeric micelles, the CMC values are usually in μM range. In contrast, the surfactant micelles are thermodynamically less stable, exhibiting CMC values in mM range [7]. In an average individual, the total blood volume is about 5 liter and the polymer concentration will face extreme dilution after i.v. injection of micelles and circulation in blood. Because of a lower CMC, polymeric micelles might be able to withstand the diluting effect of blood and stay above CMC levels after i.v. injection. In contrast, the level of surfactant micelles is expected to fall below their CMC right after injection. The CMC of block copolymers mostly depends on the nature and length of the shell and core forming blocks, i.e., hydrophilic lipophilic balance (HLB), of the copolymer. A reverse relationship between the HLB values of block copolymers and their CMC has been shown in many studies [7, 20, 93, 94].

The entropy driven self assembly of block copolymers may be followed by a hydrophobic or electrostatic interaction in the micellar core, depending on the structure of the core forming blocks. Strong cohesive forces resulting from these interactions provides kinetic stability to micelles against dissociation. As a result, a slow dissociation rate may exist for polymeric micelles even below CMC, and polymeric micelles may not necessarily exist in

equilibrium with polymeric unimers above CMC [95, 96]. In contrast, surfactant micelles tend to break up in milliseconds upon dilution below CMC and are in continuous exchange with their unimers in solution [97]. The strength of the cohesive force in polymeric micellar core may be characterized by T_g and degree of crystallinity of the copolymer. Block copolymer micelles comprised of a hydrophobic block with T_g exceeding 37 °C are considered to have frozen cores in biological environment, i.e. the molecular motions of the chains in the core are constrained, generally accounting for this greater kinetic stability upon dilution [12, 14]. Increase of polymer core crystallinity confers stronger van der Waals interactions between polymer chains in the micellar core, resulting in a more compact conformation and denser packing of the micellar core [14]. The kinetic stability can be further improved by cross-linking of the core forming block or by attaching certain bulky groups to the core forming block [62, 98]. The attachment of bulky group to the core forming block may enhance the kinetic stability due to the hindrance of rotation. In addition, there is also evidence that the incorporation of hydrophobic compounds into block copolymer micelles may enhance micellar stability due to the hydrophobic interaction between the incorporated molecules [99]. Kinetic stability in polymeric micelles will result in slow dissociation of micellar structure after dilution in blood at concentrations below CMC. Both thermodynamic and kinetic stability are extremely important for maintaining the integrity of polymeric micelles for a sufficient period of time in blood circulation. So polymeric micelles can either deliver the drug to its site of action or release it in a sustained manner. A micellar carrier with less stability might release the encapsulated drug prematurely due to the dissociation of the micelle structure in blood circulation.

1.3.2. Micellar size - The size of nanocarriers is one of the most important properties that largely influence their circulation time and organ disposition. The threshold molecular weight for glomerular filtration is 40-50 KDa for water soluble polymers. The combined molecular weight of block copolymers in the micellar aggregates is in the order of 10^6 g.mol⁻¹ and this size range is enough to prevent glomerular excretion [54, 100]. Therefore, elimination of polymeric micelles by kidney is not expected unless the micellar structure dissociates into polymeric unimers. Delivery systems smaller than 200 nm have lower chance for capture by MPS [12, 101, 102]. Polymeric micelles are usually between 10-100 nm. At this size range they are expected to efficiently escape uptake by MPS and achieve prolonged circulation in blood [12, 101-103]. Certain inflammatory vessels as well as tumor capillaries are fenestrated and have pore cut off size ranging from 100 nm to 1.2 μ m in diameter. This size allows easy extravasation of polymeric micellar nano-carriers to the inflamed or tumor site [104, 105].

1.3.3. Morphology -Most of the polymeric micelles designed for drug delivery are reported to be spherical, evidenced by transmission electron microscopy (TEM) and atomic force microscopy (AFM) techniques. Extensive investigation on polymeric micellar morphology have been carried out by Eisenberg and his group, primarily using poly(acrylic acid)-*b*-poly(styrene) (PAA-*b*-PSt) and PEO-*b*-PSt block copolymers with a wide range of copolymer compositions [106-110]. These studies have revealed that formation of different morphologies of polymeric micelles may be explained by a force of balance involving the following three components: the free energy of the core, which relates to the degree of stretching of the core-forming block; the free energy of the interface, which relates to the interfacial tension between the core-forming block and the solvent; and the free energy of the corona, to which the electrostatic and steric interactions of the corona-forming blocks

contribute [106, 107]. This balance of forces which results in morphological control can be exercised by controlling a number of different parameters; such as block copolymer composition, copolymer concentration, and the nature of the common solvent used in micelle preparation. In addition, the presence of ions influences the morphology of the micelles [111, 112]. The morphology is also sometimes tuned by introducing specific interactions like hydrogen bonding groups or excess chirality in the monomer units [113].

Different drug loading, release and applications from rod shaped or lamellar micelles in comparison to spherical micelles is envisioned. For instance, rod like micelles may be most useful in the preparation of aerosol formulations whereby their tubular structure may facilitate access to different part of the lung [12]. The influence of morphology of the micellar delivery vehicles on their performance has not been explored to this point.

1.3.4. Drug loading- Micellar cores serve as a nanoreservoir for loading of hydrophobic molecules that are conjugated, complexed or physically encapsulated in polymeric micelles [22, 56, 84]. The extent of drug incorporation in polymeric micelles by physical means is dependent on several factors, including the molecular volume of the solubilize, its interfacial tension against water, nature and length of the core-forming block, total copolymer molecular weight, copolymer concentration and to a lesser extent, the nature and length of the corona [10, 12]. However, the most important factor identified to date is the compatibility between the solubilize and the core-forming block [12, 114].

The partition coefficient of the hydrophobic molecule between the micellar core and surrounding aqueous medium describes the extent of drug entrapment in polymeric micelles. One parameter which has been used to assess compatibility between the polymer and the

solubilize is the Flory–Huggins interaction parameter (χ_{sp}) between the solubilize and the core-forming block described by Eq. 1.3 [115].

$$\chi_{sp} = (\delta_s - \delta_p)^2 V_s / RT \quad (\text{Eq. 1.3})$$

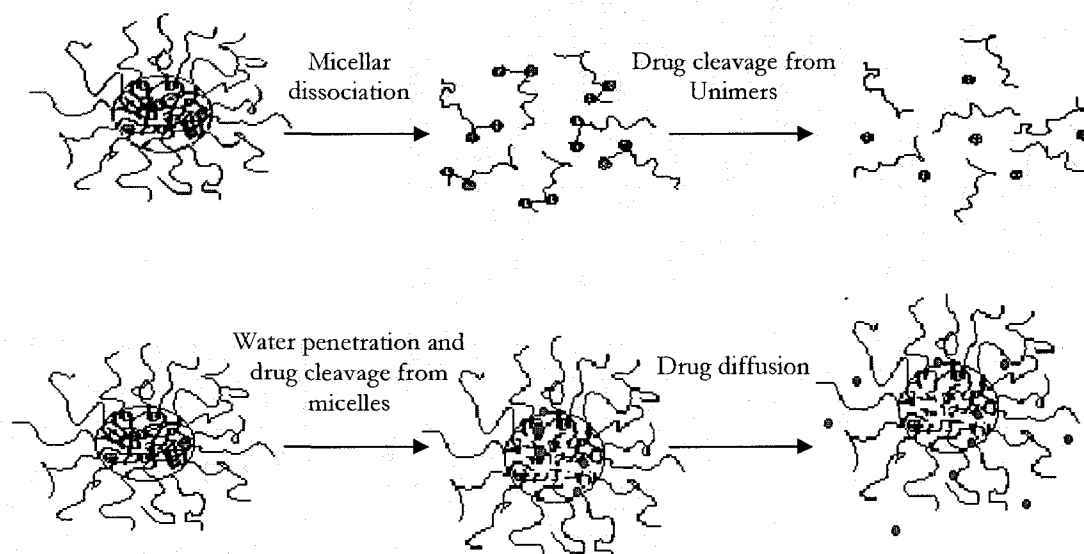
where δ_s and δ_p are the Scatchard–Hildebrand solubility parameter of the solubilize and the core-forming polymer, respectively, V_s is the molar volume of the solubilize, R is the gas constant and T the Kelvin temperature. The lower the χ_{sp} , the greater the compatibility between the solubilize and the core-forming block. The highest degree of compatibility will be reached when $\delta_s = \delta_p$. As described in section 1.2.4.2 and 1.2.4.3, the chemical conjugation of drugs or complex formation between block copolymers and charged therapeutics has been used as an alternative approach in drug delivery by polymeric micelles. In either case, existence and accessibility of functional groups on the polymeric backbone is a requirement.

1.3.5. Drug release -The mode of drug release from polymeric micelles mainly depends on the design used for the preparation of the polymeric micellar delivery system; the chemical structure of micelle-forming block copolymer and incorporated drug; their physicochemical properties; and the localization of the incorporated drug in polymeric micelles.

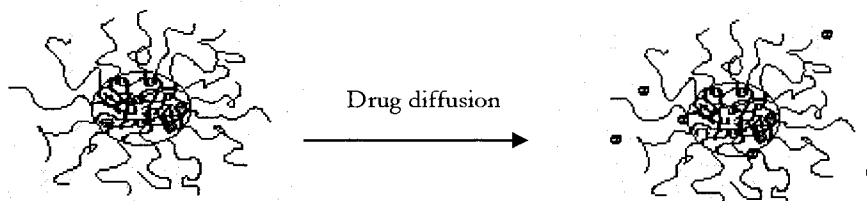
Drug release from micelle-forming block copolymer-drug conjugates may proceed via two major pathways. In first case, water penetration and hydrolysis of the liable bonds in the micellar core (erosion), followed by diffusion of drug or drug-unimer derivatives may occur (Figure 1.5 C). On the other hand, water diffusion into hydrophobic and rigid core may be restricted. Therefore, in the second case, drug release may be dependent on the rate of micellar dissociation. In this case, the slow dissociation of the micellar structure to single polymeric chains and further hydrolysis or enzymatic breakdown of the liable bonds may result in a sustained drug release (Figure 1.5 A) [72].

In case of physically encapsulated drug, release from sufficiently stable micellar nanocontainers usually proceeds by diffusion (Figure 1.5 B), whereas drug exchange with free ions and proteins in the physiological media triggers drug release in PIC micelles, formed by electrostatic complexation of block copolymers and charged drugs (Figure 1.5 C). In either case, it may be possible to tailor the chemical structure of the micelle-forming block copolymer and modify the physicochemical properties of the core/shell forming blocks to adopt an instant, sustained, or delayed mode of drug release for specific delivery requirements. For example, hydrophobicity and rigidity of the micellar core may be enhanced to restrict the penetration of water and free ions to the micellar core in micelle-forming drug conjugates and PIC micelles. This may lead to a sustained or even delayed mode of drug release from the carrier [50, 72, 116]. The application of polymeric micelles that have glassy cores under physiological condition (37°C), cross-linking of the micellar core structure and the induction of strong hydrophobic interaction or hydrogen bonds between the core-forming block and solubilisate may be used to lower the rate of micellar dissociation, drug diffusion and the overall rate of drug release from the micellar carrier [62, 73, 85, 117]. The introduction of hydrophilic or stimulus responsive groups to the core structure, on the other hand, may be used to provide an instant or pulsed mode of drug delivery. Finally, the method of drug incorporation in polymeric micelles may also be modified to improve the extent of drug loading, localization or the physical state of the loaded drug, providing other means for controlling the drug release profile from polymeric micelles [118].

A) Drug release from micelle forming block copolymer-drug conjugates



B) Drug release from micellar nanocontainers



C) Drug release from PIC micelles

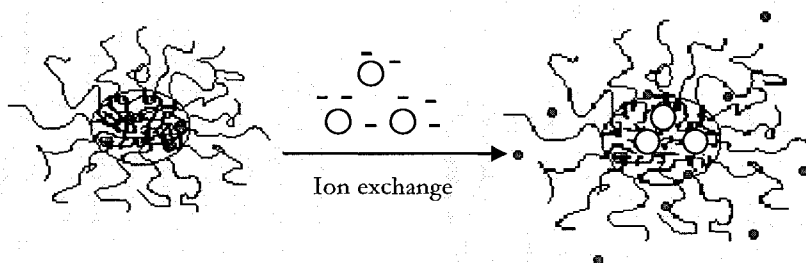


Figure 1.5- Modes of drug release from polymeric micelles.

1.4. The biological characteristics of polymeric micellar delivery systems

1.4.1. Biodistribution and pharmacokinetic properties- The major objective of using polymeric micelles is to modulate drug disposition in the body, redirecting the drug away from its site of toxicity towards its site of action so that it can achieve targeted drug delivery. The use of chemotherapeutic agents like DOX, PTX and camptothecin is limited by toxic side effects, mostly restricted from their non-specific distribution to the rapidly proliferating normal tissues in the body. In addition, they do not reach to effective levels at their site of action before toxic drug side effects are seen. For instance, the volume of distribution (Vd) for free DOX has been estimated at 25 L/kg, suggesting a significant nonspecific distribution of DOX to healthy tissues [119]. This large Vd, when combined with the relatively rapid clearance (CL) rate from the circulation results in low drug levels in the tumor and significant toxicity to normal tissues. To overcome toxic side effects and to improve the therapeutic efficacy of drugs numerous delivery systems based on specific carrier properties are studied and evaluated [120, 121]. The alteration in pharmacokinetics of the encapsulated drug induced by the carrier modifies the tissue distribution and the rate of CL of a drug providing an opportunity for maximum localization of encapsulated drugs at the tumor site.

In order to accomplish an effective drug delivery to the tumor site after systemic administration, the carriers need to achieve long circulation in the blood since the extravasation process is generally considered to be slow. The major obstacles to long circulation of colloidal drug carrier systems are considered to be renal elimination through kidney and recognition by the MPS as foreign substances (Figure 1.6). Renal elimination can be avoided for polymeric micelles due to their size being higher than the threshold for glomerular filtration. On the other hand, opsonization by serum proteins and

immunoglobulin G (IgG) antibody, which is thought to play a critical role in the recognition and subsequent clearance of colloidal particles by MPS is not expected in polymeric micelles due to their hydrophilic PEO brush on micellar surface [122, 123]. The mechanisms by which PEO prevents opsonization include shielding of the core charge, increased surface hydrophilicity [124] and enhanced repulsive interaction between polymer-coated nanocarriers and blood components due to polymer steric effect on the nanocarrier surface [125]. Preferred distribution of the carrier in tumor does not guarantee tumor targeted drug delivery. For efficient drug targeting, the carrier should be able to hold its drug content while in circulation and release the encapsulated drug preferentially in the target tissue.

The pharmacokinetics of polymeric micelles has been studied either following the pharmacokinetics of radio-labeled polymer or incorporated drug. Radio-isotope ¹²⁵Iodine (¹²⁵I) labeled tyrosine conjugated PEO-*b*-PDLLA (Tyr-PEO-*b*-PDLLA) micelles exhibited prolonged blood circulation ($t_{1/2} \sim 18\text{h}$) after i.v. administration and 25% of the injected dose remained in circulation at 24 h post-injection in male C57/BL 6N mice [126]. The half life of PEO-*b*-PDLLA micelles was comparable to that of well-established long circulating liposomes, which have reported $t_{1/2}$ values of 15-24 h [17, 127]. Regarding tissue distribution, the PEO-*b*-PDLLA micelles exhibited low uptake by lungs and kidney (less than 3% of injected dose). The minimal accumulation of the micelles in the liver and spleen ($\sim 7\%$ of the injected dose at 24 hours) suggests that they are able to avoid recognition by MPS. It is worthwhile mentioning that PEO-*b*-PDLLA micelles were slowly excreted into the urine (24% of the injected dose at 24 h-post injection), pointing to slow dissociation and elimination of block copolymer unimers through glomerular filtration [126].

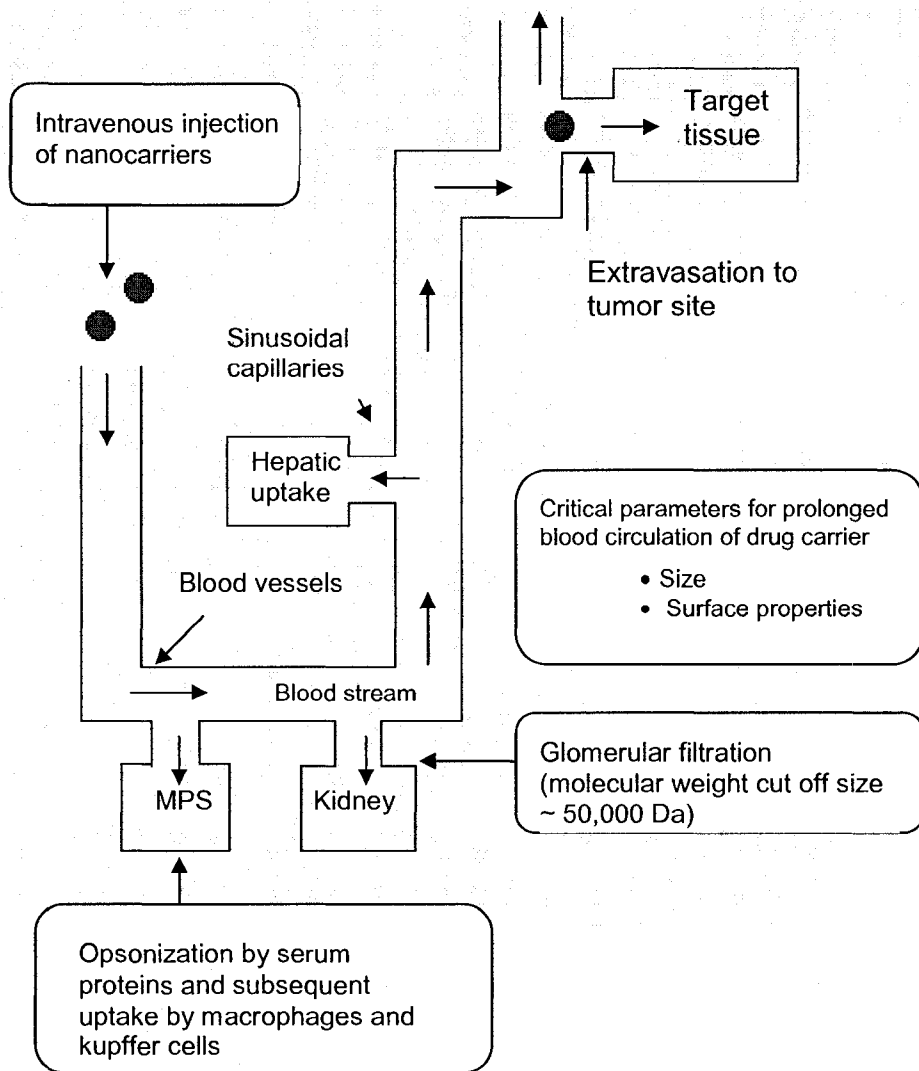


Figure 1.6- Fate of block copolymer micelles after i.v. administration

Polymeric micelles based on PEO-*b*-PDLLA block copolymer developed by Burt *et al* has been found to be one of the most successful in solubilizing PTX, which resulted in a 5000-fold increase in the solubility of PTX in aqueous media. Results of further studies on the biodistribution of PEO-*b*-PDLLA compared to the Cremophor EL formulation, Taxol[®] (Bristol-Mayer Squibb) showed a 5.5-fold decrease in the area under the concentration -time

curve (AUC) of polymeric micellar PTX in blood after its i.v. administration. This is in contrast to the expected trend in pharmacokinetic parameters for long circulating carriers. In-fact, careful investigation of the biodistribution study in Sprague-Dawley rat using ^{14}C labeled PEO-*b*-PDLLA and ^3H labeled PTX revealed a rapid dissociation of the drug from the carrier which resulted in a broad distribution of the drug into the tissue and quick elimination of unencapsulated PTX as well as micellar components through the urine [128].

The pharmacokinetics and biodistribution of micelle forming DOX conjugates, PEO-*b*-P(Asp-DOX) were studied in female, ddy mice after i.v. injection following radioiodination of the conjugate by Yokoyama *et al* [129]. Vd for free DOX was 2000 mL but (PEO-*b*-P(Asp-DOX) micelles showed a Vd of 3.6 mL, suggesting that the PEO-*b*-P(Asp-DOX) conjugate was confined to the blood pool. An increase in the molecular weight of the PEO block to 12000 g.mol^{-1} in this system resulted in further increase in DOX blood levels in healthy ddy mice (68 % of the injected dose remained in the blood at 24 h after i.v. injection) [130]. Drug level measurements 1h after its administration in healthy mice models revealed the presence of 17.1 and 2.9 % of ^{125}I -labeled PEO-*b*-P(Asp-DOX) micelles per gram of blood and heart (site of DOX toxicity), respectively. [129]. In subsequent studies, the minimal accumulation of the [^{14}C] benzylamine labeled PEO-*b*-P(Asp-DOX) micelles in the liver and spleen (17 % and 34 % of injected radiolabeled micelles per gram of organ at 24 hour, respectively) of female ddy mice suggest that the PEO-*b*-P(Asp-DOX) micelles were able to avoid MPS uptake [131].

The development of PEO-*b*-PCL micellar carriers for the encapsulation of CsA has also been pursued by Aliabadi *et al* [121]. Preliminary data indicated that PEO-*b*-PCL can effectively solubilize CsA and cause a favorable shift in the pharmacokinetics and biodistribution of this drug. Pharmacokinetic studies in healthy rat model showed a

significant increase in plasma AUC (from 32.7 to 199 $\mu\text{g}\cdot\text{h}/\text{mL}$), a decrease in Vd_{ss} (from 2.33 to 0.232 L/kg) and a decrease in CL (from 0.195 to 0.0255 l/kg/h) for the polymeric micellar formulation compared to commercial formulation of CsA, i.e., Sandimmune[®](Novartis). A detailed review on the effect of polymeric micelles on the pharmacokinetics of different drug is provided in ref. [11]. Overall, from review of literature it is evident that among different polymeric micellar formulations, only a few demonstrated desirable and meaningful changes in the pharmacokinetics and bio-distribution of the encapsulated drug for the purpose of tumor targeting (section 1.5.2 for further details). Careful and systematic engineering of the block copolymer influencing the micellar properties (e.g., appropriate micellar size, architecture, and morphology) and biological performance of the polymeric micelles such as *in vivo* stability is a necessity to prevent rapid dissociation of the carrier, MPS uptake and kidney elimination to achieve controlled biodistribution of the encapsulated drug for targeted delivery.

1.4.2 Cellular internalization and intracellular distribution- Polymeric micelles might change the sub-cellular localization of drugs and also control the time-dependant intracellular delivery of therapeutic agents. Understanding of the extent and mechanism of micellar uptake by target cells and its intracellular distribution is essential in the design and development of nano-engineered polymeric micelles for drug or gene delivery. To date, only limited numbers of studies were made available on the interaction of micelles and cells as well as their intracellular distributions.

The internalization of polymeric micelles was first investigated by Kabanov *et al*, who demonstrated the internalization of Pluronic[®] micelles by Jurkat and Madin-Darby Canine Kidney (MDCK) epithelial cells [41]. Cellular internalization of PEO-*b*-PCL micelles by

mouse embryonal carcinoma cells [63] and rat adrenal pheochromocytoma (PC12) cells [132]; as well as PEO-*b*-PLGA micelles by human hepatoblastoma (HepG2) cells [71] has also been studied. The results of these studies demonstrate that the micellar uptake is time, temperature and pH-dependent. A decrease in temperature from 37 °C to 4 °C and acidification of cytoplasm known to inhibit endocytosis [133-136], severely inhibits the uptake of PEO-*b*-PCL micelles by cancer cells [132]. Also, decreased uptake of polymeric micelles in MCF-7 breast cancer cells and PC12 cells compared to free dye indicates the possible involvement of energy dependant process, i.e., endocytosis, in micellar uptake [132, 137] (Figure 1.7). The endocytosis of polymeric micelles may take place via either clathrin mediated mechanisms [138, 139] or macropinocytosis [139]. The mechanistic details remain to be elucidated. Studies also demonstrate that polymeric micelles with PEO as corona may reduce the internalization of hydrophobic drugs by various cells [132]. However, the structure of block copolymers used, size of the micelles, and cell lines in which the studies are carried out all play a role in the extent, rate and mechanism of internalization of micelles into the cells [139].

Savic *et al* investigated the detailed intracellular distribution of tetramethylrhodamine-5-carbonyl azide (TMRCA) conjugated PEO-*b*-PCL micelles in PC12 cells by confocal microscopy utilizing organelle selective fluorescent dyes, i.e., Hoechst 33342 for nucleus and 5-dodecanoylaminofluorescein (DAF) for plasma membrane [140]. TMRCA conjugated PEO-*b*-PCL micelles was detected in the cytoplasm but not in the nuclear compartment. Triple-labeling experiments with a nucleus-selective dye; the fluorescent micelles; and dyes selective for acidic organelles, e.g. lysosomes, demonstrated the micellar distribution to the various cytoplasmic organelles including lysosomes, golgi apparatus, endoplasmic reticulum and mitochondria. Similar sub-cellular distribution of the

PEO-*b*-PCL-TMRCA micelles was observed in mouse embryonic fibroblast (NIH 3T3) cells suggesting that micelles with an unfunctionalized PEO corona and a PCL core are suitable for multiple cytoplasmic targeting. Similar to the findings with fluorescent-labeled micelles, Maysinger *et al* demonstrated that gold-incorporated micelles do not enter the nucleus but localize in endosome/lysosomes [141, 142]. Heavy atoms such as gold, because of its high electron density and stability, can be incorporated into micelles to allow visualization of individual micelles by TEM.

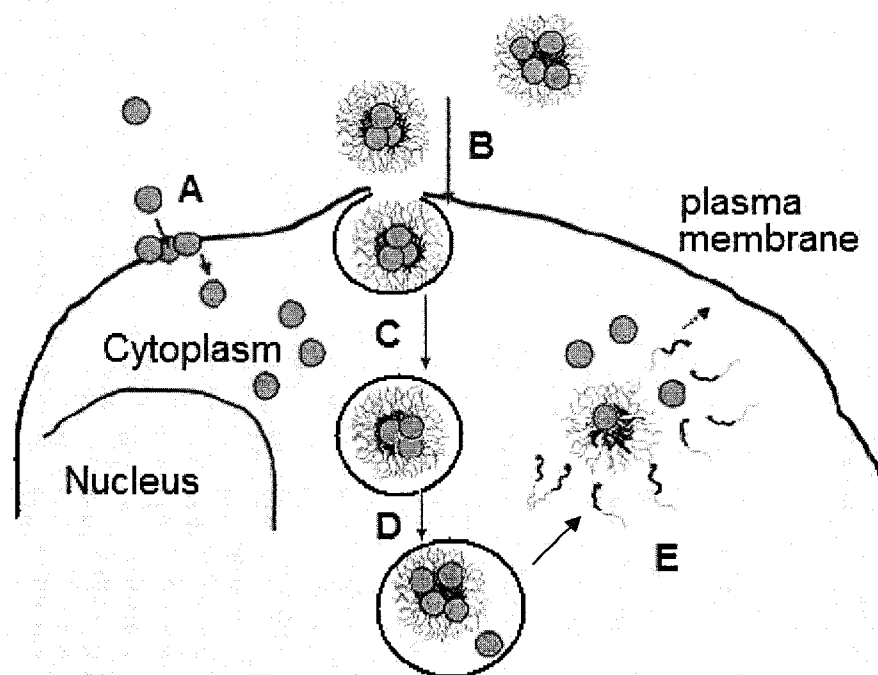


Figure 1.7- A proposed model for the cellular internalization of free fluorescent dye and dye incorporated in micelles. (A) Free dye diffuses first through the cell membrane and then enters the cytosol. (B) Dye loaded micelle enters the cytoplasmic compartment by endocytosis. (C) Trafficking of dye loaded micelles into endosome. (D) Localization of the dye loaded micelles into the acidic lysosomal compartment. (E) Drug/Dye molecule eventually diffuse out from the micelle and distribute through the cytoplasm (Adopted from ref. [140] with modification).

Polymeric micelles end up in the lysosome via endosome after internalization by endocytosis (Figure 1.7). In the endosomal compartment, the micellar carrier will be subjected to an acidic environment (typically pH 5.0 – 5.5) and degrading enzymes. Polymeric micelles containing pH responsive groups in their core structure were developed based on this explanation, where the acidic pH and harsh enzymatic environment in the lysosome can trigger drug release and micellar dissociation enabling effective drug access to its intracellular targets.

Significant attention has been focused on the improvement of the cellular internalization of the polymeric micelles. In this regard, various specific ligands, i.e., antibodies [143], sugar moieties [144], folate [68], peptides [145] and transferrin [146], have been attached to the micellar surface to improve the targeting of micelles and micelle-incorporated drugs since many target cells, over-express specific receptors on their surfaces. Cell membrane-penetrating peptides, such as TAT (*trans* activating transcriptional activator) peptide were also attached to polymeric micelles, which helps to translocate the carrier directly to cytosol circumventing endocytosis [147]. PIC micelles developed for the delivery of nucleic acid based drugs and genes, on the other hand, are expected to be able to escape endosomes, lysosomes and release their content in the cytosol [148]. Polycations with low pK_a value such as polyethyleneimine (PEI) (pK_a 5-6) by themselves have the ability to disrupt the endosomal membrane through proton sponge effect, where the protonation of PEI in the endosomal compartment (pH 5.0-5.5) causes osmotic swelling of the endosome, leading to the disruption of the endosomal membrane and the subsequent release of DNA or RNA into the cytoplasm [149-151]. Polyion block copolymers expected to form PIC micelles with DNA or RNA, protect them against nucleases and release them in cytoplasm for successful gene transfection.

1.5. Polymeric micelles for drug targeting

1.5.1. Physiological properties of tumor microvasculature and enhanced permeability

and retention (EPR) effect- Mammalian cells require oxygen and nutrients for survival.

Cells located within 100 to 200 μm of blood vessels are within the diffusion limit for oxygen and can receive adequate amount of oxygen. For multicellular organisms to grow beyond this size, they must recruit new blood vessels by vasculogenesis and angiogenesis. This process is regulated by a balance between pro- and anti-angiogenic molecules, and is derailed in various diseases, especially cancer [152, 153]. The tumor cells lying beyond 0.5 mm become profoundly hypoxic and suffer from lack of nutrients [154]. Hypoxic tumor cells upregulate the production of vascular endothelial growth factor (VEGF) and basic fibroblast growth factors (bFGF) [155]. These molecules are referred to as "direct" angiogenic growth factors and are considered key regulators of angiogenesis [156]. Secretion of these molecules in turn induce the expression of vascular endothelial growth factor receptor (VEGFR), basic fibroblast growth factor receptor (bFGFR) [155], and many other pro-angiogenic and vascular permeability factors such as; tumor necrosis factor- α (TNF- α), interleukin 8 (IL-8), matrix metalloproteinases (MMPs), bradykinin, prostaglandins (PGs), nitric oxide (NO), and peroxynitrite (ONOO^-) [157-159]. During sprouting angiogenesis, vessels initially dilate and become leaky in response to VEGF. Vascular endothelial cells (VECs) induced by the growth factors secrete proangiogenic factor Angiopoietin 2 (Ang 2) and MMPs into the surrounding matrix in the direction of the tumor. The action of Angiopoietin 1 (Ang 1) and junction molecules, VE-Cadherin (vascular endothelial-Cadherin) and platelet-endothelial cell-adhesion molecule (PECAM) which tighten the vessels is also stopped during angiogenesis. MMPs and Ang 2 mediate dissolution of the existing basement membrane and the interstitial matrix and prepare the way for vessel tube-formation towards the tumor.

VEGF, Ang1 and bFGF stimulate proliferation, migration and assembly of VECs and formation of new basement membrane [155, 160]. Once tumor blood supply is established, neoplastic growth progresses at a rapid rate.

Due to the abnormal angiogenesis, tumor vessels are immature, structurally and functionally abnormal. In contrast to normal vessels, tumor vasculatures are highly disorganized; vessels are tortuous and dilated, with uneven diameter, excessive branching and shunts. Consequently, tumor blood flow is chaotic and variable [161, 162]. As a consequence, areas of hypoxia and necrosis often develop distant from blood vessels (Figure 1.8 A-B). In terms of their ultrastructure, tumor vessels are also abnormal: their walls have numerous openings (endothelial fenestrae, vesicles and transcellular holes), widening inter-endothelial junctions, and a discontinuous or absent basement membrane (Figure 1.8 C-D). In addition, the endothelial cells are abnormal in shape, growing on top of each other and projecting into the lumen.

These defects make tumor vessels leaky [104, 163, 164]. However, the vascular permeability and angiogenesis depend on the type of tumor and the host organ where the tumor is growing. Intercellular gap size in certain tumor microvasculature ranges from 200 nm to 1.2 μm in diameter [104]. The pore size in some tumors is restricted to less than 100 nm [105]. On the contrary, in most healthy tissues, including connective tissue and tissues of the muscle, heart, brain, and lung, intercellular tight junctions result in openings of 2 nm. These openings can approach 6 nm in post-capillary venules and are considerably smaller than the size of macromoleucular nanocarriers [165].

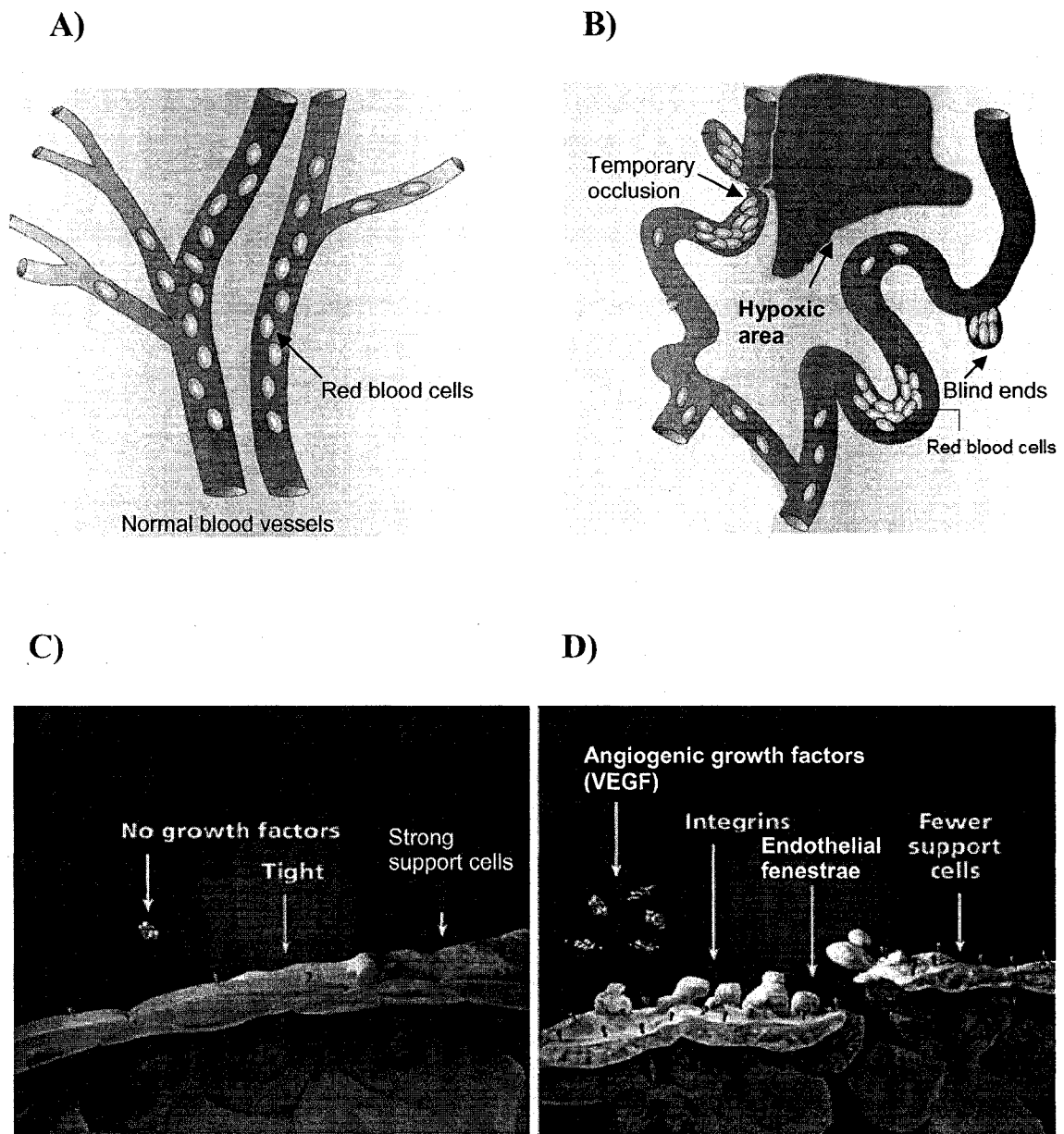


Figure 1.8- The vascular network in normal and tumor tissue: **A)** Normal tissues have relatively uniform and well-ordered blood vessels that are sufficiently close together to oxygenate all of the tissue, **B)** Blood vessels in tumors are tortuous, have incomplete vessel walls, have sluggish and irregular blood flow and have regions of hypoxia between the vessels, **C)** Structure of normal blood vessel, **D)** Structure of fenestrated, discontinuous vessels in tumor area (Adopted from ref. [162, 166] with modification).

The presence of leaky vasculature at tumor site facilitates the extravasation of nanocarriers in solid tumors. The permeated nanocarriers usually get trapped in tumor because the lymphatic system that drains fluids out of the organ is non-functional in tumors. This phenomenon, known as EPR effect is believed to be the reason for the passive accumulation of nano-carriers of < 200 nm with prolonged blood circulation properties (e.g. polymeric micelles and stealth liposomes) in solid tumors [16, 167, 168]. To date, there is firm evidence that polymeric micelles can exhibit enhanced accumulation in various types of human solid tumors by EPR effect [50, 169-171].

Despite the obvious advantage provided by leaky tumor vasculature, the distribution of nanocarriers inside tumors is heterogeneous with respect to tumor type, location of the vessel within the tumor, and the tumor microenvironment [104, 156]. Several investigators have shown that interstitial pressure in tumors is significantly higher than the normal tissue. Further, as tumor grows, interstitial pressure rises up to 30 mmHg, presumably because of the proliferation of tumor cells in a confined space and the absence of functioning lymphatic vessels, while the interstitial pressure in normal healthy tissue is 5-15 mm Hg. This increase in interstitial pressure also correlates with a reduction in tumor blood flow and the development of necrosis in a growing tumor [172]. Since the principal pathway for the movement of nanocarriers into the tumor interstitium is via extravasation through the discontinuous endothelium of the tumor microvasculature a decrease in fluid extravasation due to high tumor interstitial pressure may jeopardize the efficiency of passive drug targeting by nanocarriers [173, 174]. The small size of polymeric micelles may facilitate the extravasation of polymeric micelles at tumor site and ease further penetration of polymeric micelles within tumor tissue. Moreover, different active targeting strategies such as decoration of polymeric micelles with tumor specific ligands [175], or stimulus responsive

drug release [25] from the nanocarrier to tumor site may be applied to increase the bioavailability and facilitate the uniform distribution of polymeric micellar drugs to the more-difficult-to-reach cells within the solid tumor mass.

1.5.2. Polymeric micelles for passive drug targeting - Polymeric micelles are considered to be one of the most promising carriers for passive targeting by EPR in cancer, especially for hydrophobic drugs. In reality; however, to this point, only a few polymeric micellar formulations have demonstrated success in passive targeting of the incorporated drug to solid tumors [11]. The results of investigations on the development of polymeric micellar delivery systems for passive drug targeting are summarized in Table 1.1. The first attempt for the design of polymeric micellar system for targeted delivery of anticancer drugs has been made by Ringsdorf *et al* who prepared micelle forming block copolymer-drug conjugates of cyclophosphamide (CP) sulfide and PEO-*b*-PLL [176]. This formulation was found to be efficient in the stabilization of the active CP metabolite and caused a five-fold increase in the lifespan of mouse lymphocytic leukemia (L1210) tumor-bearing mice even at reduced CP-equivalent doses.

In 1987, Kataoka *et al* reported on the preparation of micelle-forming DOX conjugates of PEO-*b*-P(Asp). In biodistribution studies in solid tumor (C26 murine colon carcinoma) bearing mice, the delivery of DOX to the solid tumor was improved for PEO-*b*-P(Asp-DOX) micelles compared to the drug alone, and the tumor/heart selectivity of DOX was enhanced from 0.9 to 12 at 24 hour after i.v. injection [170]. Superior therapeutic efficacy of PEO-*b*-P(Asp-DOX) micelles over free drug was also achieved in C26 solid tumor bearing animal model, mainly, due to the decreased toxicity characterized by almost 20 times increase in DOX maximum tolerable dose (MTD) [129, 177]. In fact, careful

characterization of PEO-*b*-P(Asp-DOX) micelles revealed that it is the un-conjugated physically entrapped DOX that plays a significant role in the antitumor activity of this system [81]. This has led to the application of PEO-*b*-P(Asp-DOX) micelles as nanocontainer for physically encapsulated DOX [178]. This formulation, named as NK911, entered clinical trial in Japan in 2001 (Table 1.1) [179]. NK911 is one of the few polymeric micellar formulations that have shown a favorable pharmacokinetic and biodistribution pattern for passive drug targeting. Compared to free DOX, NK911 showed 28.9 fold higher AUC in plasma (within 24 h), higher tumor drug levels, less toxicity and superior *in vivo* activity in solid and hematological cancers in mice (Table 1.1) [180]. In human, NK911 exhibited only 2.5 fold increase in serum half-life and 2-fold increase in plasma AUC and changes in the pharmacokinetic parameters of DOX were not as impressive as liposomal formulation, DOXIL®. NK911 is currently under phase II clinical trial for the treatment of metastatic pancreatic cancer.

Kabanov *et al* reported development of Pluronic® micellar formulation of DOX for passive drug targeting of solid tumor [43]. DOX loaded Pluronic® micelles exhibited superior anti-tumor effect in the multi-drug resistant (MDR) tumor *in vitro* due to the increase in the influx of DOX, a reduction in drug efflux possibly due to ATP (adenosine triphosphate) depletion and changes in the intracellular trafficking of DOX in resistant tumor cells by block copolymer unimers [181]. Pluronic® formulations of DOX, known as SP1049C, entered preclinical and clinical trials in Canada in 1999 [182]. In phase I clinical trial, the pharmacokinetic profile of SP1049C was found similar to conventional DOX, with the exception of a slower terminal CL. The formulation was shown to be effective at inducing partial responses in several patients with advanced solid tumor although its effects were temporary. The results were considered to be promising, and a phase II clinical trial

was designed for the SP1049C formulation. An update of the phase II clinical trial was reported by Valle *et al* in 2004 [183]. This time the effect of SP1049C in patients with less severe forms of cancer was evaluated. Data from this study show the partial responses in some patients with the appearance of hematological and nonhematological signs of toxicity and a significant fall in left ventricular ejection fraction, a measure of cardiac function, in some patients.

Table 1.1. Polymeric micellar delivery systems in clinical trials.

Trade Name	Polymer Category	Incorporated drug	Progress	Most significant outcome	Ref.
NK911	PEO- <i>b</i> -PLAA	DOX	Phase II	Pharmacokinetic improvement and tumor accumulation in comparison to free drug in human, no significant benefit in comparison to DOXIL®	[180]
NK105	PEO- <i>b</i> -PLAA	PTX	Phase I	Improved tumor accumulation and anti-tumor activity in mice	[171]
NC6004	PEO- <i>b</i> -PLAA	CDDP	Phase I	Reduced nephrotoxicity and neurotoxicity in rats	[89]
SP1049C	Pluronic®	DOX	Phase II	Partial response in some patients	[182]
PAXCEED®	PEO- <i>b</i> -poly(ester)	PTX	Phase I/II	Increase in solubility, lower toxicity in mice, no pharmacokinetic improvement in mice	[184]
Genexol®-PM	PEO- <i>b</i> -poly(ester)	PTX	Phase II	Increase in solubility, lower toxicity in mice, no pharmacokinetic improvement	[185]

CDDP: Cisplatin; DOX: Doxorubicin; PEO: Polyethylene oxide; PLAA: Poly(L-amino acid); PTX: Paclitaxel

Development of polymeric micellar formulations for the delivery of PTX have been pursued by different research groups (Table 1.1). Both PEO-*b*-PDLLA and PEO-*b*-P(Asp) based micellar formulations of PTX were successful in increasing the water solubilized levels of PTX [171, 184]. However, except for the NK105 (PTX in PEO-*b*-poly(4-phenyl-1-butanoate L-aspartamide) micelles) other polymeric micelles failed to show any benefit over PTX commercial formulation, Taxol®, in terms of passive drug targeting. NK105 has shown 86-fold increase in PTX AUC in plasma, 86-fold decrease in CL and 15-fold decrease in Vd_{ss} compared to Taxol® after i.v. injection, which has resulted in a 25-fold increase in drug AUC in tumor and stronger anti-tumor activity in C-26 tumor bearing mice model [171, 186]. At PTX-equivalent dose of 100 mg/kg, a single administration of NK105 resulted in the disappearance of tumors and all mice remained tumor free thereafter. Due to promising pre-clinical results the formulation entered phase I clinical trial in Japan. Hamaguchi *et al* reported the result of phase I clinical trial and recommended for the design of phase II trial [187]. In phase I clinical trial, the pharmacokinetics of NK105 was found similar to the preclinical study exhibiting about 15-fold increase in plasma AUC, 26-fold decrease in CL and 13-fold decrease in Vd_{ss} compared to Taxol® after i.v. administration. The hematological and non hematological toxicities were mild and well managed, which offers advantage in terms of safety and patient convenience compared to Taxol®. In addition, the partial antitumor responses observed in 2 patients of metastatic pancreatic cancer and stomach cancer out of 6 patients is encouraging for further clinical evaluation.

The most recent polymeric micellar formulation that has entered clinical trials and shown impressive results in passive drug targeting is the PEO-*b*-PLAA based micellar formulation of CDDP. The PEO-*b*-p(Glu) formulation of CDDP, i.e., NC6004, has shown to increase the AUC (65 fold) and decrease the CL (19 fold) of the encapsulated drug in rats.

It also demonstrated a comparable or higher antitumor activity compared to free CDDP in MKN-4 (human gastric cancer cell) tumor bearing BALB/c nu/nu mice. Toxicity experiments in rats also revealed a potential for this formulation to control the nephrotoxic and neurotoxic effects of CDDP; however, signs of a transient hepatotoxicity was observed in the animals that received NC6004 [89].

1.5.3. Polymeric micelles for active drug targeting- Second generation of polymeric micelles for drug targeting, i.e., *polymeric micelles with tumor specific probes* or *polymeric micelles for stimuli-responsive targeting*, have been developed to increase their selectivity for target cells and insure effective intracellular drug delivery in diseased organ by the polymeric micellar carrier.

1.5.3.1. Ligand mediated targeting by polymeric micelles-

The delivery of micellar carrier to cancer cells or cancer associated tissue such as tumor vasculature can be selectively increased by decorating the micelles with molecules that bind to receptors that are either uniquely expressed or overexpressed on the target cells relative to normal cells. The over-expression of tumor associated antigen on cancer cells as well as high binding affinity of monoclonal antibodies (mAb)s to tumor specific antigens has provided the rational basis for the decoration of mAb decorated polymeric micelles, also termed as immunomicelles [74, 188]. Immunomicelles are usually developed through chemical conjugation of mAbs or the Fab fragments of antibodies to the functionalized shell forming block of polymeric micelles. Torchilin *et al* developed immunomicelles by chemical conjugation of 2C5 mAb (nucleosome-restricted specificity reactive towards a variety of different cancer cells) to the corona of p-nitrophenylcarbonyl-polyethylene oxide-phosphatidylethanolamine (pNP-PEO-PE) which exhibited higher drug accumulation in

LLC tumors in mice as well as higher therapeutic efficacy compared to free PTX and PTX loaded in plain micelles [143, 189]. Besides mAbs, several cell specific ligands such as carbohydrates [144], peptides [145], vitamins [190], and glycoproteins [191], which are selective for specific receptors on the cell surface have been under investigation to achieve active targeting by polymeric micelles. Carbohydrate receptors like asialoglycoprotein (ASGP) on hepatocytes and mannose receptors on kupffer and liver endothelial cells [192] are known to play a crucial role in biorecognition. Kataoka *et al* reported the formation of carbohydrate (lactose, galactose and mannose) decorated PEO-*b*- PDLLA [144, 193] and PEO-*b*-poly(2-(dimethylamino)ethyl methacrylate) (PEO-*b*-PAMA) block copolymers. Lactose modified PEO-*b*-PAMA complexed with plasmid DNA and demonstrated a significantly higher transfection efficiency compared to unmodified PIC micelles in HepG2 cells possessing ASGP receptors [87].

Folic acid (folate) has become an attractive ligand for targeting cancer cells because its receptor is overexpressed in many human cancers, including malignancies of the ovary, brain, kidney, breast, myeloid cells, and lung [194, 195]. Folate has been covalently attached to a wide variety of delivery systems such as liposomes, polymer conjugates and nanoparticles [196-198]. Recently, Park *et al* developed a mixed block copolymer micellar system composed of (folate-PEO-*b*-PLGA) and PEO-*b*-PLGA-DOX conjugates [68]. Folate conjugated micellar formulation was found to be more effective against human pharyngeal cancer cell line (KB cells) which express folate receptor in both *in vitro* and *in vivo* studies compared to unmodified micelles.

To ensure targeted delivery, the use of tumor specific peptide sequences has also been investigated. Gao *et al* developed cyclic pentapeptide C (Arg-Gly-Asp-d-Phe-Lys) (cRGDfK) bearing cRGDfK-PEO-*b*-PCL micelle with 76 % peptide density for DOX

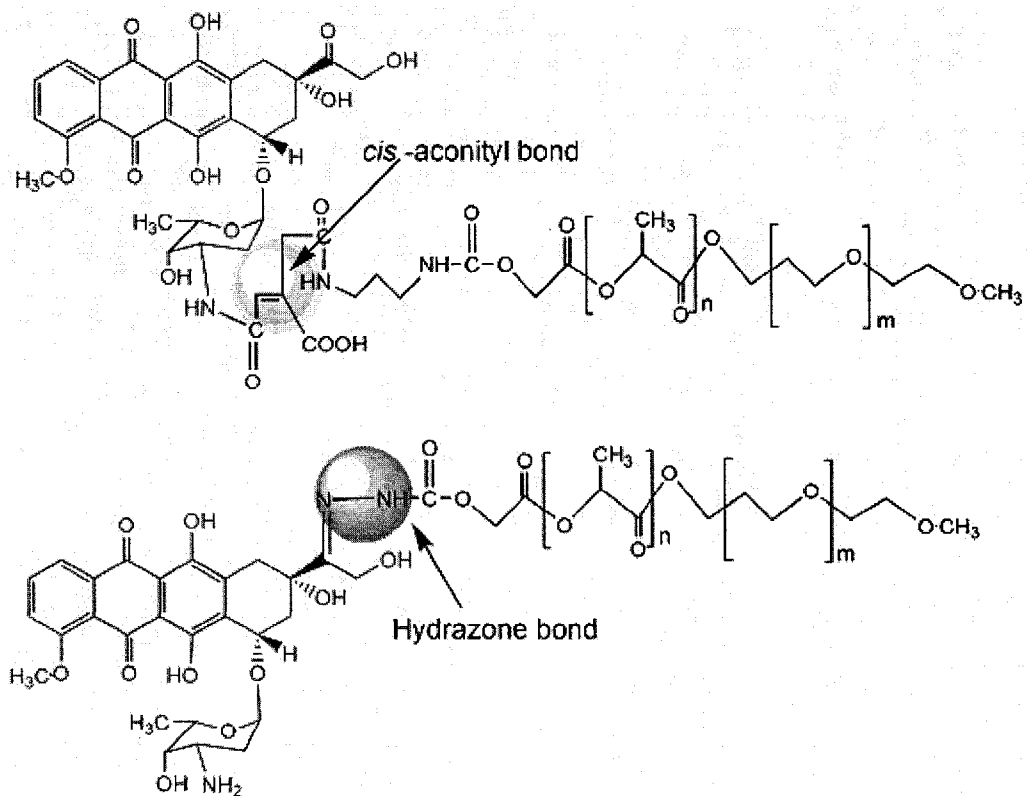
delivery that can selectively deliver hydrophobic drugs to angiogenic tumor endothelial cells that overexpressed $\alpha v\beta 3$ integrin [145]. Confocal laser scanning microscopy exhibited 30 times higher accumulation of cRGDfK modified micelles compared to unmodified micelles to human Kaposi's sarcoma tumor endothelial SLK cells. The internalization of encapsulated DOX was found to increase as the density of the conjugated peptide on micellar surface was raised. Recently, Xiong *et al* developed a relatively small internalizing linear peptide, GRGDS (Gly-Arg-Gly-Asp-Ser) modified PEO-*b*-PCL micelles and demonstrated enhanced accumulation of GRGDS modified micelles in mouse melanoma B16.F10 cells over expressing tumor specific integrin receptors [199].

1.5.3.2. pH responsive polymeric micelles for drug targeting-

Two strategies have been investigated to develop pH sensitive polymeric micellar nanocarrier by different groups. The first strategy involves the selective protonation of acid sensitive component of the block copolymers at acidic pHs. This strategy may be used to enhance intratumoral drug delivery since tumor environment is believed to be slightly acidic. In this category, the polymers mostly bear ionizable groups of a weak base. For instance, Bae *et al* constructed pH sensitive micelles from PEO-*b*-poly(L-histidine) (PEO-*b*-P(His)) block copolymer based on selective protonation of P(His) block which has a pK_a value similar to physiological pH. At physiological pH, deprotonated P(His) behaves as hydrophobic segment while at low pH(<7.0) it becomes hydrophilic due to protonation [200]. In *in-vivo* evaluation, DOX loaded PEO-*b*-P(His) micellar formulation demonstrated higher DOX level in the tumor as well as superior antitumor activity compared to free DOX in human ovarian A2780 tumor bearing mice [201].

The second strategy that is less explored involves the pH dependant cleavage of the chemotherapeutic agent from micellar nanoconjugates at the tumor extracellular or intracellular endosomal pH (Figure 1.9 A-B). One limiting factor in the application of this strategy is the requirement for the existence of functional groups on the drug molecule as well as on the polymer backbone. Park *et al* have developed one of the first pH sensitive micelle-forming drug conjugates through linking DOX to the terminal end of PEO-*b*-PLLA via two acid-cleavable bonds: a hydrazone bond between amino terminated PLLA and the ketone group of DOX or cis-aconityl bond between amino terminated PLLA and the amino group of glycosidyl residue on DOX (Figure 1.9 A) [66]. In *in vitro* cytotoxicity studies, micellar DOX conjugate bearing hydrazone linkage exhibited slightly higher cytotoxicity than free DOX against human lymphoblast HSB-2 cells after 48 hour incubation. Kataoka *et al* used a similar strategy and conjugated DOX to the carboxylic side chain of PEO-*b*-P(Asp) via hydrazone linkage forming PEO-*b*-P(Asp-Hyd-DOX) micelles (Figure 1.9 B) [202]. The release pattern of DOX below pH 5.5 was about 10 times higher compared to the release at pH 7.4 after 72 h. In *in vivo* biodistribution and antitumor efficacy study, PEO-*b*-P(Asp-Hyd-DOX) micelles clearly increased the MTD of DOX from 10 mg.kg⁻¹ to around 40 mg.kg⁻¹ in murine colon adenocarcinoma 26 (C26) bearing SPF-CDF1 mice. The pH-sensitive micellar DOX showed better efficacy (characterized by lower tumor volume) than free drug at corresponding MTD. At equal doses; however, micellar DOX was less effective than free drug [25].

A)



B)

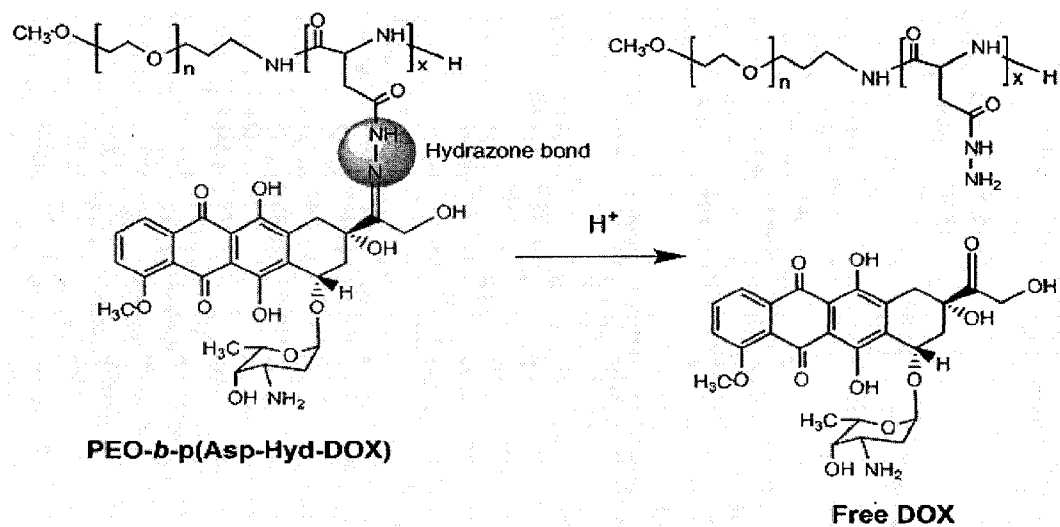


Figure 1.9- A) PEO-*b*-PLLA-DOX conjugate via hydrazone linkage and *cis*-aconityl linkage
 B) PEO-*b*-p(Asp-Hyd-DOX) conjugates with hydrazone acid liable bonds.

1.5.4. Multifunctional polymeric micelles for drug targeting- Multifunctional polymeric micelles are designed to bear a combination of structural components required for various targeting strategies on an individual carrier. This is expected to enhance the selectivity of the delivery system for the target site. Polymeric micelles with multiple ligands on the surface, block copolymers bearing a ligand and stimulus responsive moiety in their structure are example designs categorized under multifunctional polymeric micelles. Folate-PEO-*b*-p(Asp-Hyd-DOX) having cancer specific targeting ligand on the micelle surface and conjugated DOX through acid-cleavable bond in the core, developed by Kataoka and his group can be mentioned as an example of this category of polymeric micelles [25, 203]. Because folate-binding proteins (FBP) are selectively overexpressed on the cancer cell membranes, the folate-bound micelles can be guided to cancer cells in the body and internalized by cancer cells through receptor mediated endocytosis. After micellar entry to the cells, hydrazone bonds are cleaved by the intra-endosomal acidic environment. *In vitro* cytotoxicity study of folate-PEO-*b*-p(Asp-Hyd-DOX) micelles against FBP expressing KB cells after 24 h incubation exhibited equal cytotoxicity to free DOX. The cytotoxicity of this system was 8-fold higher than polymeric micellar DOX conjugates without folate modification. *In vivo* pharmacokinetic study in human KB tumor bearing mice did not show any significant difference in tumor accumulation of micelles before and after folate conjugation. This probably resulted from the increased accumulation in liver and non specific organ uptake of the folate modified micelles. Nevertheless, folate-conjugated micelles exhibited higher antitumor activity compared to unmodified micelles measured by decreased effective dose of DOX from 20 to 7.5 mg/kg which is even less than free DOX (10 mg/kg). The system maintained lower toxicity than free drug [204].

1.6. Model anticancer drugs under current study

1.6.1. Doxorubicin- DOX is an anthracycline antibiotic and one of the most important anti-cancer agents, widely used in the treatment of acute leukemias and malignant lymphomas as well as a number of solid tumors. It is isolated from cultures of a bacterium *Streptomyces peucetius* var. *caesius*. Unfortunately, the clinical use of DOX is limited by an unusual and potentially lethal cardiac toxicity. The chemical structure of DOX, i.e., (8S, 10S)-10-[(3-amino-2, 3, 6-trideoxy- α -L-lyxo-hexopyranosyl)oxy]-8-glycolyl-7, 8, 9, 10-tetrahydro-6, 8, 11-trihydroxy 1-methoxy-5, 12-naphthacenedione hydrochloride is shown in Figure 1.10. It has a molecular formula of $C_{27}H_{29}NO_{11}$. HCl and its molecular weight is 579.99. The anthracycline antibiotics have tetracycline ring structures with an unusual sugar, daunosamine moieties, attached by glycosidic linkage. Cytotoxic agents of this class all have quinone and hydroquinone moieties on adjacent rings that permit them to function as electron-accepting and donating agents. DOX is a 14-hydroxylated version of daunorubicin, the immediate precursor of DOX in its biosynthetic pathway. Daunorubicin is more abundantly found as a natural product because it is produced by a number of different wild type strains of *streptomyces*. The anthracycline ring of DOX molecule is lipophilic, but the saturated end of the ring system contains abundant hydroxyl groups adjacent to the amino sugar, producing a hydrophilic center. The molecule is amphoteric, containing acidic functions in the phenolic ring.

Studies have suggested that DOX may have at least two mechanisms of action that cause cellular damage. One mechanism involves generation of oxygen free radicals, the damage which is inhibited by free radical scavengers. This appears to play a major role in the development of cardiomyopathy by DOX [205-207]. DOX is highly reactive with metal ions such as Cu^{++} and Fe^{+++} . Following entry into the cell, free drug in the cytosol is thought to

bind ferric iron (DOX-Fe³⁺), which then generates highly reactive hydroxyl radical species (\bullet OH) by a one-electron reduction of the hydroxyquinone structure. The drug-iron complex binds to cell membranes and results in the conversion of the unsaturated fatty acids of the membranes to lipid peroxides causing oxidative cell damage; most tissues possess adequate defenses against this type of event in the form of super-oxide dismutase, glutathione, and so on and are able to repair the damage [207]. Cardiac tissue, however, is notably deficient in this respect and is highly vulnerable to oxidative attack. The cardiotoxicity caused by anthracyclines is not the result of a particular affinity for cardiac tissue but rather the result of a deficiency in host protective factors.

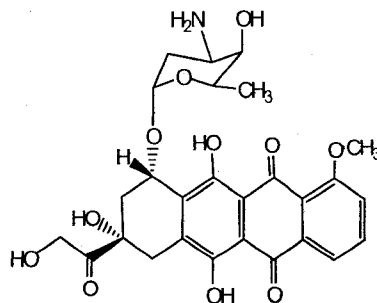


Figure 1.10- Chemical structure of doxorubicin

The other mechanism is mediated by the intercalation of the drug to DNA and is unaffected by free radical scavengers. This appears to be the major determinant of DOX cytotoxicity to tumor cells [207]. Interference with the action of DNA topoisomerase II in regions of transcriptionally active DNA is the most widely cited and generally accepted mechanism of action for the anthracyclines. This enzyme acts by binding to DNA and nicking one of its strands, thus allowing the supercoiled macromolecule to relax as the

opposite strand passes through the break. The enzyme then reanneals the broken ends. DOX is thought to act by stabilizing the topoisomerase-DNA complex in the cleaved configuration. This event not only maintains the single-strand breaks but also helps to create further double-strand breaks. During mitosis, topoisomerase II levels rise rapidly, and the cell becomes more vulnerable to the effects of DOX, thus possibly accounting for selective effects on rapidly dividing tumors.

In addition to nucleic acids and cellular membranes, the cytotoxic action by anthracyclines involves the cytoskeleton of both tumor cells and cardiomyocytes [208]. Cytoskeletal changes following DOX administration include reduction in the density of myofibrillar bundles [209], alterations on the Z-disc structure, and disarray and depolymerization of actin filaments [210]. Histologically, cytoplasmic vacuolization due to dilation of the sarcotubules and loss of myofibrils characterize DOX cardiomyopathy [211].

1.6.1.1. Commercial formulations of DOX

Doxorubicin is available commercially in two forms: traditional formulation and liposomal formulation. Traditional formulations, Adriamycin[®] (Pfizer) and Rubex[®] (Bristol-Myers Squibb) contain DOX.HCl for intravenous injection. Liposomal formulation, Doxil[®] manufactured by Alza corporation, United States contains DOX.HCl encapsulated in PEGylated (STEALTH[®]) liposome for intravenous administration which is the first and only liposomal cytotoxic agent approved to treat a solid tumor. The STEALTH[®] liposome carriers are composed of N-(carbonyl-methoxy poly(ethylene glycol) 2000)-1,2-distearoyl-sn-glycero-3-phosphoethanolamine (MePEG-DSPE), 3.19 mg/mL; hydrogenated soy phosphatidylcholine (HSPC), and cholesterol. Doxil[®] was originally approved in 1995 for the treatment of AIDS-related Kaposi's sarcoma. In June 29, 1999, the United States Food and

Drug Administration have approved Doxil[®] for the treatment of refractory ovarian cancer. Doxil[®] is indicated for women with ovarian cancer who have disease that is refractory to PTX and platinum-based chemotherapy regimens, which are current first-line therapies. Recently, Doxil[®] exhibited reduced cardiotoxicity and comparable efficacy compared to conventional DOX for first-line treatment of metastatic breast cancer in a phase III trial [212]. This liposomal formulation under the brand name of Caelyx[®] is marketed in Europe by Schering-Plough Corporation for the treatment of advanced ovarian cancer in women who have failed a first-line platinum-based chemotherapy regimen.

Myocet[®], manufactured by Elan Pharmaceuticals is DOX citrate encapsulated in liposomes (composed of egg phosphatidylcholine (EPC) and cholesterol) and which are not pegylated. Myocet[®] has been approved by the European and Canadian regulatory agencies for first line therapy in combination with cyclophosphamide for patients with metastatic breast cancer. Myocet[®], a less cardiotoxic, better tolerated and equally efficacious form of DOX extends the therapeutic options in the overall management of breast cancer.

1.6.1.2. Polymer conjugates of DOX in clinical trials

Conjugation of hydrophobic chemotherapeutic agents to hydrophilic polymers markedly improves their solubility. The application of macromolecular prodrug dramatically alters biodistribution of the therapeutic agents as well. Efforts in the 1970s and 1980s allowed rational design of the first polymer therapeutic candidates that later entered clinical testing. (N-(2-hydroxypropyl) methacrylamide) (HPMA) copolymer-Gly-Phe-Leu-Gly-DOX conjugates (PK1) (Mw: $\sim 30,000 \text{ g.mol}^{-1}$; drug content $\sim 8 \text{ wt}\%$) began phase I clinical trial in 1994 [213]. In phase I study, the MTD of PK1 was found to be 320 mg/m^2 , 4-5 times greater than the usual dose of DOX without any signs of cardiotoxicity. Activity was also

observed in chemotherapy-resistant patients; and doses as low as 80 mg/m² caused activity in patients with non-small-cell lung cancer (NSCLC), colorectal cancer and anthracycline-resistant breast cancer. Clinical pharmacokinetics showed prolonged plasma circulation ($t_{1/2\alpha}$ =1.8 h) compared to free DOX ($t_{1/2\alpha}$ =5 min), an absence of liver accumulation and significant renal elimination [213]. Phase II trials showed no activity in patients with colorectal cancer, but partial responses were observed in breast cancer and NSCLC. Another HPMA copolymer–Gly-Phe-Leu-Gly-DOX conjugate also contained galactosamine (PK2) as targeting ligand against hepatocyte ASGP receptor to treat primary liver cancer. In a phase I/II trial, this galactosamine-containing conjugate was found more toxic than the conjugate without galactosamine demonstrating MTD of 160 mg/m². Of the 23 patients treated who had primary hepatocellular carcinoma, two displayed partial responses, and a third showed a reduction in tumor volume [214]. Natural polymer dextran was thought to be a safer platform for the development of polymer-DOX conjugates. The starting dose of 40 mg/m² for dextran-DOX (AD-70, MWt. 70,000 gmol⁻¹) showed significant clinical toxicity i.e., thrombocytopenia and hepatotoxicity in phase I trial. Significant uptake by the MPS and dextran binding to platelet membranes were figured out as possible cause of severe toxicities. The recommended DOX equivalent dose for clinical phase II studies of this system was 12.5 mg/m².

1.6.1.3. Polymeric micellar formulations of DOX in clinical trials

Two formulations, NK-911, a micellar carrier of DOX composed of PEO-*b*-P(Asp-DOX) block copolymers containing physically encapsulated DOX; and SP1049C composed of Pluronic[®] (combination of L61 and F127) micellar formulation of DOX are in phase II clinical trials. In phase I clinical trial, NK-911 demonstrated a similar spectrum of toxicity

profile and recommended dose to that of free DOX. A comparison between pharmacokinetic parameters for NK-911 and liposomal formulation DOXIL[®] indicated a lower stability of NK-911 in the blood stream. However, infusion related reactions that occur after the administration of liposomal DOX were not seen for NK-911 [180]. A partial antitumor response observed in one patient with metastatic pancreatic cancer and toxicity profile recommends further clinical evaluation of NK-911. SP-1049C entered clinical trial in Canada in 1999. In phase I clinical trial, SP-1049C showed similar pharmacokinetic profile to that of conventional DOX and demonstrated temporary partial responses in several patients with advanced solid tumors [182]. In phase II clinical trials, the formulation showed partial responses in some patients. However, the results also showed the appearance of haematological and nonhaematological signs of toxicity and a significant fall in left ventricular ejection fraction, a measure of cardiac function, in some patients [183].

1.6.2. Cucurbitacin I

Cucurbitacins I (CuI) (Figure 1.11) is a potent anti-cancer agent with selective inhibitory effect on signal transducer and activator of transcription (STAT3) pathway [215, 216]. It belongs to a group of natural product called cucurbitacins, which are isolated from varieties of plant families such as cucurbitaceae and cruciferae. Cucurbitacins are divided into twelve categories, incorporating cucurbitacins A-T and structurally, they are characterized by the tetracyclic cucurbitane nucleus skeleton, namely, 19-(10→9b)-abeo-10alanost-5-ene (also known as 9b-methyl-19-nor lanosta-5-ene), with a variety of oxygenation functionalities at different positions (Figure 1.11) [217].

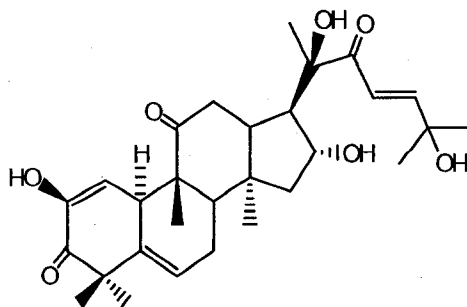


Figure 1.11 - Chemical structure of cucurbitacin I

Signal transducer and activator of transcription (STAT) proteins were originally discovered as latent cytoplasmic transcription factors a decade ago [218]. There are seven known mammalian STAT proteins, STAT 1, 2, 3, 4, 5a, 5b and 6, which are involved in cell proliferation, differentiation and apoptosis. STAT tyrosine phosphorylation is required for the biological function of STATs. This occurs when cytokines such as interleukin 6 (IL-6) and interferons or growth factors such as platelet-derived growth factor and epidermal growth factor bind their respective receptors, which results in STAT protein recruitment to the inner surface of the plasma membrane in the vicinity of the cytoplasmic portion of the receptors [219, 220].

Several lines of evidence have implicated the role of some STAT family members in malignant transformation and tumor cell survival. STAT3 involvement in oncogenesis is the most thoroughly characterized. Consideration of STAT3 as a target for anti-cancer drug design is based upon the findings that STAT3 is a critical mediator of oncogenic signaling. STAT3 is activated in many human cancers, including 82% of prostate cancers, 70% of breast cancers, more than 82% of squamous cell carcinoma of the head and neck, and 71% of nasopharyngeal carcinoma [221]. STAT3 participates in oncogenesis through up-

regulation of genes encoding apoptosis inhibitors (Bcl-xL, Mcl-1 and survivin), cell-cycle regulators (cyclin D1) and inducers of angiogenesis, vascular endothelial growth factor (VEGF) [221].

Cucurbitacins possess a broad range of potent biological activity derived largely from their cytotoxic properties. A number of compounds of this group have been investigated for their hepatoprotective, anti-inflammatory, anti-microbial and most importantly anti-cancer properties [217]. The molecular mechanism of the various biological activities of cucurbitacins has not been fully investigated. However, CuI was reported to reduce the levels of constitutively activated STAT3 in many cancer cells, and to reduce STAT3 DNA-binding activity and STAT3-mediated gene transcription [221]. It was found that CuI administration inhibited the growth of nude mice tumor xenografts including lung adenocarcinoma and breast cancer (MDA-MB-468) in which STAT3 is constitutively active, and significantly increased the survival duration of these mice [222]. Also, CuI has been shown to modulate tumor-induced immunosuppression and enhance anti tumor activity of cancer immunotherapy *in vivo* [222].

STAT3 inhibitory and potent anti-proliferative activity of CuI makes it excellent and novel drug candidate in cancer therapy. For the cytotoxic activity, cucurbitacins were a hot topic within the medicinal chemistry and drug discovery community from an anti-cancer drug development perspective, particularly in the 1960's. However, the application potential of CuI was substantially hindered due to its poor water solubility (0.05 mg/mL) and nonspecific toxicity [223]. Development of a suitable carrier might be able to increase the water solubility of the drug and overcome its nonspecific toxicity.

1.7. Thesis proposal

1.7.1. Rationale

Polymeric micelles prepared from amphiphilic block copolymers have been explored as delivery systems for the effective solubilization and controlled delivery of poorly water soluble drugs. Among different block copolymers designed for drug delivery, those with PEO as the shell forming block and PLAA or poly(ester) as the core forming block are of increasing interest. PLAA structures are advantageous over poly(ester)s due to the presence of free functional groups on the PLAA block which allows for core modification to achieve desired stability, drug loading and release properties. However, the biodegradability, long term biocompatibility and immunogenicity of PLAAs is still of concern. On the other hand, PEO-*b*-poly(ester) block copolymers have a history of safe application in human, but are less suitable for chemical engineering due to the lack of functional groups on the poly(ester) block. Introduction of functional groups to the poly(ester) segment of PEO-*b*-poly(ester) such as PEO-*b*-PCL may result in the development of biodegradable self assembling biomaterials with a potential for chemical engineering of the micellar core. Chemical tailoring of the core may modify the thermodynamic and kinetic stability, biodegradation, drug solubilization and release properties of PEO-*b*-PCL micelles. Such structures have a capacity for the covalent attachment of therapeutic agents, formation of hydrogen bonds with drugs that bear hydrogen binding groups and electrostatic interactions with therapeutic agents that carry charge. In addition, the superior hydrophobicity of PCL in comparison to PLAA based cores may induce greater tendency for micellization and results in improved thermodynamic stability for polymeric micelles. Finally, while the presence of hydrolysable PCL core in comparison to PLAAs is considered an important advantage in terms of biocompatibility and long term toxicity, it offers further potential for the development of

pH-responsive polymeric micellar drug conjugates and nanocontainers, since hydrolysis of PCL is catalyzed in acidic pH.

1.7.2. Hypothesis

Methoxy poly(ethylene oxide)-*block*-poly(ϵ -caprolactone) (MePEO-*b*-PCL) block copolymers with reactive groups on the PCL block can be synthesized and used to prepare polymeric micellar drug conjugates and nanocontainers for optimized solubilization and controlled delivery of model anticancer drugs.

1.7.3. Objective

1. To develop micelle-forming methoxy poly(ethylene oxide)-*block*-poly(ϵ -caprolactone) (MePEO-*b*-PCL) based block copolymers bearing functional groups on the PCL block.
2. To investigate the potential of functionalized MePEO-*b*-PCL block copolymers for the development of novel polymeric micellar-drug conjugates and micellar nanocontainer for the delivery of model anticancer drugs, i.e., DOX and CuI.

1.7.4. Specific aims

1. To optimize the synthesis of MePEO-*b*-PCL and assess the effect of PEO/PCL molecular weights on the relevant characteristics of MePEO-*b*-PCL micelles for drug delivery.
2. To synthesize MePEO-*b*-PCL block copolymers bearing functional side groups on the PCL block and characterize their self assembled structures.

3. To assess the potential of core functionalized self assembled structures for the preparation of novel polymeric micellar DOX conjugates and nanocontainers bearing hydrolysable cores and identify the best micellar design among developed structures for efficient DOX delivery.
4. To assess the effect of cholesteryl carboxylate substitution on the PCL block of MePEO-*b*-PCL for the solubilization and release of CuI from its polymeric micellar carrier.
5. To assess the effect of core shell structure in MePEO-*b*-PCL micelles on their extent, rate and mechanism of internalization by human cancer cells.

1.8. References

- [1] P. Couvreur, F. Puisieux, *Advanced Drug Delivery Reviews* 10 (1993) 141-162.
- [2] W. Morris, M.C. Steinhoff, P.K. Russell, *Vaccine* 12 (1994) 5-11.
- [3] Y. Tomii, *Current Pharmaceutical Design* 8 (2002) 467-474.
- [4] D.D. Lasic, *Nature* 380 (1996) 561-562.
- [5] I. Brigger, C. Dubernet, P. Couvreur, *Advanced Drug Delivery Reviews* 54 (2002) 631-651.
- [6] V. Omelyanenko, P. Kopeckova, C. Gentry, J. Kopecek, *Journal of Controlled Release* 53 (1998) 25-37.
- [7] G. Kwon, M. Naito, M. Yokoyama, T. Okano, Y. Sakurai, K. Kataoka, *Langmuir* 9 (1993) 945-949.
- [8] K. Kataoka, A. Harada, Y. Nagasaki, *Adv Drug Deliv Rev* 47 (2001) 113-131.
- [9] N. Nishiyama, K. Kataoka, *Nanostructured devices based on block copolymer assemblies for drug delivery: Designing structures for enhanced drug function, Polymer Therapeutics II: Polymers as Drugs, Conjugates and Gene Delivery Systems*, vol. 193, 2006, pp. 67-101.
- [10] A. Lavasanifar, J. Samuel, G.S. Kwon, *Advanced Drug Delivery Reviews* 54 (2002) 169-190.
- [11] H.M. Aliabadi, A. Lavasanifar, *Expert Opinion on Drug Delivery* 3 (2006) 139-162.
- [12] C. Allen, D. Maysinger, A. Eisenberg, *Colloids and Surfaces B-Biointerfaces* 16 (1999) 3-27.
- [13] G.S. Kwon, *Advanced Drug Delivery Reviews* 54 (2002) 167.
- [14] G. Gaucher, M.H. Dufresne, V. Sant, N. Kang, D. Maysinger, J. Leroux, *J Control Release* 109 (2005) 169-188.
- [15] H. Maeda, *Advanced Drug Delivery Reviews* 6 (1991) 181-202.
- [16] H. Maeda, *Advanced Drug Delivery Reviews* 46 (2001) 169-185.
- [17] D. Papahadjopoulos, T.M. Allen, A. Gabizon, E. Mayhew, K. Matthay, S.K. Huang, K.D. Lee, M.C. Woodle, D.D. Lasic, C. Redemann, F.J. Martin, *Proceedings of the National Academy of Sciences of the United States of America* 88 (1991) 11460-11464.
- [18] J.E. Chung, M. Yokoyama, T. Okano, *Journal of Controlled Release* 65 (2000) 93-103.
- [19] A. Lavasanifar, J. Samuel, G.S. Kwon, *J Control Release* 79 (2002) 165-172.
- [20] A. Mahmud, X.B. Xiong, A. Lavasanifar, *Macromolecules* 39 (2006) 9419-9428.
- [21] M. Yokoyama, S. Inoue, K. Kataoka, N. Yui, Y. Sakurai, *Makromol. Chem.* 8 (1987) 431 - 435.
- [22] Y. Li, G.S. Kwon, *Colloids and Surfaces. B, Biointerfaces* 16 (1999) 217-226.
- [23] M. Yokoyama, T. Okano, Y. Sakurai, S. Suwa, K. Kataoka, *Journal of Controlled Release* 39 (1996) 351-356.
- [24] M. Yokoyama, A. Satoh, Y. Sakurai, T. Okano, Y. Matsumura, T. Kakizoe, K. Kataoka, *J Control Release* 55 (1998) 219-229.
- [25] Y. Bae, N. Nishiyama, S. Fukushima, H. Koyama, M. Yasuhiro, K. Kataoka, *Bioconjug Chem* 16 (2005) 122-130.
- [26] J.C. Middleton, A.J. Tipton, *Biomaterials* 21 (2000) 2335-2346.

- [27] S. Gimenez, S. Ponsart, J. Coudane, M. Vert, *Journal of Bioactive and Compatible Polymers* 16 (2001) 32-46.
- [28] I.K.V. Ann-Christine Albertsson, *Biomacromolecules* 4 (2003) 1466-1486.
- [29] M. Yokoyama, *Critical Reviews in Therapeutic Drug Carrier Systems* 9 (1992) 213-248.
- [30] J. Young, A. Lovell, 2nd ed., Chapman & Hall, London, UK, 1991.
- [31] Z.S. Gao, A. Eisenberg, *Macromolecules* 26 (1993) 7353-7360.
- [32] J. Plestil, J. Baldrian, *Makromolekulare Chemie-Macromolecular Chemistry and Physics* 174 (1973) 183-191.
- [33] L.B. Alexandridis P, Elsevier 2000.
- [34] C. Tanford, *The hydrophobic effect: formation of micelles and biological membranes*, Wiley-Interscience, New York, 1980.
- [35] Z.K. Zhou, B. Chu, *Journal of Colloid and Interface Science* 126 (1988) 171-180.
- [36] M.L. Adams, A. Lavasanifar, G.S. Kwon, *J Pharm Sci* 92 (2003) 1343-1355.
- [37] S. Cammas, K. Suzuki, C. Sone, Y. Sakurai, K. Kataoka, T. Okano, *Journal of Controlled Release* 48 (1997) 157-164.
- [38] J.E. Chung, M. Yokoyama, T. Aoyagi, Y. Sakurai, T. Okano, *J Control Release* 53 (1998) 119-130.
- [39] T.P. Johnston, S.C. Miller, *J Parenter Sci Technol* 39 (1985) 83-89.
- [40] F. Quirion, S. St-Pierre, *Biophysical chemistry* 40 (1991) 129-134.
- [41] A.V. Kabanov, E.V. Batrakova, N.S. Meliknubarov, N.A. Fedoseev, T.Y. Dorodnich, V.Y. Alakhov, V.P. Chekhonin, I.R. Nazarova, V.A. Kabanov, *Journal of Controlled Release* 22 (1992) 141-157.
- [42] S.Y. Lin, Y. Kawashima, *Pharmaceutica acta Helvetiae* 60 (1985) 345-350.
- [43] E.V. Batrakova, T.Y. Dorodnych, E.Y. Klinskii, E.N. Kliushnenkova, O.B. Shemchukova, O.N. Goncharova, S.A. Ajakov, V.Y. Alakhov, A.V. Kabanov, *British Journal of Cancer* 74 (1996) 1545-1552.
- [44] D. Forster, C. Washington, S.S. Davis, *J Pharm Pharmacol* 40 (1988) 325-328.
- [45] P. Gaehtgens, K.U. Benner, *Acta Haematologica* 53 (1975) 82-89.
- [46] R. Hunter, F. Strickland, F. Kezdy, *J Immunol* 127 (1981) 1244-1250.
- [47] E.V. Batrakova, H.Y. Han, V. Alakhov, D.W. Miller, A.V. Kabanov, *Pharm Res* 15 (1998) 850-855.
- [48] E.V. Batrakova, H.Y. Han, D.W. Miller, A.V. Kabanov, *Pharmaceutical Research* 15 (1998) 1525-1532.
- [49] N. Nishiyama, K. Kataoka, *Journal of Controlled Release* 74 (2001) 83-94.
- [50] N. Nishiyama, S. Okazaki, H. Cabral, M. Miyamoto, Y. Kato, Y. Sugiyama, K. Nishio, Y. Matsumura, K. Kataoka, *Cancer Research* 63 (2003) 8977-8983.
- [51] S. Katayose, K. Kataoka, *Bioconjugate Chemistry* 8 (1997) 702-707.
- [52] K. Itaka, K. Yamauchi, A. Harada, K. Nakamura, H. Kawaguchi, K. Kataoka, *Biomaterials* 24 (2003) 4495-4506.
- [53] K. Kataoka, T. Matsumoto, M. Yokoyama, T. Okano, Y. Sakurai, S. Fukushima, K. Okamoto, G.S. Kwon, *J Control Release* 64 (2000) 143-153.
- [54] A. Lavasanifar, J. Samuel, S. Sattari, G.S. Kwon, *Pharmaceutical Research* 19 (2002) 418-422.
- [55] R. Gref, Y. Minamitake, M.T. Peracchia, V. Trubetskoy, V. Torchilin, R. Langer, *Science* 263 (1994) 1600-1603.

- [56] X. Zhang, J.K. Jackson, H.M. Burt, *International Journal of Pharmaceutics* 132 (1996) 195-206.
- [57] D.C. Kim, Y. Yoo, *Polymer-Korea* 21 (1997) 674-681.
- [58] S.Y. Kim, I.G. Shin, Y.M. Lee, C.S. Cho, Y.K. Sung, *Journal of Controlled Release* 51 (1998) 13-22.
- [59] C. Allen, J. Han, Y. Yu, D. Maysinger, A. Eisenberg, *Journal of Controlled Release* 63 (2000) 275-286.
- [60] H.M. Aliabadi, A. Mahmud, A.D. Sharifabadi, A. Lavasanifar, *J Control Release* 104 (2005) 301-311.
- [61] X. Shuai, H. Ai, N. Nasongkla, S. Kim, J. Gao, *J Control Release* 98 (2004) 415-426.
- [62] X. Shuai, T. Merdan, A.K. Schaper, F. Xi, T. Kissel, *Bioconjugate Chemistry* 15 (2004) 441-448.
- [63] C. Allen, Y. Yu, D. Maysinger, A. Eisenberg, *Bioconjugate Chemistry* 9 (1998) 564-572.
- [64] S.Y. Kim, I.G. Shin, Y.M. Lee, *Biomaterials* 20 (1999) 1033-1042.
- [65] H.S. Yoo, J.E. Oh, K.H. Lee, T.G. Park, *Pharm Res* 16 (1999) 1114-1118.
- [66] H.S. Yoo, E.A. Lee, T.G. Park, *J Control Release* 82 (2002) 17-27.
- [67] H.S. Yoo, K.H. Lee, J.E. Oh, T.G. Park, *Journal of Controlled Release* 68 (2000) 419-431.
- [68] H.S. Yoo, T.G. Park, *Journal of Controlled Release* 96 (2004) 273-283.
- [69] H. Bader, H. Ringsdorf, B. Schmidt, *Angewandte Makromolekulare Chemie* 123 (1984) 457-485.
- [70] M. Yokoyama, M. Miyauchi, N. Yamada, T. Okanao, Y. Sakurai, K. Kataoka, S. Inoue, *Journal of Controlled Release* 11 (1990) 269-278.
- [71] H.S. Yoo, T.G. Park, *Journal of Controlled Release* 70 (2001) 63-70.
- [72] Y. Li, G.S. Kwon, *Pharm Res* 17 (2000) 607-611.
- [73] N. Rapoport, *Colloids and Surfaces B: Biointerfaces* 16 (1999) 93-111.
- [74] A.V. Kabanov, V.P. Chekhonin, V. Alakhov, E.V. Batrakova, A.S. Lebedev, N.S. Melik-Nubarov, S.A. Arzhakov, A.V. Levashov, G.V. Morozov, E.S. Severin, et al., *FEBS Lett* 258 (1989) 343-345.
- [75] E.V. Batrakova, S. Li, D.W. Miller, A.V. Kabanov, *Pharmaceutical Research* 16 (1999) 1366-1372.
- [76] G.S. Kwon, M. Naito, M. Yokoyama, T. Okano, Y. Sakurai, K. Kataoka, *Pharmaceutical Research* 12 (1995) 192-195.
- [77] S.C. Kim, D.W. Kim, Y.H. Shim, J.S. Bang, H.S. Oh, S. Wan Kim, M.H. Seo, *J Control Release* 72 (2001) 191-202.
- [78] G. Kwon, M. Naito, M. Yokoyama, T. Okano, Y. Sakurai, K. Kataoka, *Journal of Controlled Release* 48 (1997) 195-201.
- [79] X. Zhang, H.M. Burt, D. Von Hoff, D. Dexter, G. Mangold, D. Degen, A.M. Oktaba, W.L. Hunter, *Cancer Chemother Pharmacol* 40 (1997) 81-86.
- [80] Piskin, X. Kaitian, E.B. Denkbaz, Z. Kucukyavuz, *J Biomater Sci Polym Ed* 7 (1995) 359-373.
- [81] M. Yokoyama, T. Okano, Y. Sakurai, K. Kataoka, *Journal of Controlled Release* 32 (1994) 269-277.

- [82] Y. Matsumura, M. Yokoyama, K. Kataoka, T. Okano, Y. Sakurai, T. Kawaguchi, T. Kakizoe, *Jpn J Cancer Res* 90 (1999) 122-128.
- [83] Y. Mizumura, Y. Matsumura, M. Yokoyama, T. Okano, T. Kawaguchi, F. Moriyasu, T. Kakizoe, *Jpn J Cancer Res* 93 (2002) 1237-1243.
- [84] N. Nishiyama, M. Yokoyama, T. Aoyaga, T. Okano, Y. Sakurai, K. Kataoka, *Langmuir* 15 (1999) 377-383.
- [85] X. Yuan, A. Harada, Y. Yamasaki, K. Kataoka, *Langmuir* 21 (2005) 2668-2674.
- [86] D. Wakebayashi, N. Nishiyama, K. Itaka, K. Miyata, Y. Yamasaki, A. Harada, H. Koyama, Y. Nagasaki, K. Kataoka, *Biomacromolecules* 5 (2004) 2128-2136.
- [87] D. Wakebayashi, N. Nishiyama, Y. Yamasaki, K. Itaka, N. Kanayama, A. Harada, Y. Nagasaki, K. Kataoka, *J Control Release* 95 (2004) 653-664.
- [88] Y. Kakizawa, A. Harada, K. Kataoka, *Journal of the American Chemical Society* 121 (1999) 11247-11248.
- [89] H. Uchino, Y. Matsumura, T. Negishi, F. Koizumi, T. Hayashi, T. Honda, N. Nishiyama, K. Kataoka, S. Naito, T. Kakizoe, *British Journal of Cancer* 93 (2005) 678-687.
- [90] A.V. Kabanov, S.V. Vinogradov, Y.G. Suzdaltseva, V. Alakhov, *Bioconjugate Chemistry* 6 (1995) 639-643.
- [91] A.V. Kabanov, V.A. Kabanov, *Advanced Drug Delivery Reviews* 30 (1998) 49-60.
- [92] M.A. Wolfert, E.H. Schacht, V. Toncheva, K. Ulbrich, O. Nazarova, L.W. Seymour, *Human Gene Therapy* 7 (1996) 2123-2133.
- [93] Y.I. Jeong, J.B. Cheon, S.H. Kim, J.W. Nah, Y.M. Lee, Y.K. Sung, T. Akaike, C.S. Cho, *J Control Release* 51 (1998) 169-178.
- [94] A. Lavasanifar, J. Samuel, G.S. Kwon, *Colloids Surf B Biointerfaces* 22 (2001) 115-126.
- [95] G.S. Kwon, T. Okano, *Advanced Drug Delivery Reviews* 21 (1996) 107-116.
- [96] G.S. Kwon, *Crit Rev Ther Drug Carrier Syst* 15 (1998) 481-512.
- [97] K. Kataoka, G.S. Kwon, M. Yokoyama, T. Okano, Y. Sakurai, *Journal of Controlled Release* 24 (1993) 119-132.
- [98] M. Yokoyama, T. Sugiyama, T. Okano, Y. Sakurai, M. Naito, K. Kataoka, *Pharmaceutical Research* 10 (1993) 895-899.
- [99] S. Cammas, T. Matsumoto, T. Okano, Y. Sakurai, K. Kataoka, *Materials Science & Engineering C-Biomimetic Materials Sensors and Systems* 4 (1997) 241-247.
- [100] R.L. Xu, M.A. Winnik, F.R. Hallett, G. Riess, M.D. Croucher, *Macromolecules* 24 (1991) 87-93.
- [101] S. Stolnik, L. Illum, S.S. Davis, *Advanced Drug Delivery Reviews* 16 (1995) 195-214.
- [102] D.C. Litzinger, A.M. Buiting, N. van Rooijen, L. Huang, *Biochim Biophys Acta* 1190 (1994) 99-107.
- [103] F. Yuan, M. Leunig, S.K. Huang, D.A. Berk, D. Papahadjopoulos, R.K. Jain, *Cancer Res* 54 (1994) 3352-3356.
- [104] S.K. Hobbs, W.L. Monsky, F. Yuan, W.G. Roberts, L. Griffith, V.P. Torchilin, R.K. Jain, *Proceedings of the National Academy of Sciences of the United States of America* 95 (1998) 4607-4612.
- [105] G. Kong, R.D. Braun, M.W. Dewhirst, *Cancer Research* 60 (2000) 4440-4445.

- [106] L.F. Zhang, A. Eisenberg, *Journal of the American Chemical Society* 118 (1996) 3168-3181.
- [107] L.F. Zhang, A. Eisenberg, *Polymers for Advanced Technologies* 9 (1998) 677-699.
- [108] L. Zhang, A. Eisenberg, *Science* 268 (1995) 1728-1731.
- [109] K. Yu, L.F. Zhang, A. Eisenberg, *Langmuir* 12 (1996) 5980-5984.
- [110] Y.S. Yu, L.F. Zhang, A. Eisenberg, *Langmuir* 13 (1997) 2578-2581.
- [111] L. Zhang, K. Yu, A. Eisenberg, *Science* 272 (1996) 1777-1779.
- [112] L.F. Zhang, A. Eisenberg, *Macromolecules* 29 (1996) 8805-8815.
- [113] J. Cornelissen, M. Fischer, N. Sommerdijk, R.J.M. Nolte, *Science* 280 (1998) 1427-1430.
- [114] J. Liu, Y. Xiao, C. Allen, *J Pharm Sci* 93 (2004) 132-143.
- [115] J.P.L. Dwan'Isa, L. Rouxhet, V. Preat, M.E. Brewster, A. Arien, *Pharmazie* 62 (2007) 499-504.
- [116] N. Nishiyama, F. Koizumi, S. Okazaki, Y. Matsumura, K. Nishio, K. Kataoka, *Bioconjugate Chemistry*. 14 (2003) 449-457.
- [117] T. Matsuya, S. Tashiro, N. Hoshino, N. Shibata, Y. Nagasaki, K. Kataoka, *Anal Chem* 75 (2003) 6124-6132.
- [118] A. Lavasanifar, J. Samuel, G.S. Kwon, *J Control Release* 77 (2001) 155-160.
- [119] P.A.J. Speth, Q. Vanhoesel, C. Haanen, *Clinical Pharmacokinetics* 15 (1988) 15-31.
- [120] T.M. Allen, P.R. Cullis, *Science* 303 (2004) 1818-1822.
- [121] H.M. Aliabadi, D.R. Brocks, A. Lavasanifar, *Biomaterials* 26 (2005) 7251-7259.
- [122] J.H. Senior, *Crc Critical Reviews in Therapeutic Drug Carrier Systems* 3 (1987) 123-193.
- [123] H.M. Patel, *Critical Reviews in Therapeutic Drug Carrier Systems* 9 (1992) 39-90.
- [124] D. Needham, T.J. McIntosh, D.D. Lasic, *Biochimica Et Biophysica Acta* 1108 (1992) 40-48.
- [125] A. Gabizon, D. Papahadjopoulos, *Biochimica Et Biophysica Acta* 1103 (1992) 94-100.
- [126] Y. Yamamoto, Y. Nagasaki, Y. Kato, Y. Sugiyama, K. Kataoka, *J Control Release* 77 (2001) 27-38.
- [127] M.C. Woodle, K.K. Matthay, M.S. Newman, J.E. Hidayat, L.R. Collins, C. Redemann, F.J. Martin, D. Papahadjopoulos, *Biochimica Et Biophysica Acta* 1105 (1992) 193-200.
- [128] H.M. Burt, X. Zhang, P. Toleikis, L. Embree, W.L. Hunter, *Colloids and Surfaces. B, Biointerfaces* 16 (1999) 161-171.
- [129] M. Yokoyama, T. Okano, Y. Sakurai, H. Ekimoto, C. Shibasaki, K. Kataoka, *Cancer Res* 51 (1991) 3229-3236.
- [130] G.S. Kwon, M. Yokoyama, T. Okano, Y. Sakurai, K. Kataoka, *Journal of Controlled Release* 28 (1994) 334-335.
- [131] G.S. Kwon, M. Yokoyama, T. Okano, Y. Sakurai, K. Kataoka, *Pharmaceutical Research* 10 (1993) 970-974.
- [132] C. Allen, Y. Yu, A. Eisenberg, D. Maysinger, *Biochimica et Biophysica Acta - Biomembranes* 1421 (1999) 32-38.

- [133] K. Sandvig, S. Olsnes, O.W. Petersen, B. Vandeurs, *Journal of Cell Biology* 105 (1987) 679-689.
- [134] S.H. Hansen, K. Sandvig, B. Vandeurs, *Journal of Cell Biology* 121 (1993) 61-72.
- [135] J.E. Heuser, *Journal of Cell Biology* 108 (1989) 401-411.
- [136] R.M. Steinman, I.S. Mellman, W.A. Muller, Z.A. Cohn, *The Journal of cell biology* 96 (1983) 1-27.
- [137] A.V. Kabanov, V.I. Slepnev, L.E. Kuznetsova, E.V. Batrakova, V.Y. Alakhov, N.S. Meliknubarov, P.G. Sveshnikov, V.A. Kabanov, *Biochemistry International* 26 (1992) 1035-1042.
- [138] L.B. Luo, J. Tam, D. Maysinger, A. Eisenberg, *Bioconjugate Chemistry* 13 (2002) 1259-1265.
- [139] A. Mahmud, A. Lavasanifar, *Colloids Surf B Biointerfaces* 45 (2005) 82-89.
- [140] R. Savic, L.B. Luo, A. Eisenberg, D. Maysinger, *Science* 300 (2003) 615-618.
- [141] T. Sakai, P. Alexandridis, *Langmuir* 21 (2005) 8019-8025.
- [142] S.N. Sidorov, L.M. Bronstein, Y.A. Kabachii, P.M. Valetsky, P.L. Soo, D. Maysinger, A. Eisenberg, *Langmuir* 20 (2004) 3543-3550.
- [143] V.P. Torchilin, A.N. Lukyanov, Z. Gao, B. Papahadjopoulos-Sternberg, *Proc Natl Acad Sci U S A* 100 (2003) 6039-6044.
- [144] Y. Nagasaki, K. Yasugi, Y. Yamamoto, A. Harada, K. Kataoka, *Abstracts of Papers of the American Chemical Society* 221 (2001) U434-U434.
- [145] N. Nasongkla, X. Shuai, H. Ai, B.D. Weinberg, J. Pink, D.A. Boothman, J.M. Gao, *Angewandte Chemie-International Edition* 43 (2004) 6323-6327.
- [146] S.V. Vinogradov, T.K. Bronich, A.V. Kabanov, *Bioconjug Chem* 9 (1998) 805-812.
- [147] E.V. Batrakova, S. Li, W.F. Elmquist, D.W. Miller, V.Y. Alakhov, A.V. Kabanov, *British Journal of Cancer* 85 (2001) 1987-1997.
- [148] V.A. Sethuraman, Y.H. Bae, *J Control Release* (2006).
- [149] O. Boussif, F. Lezoualch, M.A. Zanta, M.D. Mergny, D. Scherman, B. Demeneix, J.P. Behr, *Proceedings of the National Academy of Sciences of the United States of America* 92 (1995) 7297-7301.
- [150] S. Ferrari, E. Moro, A. Pettenazzo, J.P. Behr, F. Zacchello, M. Scarpa, *Gene Therapy* 4 (1997) 1100-1106.
- [151] K. Itaka, A. Harada, Y. Yamasaki, K. Nakamura, H. Kawaguchi, K. Kataoka, *Journal of Gene Medicine* 6 (2004) 76-84.
- [152] D. Hanahan, R.A. Weinberg, *Cell* 100 (2000) 57-70.
- [153] N. Bouck, V. Stellmach, S.C. Hsu, *Advances in cancer research* 69 (1996) 135-174.
- [154] J. Folkman, *Cancer research* 46 (1986) 467-473.
- [155] C.R. Dass, *Journal of Drug Targeting* 12 (2004) 245-255.
- [156] R.K. Jain, *Adv Drug Deliv Rev* 46 (2001) 149-168.
- [157] H. Maeda, *Advances in Enzyme Regulation* 41 (2001) 189-207.
- [158] J. Fang, T. Sawa, H. Maeda, *Advances in Experimental Medicine & Biology* 519 (2003) 29-49.
- [159] J. Folkman, M. Klagsbrun, *Science* 235 (1987) 442-447.
- [160] P. Carmeliet, R.K. Jain, *Nature* 407 (2000) 249-257.
- [161] J.W. Baish, R.K. Jain, *Cancer Res* 60 (2000) 3683-3688.

- [162] J.M. Brown, A.J. Giaccia, *Cancer Research* 58 (1998) 1408-1416.
- [163] H. Hashizume, P. Baluk, S. Morikawa, J.W. McLean, G. Thurston, S. Roberge, R.K. Jain, D.M. McDonald, *American Journal of Pathology* 156 (2000) 1363-1380.
- [164] H.F. Dvorak, J.A. Nagy, D. Feng, L.F. Brown, A.M. Dvorak, *Current topics in microbiology and immunology* 237 (1999) 97-132.
- [165] D.C. Drummond, O. Meyer, K. Hong, D.B. Kirpotin, D. Papahadjopoulos, *Pharmacol Rev* 51 (1999) 691-743.
- [166] P. Carmeliet, *Oncology* 69 (2005) 4-10.
- [167] H. Maeda, Y. Matsumura, *Critical Reviews in Therapeutic Drug Carrier Systems* 6 (1989) 193-210.
- [168] F.M. Muggia, *Clinical Cancer Research* 5 (1999) 7-8.
- [169] M. Yokoyama, T. Okano, Y. Sakurai, S. Fukushima, K. Okamoto, K. Kataoka, *Journal of Drug Targeting* 7 (1999) 171-186.
- [170] G. Kwon, S. Suwa, M. Yokoyama, T. Okano, Y. Sakurai, K. Kataoka, (1994).
- [171] T. Hamaguchi, Y. Matsumura, M. Suzuki, K. Shimizu, R. Goda, I. Nakamura, I. Nakatomi, M. Yokoyama, K. Kataoka, T. Kakizoe, *British Journal of Cancer* 92 (2005) 1240-1246.
- [172] R.K. Jain, *Cancer & Metastasis Reviews* 6 (1987) 559-593.
- [173] R.K. Jain, L.T. Baxter, *Cancer Research* 48 (1988) 7022-7032.
- [174] L.T. Baxter, R.K. Jain, *Microvascular Research* 37 (1989) 77-104.
- [175] D. Papahadjopoulos, D.B. Kirpotin, J.W. Park, K.L. Hong, Y. Shao, R. Shalaby, G. Colbern, C.C. Benz, *Journal of Liposome Research* 8 (1998) 425-442.
- [176] H. Ringsdorf, K. Dorn, G. Hoerpel, Plenum Press, New York. (1985) 531-585.
- [177] M.K. Yokoyama, T. Okano, Y. Sakurai, H. Ekimoto, K. Okamoto, H. Mashiba, T. Seto, K. Kataoka, *Drug Deliv* 1 (1993) 11-19.
- [178] M. Yokoyama, S. Fukushima, R. Uehara, K. Okamoto, K. Kataoka, Y. Sakurai, T. Okano, *Journal of Controlled Release* 50 (1998) 79-92.
- [179] T. Nakanishi, S. Fukushima, K. Okamoto, M. Suzuki, Y. Matsumura, M. Yokoyama, T. Okano, Y. Sakurai, K. Kataoka, *Journal of Controlled Release* 74 (2001) 295-302.
- [180] Y. Matsumura, T. Hamaguchi, T. Ura, K. Muro, Y. Yamada, Y. Shimada, K. Shirao, T. Okusaka, H. Ueno, M. Ikeda, N. Watanabe, *Br J Cancer* 91 (2004) 1775-1781.
- [181] A.V. Kabanov, E.V. Batrakova, V.Y. Alakhov, *Journal of Controlled Release* 91 (2003) 75-83.
- [182] S. Danson, D. Ferry, V. Alakhov, J. Margison, D. Kerr, D. Jowle, M. Brampton, G. Halbert, M. Ranson, *Br J Cancer* 90 (2004) 2085-2091.
- [183] J.W. Valle, J. Lawrance, J. Brewer, A. Clayton, P. Corrie, V. Alakhov, M. Ranson, *Journal of Clinical Oncology* 22 (2004) 362S-362S.
- [184] Angiotech Pharmaceuticals, Inc. website.
- [185] T.Y. Kim, D.W. Kim, J.Y. Chung, S.G. Shin, S.C. Kim, D.S. Heo, N.K. Kim, Y.J. Bang, *Clin Cancer Res* 10 (2004) 3708-3716.
- [186] T.Y. Kim, D.W. Kim, J.Y. Chung, S.G. Shin, S.C. Kim, D.S. Heo, N.K. Kim, Y.J. Bang, *Clinical Cancer Research* 10 (2004) 3708-3716.

- [187] T. Hamaguchi, K. Kato, H. Yasui, C. Morizane, M. Ikeda, H. Ueno, K. Muro, Y. Yamada, T. Okusaka, K. Shirao, Y. Shimada, H. Nakahama, Y. Matsumura, *Br J Cancer* 97 (2007) 170-176.
- [188] V.P. Torchilin, *J Control Release* 73 (2001) 137-172.
- [189] V.P. Torchilin, *Cell Mol Life Sci* 61 (2004) 2549-2559.
- [190] E.K. Park, S.Y. Kim, S.B. Lee, Y.M. Lee, *J Control Release* 109 (2005) 158-168.
- [191] S. Vinogradov, E. Batrakova, S. Li, A. Kabanov, *Bioconjug Chem* 10 (1999) 851-860.
- [192] G. Ashwell, J. Harford, *Annual Review of Biochemistry* 51 (1982) 531-554.
- [193] E. Jule, Y. Nagasaki, K. Kataoka, *Bioconjug Chem* 14 (2003) 177-186.
- [194] Y. Lu, P.S. Low, *J Control Release* 91 (2003) 17-29.
- [195] C.P. Leamon, J.A. Reddy, *Adv Drug Deliv Rev* 56 (2004) 1127-1141.
- [196] R.J. Lee, P.S. Low, *Biochim Biophys Acta* 1233 (1995) 134-144.
- [197] D. Goren, A.T. Horowitz, D. Tzemach, M. Tarshish, S. Zalipsky, A. Gabizon, *Clin Cancer Res* 6 (2000) 1949-1957.
- [198] J.A. Reddy, P.S. Low, *J Control Release* 64 (2000) 27-37.
- [199] X.B. Xiong, A. Mahmud, H. Uludag, A. Lavasanifar, *Biomacromolecules* (2007).
- [200] E.S. Lee, H.J. Shin, K. Na, Y.H. Bae, *J Control Release* 90 (2003) 363-374.
- [201] Z.G. Gao, D.H. Lee, D.I. Kim, Y.H. Bae, *Journal of Drug Targeting* 13 (2005) 391-397.
- [202] Y. Bae, S. Fukushima, A. Harada, K. Kataoka, *Angew Chem Int Ed Engl* 42 (2003) 4640-4643.
- [203] Y. Bae, W.D. Jang, N. Nishiyama, S. Fukushima, K. Kataoka, *Mol Biosyst* 1 (2005) 242-250.
- [204] Y. Bae, N. Nishiyama, K. Kataoka, *Bioconjugate Chemistry* 18 (2007) 1131-1139.
- [205] H.G. Keizer, H.M. Pinedo, G.J. Schuurhuis, H. Joenje, *Pharmacology & Therapeutics* 47 (1990) 219-231.
- [206] V. Lee, A.K. Randhawa, P.K. Singal, *American Journal of Physiology* 261 (1991) H989-H995.
- [207] C.E. Myers, W.P. McGuire, R.H. Liss, I. Ifrim, K. Grotzinger, R.C. Young, *Science* 197 (1977) 165-167.
- [208] A. Molinari, A. Calcabrini, P. Crateri, G. Arancia, *Experimental and Molecular Pathology* 53 (1990) 11-33.
- [209] R.S. Jaenke, *Laboratory Investigation* 30 (1974) 292-304.
- [210] W. Lewis, B. Gonzalez, *Laboratory Investigation* 54 (1986) 416-423.
- [211] O.J. Arola, A. Saraste, K. Pulkki, M. Kallajoki, M. Parvinen, L.M. Voipio-Pulkki, *Cancer Research* 60 (2000) 1789-1792.
- [212] M.E.R. O'Brien, N. Wigler, M. Inbar, R. Rosso, E. Grischke, A. Santoro, R. Catane, D.G. Kieback, P. Tomczak, S.P. Ackland, F. Orlandi, L. Mellars, L. Alland, C. Tendler, *Annals of Oncology* 15 (2004) 440-449.
- [213] P.A. Vasey, S.B. Kaye, R. Morrison, C. Twelves, P. Wilson, R. Duncan, A.H. Thomson, L.S. Murray, T.E. Hilditch, T. Murray, S. Burtles, D. Fraier, E. Frigerio, J. Cassidy, *Clinical Cancer Research* 5 (1999) 83-94.

- [214] L.W. Seymour, D.R. Ferry, D. Anderson, S. Hesslewood, P.J. Julyan, R. Poyner, J. Doran, A.M. Young, S. Burtles, D.J. Kerr, *Journal of Clinical Oncology* 20 (2002) 1668-1676.
- [215] M.A. Blaskovich, J. Sun, A. Cantor, J. Turkson, R. Jove, S.M. Sebti, *Cancer Res* 63 (2003) 1270-1279.
- [216] B. Jayaprakasam, N.P. Seeram, M.G. Nair, *Cancer letters* 189 (2003) 11-16.
- [217] J.C. Chen, M.H. Chiu, R.L. Nie, G.A. Cordell, S.X. Qiu, *Natural product reports* 22 (2005) 386-399.
- [218] J.E. Darnell, Jr., *Science* 277 (1997) 1630-1635.
- [219] L.M. Karnitz, R.T. Abraham, *Current opinion in immunology* 7 (1995) 320-326.
- [220] Z. Zhong, Z. Wen, J.E. Darnell, Jr., *Science* 264 (1994) 95-98.
- [221] N. Jing, D.J. Twardy, *Anticancer Drugs* 16 (2005) 601-607.
- [222] Y. Nefedova, S. Nagaraj, A. Rosenbauer, C. Muro-Cacho, S.M. Sebti, D.I. Gabrilovich, *Cancer research* 65 (2005) 9525-9535.
- [223] O. Molavi, A. Shayeganpour, V. Somayaji, S. Hamdy, D.R. Brocks, A. Lavasanifar, G.S. Kwon, J. Samuel, *Journal of Pharmacy and Pharmaceutical Sciences* 9 (2006) 158-164.

Chapter 2

Preparation and characterization of methoxy poly(ethylene oxide)-*b*-poly(ϵ -caprolactone) block copolymer micelles

A version of this Chapter has been published as part of: Hamidreza Montazeri Aliabadi, Abdullah Mahmud, Annahita Dehmoobed Sharifabadi, and Afsaneh Lavasanifar *Journal of Controlled Release* 104 (2005) 301-311.

2.1. Introduction

Self associating block copolymers of methoxy poly(ethylene oxide)-*block*-poly(ϵ -caprolactone) (MePEO-*b*-PCL) have been used extensively as a potential drug delivery vehicle [1-4]. The hydrophobic block of this copolymer, i.e., PCL, is a semicrystalline biodegradable polymer in solid state. Due to the biodegradability of the PCL homopolymer, it has been used both as a structural material in the production of medical devices, such as implants, sutures, stents, and prosthetics, and as delivery vehicles for the formation of polymeric micelles, nanoparticles, nanocapsules, and microsphere for a variety of drugs [1, 5-7]. The hydrophilic block, PEO is commonly used to impart biocompatibility and steric effect to the surface of many delivery systems [8, 9].

The traditional way of synthesizing poly(ester)s has been by polycondensation using diols and a diacid (or an acid derivative), or from a hydroxy acid. This method, however, needs high temperature, long reaction times and removal of reaction by-products, also, it is difficult to achieve high degree of polymerization [10]. In contrast, ring opening polymerization of lactones, cyclic diesters (lactides and glycolides), and cyclic ketene acetals can be used to yield high molecular mass polymers under relatively mild conditions [11, 12]. Synthesis of MePEO-*b*-PCL block copolymers may be achieved through ring opening polymerization of ϵ -caprolactone initiated with MePEO without any catalyst [13] or in the presence of catalysts [14-16]. The ring opening polymerization using catalysts has been reported to be conducted at different temperatures ranging from room temperature to 190 °C and various reaction time lengths from few minutes to several days depending on catalyst type, and reaction conditions [14, 16-19]. Different ring opening polymerization mechanisms such as free radical, anionic, carbocationic, zwitterionic, coordinative, or mechanisms based

on active hydrogen species have been reported in the literature [10, 12]. However, the highest yields and controlled molecular weights have been obtained mainly by the anionic and coordinative ring opening polymerization [10].

In this study, first, through changes in the reaction time and temperature, we tried to optimize the synthesis of MePEO-*b*-PCL using ring opening polymerization. In further studies, MePEO-*b*-PCL block copolymers of different length of PCL units were synthesized using the optimized synthetic procedure. The effect of PCL chain length on the physicochemical characteristics of MePEO-*b*-PCL nano-aggregates such as size, morphology, critical micellar concentration (CMC) and core viscosity of the prepared nanocarriers was measured by dynamic light scattering technique (DLS), transmission electron microscopy (TEM) and fluorescent probe techniques.

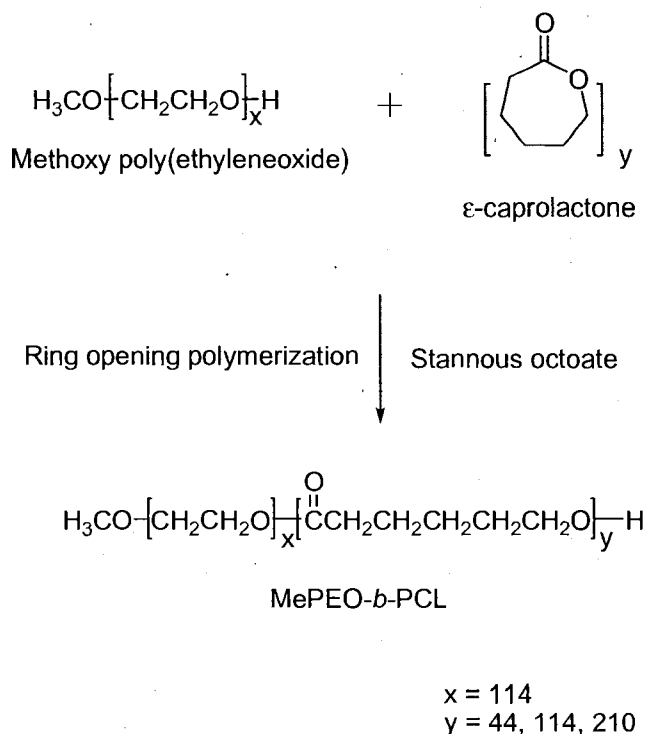
2.2 Experimental section

2.2.1. Materials- Stannous (II) 2-ethylhexanoate (stannous octoate) (96%) and biphenyl (99.5%) were obtained from Aldrich (Milwaukee, WI, USA). MePEO (average molecular weight of 5000 g.mol⁻¹), polystyrene standards, pyrene, and Cremophor EL were purchased from Sigma (St. Louis, MO). Chloroform was supplied by Fisher Scientific (Nepean, Ontario, Canada). 1,3-(1,1'-dipyrenyl)propane was purchased from Molecular Probes. ϵ -caprolactone was purchased from Lancaster Synthesis, UK. All other chemicals were reagent grade.

2.2.2. Synthesis and characterization of MePEO-*b*-PCL block copolymers- MePEO-*b*-PCL block copolymers were synthesized by ring opening polymerization of ϵ -caprolactone using MePEO (MW: 5000 g.mol⁻¹) as initiator and stannous octoate as catalyst (Scheme 2.1).

MePEO (5g), ϵ -caprolactone and stannous octoate were added to a previously flamed 10 mL ampoule, nitrogen purged, then sealed under vacuum. ^1H NMR spectrum of MePEO-*b*-PCL in deuterated chloroform (CDCl_3) was obtained by a 300 MHz, Bruker Unity-300 NMR spectrometer at room temperature and used to determine the number average molecular weight (M_n) of the block copolymers. The percentage of ϵ -caprolactone conversion to PCL was determined comparing peak intensity of -O-CH₂- (δ 4.223 ppm) for ϵ -caprolactone monomer to the intensity of the same peak for PCL (δ 4.075 ppm) in the ^1H NMR spectrum of MePEO-*b*-PCL. The effect of reaction time, temperature, and catalyst concentration on the percentage of ϵ -caprolactone conversion to PCL was assessed to optimize the conditions of the reaction further. Different ϵ -caprolactone to MePEO feed ratios were used to prepare MePEO-*b*-PCL block copolymers with varying degrees of ϵ -caprolactone polymerization. The reaction product was dissolved in chloroform, precipitated, and washed with an excess of cold methanol, followed by centrifugation. Comparison of peak intensity of MePEO (-CH₂CH₂O-, δ 3.65 ppm) to that of purified polymer PCL (-O-CH₂-, δ 4.075 ppm) provided an estimate for the degree of ϵ -caprolactone polymerization. The IR spectrum of MePEO-*b*-PCL block copolymer in CHCl_3 was obtained by preparing a thin film on sodium chloride disc using a FT-IR spectrometer (Nicolet Magna-IR[®] 550, USA). Prepared polymers were further characterized for their M_n and polydispersity (weight average molecular weight/number average molecular weight) (M_w/M_n) by gel permeation chromatography (GPC). Samples (20 μL from 10 mg/mL polymer stock solutions in tetrahydrofuran (THF) were injected into a 4.6 \times 300 mm Waters Styragel[®] HT4 column (Waters Inc., Milford, MA). The elution pattern was detected at 35°C by refractive index (PD2000, Percision Detectors, Inc.)/light scattering detectors (Model 410, Waters Inc). THF

was used as eluent at a flow rate of 1.0 mL/min. The column was calibrated with a series of standard polystyrenes of varying molecular weights (M_w : from 4750 g.mol⁻¹ to 13700 g.mol⁻¹).



Scheme 2.1- General reaction scheme for the synthesis of MePEO-*b*-PCL block copolymers through ring opening polymerization of ϵ -caprolactone by MePEO in the presence of stannous octoate.

2.2.3. Assembly of MePEO-*b*-PCL and Cremophor EL and characterization of associated structures- Assembly of block copolymers was achieved by co-solvent evaporation where MePEO-*b*-PCL (10 mg) dissolved in acetone (0.5 mL) was added in a drop wise manner (1 drop/ 15 sec) to stirring distilled water (1 mL). The remaining acetone was removed by evaporation at room temperature under vacuum. Average diameter (intensity mean) and size distribution of self assembled structures were estimated by dynamic

light scattering (DLS) technique (3000HS_A Zetasizer Malvern, Zeta-Plus™ zeta potential analyzer, Malven Instrument Ltd., UK) at a polymer concentration of 10 mg/mL in water at 25°C after filtration through 0.45 μm filters.

Morphology of self assembled structures was investigated by transmission electron microscopy (TEM). An aqueous droplet of micellar solution (20 μL) with a polymer concentration of 1-1.5 mg/mL was placed on a copper coated grid. The grid was held horizontally for 20 second to allow the colloidal aggregates to settle. A drop of 2 % solution of phosphotungstic acid (PTA) in PBS (pH=7.0) was then added to provide the negative stain. After 1 min, the excess fluid was removed by filter paper. The samples were then air dried and loaded into a Hitachi H 700 transmission electron microscope. Images were obtained at a magnification of × 18000 at 75 KV.

A change in the fluorescence excitation spectra of pyrene in the presence of varied concentrations of block copolymers was used to measure CMC of block copolymers. Pyrene was dissolved in acetone and added to 5 mL volumetric flasks to provide a concentration of 6×10^{-7} M in the final solutions. Acetone was then evaporated and replaced with aqueous block copolymer micellar solutions with concentrations ranging from 0.05 to 500 μg/mL. Samples were heated at 65°C for an hour, cooled to room temperature overnight, and deoxygenated with nitrogen gas prior to fluorescence measurements. The excitation spectrum of pyrene for each sample was obtained at room temperature using a Fluoromax DM-3000 spectrometer. The emission wavelength and excitation bandwidth were set at 390 and 4.25 nm, respectively. The intensity ratio of peaks at 337 nm to those at 333 nm was plotted against the logarithm of copolymer concentration to measure CMC. A sharp rise in

the intensity ratio of peaks at 337 nm to those at 333 nm from the excitation spectra of pyrene indicates the on-set of micellization for block copolymers.

The viscosity of the micellar cores was estimated by measuring excimer to monomer intensity ratio (I_e/I_m) from the emission spectra of 1,3-(1,1'-dipyrenyl)propane at 373 and 480 nm, respectively. 1,3-(1,1'-dipyrenyl)propane was dissolved in a known volume of chloroform to give a final concentration of 2×10^{-7} M. Chloroform was then evaporated and replaced with 5 mL of MePEO-*b*-PCL solutions at a concentration of 500 $\mu\text{g/mL}$. Samples were heated at 65°C for an hour and cooled to room temperature overnight. A stream of nitrogen gas was used to deoxygenate samples prior to fluorescence measurements. Emission spectrum of 1,3-(1,1'-dipyrenyl)propane was obtained at room temperature using an excitation wavelength of 333 nm, and an emission bandwidth was set at 4.25 nm [20]. The ratio of peak intensity from the excimer to monomer (I_e/I_m) was used to estimate the relative microviscosity of different polymeric micellar structures. Cremophor EL was used as a representative low molecular weight surfactant and micelles were prepared by direct drop-wise addition of the surfactant (300 mg) to distilled water (6 mL) under moderate stirring. The prepared surfactant micelles were characterized for their size using DLS technique at 50 mg/mL concentration. The CMC was determined at Cremophor EL concentrations ranging from 0.5 $\mu\text{g/mL}$ to 1000 $\mu\text{g/mL}$ and the core viscosity was estimated at a concentration of 5000 $\mu\text{g/mL}$ through fluorescent probe techniques as described for polymeric micelles.

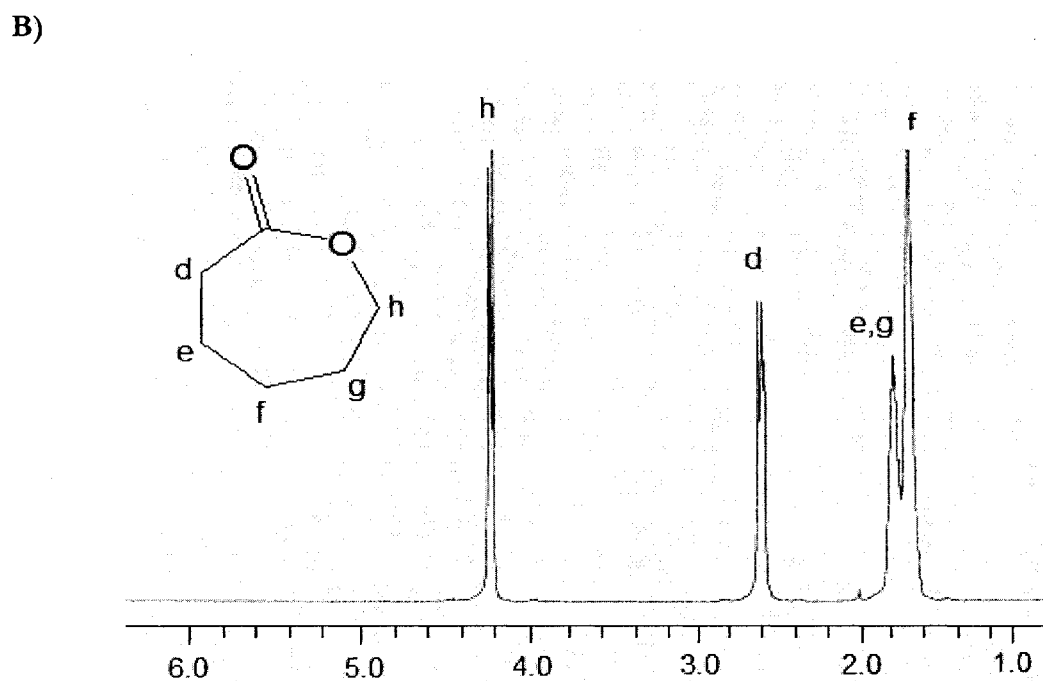
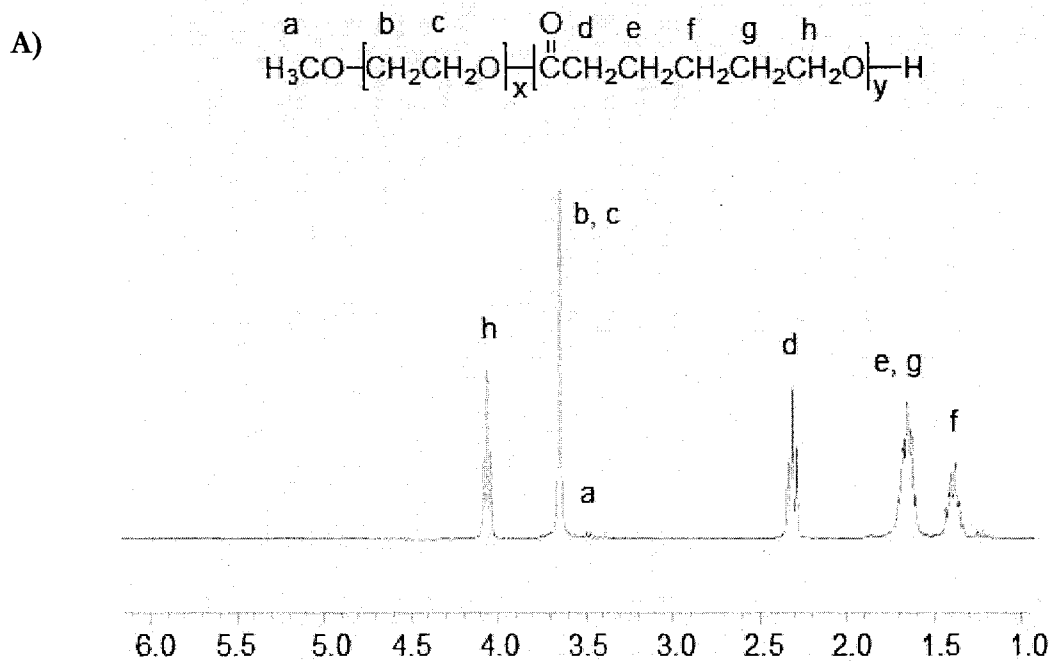
2.2.4. Statistical analysis- Data are reported as mean \pm standard deviation (S.D.). Differences among the mean of formulation characteristics for polymeric micelles were compared by Student's unpaired t-test assuming unequal variance.

2.3. Results

Synthesis of MePEO-*b*-PCL block copolymers through ring opening polymerization of ϵ -caprolactone by MePEO in the presence of stannous octoate has been reported previously [18]. In the present study to determine optimal conditions, the catalyst level and temperature of the reaction were altered and the amount of residual monomer in the reaction product was measured over time by ^1H NMR as described in section 2.2.2 (Figure 2.1 A). The ^1H NMR spectrum of MePEO-*b*-PCL block copolymer showed the presence of characteristic peaks at δ (ppm) 4.075 (tri, 2H); 3.65 (s, 4H); 2.32 (tri, 2H); 1.68 (m, 4H); 1.38 (m, 2H). The characteristic downfield shift of ϵ -caprolactone protons, i.e., h: δ 4.223 to 4.075; d: δ 2.6 to 2.32; e,g: δ 1.78 to 1.68; and f: δ 1.62 to 1.38 ppm in the ^1H NMR spectrum of PCL strongly indicates the ring opening polymerization of ϵ -caprolactone and formation of block copolymers (Figure 2.1 A and B). The IR spectrum of MePEO-*b*-PCL block copolymers (Figure 2.1 C) demonstrate the presence of characteristic sharp single peak at $1725\text{-}^1\text{cm}$ related to the carbonyl (C=O) group in the PCL block.

Figure 2.2 A illustrates the progress of polymerization for MePEO-*b*-PCL block copolymers synthesized with a catalyst to monomer molar ratio of 0.002 at temperatures ranging between 120-160°C. When reaction temperatures were set at 120, 140 and 160°C, the maximum conversion of ϵ -caprolactone to PCL was achieved at 6, 3 and 2 hours, respectively. The effect of catalyst concentration on the monomer to polymer conversion was assessed in a second experiment when the reaction temperature and time were set at 140°C and 4 hours, respectively. As shown in Figure 2.2 B, the highest conversion was achieved at catalyst to ϵ -caprolactone monomer molar ratios of more than 0.002. As a result,

applying a temperature of 140°C for 4 hrs and a catalyst to monomer ratio of 0.002 was chosen as an optimal condition for the preparation of MePEO-*b*-PCL block copolymers.



C)

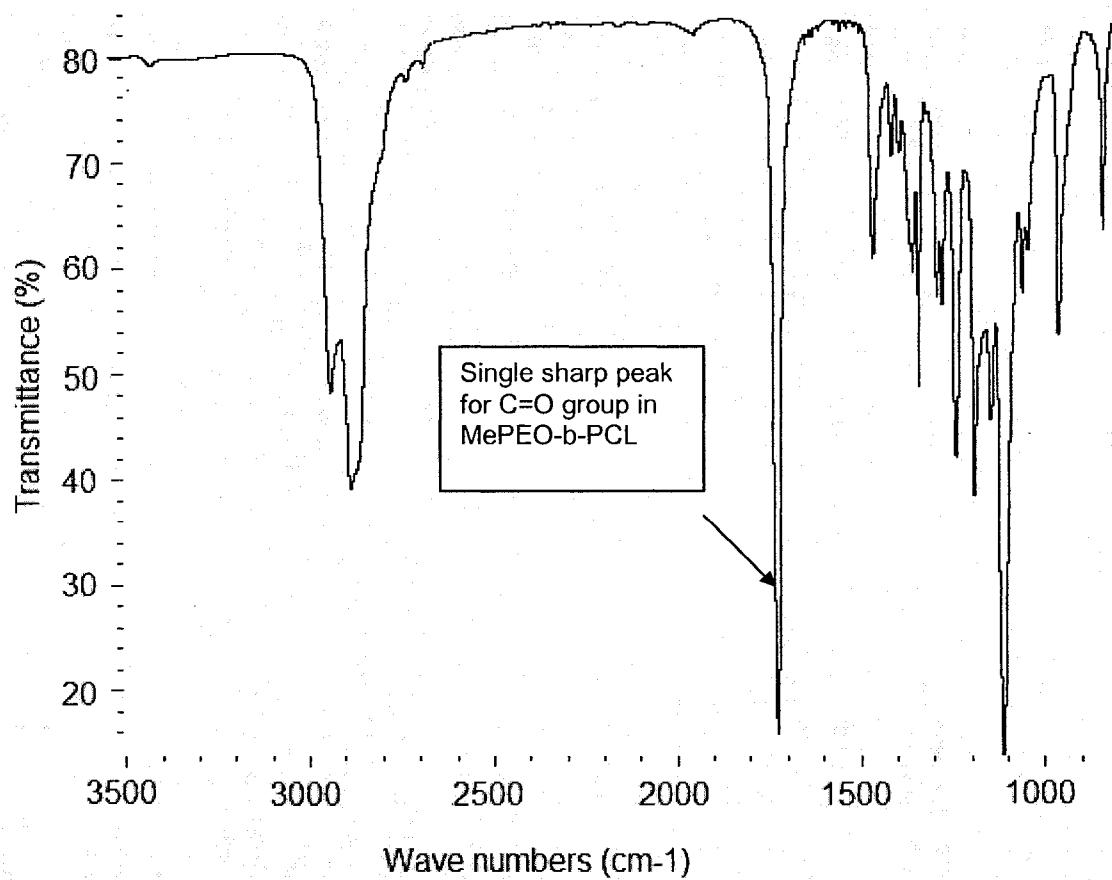
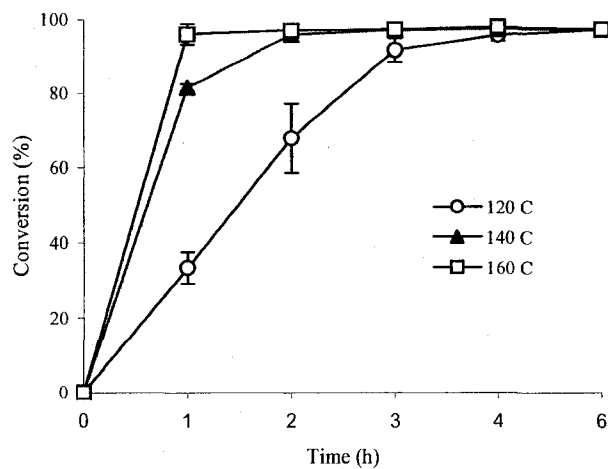


Figure 2.1- ^1H NMR spectrum and peak assignments of **A)** MePEO-*b*-PCL block copolymer and **B)** ϵ -Caprolactone monomer. The ^1H NMR spectra were obtained in CDCl_3 . **C)** IR spectrum of MePEO-*b*-PCL block copolymer. The IR spectrum was obtained by preparing a thin film of block copolymer on sodium chloride disc using a FT-IR spectrometer (Nicolet Magna-IR[®] 550, USA).

A)



B)

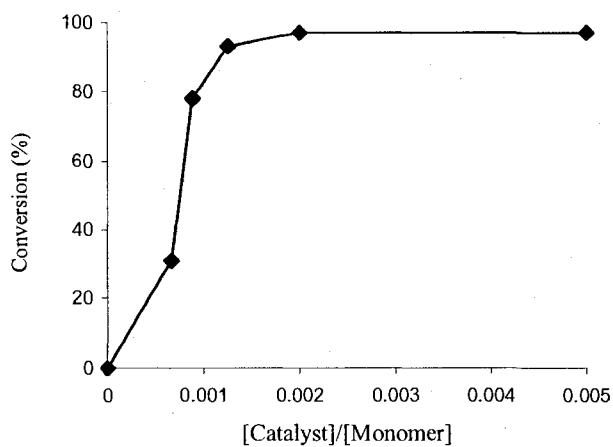


Figure 2.2- A) The effect of temperature on the percentage of ε-caprolactone conversion to PCL in the synthesis of MePEO-*b*-PCL di-block copolymers at a catalyst to monomer molar ratio of 0.002. **B)** The effect of catalyst concentration on the percentage of ε-caprolactone conversion to PCL in the synthesis of MePEO-*b*-PCL di block copolymer at 140 °C after 4 hours of reaction.

In the next step, the molar ratio of ϵ -caprolactone monomer to MePEO initiator (M/I) was changed to prepare MePEO-*b*-PCL block copolymers having different degrees of ϵ -caprolactone polymerization. Prepared block copolymers were characterized for their average molecular weights by ^1H NMR and GPC. Considering a MePEO molecular weight of $5000 \text{ g}\cdot\text{mol}^{-1}$, at M/I molar ratios of 44, 114 and 210, MePEO-*b*-PCL block copolymers with approximate PCL molecular weights of 5000, 13000 and $24000 \text{ g}\cdot\text{mol}^{-1}$ were synthesized. A nomenclature of 5000-5000, 5000-13000 and 5000-24000 in which the left and right number define the molecular weight of PEO and PCL respectively is used throughout this chapter to distinguish between the MePEO-*b*-PCL block copolymers with characteristics described in Table 2.1. As shown in Table 2.1, a good agreement between calculated and actual molecular weights was observed in most of the cases. Prepared block copolymers showed relatively narrow polydispersity (<1.065) (Table 2.1).

Table 2.1- Characteristics of the prepared MePEO-*b*-PCL block copolymers.

MePEO M wt. ($\text{g}\cdot\text{mol}^{-1}$)	PCL M wt. ($\text{g}\cdot\text{mol}^{-1}$) ^a	[M]/ [I] ^b	MePEO- <i>b</i> -PCL M_n^c	MePEO- <i>b</i> -PCL M_n^d	PEO- <i>b</i> -PCL PDI ^e
5000	5000	44	9825	11007	1.035
5000	13000	114	17318	23008	1.063
5000	24000	210	27800	30035	1.065

^a Theoretical molecular weight

^b Theoretical monomer to initiator molar ratios

^c Number average molecular weight (M_n) determined by ^1H NMR

^d Number average molecular weight (M_n) determined by GPC

^e Polydispersity index (M_w/M_n) determined by GPC

Self assembly of MePEO-*b*-PCL block copolymers was achieved by co-solvent evaporation method. Acetone was used as the organic co-solvent to dissolve the polymers and added to the aqueous phase at a defined organic:aqueous phase ratio of 1:2. The average size measured by DLS technique was found to be 68-99 nm for MePEO-*b*-PCL nanoassemblies of different PCL chain length (Table 2.2). In contrast, low molecular weight surfactant, Cremophor EL produced much smaller micelles with an average diameter of 11.3 nm. The TEM pictures of nanoassembled structures show the formation of true spherical micelles with a clear boundary for different MePEO-*b*-PCL block copolymers under study (Figure 2.3).

Table 2.2- Characteristics of Cremophor EL and MePEO-*b*-PCL micelles with different PCL molecular weights (n=3)

Amphiphilic agent	Micellar size ^a ± SD (nm)	PDI ^b	CMC ^c ± SD (μM)	I _c /I _m ^d ± SD
Cremophor EL	11.3 ± 0.2	0.108	397 × 10 ⁻² ± 0.15	0.43 ± .10
MePEO- <i>b</i> -PCL (5000-5000)	68.5 ± 2.0 [†]	0.198	18.2 × 10 ⁻² ± 0.01 [†]	0.19 ± .02 [†]
MePEO- <i>b</i> -PCL (5000-13000)	87.8 ± 5.4 [‡]	0.111	4.30 × 10 ⁻² ± 0.01 [‡]	0.11 ± .03
MePEO- <i>b</i> -PCL (5000-24000)	98.5 ± 3.5	0.119	1.80 × 10 ⁻² ± 0.01	0.13 ± .02

^a Intensity mean measured by DLS technique

^b Polydispersity index of size distribution estimated by DLS technique

^c Measured from the onset of a rise in the intensity ratio of peaks at 337 nm to peaks at 333 nm in the fluorescence spectra of pyrene plotted versus logarithm of polymer or Cremophor EL concentration.

^d Intensity ratio (excimer/monomer) from emission spectrum of 1,3-(1,1' dipyrenyl) propane in presence of polymeric or Cremophor EL micelles

[†] Significantly different from MePEO-*b*-PCL (5000-13000) and MePEO-*b*-PCL (5000-24000) (P<0.05)

[‡] Significantly different from MePEO-*b*-PCL (5000-24000) (P<0.05)

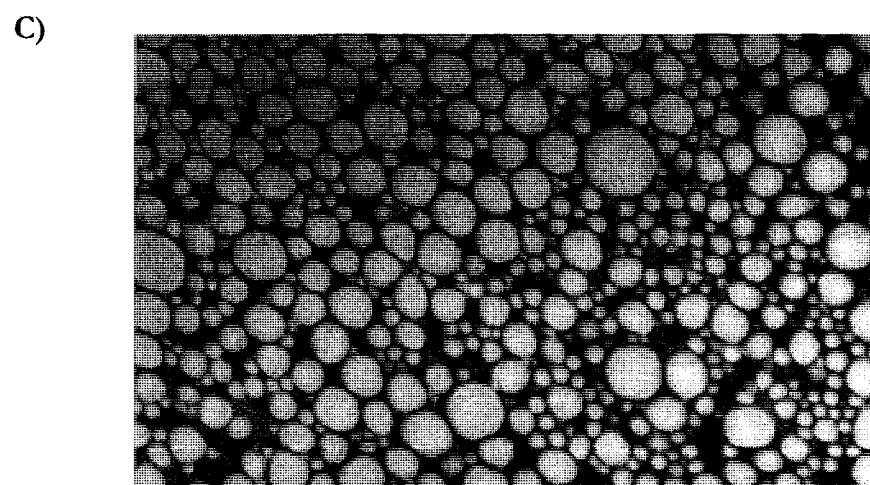
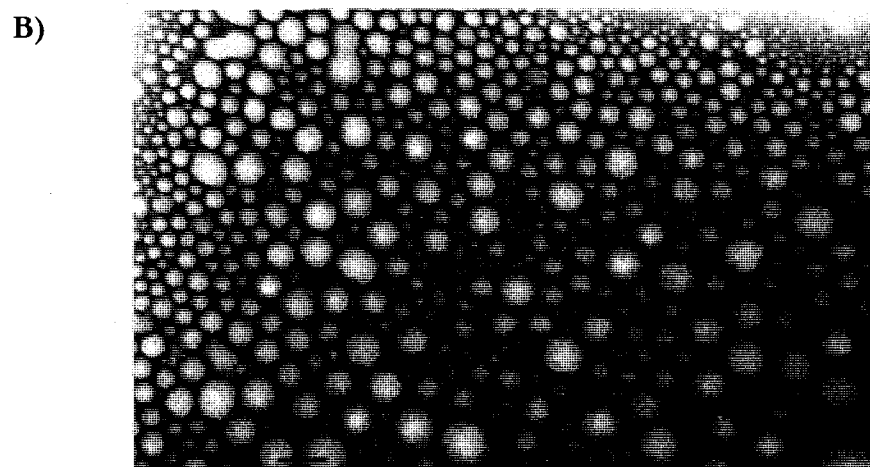
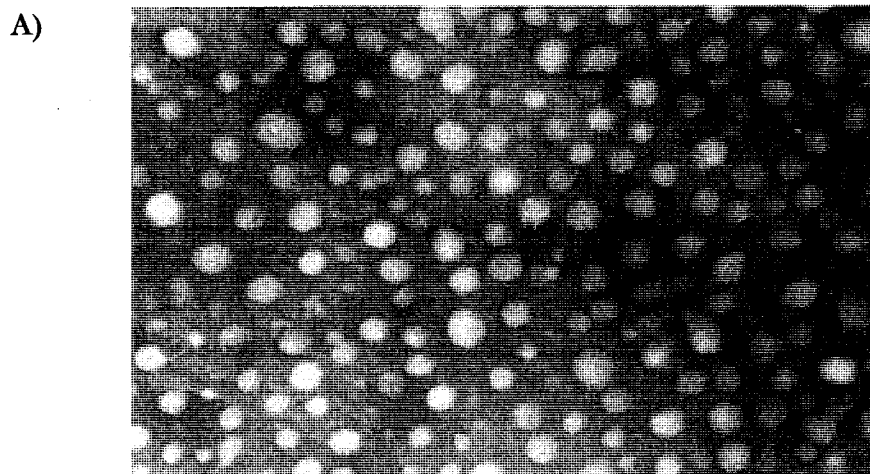


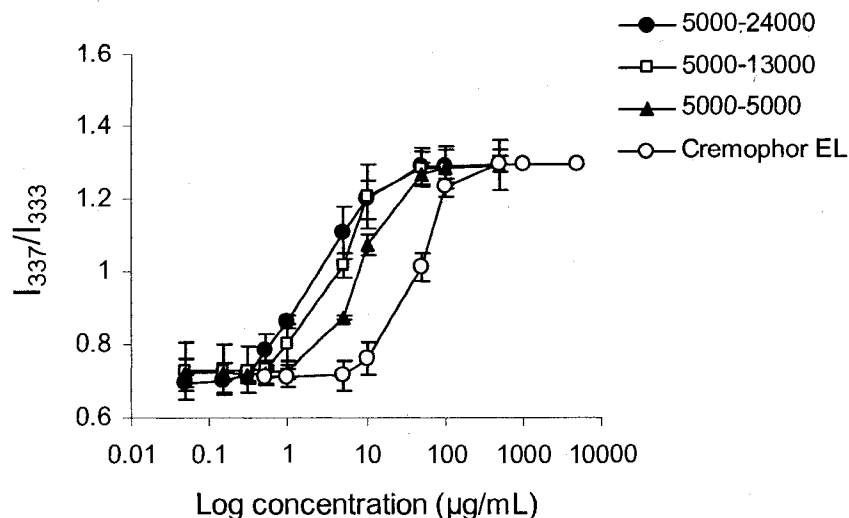
Figure 2.3- TEM pictures of colloidal particles assembled from MePEO-*b*-PCL block copolymers: **A)** 5000-5000, **B)** 5000-13000, **C)** 5000-24000 (magnification of 18000×6.1). The bar in the image represents 100 nm.

The CMC of MePEO-*b*-PCL micelles was determined using pyrene as fluorescent probe. Pyrene preferentially partitions into hydrophobic microdomains with a concurrent change in the molecule's photophysical properties. Using this method, the average CMC for MePEO-*b*-PCL block copolymers with varied PCL length under study ranged from 4.3×10^{-2} to 18.2×10^{-2} μM . Elongation of the PCL length from 5000 to 24000 was found to decrease the CMC values of MePEO-*b*-PCL micelles ($p < 0.05$, unpaired student's *t* test) (Table 2.2). For Cremophor EL, with pyrene as the fluorescent probe, the calculated CMC was observed at a much higher concentration (397×10^{-2} μM) compared to polymeric micelles (Table 2.2, Figure 2.4 A).

Evidence for the limited motion of MePEO-*b*-PCL micellar core was obtained from the fluorescence emission spectrum of 1,3-(1,1'-dipyrenyl)propane in the presence of polymeric micelles. Like pyrene, 1,3-(1,1'-dipyrenyl)propane is a hydrophobic fluorescent probe that preferentially partitions into the hydrophobic micro-domains of micelles at polymer concentrations above the CMC. By changing its conformation, 1, 3-(1,1'-dipyrenyl)propane forms intramolecular pyrene excimers that emit light at 480 nm when excited at 390 nm. Therefore, the ratio of the intensity of the light emitted from excited dipyrene excimer (I_e) to that of isolated pyrene monomer (I_m) in its emission spectrum could be used as a measure of effective viscosity (Figure 2.4 B). As shown in Table 2.2, I_e/I_m ratios are found to be very low (0.11-0.19) for all the copolymers under study, reflecting rigid structures for the polymeric micellar cores. In contrast, a high value of I_e/I_m ratio indicates the excimer formation in Cremophor EL micelles, which reflects the liquid like core of low molecular weight surfactant micelle. I_e/I_m ratios of dipyrene probe in the presence of 5000-13000 and 5000-24000 MePEO-*b*-PCL micelles was significantly lower than 5000-5000 MePEO-*b*-PCL

micelles ($p < 0.05$, unpaired student's t test) reflecting the presence of more rigid core in the micelles with longer hydrophobic blocks.

A)



B)

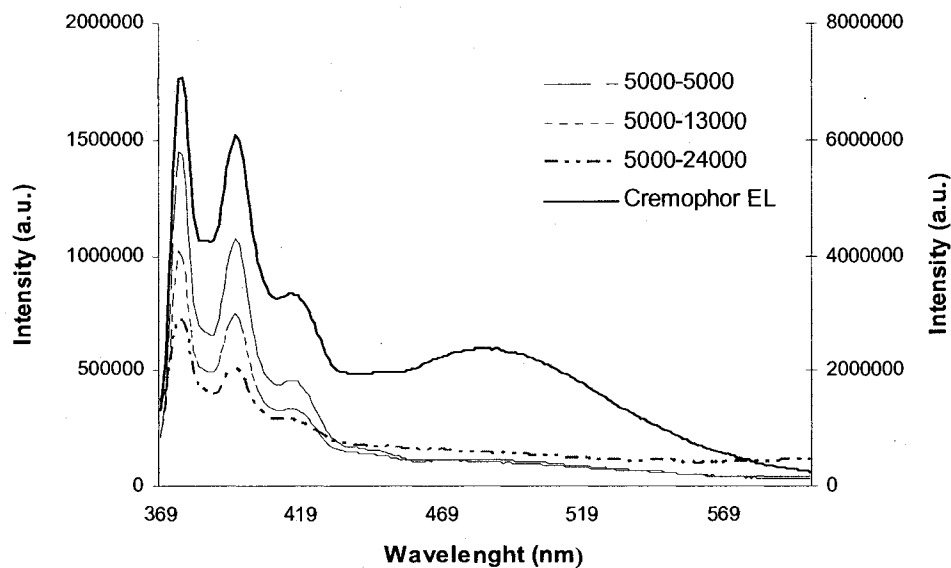


Figure 2.4- A) Intensity ratio (337 nm/333 nm) of pyrene ($6 \times 10^{-7} \text{M}$) from excitation spectrum as a function of block copolymer concentration. B) Fluorescence emission spectrum of 1,3-(1,1'-dipyrenyl)propane in micellar solutions of MePEO-*b*-PCL (different PCL chain lengths) in comparison to Cremophor EL as an indication of micellar core viscosity. No significant change in I_e/I_m ratios of dipyrrene probe was detected between micelles of 5000-13000 and 5000-24000 ($p > 0.05$, unpaired student's t test).

2.4. Discussion

It is known that amphiphilic block copolymers can form supramolecular core/shell structures in aqueous environment through the expulsion of their hydrophobic segments from water and further hydrophobic association of these blocks. Supramolecular self-assembled structures play an analogous role to natural carriers with several advantages such as possibility for chemical modifications, stability and safety [21, 22]. Compatibility between the solubilizate and the core forming block is proven to be necessary for efficient solubilization of poorly water soluble drugs in micellar systems [23-25]. To achieve optimized micellar properties and drug loading capacities we engineered the chemical structure of the core forming block in MePEO-*b*-PCL to different length of PCL chain. The purpose of the current study was to optimize the synthesis process of MePEO-*b*-PCL block copolymer and investigate the role of structural modifications on the key micellar properties, which determine the effectiveness of the drug delivery system.

Synthesis of MePEO-*b*-PCL having different lengths of PCL block was carried out through ring opening polymerization of ϵ -caprolactone using MePEO as initiator in the presence of stannous octoate as catalyst. Yuan *et al* have reported on the application of a similar process at a temperature of 140°C for 24 h [18]. In the present study, reaction conditions for the preparation of MePEO-*b*-PCL block copolymers through ring opening polymerization were optimized with respect to time, temperature and catalyst concentration. Inadequate time or temperature of the reaction in the ring opening polymerization of lactones may lead to the incomplete conversion of the monomer to polymer, whereas long reaction times or high temperatures may result in transesterification or back biting degradation of the polyester chain leading to an increase in the polydispersity of the prepared block copolymers [12, 17]. At a reaction temperature of 140°C and a reaction period of 4 h

(instead of 24 h) sufficient conversion of ϵ -caprolactone to PCL occurs (Figure 2.2 A). Block copolymers synthesized at this condition showed narrow polydispersity (Table 2.1), which indicates the absence of homopolymers and purity of the synthesized block copolymers. Narrow polydispersity of the synthesized block copolymers is a prerequisite for the preparation of micellar structure with unimodal size distribution. A reaction temperature of 160°C for 3 h was also shown to be sufficient for optimum conversion of ϵ -caprolactone to PCL (Figure 2.2 A). Stannous octoate is one of the most widely used compounds for initiating the ring opening polymerization of various lactones and lactides [26-29]. It produces polymers of high molecular weight with high yields [27, 30]. It is a very effective and versatile catalyst, which is easy to handle and is soluble in common organic solvents and lactones. The Food and Drug Administration has approved it as a food additive [12]. The ring opening polymerization reaction with stannous octoate is carried out in the presence of active hydrogen compounds. The polymerization mechanism with this catalyst is rather complex and several mechanisms have been proposed in the past [31-33]. Penczek and co-workers proposed that when stannous octoate is mixed with an initiator i.e., alcohol an initiating complex is formed prior to polymerization. The tin alkoxide complex initiates the polymerization reaction. The reaction is terminated by hydrolysis forming a hydroxyl end group [32]. However, the use of stannous octoate in ring opening polymerization can catalyze transesterification reactions of lactones and lactides [34]. It is extremely important to optimize the catalyst concentration in the polymerization reaction to minimize the residual heavy metals such as tin in biomedical intended for parenteral use. In this study, a catalyst to monomer molar ratio of 0.002 at temperatures 140 °C was found to be enough for optimum polymerization.

Prepared block copolymers were assembled to micellar structures by a co-solvent evaporation method and characterized for their functional properties in drug delivery. Self assembly of block copolymers may be accomplished through direct dissolution [35], solvent evaporation/film formation [36] or dialysis methods [37]. Direct dissolution and solvent evaporation/film formation were shown to be inappropriate methods for the self assembly of MePEO-*b*-PCL block copolymers, especially for those with long PCL chain lengths, because of the high hydrophobicity of the PCL which prevents the reconstitution or solubilization of the block copolymer. Preparation of MePEO-*b*-PCL micelles with low PCL molecular weights (1000-4000 g.mol⁻¹) through the evaporation of a co-solvent azeotrope (acetonitrile/water) has been reported by Jetta *et al* [38]. In the current study, an acetone/water co-solvent system has been used to match the higher hydrophobicity of the core-forming block (5000 to 24000 g.mol⁻¹). Recently, THF/water co-solvent systems have been used by Gao *et al* for the micellization of MePEO-*b*-PCL block copolymers having long PCL blocks (PCL molecular weights of 2500 to 24700 g.mol⁻¹) [14]. The acetone: water system may be beneficial in terms of scale-up because of a lower boiling point of acetone to THF, however.

A comparison between various studies on the preparation of MePEO-*b*-PCL micelles demonstrates that aside from block copolymer molecular weight other factors such as micellization procedure or solvent composition play a significant role in determining the average diameter and size distribution of assembled nano-carriers. Using acetone:water (1:2) system, MePEO-*b*-PCL block copolymers with a MePEO molecular weight of 5000 g.mol⁻¹ and PCL molecular weights of 5000 to 24000 g.mol⁻¹ produced polymeric micelles with an average diameter of 68-99 nm (Table 2.2). At a similar block copolymer molecular weight range, application of a THF: water (1:10) system has resulted in the formation of smaller

micelles (an average diameter of 41-86 nm). The difference in size is specially marked for self-assembled structures formed from 5000-5000 MePEO-*b*-PCL block copolymers (an average diameter of 41.0 nm for THF:water versus a diameter of 68.5 nm for acetone:water system). Although the size distribution of the self-assembled structures prepared from 5000-5000 MePEO-*b*-PCL micelles in the acetone:water co-solvent mixture in this study were unimodal, a higher polydispersity index (Table 2.2) might be an indication of a trend towards aggregate formation. Application of dialysis methods for the self-assembly of MePEO-*b*-PCL block copolymers having similar PCL chain lengths has resulted in the formation of larger particles, even when THF has been used as the selective solvent for the core-forming block in the micellization of MePEO-*b*-PCL [39].

Lower CMC values for block copolymers reflect reduced free energy of micellization for those polymers compared to Cremophor EL. A CMC value of 90 µg/mL (equivalent to 40.0 µM in molar concentration) for Cremophor EL has been reported in previous studies [40]. The fluorescent intensity ratio (I_{337}/I_{333}) of block copolymers was levelled off at an approximate concentration of 100 µg/mL (Figure 2.4 A), which is close to the reported CMC for Cremophor EL. Changes in the excitation spectrum of pyrene in the presence of Cremophor EL at levels below its reported CMC may be attributed to the interaction of fluorescent probe with surfactant unimers or the existence of premicellar aggregates. The lower CMCs reflect the thermodynamic stability of polymeric micellar structure, allowing a lower dose of injection to keep block copolymers above the CMC and in a micellar form upon dilution in blood after i.v. administration. The decrease in CMC values with increase of PCL block in MePEO-*b*-PCL micelles (Table 2.2) shows that elongation of hydrophobic PCL block makes self-association of block copolymers, thermodynamically, more favorable.

Very low I_c/I_m ratios (0.11 - 0.19) from the emission spectrum of 1,3-(1,1 dipyrenyl) propane for MePEO-*b*-PCL micelles reflects a high viscosity for the PCL core. Higher viscosity of the core in polymeric micelles compared to Cremophor EL micelles reflects higher kinetic stability that may postpone the dissociation of micellar structure into polymeric unimers below the CMC and restrict the diffusion of the encapsulated drug leading to sustained drug release properties from the micellar carrier. This is consistent with the results of previous studies that have shown lower CMC and higher core viscosity for PEO-*b*-poly[N-(6-hexyl stearate)-L-aspartamide] (PEO-*b*-PHSA) compared to sodium dodecyl sulfate (SDS) micelles [20]. SDS has higher CMC (8.7 mM) and less viscous core ($I_c/I_m=0.93$) compared to Cremophor EL micelles. Higher core viscosity of PEO-*b*-PCL micelles of 5000-13000 and 5000-24000 compared to 5000-5000 may be due to the enhanced hydrophobic interaction among long PCL chains in the micellar core.

2.5. Conclusion

The synthesis of MePEO-*b*-PCL was optimized in terms of time, temperature and catalyst concentration to prepare block copolymers with narrow polydispersity. The prepared micelles were found more thermodynamically and kinetically stable than low molecular surfactant micelles prepared from Cremophor EL. Thus, the MePEO-*b*-PCL micelles may serve as a better carrier than surfactant micelles for the solubilization of hydrophobic drugs and have the potential to alter the biodistribution of the incorporated drugs. Changes in the molecular weight of core forming block may be used to modify the relevant characteristics of MePEO-*b*-PCL micelles for drug delivery such as micellar size, CMC and core viscosity.

2.6. References

- [1] S.C. Woodward, P.S. Brewer, F. Moatamed, A. Schindler, C.G. Pitt, *J Biomed Mater Res* 19 (1985) 437-444.
- [2] W.J. van der Giessen, A.M. Lincoff, R.S. Schwartz, H.M. van Beusekom, P.W. Serruys, D.R. Holmes, Jr., S.G. Ellis, E.J. Topol, *Circulation* 94 (1996) 1690-1697.
- [3] J.K. Jackson, W. Min, T.F. Cruz, S. Cindric, L. Arsenault, D.D. Von Hoff, D. Degan, W.L. Hunter, H.M. Burt, *Br J Cancer* 75 (1997) 1014-1020.
- [4] P. Calvo, A. Sanchez, J. Martinez, M.I. Lopez, M. Calonge, J.C. Pastor, M.J. Alonso, *Pharmaceutical Research* 13 (1996) 311-315.
- [5] P. Calvo, J.L. VilaJato, M.J. Alonso, *Journal of Pharmaceutical Sciences* 85 (1996) 530-536.
- [6] S.Y. Kim, Y.M. Lee, H.J. Shin, J.S. Kang, *Biomaterials* 22 (2001) 2049-2056.
- [7] M. Berrabah, D. Andre, F. Prevot, A.M. Orecchioni, O. Lafont, *Journal of Pharmaceutical and Biomedical Analysis* 12 (1994) 373-378.
- [8] D.L. Elbert, J.A. Hubbell, *Annual Review of Materials Science* 26 (1996) 365-394.
- [9] J.H. Lee, H.B. Lee, J.D. Andrade, *Progress in Polymer Science* 20 (1995) 1043-1079.
- [10] A.C. Albertsson, I.K. Varma, *Aliphatic polyesters: Synthesis, properties and applications, Degradable Aliphatic Polyesters*, vol. 157, 2002, pp. 1-40.
- [11] X.D. Lou, C. Detrembleur, R. Jerome, *Macromolecular Rapid Communications* 24 (2003) 161-172.
- [12] A.C. Albertsson, I.K. Varma, *Biomacromolecules* 4 (2003) 1466-1486.
- [13] P. Cerrai, G.D. Guerra, L. Lelli, M. Tricoli, R.S. Delguerra, M.G. Cascone, P. Giusti, *Journal of Materials Science-Materials in Medicine* 5 (1994) 33-39.
- [14] X. Shuai, H. Ai, N. Nasongkla, S. Kim, J. Gao, *J Control Release* 98 (2004) 415-426.
- [15] C. Allen, Y. Yu, A. Eisenberg, D. Maysinger, *Biochimica et Biophysica Acta - Biomembranes* 1421 (1999) 32-38.
- [16] S.M. Li, H. Garreau, B. Pauvert, J. McGrath, A. Toniolo, M. Vert, *Biomacromolecules* 3 (2002) 525-530.
- [17] R.T. Liggins, H.M. Burt, *Adv Drug Deliv Rev* 54 (2002) 191-202.
- [18] M. Yuan, Y. Wang, X. Li, C. Xiong, X. Deng, *Macromolecules* 33 (2000) 1613-1617.
- [19] Z. Zhu, C. Xiong, L. Zhang, X. Deng, *Journal of Polymer Science: Part A: Polymer Chemistry* 35 (1997) 709-714.
- [20] A. Lavasanifar, J. Samuel, G.S. Kwon, *Colloids Surf B Biointerfaces* 22 (2001) 115-126.
- [21] G.S. Kwon, *Crit Rev Ther Drug Carrier Syst* 15 (1998) 481-512.
- [22] G.S. Kwon, T. Okano, *Pharm Res* 16 (1999) 597-600.
- [23] M. Yokoyama, A. Satoh, Y. Sakurai, T. Okano, Y. Matsumura, T. Kakizoe, K. Kataoka, *J Control Release* 55 (1998) 219-229.

- [24] M. Yokoyama, S. Fukushima, R. Uehara, K. Okamoto, K. Kataoka, Y. Sakurai, T. Okano, *Journal of Controlled Release* 50 (1998) 79-92.
- [25] R. Nagarajan, M. Barry, E. Ruckenstein, *Langmuir* 2 (1986) 210-215.
- [26] D.K. Gilding, A.M. Reed, *Polymer* 20 (1979) 1459-1464.
- [27] J. Dahlmann, G. Rafler, K. Fechner, B. Mehlis, *British Polymer Journal* 23 (1990) 235-240.
- [28] A.C. Albertsson, A. Lofgren, *Journal of Macromolecular Science-Pure and Applied Chemistry* A32 (1995) 41-59.
- [29] A. Kowalski, A. Duda, S. Penczek, *Macromolecular Rapid Communications* 19 (1998) 567-572.
- [30] H.R. Kricheldorf, I. Kreiseraunders, C. Boettcher, *Polymer* 36 (1995) 1253-1259.
- [31] J.W. Leenslag, A.J. Pennings, *Makromolekulare Chemie-Macromolecular Chemistry and Physics* 188 (1987) 1809-1814.
- [32] A. Kowalski, A. Duda, S. Penczek, *Macromolecules* 33 (2000) 689-695.
- [33] Y.J. Du, P.J. Lemstra, A.J. Nijenhuis, H.A.M. Vanaert, C. Bastiaansen, *Macromolecules* 28 (1995) 2124-2132.
- [34] M. Ryner, K. Stridsberg, A.C. Albertsson, H. von Schenck, M. Svensson, *Macromolecules* 34 (2001) 3877-3881.
- [35] C. Allen, D. Maysinger, A. Eisenberg, *Colloids and Surfaces B-Biointerfaces* 16 (1999) 3-27.
- [36] A. Lavasanifar, J. Samuel, G.S. Kwon, *J Control Release* 77 (2001) 155-160.
- [37] C. Allen, J. Han, Y. Yu, D. Maysinger, A. Eisenberg, *Journal of Controlled Release* 63 (2000) 275-286.
- [38] K.K. Jette, D. Law, E.A. Schmitt, G.S. Kwon, *Pharm Res* 21 (2004) 1184-1191.
- [39] S.Y. Kim, I.G. Shin, Y.M. Lee, C.S. Cho, Y.K. Sung, *Journal of Controlled Release* 51 (1998) 13-22.
- [40] D. Kessel, *Photochemistry & Photobiology* 56 (1992) 447-451.

Chapter 3

Synthesis and Characterization of novel self associating methoxy poly(ethylene oxide)-*b*-poly(ϵ -caprolactone) block copolymers with functional side groups on the polyester block for drug delivery

A version of this Chapter has been published: Abdullah Mahmud, Xiao-Bing Xiong, and Afsaneh Lavasanifar, *Macromolecules*; 39 (2006) 9419-9428.

3.1. Introduction

Among different amphiphilic block copolymers designed for the preparation of polymeric micelles, those containing poly(ester) as the core-forming block are considered promising due to their superior hydrophobic nature and excellent biodegradability and biocompatibility[1-4]. However, the application potential of this class of block copolymer was limited due to the lack of functional groups in their structure. In this context, block copolymers containing poly(L-amino acid)s (PLAA)s are advantageous over poly(ester)s due to the presence of free functional groups in their structure which allow them to engineer the core structure to achieve desired micellar properties for drug delivery application. Through chemical engineering of the PLAA core in poly(ethylene oxide)-*block*-poly(L-amino acid) (PEO-*b*-PLAA) based micelles, desired properties for the delivery of doxorubicin (DOX) [5, 6], amphotericin B [7], methotrexate [8], cisplatin [9] and KRN-5500 [10] has been achieved.

Introduction of functional groups to the poly(ester) segment of poly(ethylene oxide)-*block*-poly(ester) block copolymers such as methoxy PEO-*b*-poly(ϵ -caprolactone) (MePEO-*b*-PCL) may result in the development of biodegradable self-assembling biomaterials with a potential for the attachment of different reactive compounds to the core-forming structure. Micelles of MePEO-*b*-PCL have been used to encapsulate therapeutic agents with hydrophobic properties [11-18]. PCL is a hydrophobic, semi-crystalline polymer with a low glass transition temperature. Owing to these properties, MePEO-*b*-PCL micelles have shown sufficient *in vivo* stability and great promise in tumor targeted drug delivery by enhanced permeability and retention (EPR) effect in several studies [11, 19].

In this chapter we report on the successful synthesis and self assembly of MePEO-*b*-PCL block copolymers bearing benzylcarboxylate and carboxyl side groups on the PCL

block, i.e, MePEO-*b*-poly(α -benzylcarboxylate ϵ -caprolactone) (MePEO-*b*-PBCL) and MePEO-*b*-poly(α -carboxyl ϵ -caprolactone) (MePEO-*b*-PCCL), respectively. The presence of aromatic or carboxylic side groups on the core forming block and changes in the level of side groups is shown to provide additional opportunities for the modification of micellar properties such as micellar size as well as thermodynamic/kinetic stability. The core-functionalized micelles may also change the encapsulation and release properties for certain drugs through formation of π - π interactions, hydrogen bonds or electrostatic complexation between the core forming block and drug and/or lead to the development of pH sensitive micelles with triggered drug release at basic pHs [20-22].

3.2. Experimental section

3.2.1. Materials- MePEO (average molecular weight of 5000 g.mol⁻¹), diisopropyl amine (99%), benzyl chloroformate (tech. 95%), sodium (in kerosin), butyl lithium (Bu-Li) in hexane (2.5 M solution), palladium coated charcoal and pyrene were purchased from Sigma, St. Louis, MO, USA. ϵ -Caprolactone was purchased from Lancaster Synthesis, UK. Stannous octoate was purchased from MP Biomedicals Inc, Germany. Fluorescent probe 1,3-(1,1'-dipyrenyl)propane was purchased from Molecular Probes, USA. All other chemicals were reagent grade.

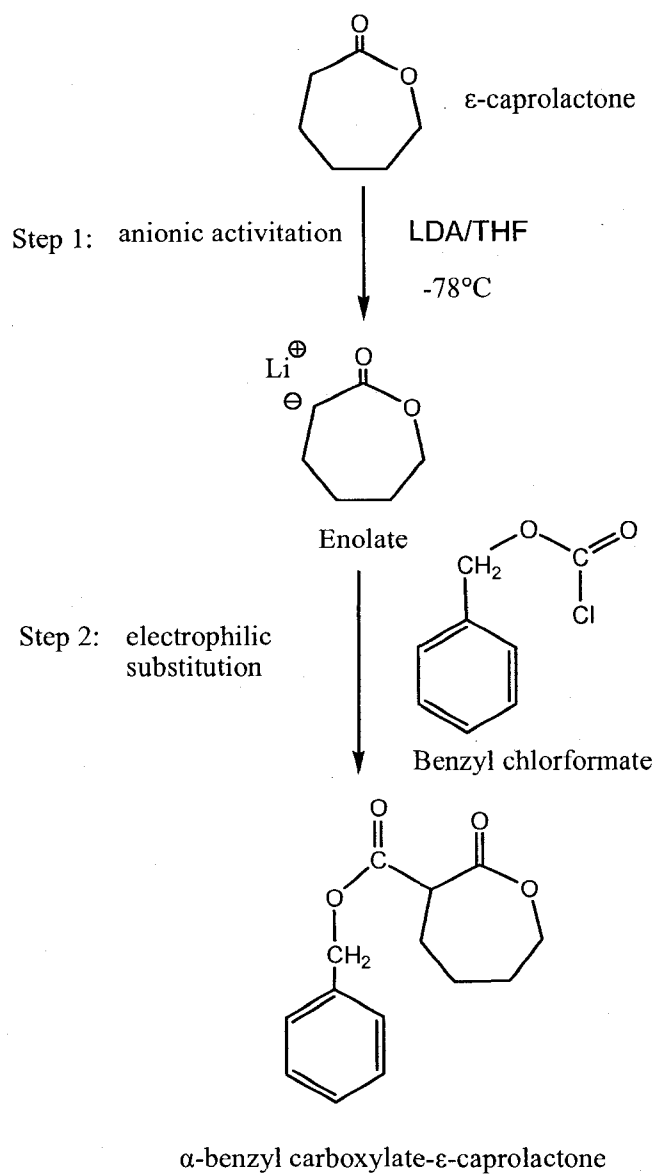
3.2.2. Synthesis of α -benzylcarboxylate ϵ -caprolactone- The method used for the synthesis of α -benzylcarboxylate- ϵ -caprolactone is shown in Scheme 3.1. Briefly, Bu-Li (24 mL) in hexane was slowly added to dry diisopropylamine (8.4 mL) in 60 mL of dry tetrahydrofuran (THF) in a 3 neck round bottomed flask at -30 °C under vigorous stirring with continuous argon supply. The solution was cooled to -78 °C. ϵ -Caprolactone (3.42 g)

was dissolved in 8 mL of dry THF and added to the above mentioned mixture slowly, followed by the addition of benzyl chloroformate (5.1 g). The temperature was allowed to rise to 0 °C and the reaction was quenched with 5 mL of saturated ammonium chloride solution [23]. The reaction mixture was diluted with water and extracted with ethyl acetate. The combined extracts were dried over Na₂SO₄ and evaporated. The yellowish oily crude mixture was purified twice over a silica gel column and the purity of the compound was confirmed with thin layer chromatography (TLC). ¹H NMR of the synthesized compound in deuterated chloroform (CDCl₃) at 300 MHz and ¹³C NMR at 75.4 MHz were performed by a Bruker Unity-300 NMR spectrometer. IR spectrum was obtained from a FT-IR spectrometer (Nicolet Magna-IR[®] 550, USA) by preparing a thin film of the synthesized compound on NaCl disc. Finally, mass spectrum was obtained by a quadrupole mass analyser (Waters, Micromass ZQ[™] 4000, USA). The combined spectroscopic data were used to confirm the structure of the synthesized compound, α-benzylcarboxylate-ε-caprolactone. The reaction yield was calculated using the equation outlined as Eq. 3.1.

Yield (%) =

$$\frac{\text{Amount of } \alpha\text{-benzylcarboxylate } \varepsilon\text{-caprolactone produced in the reaction}}{\text{Predicted amount of } \alpha\text{-benzylcarboxylate } \varepsilon\text{-caprolactone to be produced in the reaction}} \times 100 \quad (\text{Eq. 3.1})$$

3.1)



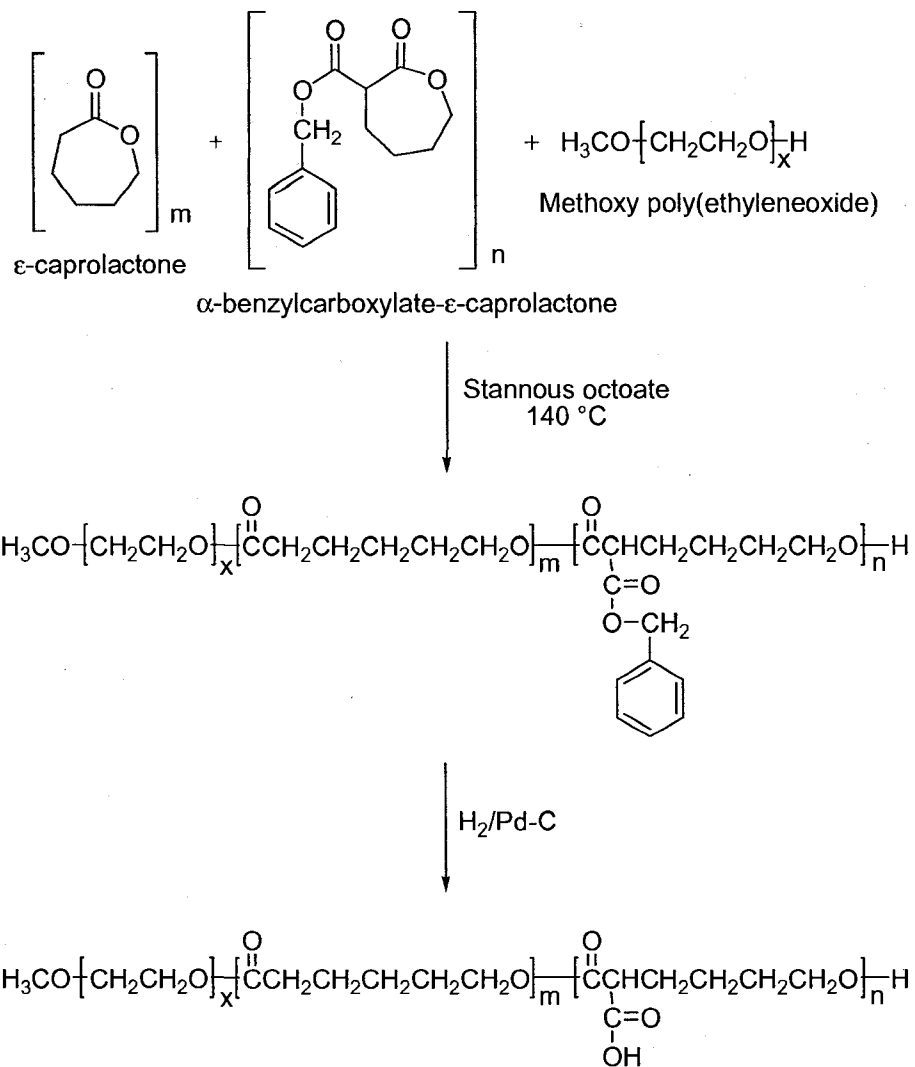
Scheme 3.1- Synthetic scheme for the preparation of α -benzylcarboxylate- ϵ - caprolactone (α -carbon substituted monomer)

3.2.3. Synthesis of MePEO-*b*-PBCL Block copolymers of MePEO-*b*-PBCL were synthesized by ring opening polymerization of α -benzylcarboxylate- ϵ -caprolactone using MePEO as initiator and stannous octoate as catalyst [24, 25]. Synthetic method for the preparation of the block copolymer is shown in Scheme 3.2. MePEO (MW: 5000 g.mol⁻¹) (3.5 g), α -benzylcarboxylate- ϵ -caprolactone (3.5 g) and stannous octoate (0.002 eq of monomer) were added to a 10 mL previously flamed ampoule, nitrogen purged and sealed under vacuum. The polymerization reaction was allowed to proceed for 4 h at 140 °C in oven. The reaction was terminated by cooling the product to room temperature. ¹H NMR spectrum of α -benzylcarboxylate- ϵ -caprolactone bearing block copolymer in CDCl₃ was carried out at 300 MHz and used to assess the conversion of α -benzylcarboxylate- ϵ -caprolactone monomer to PBCL comparing the intensity of -O-CH₂- (δ 4.25 ppm) related peak for α -benzylcarboxylate- ϵ -caprolactone monomer to the intensity of the same protons for PBCL (δ 4.05 ppm). Block copolymers of MePEO-*b*-poly(ϵ -caprolactone)-*co*-poly(α -benzylcarboxylate- ϵ -caprolactone) (MePEO-*b*-PCL-*co*-PBCL) were also synthesized by ring opening polymerization of a mixture of ϵ -caprolactone and α -benzylcarboxylate- ϵ -caprolactone at 50:50 and 75:25 molar ratios.

3.2.4. Reduction of α -benzylcarboxylate bearing block copolymer to α -carboxyl bearing block copolymer- Carboxyl group bearing block copolymers, i.e, MePEO-*b*-PCCL and MePEO-*b*-PCL-*co*-PCCL were obtained by the catalytic debenzylation of MePEO-*b*-PBCL and MePEO-*b*-PCL-*co*-PBCL in the presence of hydrogen gas, respectively (Scheme 3.2) [21, 26]. Briefly, a solution of MePEO-*b*-PBCL or MePEO-*b*-PCL-*co*-PBCL (1 g in 25 mL of THF) was placed into a 100 mL round bottom flask. Charcoal coated with palladium (300 mg) was dispersed in this solution. The flask was sealed with septum and vacuum was

applied through a needle for 10 minutes. The reaction flask was filled with hydrogen gas and maintained a continuous supply of hydrogen gas. The mixture was stirred vigorously with a magnetic stirrer and reacted with hydrogen for 24 h at room temperature. The reaction mixture was centrifuged at $1610 \times g$ to remove the catalyst. The supernatant was collected, condensed under reduced pressure, precipitated in diethyl ether and washed repeatedly to remove impurities. The final product was collected and dried under vacuum at room temperature for 48 h. ^1H NMR spectrum of reduced block copolymer in dimethyl sulfoxide- d_6 (DMSO- d_6) at 300 MHz was used to assess the conversion of benzylcarboxylate to carboxyl group following the disappearance of the characteristic aromatic peak at δ 7.4 ppm.

3.2.5. Characterization of synthesized block copolymers- The number average molecular weight (M_n) of MePEO-*b*-PBCL and MePEO-*b*-PCCL block copolymers was determined from ^1H NMR spectra comparing peak intensity of MePEO ($-\text{CH}_2\text{CH}_2\text{O}-$, δ 3.65 ppm) to that of PBCL or PCCL ($-\text{OCH}_2-$, δ 4.05 ppm), respectively, considering a $5000 \text{ g}\cdot\text{mol}^{-1}$ molecular weight for MePEO. The M_n of MePEO-*b*-PCL-*co*-PCCL block copolymers was determined by comparing the MePEO peak intensity ($-\text{CH}_2\text{CH}_2\text{O}-$, δ 3.65 ppm) to that of PCL ($\text{O}=\text{C}-\text{CH}_2$, δ 2.31 ppm) and PCCL (CH_2 protons of $-\text{CH}-\text{CH}_2$, δ 1.90 ppm) in its ^1H NMR spectra. The molar proportion of PCL and PCCL in MePEO-*b*-PCL-*co*-PCCL was determined by comparing the peak intensity ratio of PCL ($\text{O}=\text{C}-\text{CH}_2$, δ 2.31 ppm) to PCCL (CH_2 protons of $\text{CH}-\text{CH}_2$, δ 1.90 ppm). The degree of polymerization of each block of the synthesized block copolymers calculated from ^1H NMR is indicated by the number as subscript in each block. IR spectrum was obtained by dissolving the block copolymers in chloroform and preparing a thin film on NaCl disc.



$m=0$ for MePEO-*b*-PBCL or MePEO-*b*-PCCL
 $m>0$ for MePEO-*b*-PCL-*co*-PBCL or MePEO-*b*-PCL-*co*-PCCL

Scheme 3.2- General synthesis scheme for the preparation of MePEO-*b*-PBCL, MePEO-*b*-PCCL, MePEO-*b*-PCL-*co*-PBCL and MePEO-*b*-PCL-*co*-PCCL block copolymers

The M_n and weight average molecular weight (M_w) as well as polydispersity of prepared polymers were assessed by gel permeation chromatography (GPC). Briefly, 20 μ L of polymer solution (20 mg/mL in THF) was manually injected into a 7.8×300 mm Styragel HMW 6E column (Waters Inc. Milford, MA). The column was eluted with 1 mL/min THF using a HP 1100 pump. The elution pattern was detected by refractive index (Model 410; Waters Inc.) and dynamic light scattering (PD 2000 DLS; Precision Detectors, Franklin, MA, USA) detectors. Polystyrene standard of varying molecular weights (from M_w : 4750 g.mol⁻¹ to 13700 g.mol⁻¹) were used to calibrate the GPC process.

3.2.6. Assembly of block copolymers and characterization of the assembled structures- Block copolymer assembly was achieved by dissolving copolymers (30 mg) in acetone (0.5 mL) and drop-wise addition (~1 drop/15 sec) of polymer solutions to doubly distilled water (3 mL) under moderate stirring at 25°C, followed by the evaporation of acetone under vacuum [12]. Average diameter (intensity mean) and size distribution of self assembled structures were estimated by dynamic light scattering (DLS) using Malvern Zetasizer 3000 at a polymer concentration of 10 mg/mL in water at 25°C after filtration through 0.45 μ m filters. Morphology of self assembled structures was investigated at a polymer concentration of 1 mg/mL, using a Hitachi H 700 transmission electron microscope (TEM) according to the procedure described in previous chapter (Chapter 2, section 2.2.3). Images were obtained at a magnification of $\times 18000$ at 75 KV.

Critical micellar concentration (CMC) of the synthesized block copolymers were determined using pyrene as fluorescent probe according to the method described in previous chapter (Chapter 2, section 2.2.3). The viscosity of prepared micellar core was estimated by measuring excimer to monomer intensity ratio (I_e/I_m) from the emission spectra of 1,3-(1,1'-

dipyrenyl)propane at 373 and 480 nm, respectively, according to the method described in previous section (Chapter 2, section 2.2.3).

3.2.7. Assessing the biocompatibility of prepared block copolymers- Biocompatibility of the prepared block copolymers, i.e., MePEO-*b*-PBCL, MePEO-*b*-PCCL and MePEO-*b*-PCL-*co*-PCCL was assessed and compared with that of MePEO-*b*-PCL by hemolysis study against rat red blood cells (RBC)s and cytotoxicity study against human fibroblast cells. For hemolysis study, blood was freshly obtained from a Sprague-Dawley rat by cardiac puncture, mixed with sterile isotonic phosphate buffer solution (PBS) and centrifuged at 3000 rpm for 5 minutes. The supernatant were pipetted out and the red blood cells were diluted with isotonic sterile PBS (pH: 7.4). The proper dilution factor was estimated from the UV-Vis absorbance of hemoglobin at 576 nm in the supernatant after RBCs were lysed by 0.1% triton X -100. A properly diluted sample of RBC gave an absorbance of 0.4 to 0.5. Micellar solution of different block copolymers at varied polymer concentrations were incubated with diluted RBC suspension (2.5 mL) at 37 °C for 30 minutes. After incubation the samples were kept in ice bath to stop further hemolysis. The samples were centrifuged at 14,000 rpm for 30 sec to precipitate the intact RBCs. The supernatant was separated and analyzed for hemoglobin by UV-Vis spectrophotometer at 576 nm. The percentage of hemolyzed RBC was calculated using the following equation:

$$\% \text{ of hemolysis} = 100 (Abs - Abs_0)/(Abs_{100}-Abs_0) \quad (\text{Eq. 3.2})$$

where Abs, Abs₀ and Abs₁₀₀ are the absorbance for the sample, control with no polymer and control with 0.1% triton X-100, respectively.

In vitro biocompatibility of the prepared block copolymers with human fibroblast cells was assessed using 3-(4,5-dimethylthiazol-2-yl)-2,5-diphenyltetrazolium bromide (MTT) assay. The cells were grown in RPMI 1640 complete growth media supplemented with 10 % fetal bovine serum, 1% w/v % L-glutamine, 100 units/mL penicillin and 100 µg/mL streptomycin and maintained at 37 °C with 5% CO₂ in a tissue culture incubator. In the logarithmic growth phase the cells were harvested and seeded into 96-well plates at a density of 5×10^3 cells/well in 100 µL of RPMI 1640 media. After 24 h, when the cells had adhered, block copolymers at different concentrations, i.e., 5 to 500 µg/mL were incubated with the cells for 24 h. After this time, MTT solution (20 µL; 5mg/mL in sterile-filtered PBS) was added to each well and the plates were reincubated for further 3 h. The formazan crystals were dissolved in DMSO, and the concentration was read by measuring the absorbance by a Power Wave _x 340 microplate reader (Bio-Tek Instruments, Inc. USA) at 550 nm. Percent of cell viability was calculated based on the equation outlined below (Eq. 3.3). A plot of the cell viability (%) versus logarithm of polymer concentration was graphed.

$$\text{Cell viability (\%)} = (\text{Abs} - \text{Abs}_0)100 / (\text{Abs}_{100} - \text{Abs}_0) \quad (\text{Eq. 3.3})$$

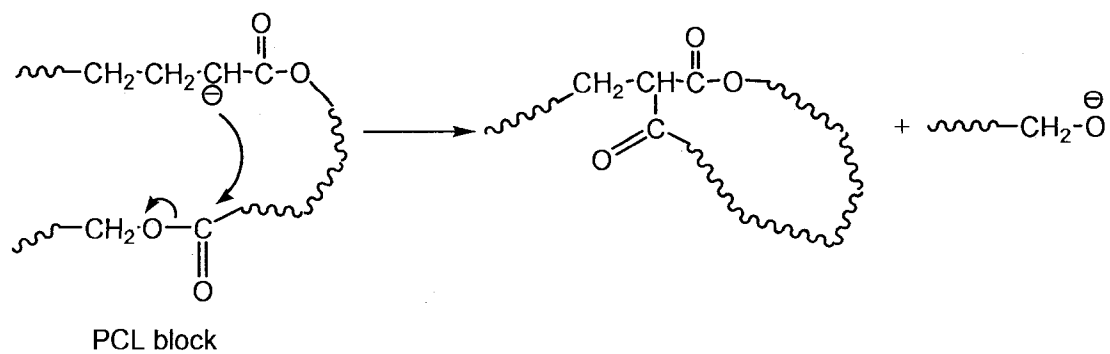
where Abs, Abs₀ and Abs₁₀₀ are the absorbance from cells incubated with varied concentrations of polymer samples, control without any cells and cells without any polymer sample respectively.

3.2.8. Statistical analysis- Data are reported as mean ± standard deviation (S.D.). Differences among the mean of formulation characteristics for polymeric micelles were compared by Student's unpaired t-test assuming unequal variance.

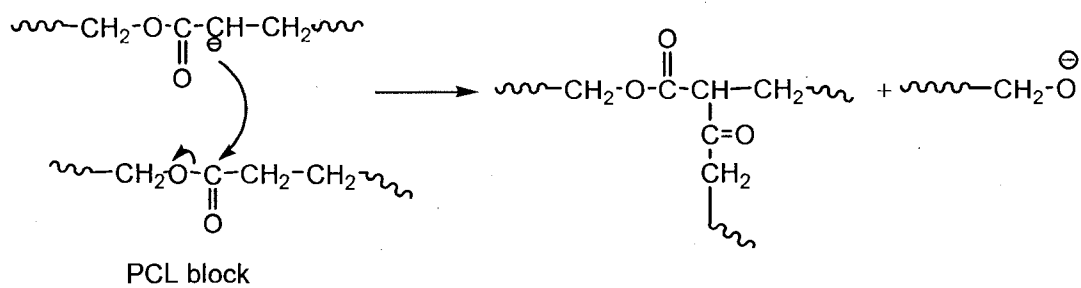
3.3. Results and discussion

3.3.1. Preparation of MePEO-*b*-PCL block copolymers with aromatic side groups on the PCL block- Attachment of aromatic side groups to MePEO-*b*-PCL block copolymers was carried out through conjugation of benzyl chloroformate with ϵ -caprolactone monomer producing α -benzylcarboxylate- ϵ -caprolactone monomer (Scheme 3.1) [23, 27] and further ring opening polymerization of this new monomer by MePEO (Scheme 3.2). In preliminary studies, direct conjugation of benzylcarboxylate group to MePEO-*b*-PCL block copolymers through generation of lithium carbanion on the PCL block following treatment with lithium diisopropylamide (LDA) was tried, as suggested by Gimenez *et al* and Ponsart *et al* for homopolymers of PCL [1, 27]. This approach led to a loss in the intensity of peak at δ 3.65 ppm in the ^1H NMR spectrum of product reflecting the loss of MePEO chain during the formation of polycarbanion (data not shown). The decrease in molar mass of substituted polymer was also evident when Ponsart *et al* carried a similar reaction with PCL homopolymer. Cleavage of the ester bonds in the block copolymer backbone during the formation of the polycarbanion is a side reaction occurring in parallel to the proton extraction by LDA. Transesterification by inter or intra-molecular autocondensation in the homo or block copolymer backbone is a possible explanation for this effect (Scheme 3.3 A and B).

A)

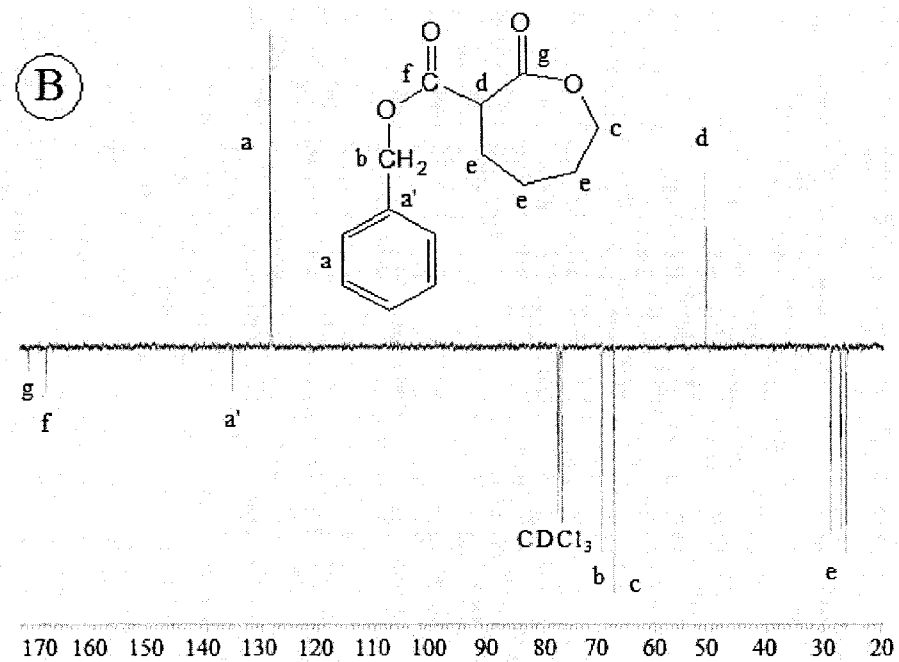
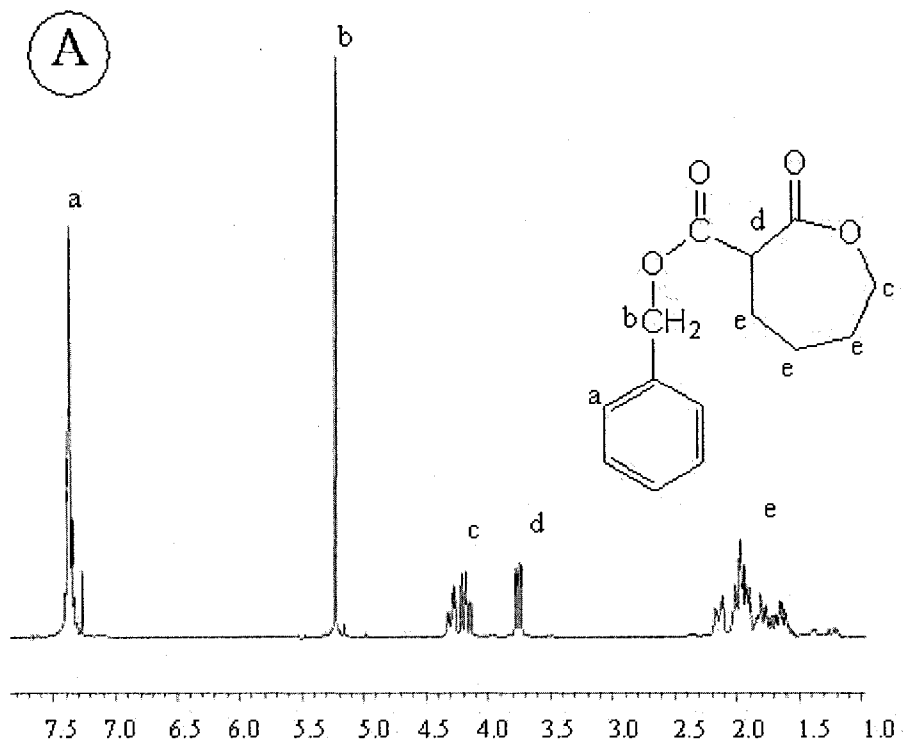


B)



Scheme 3.3- A) Intramolecular transesterification and B) Intermolecular transesterification of MePEO-*b*-PCL.

Anionic activation of ϵ -caprolactone monomer was performed using freshly prepared non-nucleophilic strong base LDA to extract a methylene proton from α -position ($-\text{CH}_2-\text{C}=\text{O}$). The generated lithium carbanion was then quenched with benzyl chloroformate to obtain α -benzylcarboxylate- ϵ -caprolactone (Scheme 3.1). After column chromatography α -benzylcarboxylate- ϵ -caprolactone was isolated as a clear thick oily liquid. The product produced a single spot at an R_f value of 0.3 in TLC. The yield of reaction was 53.8%. The structure was confirmed by combined analysis of ^1H NMR, ^{13}C NMR, IR and Mass spectroscopy (Figure 3.1). In 300 MHz ^1H NMR spectroscopy in CDCl_3 , corresponding proton peaks were observed at δ (ppm): 1.6-2.2 (m, 6H); 3.75 (dd, 1H); 4.13-4.35 (m, 2H); 5.226 (s, 2H); 7.4 (m, 5H) (Figure 3.1 A). The peak at 3.75 ppm (Figure 3.1 A) for α -benzylcarboxylate- ϵ -caprolactone, which corresponds to a single proton instead of two protons of ϵ -caprolactone monomer, indicates the successful substitution of the benzyl carboxylate on ϵ -caprolactone monomer at α -position. The presence of two negative peaks for carbonyl at 168.695 and 171.665 ppm and the generation of a new characteristic positive peak at 50.86 ppm in ^{13}C NMR spectrum also confirm the chemical structure of the reaction product (Figure 3.1 B). The presence of two sharp carbonyl peaks in the IR spectrum at 1725 and 1760 cm^{-1} corresponds to the carbonyl groups in lactone and benzylcarboxylate, respectively (Figure 3.1 C). Finally, mass spectroscopy resulted in the formation of peaks at m/z :248.99, m/z :230.95 and m/z :164.82 m/z :132.84 (Figure 3.1 D). The presence of molecular ion (M^+) peak at m/z :248.99, $\text{M}^+ + \text{Na}$ peak at m/z :271.00 and $\text{M}^+ + \text{K}$ peak at m/z :287.00 in the mass spectrum provided additional evidence for the chemical structure of the synthesized monomer.



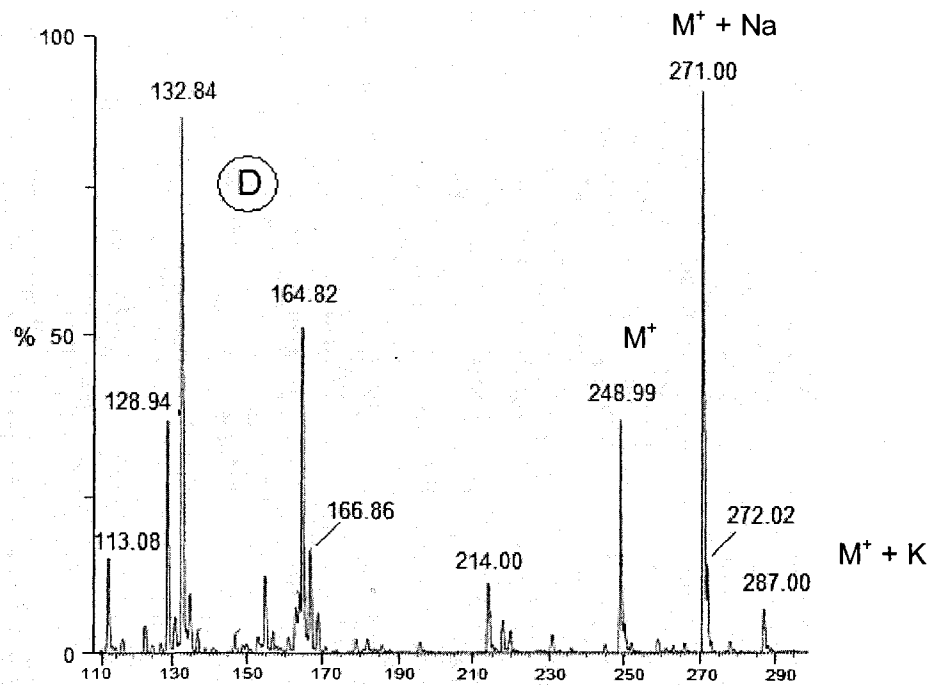
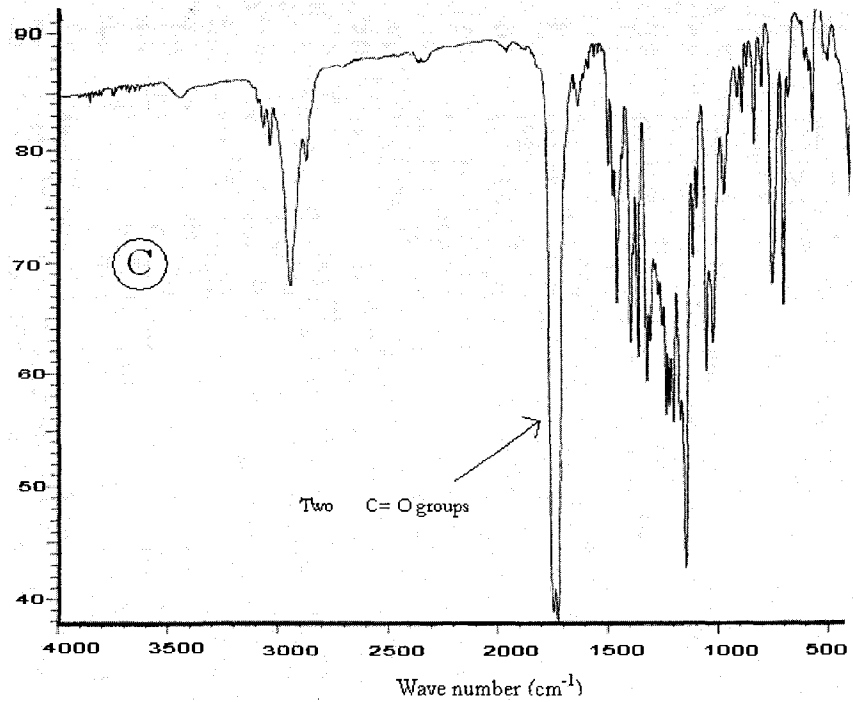


Figure 3.1- A) ^1H NMR; B) ^{13}C NMR; C) IR; and D) Mass spectra of α -benzylcarboxylate- ϵ -caprolactone and peak assignments.

MePEO-*b*-PBCL block copolymer was synthesized by ring opening polymerization of α -benzylcarboxylate- ϵ -caprolactone using MePEO as initiator and stannous octoate as catalyst according to the procedure reported previously for the polymerization of ϵ -caprolactone (Chapter 2, section 2.2.2) [12]. Synthesis of homopolymers of ϵ -caprolactone bearing carboxyl, benzylcarboxylate or benzyloxy group, on the methylene in the γ -position of ϵ -caprolactone by ring opening polymerization of the functionalized ϵ -caprolactone monomer using stannous octoate or $\text{Al}(\text{O}^i\text{Pr})_3$, has also been reported, recently [28, 29]. The percent of conversion of MePEO-*b*-PBCL block copolymer from α -benzylcarboxylate ϵ -caprolactone was found to be 91 %. In 300 MHz ^1H NMR spectroscopy in CDCl_3 , corresponding proton peaks for the product were observed at δ (ppm): 1.25-1.9 (m, 6H); 3.3-3.45 (s, 3H; tri, 1H); 3.65 (s, 4H); 4.05 (tri, 2H); 5.15 (s, 2H); 7.35 (s, 5H) (Figure 3.2 A). The presence of peaks at δ 7.35 and 5.15 ppm, which are due to the aromatic and methylene protons of the benzylcarboxylate group, respectively, confirm the polymerization of α -benzylcarboxylate- ϵ -caprolactone and the presence of aromatic groups in the structure of block copolymer. Furthermore, the characteristic downfield shift of the methylene protons ($-\text{OCH}_2-$ of α -benzylcarboxylate- ϵ -caprolactone) from δ 4.25 to 4.05 and $\text{O}=\text{C}-\text{CH}-$ proton from δ 3.75 to 3.28 in the ^1H NMR spectra (Figure 3.1 A and 3.2 A) strongly indicates the ring opening polymerization of the monomer and formation of block copolymers. The IR spectrum of MePEO-*b*-PBCL block copolymer is shown in Figure 3.3 A. The characteristic peaks observed at 1725 and 1735 cm^{-1} ($\text{C}=\text{O}$ stretching) compared to one peak at 1725 cm^{-1} for MePEO-*b*-PCL (Chapter 2, figure 2.1 C), indicates the presence of two different positions for carbonyl groups present in the structure of MePEO-*b*-PBCL. Besides, characteristic peaks related to the C-H stretching aromatic appeared in the finger print region of the IR spectrum for MePEO-*b*-PBCL at 690 -750 cm^{-1} .

The characteristics of prepared MePEO-*b*-PBCL block copolymer are summarized in Table 3.1. The molecular weight of prepared MePEO-*b*-PBCL block copolymer, measured by comparing the peak intensities of 4 methylene protons of MePEO (δ 3.65) and 2 methylene protons of PBCL (δ 4.05) in the ^1H NMR spectrum, was calculated to be $9700 \text{ g}\cdot\text{mol}^{-1}$ (equal to a degree of α -benzylcarboxylate- ϵ -caprolactone polymerization of 19). The agreement between the measured and theoretical molecular weights for MePEO-*b*-PBCL was not as good as values reported earlier for MePEO-*b*-PCL (Chapter 2, section 2.3.1) pointing to a decrease in the reactivity of α -benzylcarboxylate ϵ -caprolactone compared to unsubstituted ϵ -caprolactone (Table 2.1 and 3.1). The decrease in the polymerization reactivity of α -benzylcarboxylate ϵ -caprolactone may be due to the steric hindrance created by the attached aromatic group. However, the M_n measured by ^1H NMR was close to the one measured by GPC (Table 3.1). The unimodal distribution of the block copolymer from GPC analysis (Figure 3.4) is particularly significant since it lends further support to the view that the final product is indeed a block copolymer rather than a blend of homopolymers. The resulting copolymer showed a broad polydispersity ($M_w/M_n=1.47-1.74$) compared to the unfunctionalized MePEO-*b*-PCL block copolymer ($M_w/M_n=1.04$) and tailing in its GPC chromatogram (Figure 3.4), which may be attributed to the presence of traces of PBCL homopolymer or block copolymers with short PBCL segments in the reaction product.

Table 3.1- Characteristics of substituted and unsubstituted MePEO-*b*-PCL block copolymers

Block copolymer ^a	Actual feed ratio ^b εCL:BCL	Theoretical Mol. Wt. (g.mol ⁻¹)	M _n (g.mol ⁻¹) ^c	M _n (g.mol ⁻¹) ^d	PDI ^e
MePEO ₁₁₄ - <i>b</i> -PCL ₄₂	44: 0	10000	9800	11500	1.04
MePEO ₁₁₄ - <i>b</i> -PBCL ₁₉	0: 21	10200	9700	9200	1.74
MePEO ₁₁₄ - <i>b</i> -PCCL ₁₆	0 :19	8000	7530	7200	1.52
MePEO ₁₁₄ - <i>b</i> -PCL _{16-co} -PCCL ₁₀	15:13	8800	8400	9600	1.47
MePEO ₁₁₄ - <i>b</i> -PCL _{25-co} -PCCL ₅	23: 7	8750	8650	15600	1.53

^a The number showed as subscript indicates the polymerization degree of each block determined from ¹H NMR spectroscopy.

^b Molar feed ratio of ε-caprolactone (εCL) and α-benzylcarboxylate-ε-caprolactone (BCL) applied in the reaction mixture

^c Number average molecular weight measured by ¹H NMR.

^d Number average molecular weight measured by GPC

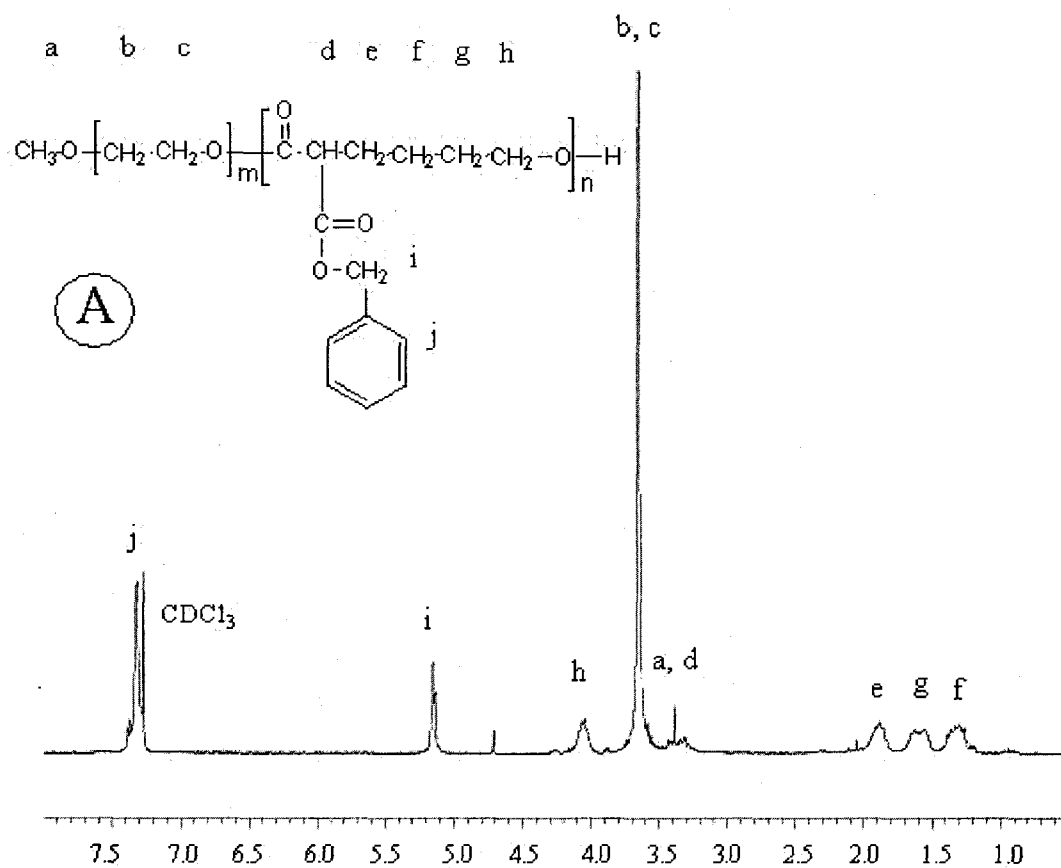
^e Polydispersity index (M_w/M_n) measured by GPC

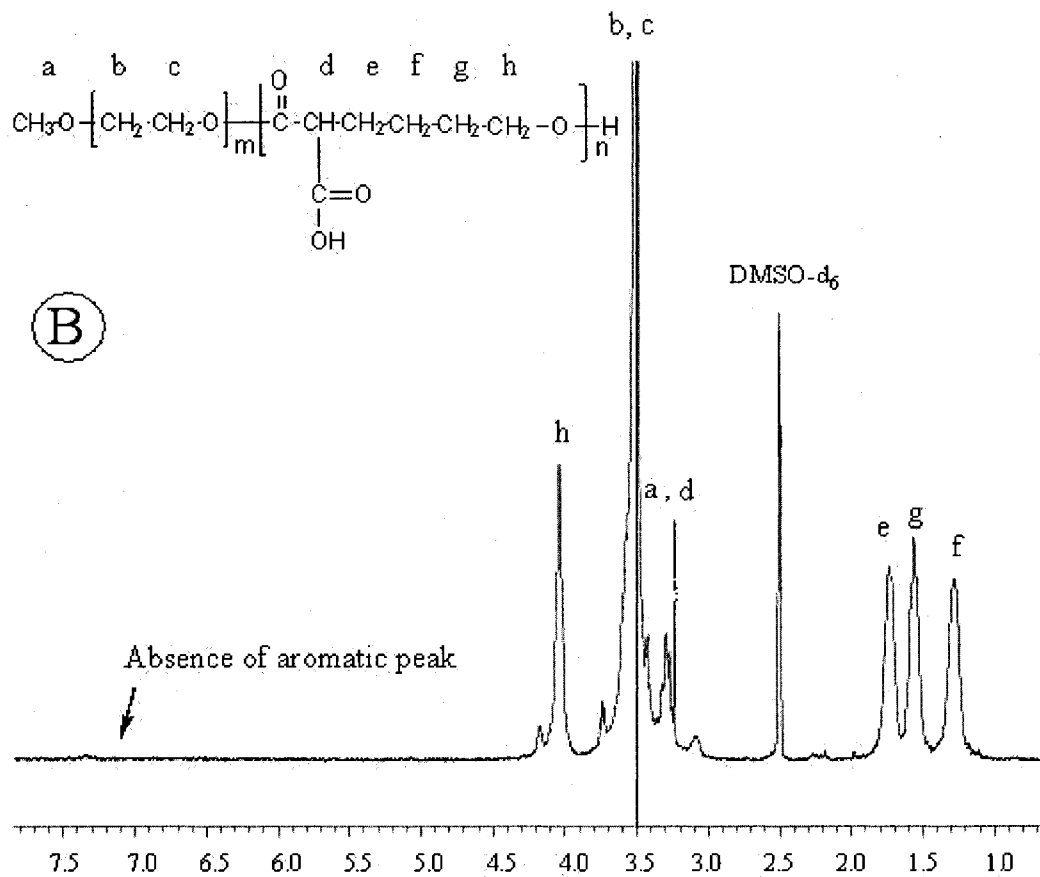
3.3.2. Synthesis and characterization of MePEO-*b*-PCCL block copolymers- Synthesis

of MePEO-*b*-PCL block copolymers bearing carboxylic groups on the PCL block was accomplished through reduction of benzylcarboxylate on the MePEO-*b*-PBCL block copolymer. The pendant benzylcarboxylate was readily removed by the catalytic hydrogenolysis to yield a carboxyl-functionalized block copolymer. ¹H NMR spectrum of synthesized block copolymer in DMSO-*d*₆ at 300 MHz showed peaks at δ (ppm): 1.20 -1.9 (m, 6H); 3.22-3.38 (s,3H; tri, 1H); 3.5 (s,4H); 4.03 (tri, 2H). No peak was observed at δ 7.4 and δ 5.15 ppm (Figure 3.2 B). The latter peaks correspond to the aromatic and the methylene protons of the benzylcarboxylate group, respectively. IR spectrum of MePEO-*b*-PCCL block copolymer showed a large broad peak from 3500 to 2500 cm^{-1} , which indicates the presence of hydrogen bonded carboxyl groups. This broad peak was absent in the IR spectrum of MePEO-*b*-PBCL block copolymer (Figure 3.3 A and B). The characteristic peaks related to the aromatic C-H stretching (at 690-750 cm^{-1}) were also absent here. The characteristic properties of MePEO-*b*-PCCL block copolymer are summarized in Table 3.1. The molecular weight of prepared MePEO-*b*-PCCL block copolymer measured by comparing the peak intensity of four methylene protons of MePEO (δ 3.65 ppm) and two methylene protons of PCCL (δ 4.05 ppm) in the ¹H NMR spectrum was calculated to be 7530 $\text{g}\cdot\text{mol}^{-1}$ (corresponding to a degree of polymerization of 16 for α -carboxyl- ϵ -caprolactone). The molecular weight measured by GPC was in good agreement with the ¹H NMR results. The polymer population was unimodal and the molecular weight distribution was also broad ($M_w/M_n=1.52$) like MePEO-*b*-PBCL block copolymer. The broad molecular weight distribution of MePEO-*b*-PCCL may be attributed to the production of trace amounts of low molecular weight PCCL homopolymer due to the possible chain cleavage during reduction procedure.

3.3.3. Synthesis and characterization of MePEO-*b*-PCL-*co*-PCCL block copolymer-

Two block copolymers MePEO₁₁₄-PCL_{16-*co*}-PCCL₁₀ (equivalent to 60 and 40% PCL and PCCL in molar basis, respectively) and MePEO₁₁₄-PCL_{25-*co*}-PCCL₅ (equivalent to 83 and 17 % PCL and PCCL in molar basis, respectively) were synthesized from copolymerization of ϵ -caprolactone and α -benzylcarboxylate- ϵ -caprolactone and further reduction of the product. Thin layer chromatography using hexane:ethyl acetate (3:1 ratio) as the mobile phase and cerium molybdate solution (Hanesian's Stain) as indicator confirmed the purity of block copolymers from free ϵ -caprolactone and α -benzylcarboxylate- ϵ -caprolactone (data not shown). ¹H NMR spectra of these block copolymers clearly show the characteristic peaks for O=C-CH₂- protons of PCL (at δ 2.31 ppm) and -CH₂ protons of PCCL (at δ 1.90 ppm) and complete reduction of benzylcarboxylate group to COOH (Figure 3.2 C). The degree of polymerization for the hydrophobic block (unsubstituted+substituted ϵ -caprolactone) was determined by comparing the peak intensities of 4 methylene protons of MePEO (δ 3.65 ppm) to 2 methylene protons of PCL (-CH₂-C=O, δ 2.31 ppm) and 2 methylene protons of PCCL (CH₂-CH-, δ 1.90 ppm) from the ¹H NMR spectrum. The calculated degree of polymerization ratios of ϵ -caprolactone and α -benzylcarboxylate- ϵ -caprolactone (ϵ CL:BCL) were 16:10 and 25:5 for MePEO₁₁₄-PCL_{16-*co*}-PCCL₁₀ and MePEO₁₁₄-PCL_{25-*co*}-PCCL₅ respectively. However, the applied feed ratios of ϵ CL:BCL in the reaction mixture were 15:13 and 23:7 for the respective copolymers which indicates more reactivity of ϵ -caprolactone compared to α -benzylcarboxylate- ϵ -caprolactone in ring opening polymerization (Table 3.1). Both copolymers gave unimodal molecular weight distributions, but produced broad peaks in GPC. The polydispersity values for MePEO₁₁₄-PCL_{16-*co*}-PCCL₁₀ and MePEO₁₁₄-PCL_{25-*co*}-PCCL₅ was 1.47 and 1.53, respectively.





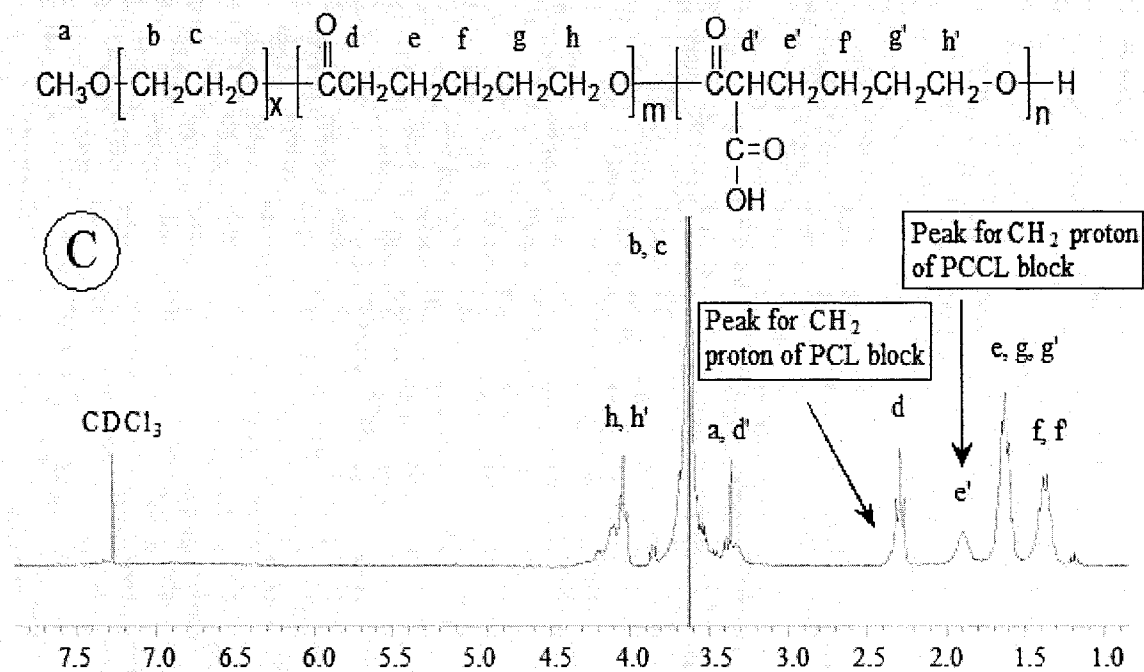


Figure 3.2- ¹H NMR spectrum and peak assignments for **A)** MePEO-*b*-PBCL in CDCl₃; **B)** MePEO-*b*-PCCL in DMSO-*d*₆; and **C)** MePEO-*b*-PCL-*co*-PCCL in CDCl₃

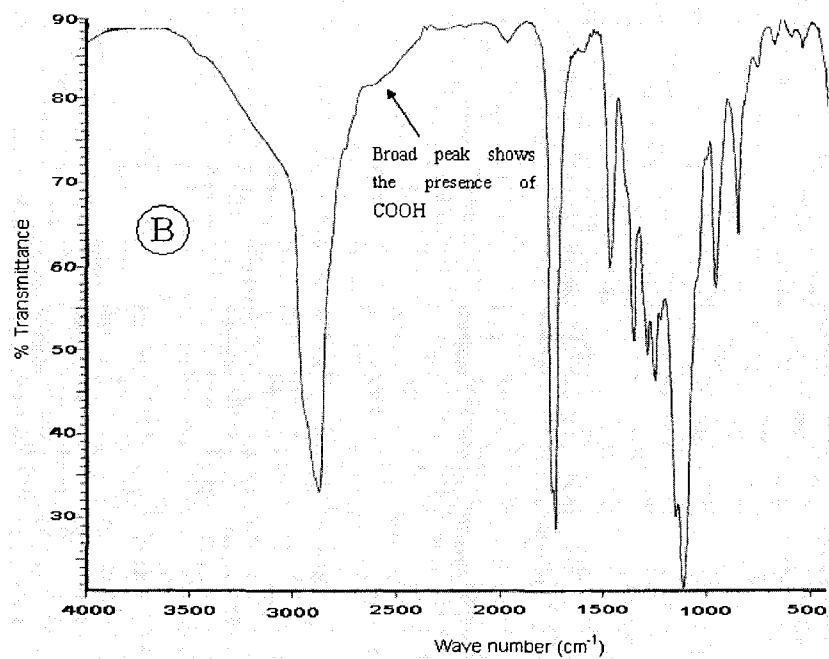
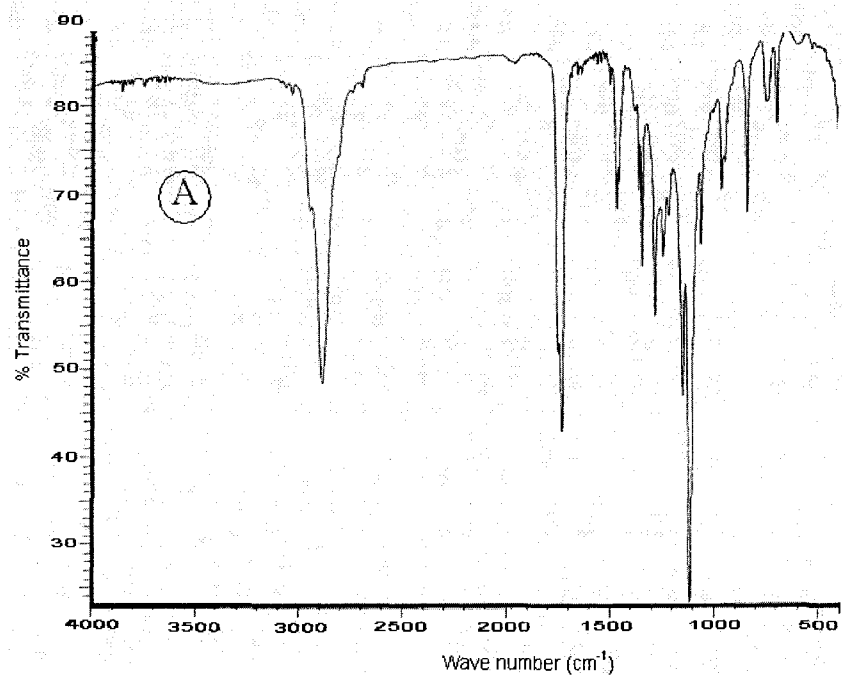


Figure 3.3- IR spectrum of **A)** MePEO-*b*-PBCL ($M_n=9700 \text{ g.mol}^{-1}$) and **B)** MePEO-*b*-PCCL ($M_n=7530 \text{ g.mol}^{-1}$). Arrow indicates the presence of broad peak caused by OH of pendant COOH group. The IR samples were prepared using sodium chloride disc method.

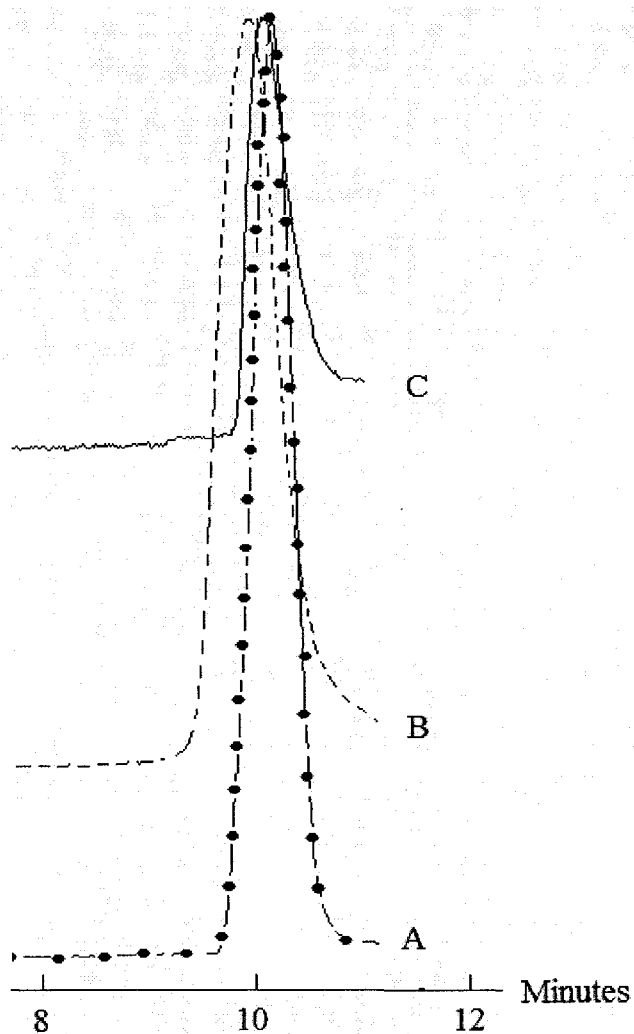


Figure 3.4- GPC chromatogram for **A)** MePEO, $M_n=5000 \text{ g.mol}^{-1}$, $M_w/M_n=1.62$; **B)** MePEO-*b*-PBCL, $M_n=9700 \text{ g.mol}^{-1}$, $M_w/M_n=1.74$; and **C)** MePEO-*b*-PCCL, $M_n=7530 \text{ g.mol}^{-1}$, $M_w/M_n=1.52$.

3.3.4. Assembly of block copolymers and characterization of self-assembled structures- Synthesized block copolymers were assembled to polymeric micelles by a co-solvent evaporation method as described in Chapter 2, section 2.2.3 [12]. Average diameter for MePEO-*b*-PBCL micelle determined by DLS technique was $61.9 \pm 2.90 \text{ nm}$. Micellar

population showed a relatively broad distribution (PI=0.39) compared to the unfunctionalized MePEO-*b*-PCL (PI=0.20) block copolymer. The results of size measurements by DLS for three carboxyl bearing block copolymers at different levels of COOH substitution revealed a relatively small average diameter (19.9-38.3 nm) for the micellar peak, but secondary peaks at larger diameters were also present. A relatively high degree of polydispersity for the self assembled structures in these polymers (0.5-0.9) may be a reflection of the secondary association of PCCL bearing micelles (Table 3.2). The size of micelles for all PCCL containing block copolymers decreased with an increase in the number of carboxyl groups on the polymeric backbone (Table 3.2). The composition and the molecular weight of the block copolymer is known to significantly influence the size and polydispersity of the resultant micelles [30]. In this case, association of the exposed COOH groups, localized in the core/shell interface during synthesis or by folding of the hydrophobic block, through hydrogen bonding is speculated to be a possible reason for the aggregation of micellar structures.

The TEM pictures of MePEO-*b*-PBCL shows formation of true spherical shaped micelle having clear boundary and the average diameter was 31.5 nm in dry state (Figure 3.5A). While micelles formed from MePEO-*b*-PCCL block copolymers were found to be much smaller (10.3 nm based on TEM images) and the shape of the micelles are not clearly defined (Figure 3.5 B). A similar trend was observed in the size measurement obtained from DLS technique. The difference in size measured by these two methods (61.9 vs 31.5 nm for MePEO-*b*-PBCL and 19.9 vs 10.3 nm for MePEO-*b*-PCCL) is due to the hydration of the MePEO chain in the aqueous medium used in DLS measurements.

Table 3.2- Characteristics of substituted and unsubstituted MePEO-*b*-PCL block copolymer micelles ($n=3$).

Block copolymer	Micellar size \pm SD (nm) ^a	Size of secondary peaks (nm)	PDI ^c	CMC ^d \pm SD (μ M)	I _e /I _m ^e \pm SD
MePEO ₁₁₄ - <i>b</i> -PCL ₄₂	40.0 \pm 2.0	-	0.20	18.2 \times 10 ⁻² \pm 0.01	0.055 \pm .007
MePEO ₁₁₄ - <i>b</i> -PBCL ₁₉	61.9 \pm 2.9	-	0.39	9.8 \times 10 ⁻² \pm 0.01	0.028 \pm .002
MePEO ₁₁₄ - <i>b</i> -PCCL ₁₆	19.9 \pm 2.3	368 (60%) ^b	0.90	1220 \times 10 ⁻² \pm 0.42	0.025 \pm .002
MePEO ₁₁₄ - <i>b</i> -PCL ₁₆ - <i>co</i> -PCCL ₁₀	24.4 \pm 2.4	256 (45%) ^b	0.58	130 \times 10 ⁻² \pm 0.05	0.027 \pm .003
MePEO ₁₁₄ - <i>b</i> -PCL ₂₅ - <i>co</i> -PCCL ₅	38.3 \pm 4.5	290 (40%) ^b	0.53	44.5 \times 10 ⁻² \pm 0.02	0.035 \pm .002

^a Intensity mean estimated by DLS technique.

^b Numbers in the parenthesis indicate the frequency of secondary peak in micellar population in percentage

^c Polydispersity index (PDI) of micellar size distribution estimated by DLS technique

^d Measured from the onset of a rise in the intensity ratio of peaks at 339 nm to peaks at 334 nm in the fluorescence excitation spectra of pyrene plotted versus logarithm of polymer concentration.

^e Intensity ratio (excimer/monomer) from emission spectrum of 1,3-(1,1' dipyrenyl) propane in presence of polymeric micelle

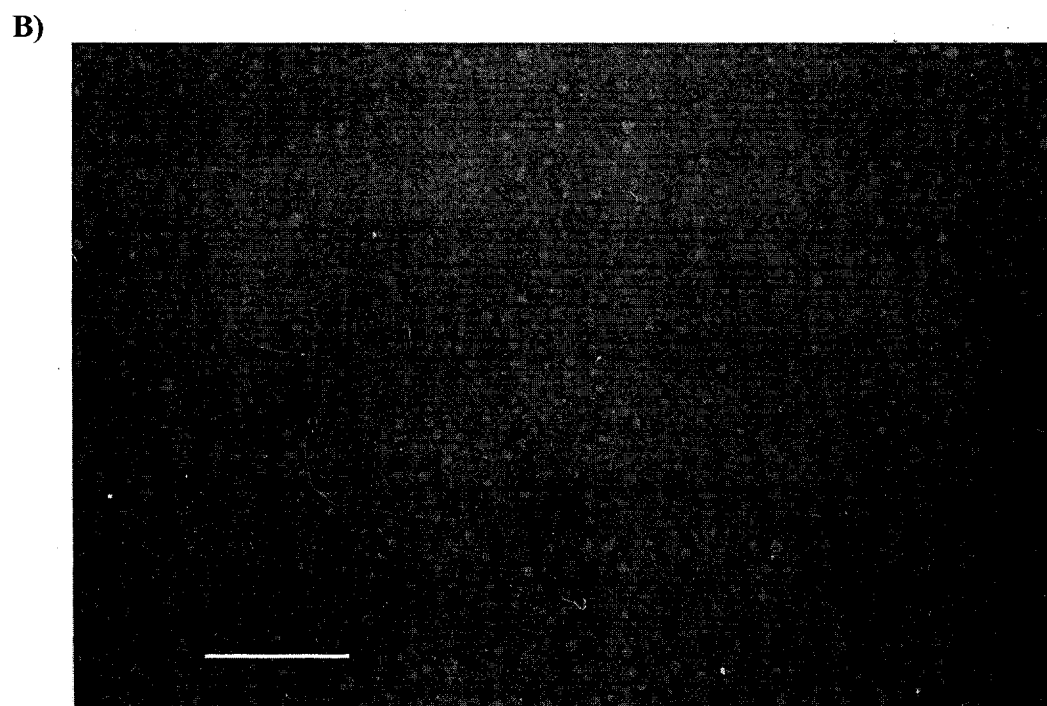
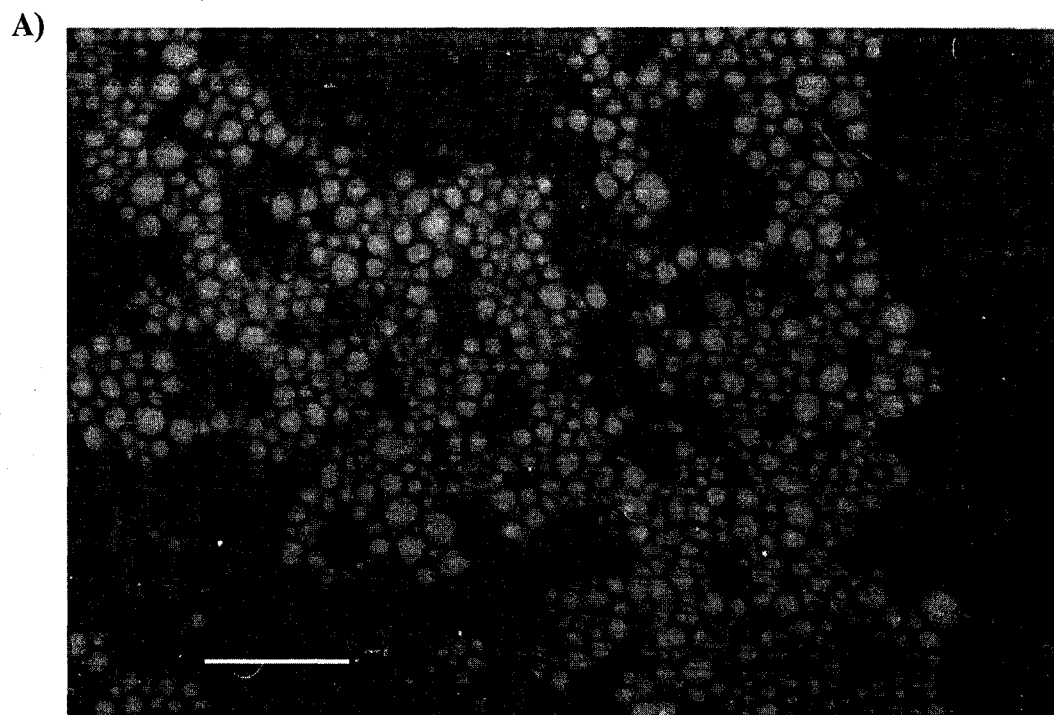


Figure 3.5- TEM picture of micelles prepared from **A)** MePEO-*b*-PBCL ($M_n=9700 \text{ g.mol}^{-1}$) and **B)** MePEO-*b*-PCCL ($M_n=7530 \text{ g.mol}^{-1}$) block copolymers (magnification 18000×6.1). The bar on the images represents 200 nm.

The CMC of all di-block copolymers were determined by fluorescence spectroscopy using pyrene as the fluorescent probe (Figure 3.6). Using this method, low CMC values (in μM range) were revealed for MePEO-*b*-PCL and MePEO-*b*-PBCL block copolymers. The average CMC for MePEO₁₁₄-*b*-PCL₄₂ and MePEO₁₁₄-*b*-PBCL₁₉ was calculated at 18.36×10^{-2} and 9.8×10^{-2} μM , respectively. The CMC for MePEO-*b*-PBCL with a degree of polymerization of 19 (hydrophobic block) is even lower than MePEO-*b*-PCL having a degree of polymerization 42 (hydrophobic block). The lower CMC values for MePEO-*b*-PBCL clearly shows that introduction of hydrophobic benzylcarboxylate group to the PCL makes self association of block copolymers, thermodynamically more favorable. More importantly, presence of aromatic group on PCL block seems to be even more effective than elongating the PCL block in pushing the CMC to lower concentrations. It is noteworthy to mention that the CMC value for MePEO-*b*-PBCL is 5 times lower than the reported CMC for MePEO-*b*-poly(β -benzyl L-aspartate) (MePEO₁₁₀-*b*-PBLA₁₉). The CMC value for MePEO-*b*-PBLA measured by an identical method is 55×10^{-2} μM . The lower CMC of MePEO-*b*-PBCL reflects a better thermodynamic stability of this micellar structure compared to MePEO-*b*-PBLA in the biological system. The CMC for MePEO₁₁₄-*b*-PCCL₁₉ (with 100 % COOH substitution on the PCL block) was 1220×10^{-2} μM , i.e., 67 fold higher than the CMC value for MePEO₁₁₄-*b*-PCL₄₂ (Table 3.2). The significant increase in the CMC of MePEO₁₁₄-*b*-PCCL₁₉ compared to MePEO₁₁₄-*b*-PCL₄₂ is attributed to the substitution of a hydrophilic group, i.e., COOH, as well as lower degree of polymerization in the core-forming block. Copolymers having large number of COOH groups in their hydrophobic block have a lower tendency for self-association [21]. Compared to MePEO₁₁₄-*b*-PCCL₁₉, a 10 fold decrease in the CMC of block copolymer was observed for MePEO₁₁₄-*b*-PCL₁₆-*co*-PCCL₁₀ (Table 3.2). This may be due to an increase in the degree of polymerization in the

core-forming block from 19 to 26, the introduction of hydrophobic PCL and/or a reduction in the number of free COOH groups on the PCL backbone. At a similar degree of polymerization for the core forming block (26-30), a decrease in the ratio of COOH substituted ϵ -caprolactone to ϵ -caprolactone in the core forming block from 10 to 5 led to a 2.9-fold decrease in CMC (Table 3.2).

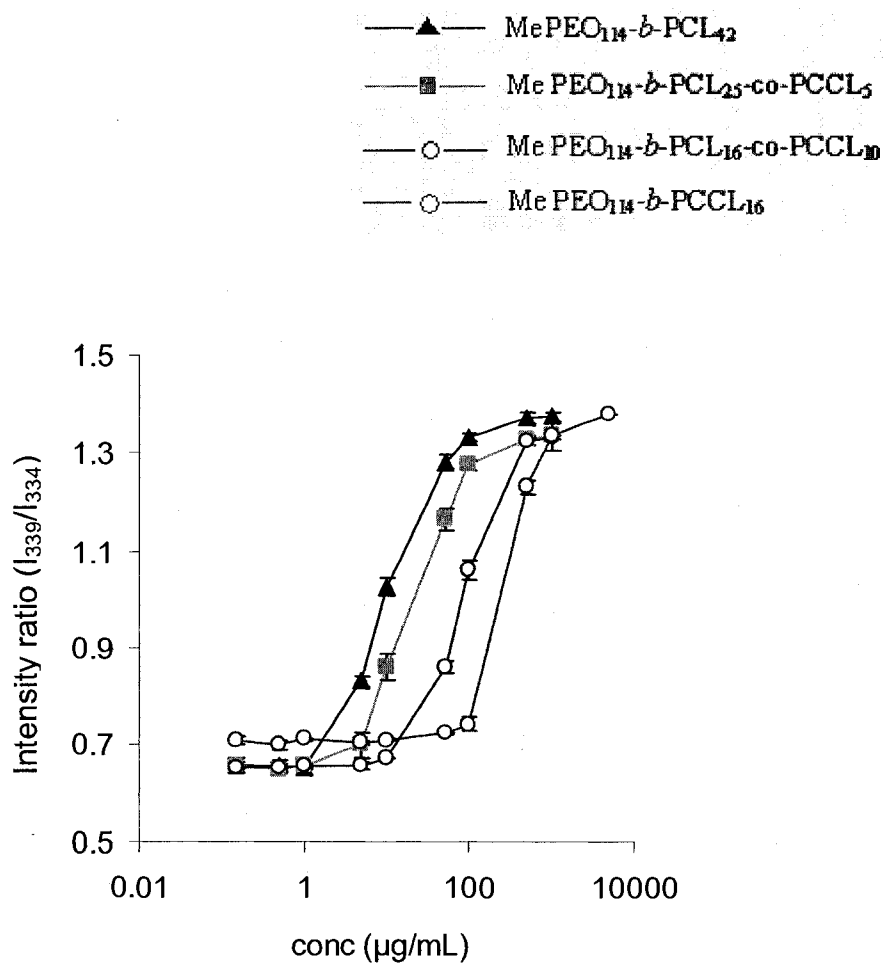


Figure 3.6- The intensity ratio (339 nm/334 nm) of pyrene (6×10^{-7} M) from excitation spectrum as a function of log concentration of different block copolymers. Each point represent average \pm SD (n=3).

These results are consistent with previous findings on the effect of core hydrophobicity on CMC value [31, 32]. Therefore, controlled introduction of aromatic or carboxylic group in the MePEO-*b*-PCL backbone may be used to adjust the CMC and stability of resulted polymeric micelles.

Evidence for the limited motion in the core of MePEO-*b*-PCL based micelles prepared in this study was obtained from the fluorescence emission spectra of 1,3-(1,1'-dipyrenyl) propane in the presence of block copolymers at concentration above CMC (~1000 µg/mL) [31, 33]. Very low excimer to monomer (I_c / I_m) intensity ratios in the emission spectrum of the dipylene probe for the prepared micelles (0.025–0.055) reflects a high viscosity for the hydrophobic core. The rigidity of the micellar core is believed to be the reason for slow dissociation of polymeric micelles and controlled rate of drug release [34]. As stated in Table 3.2, I_c/I_m ratios of dipylene probe in the presence of MePEO-*b*-PBCL and MePEO-*b*-PCCL micelles was significantly lower than unfunctionalized MePEO-*b*-PCL micelles ($p < 0.05$, unpaired student's t test) reflecting the presence of more rigid core in the aromatic or carboxylic group bearing micelles. No significant change in I_c/I_m ratios of dipylene probe was detected between MePEO-*b*-PBCL and MePEO-*b*-PCCL micelles ($p > 0.05$, unpaired student's t test). This may be due to the formation of strong intra-micellar π - π interactions between the aromatic rings of PBCL or hydrogen bonding between the carboxylic groups of the PCCL core. MePEO-*b*-PCL₂₅-*co*-PCCL₅ block copolymer had significantly higher I_c/I_m ratio (0.035) than MePEO-*b*-PCL₁₆-*co*-PCCL₁₀ (0.027) and MePEO-*b*-PCCL₁₆ (0.025) block polymers ($p < 0.05$, unpaired student's t test). The lower rigidity of the micellar core in this particular structure may be due to the presence of less carboxyl

substituents where intramicellar hydrogen bonding between carboxyl groups of the core are less significant than the block copolymers containing higher carboxyl substitution.

Further proof for the formation of core/shell structures from prepared block copolymers in an aqueous environment and limited mobility of the inner core of MePEO-*b*-PCL based micelles was obtained by ^1H NMR spectroscopy in D_2O (Figure 3.7). Due to the limited mobility of the inner core of polymeric micelles in D_2O , the intensity of proton peaks originated from the core forming block reduced dramatically compared to the one in CDCl_3 or DMSO-d_6 where the formation of micelle is not expected. Small broad peaks at δ 7.4 ppm (Figure 3.7 A) and δ 1.2-2.0 ppm (Figure 3.7 A and B) characteristics of the protons of the aromatic and ϵ -caprolactone of PBCL and PCCL segment shows restricted motions of these protons compared to the ^1H NMR spectrum of the same block copolymers in CDCl_3 or DMSO-d_6 (Figure 3.2 A and B).

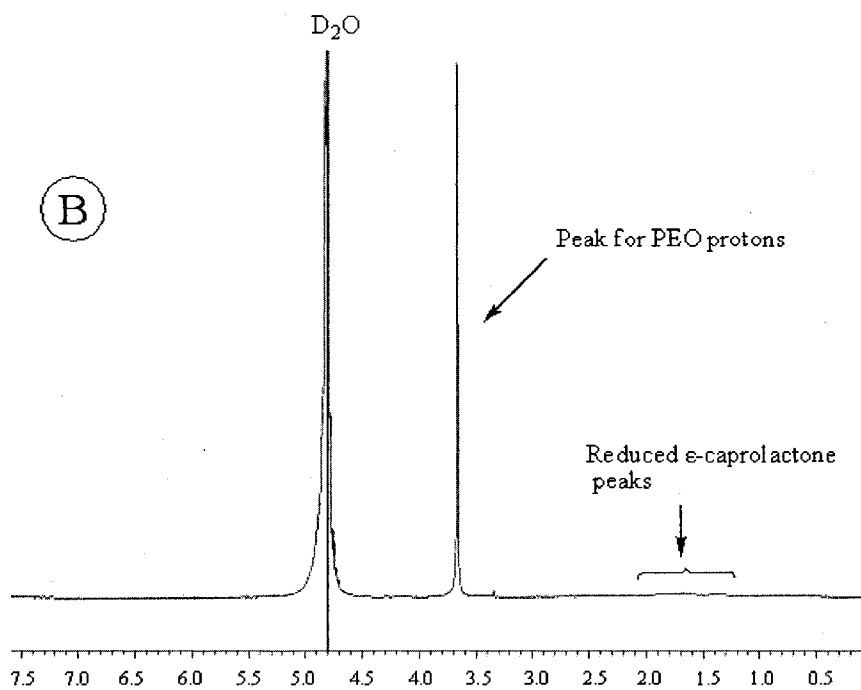
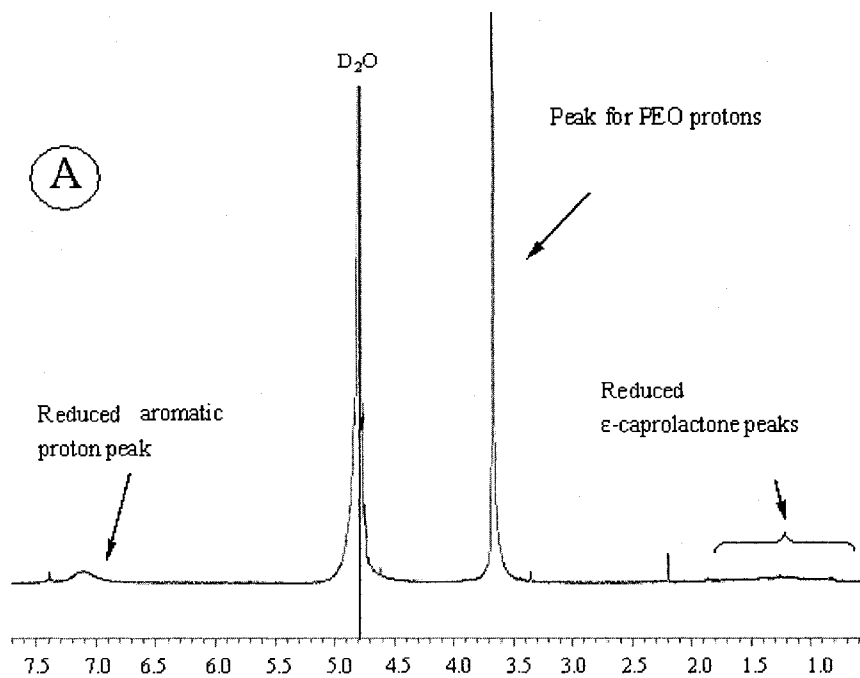
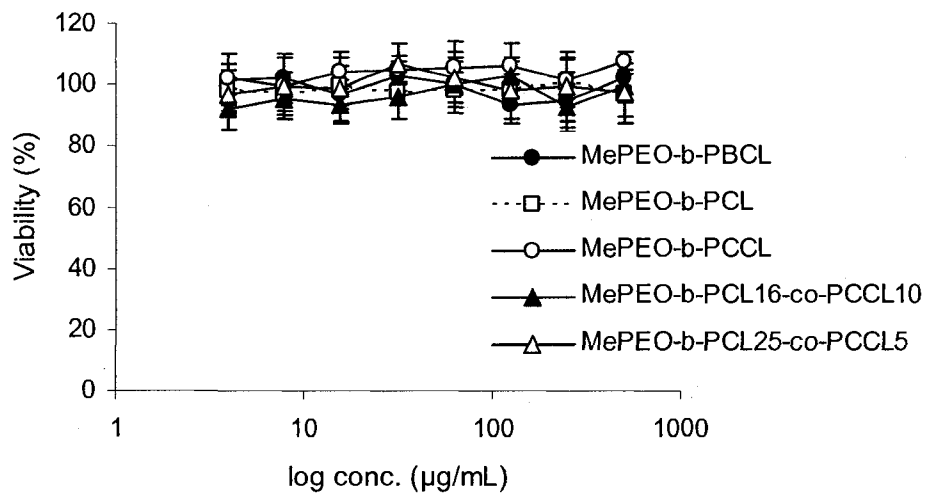


Figure 3.7- ^1H NMR spectrum of **A)** MePEO-*b*-PBCL and **B)** MePEO-*b*-PCCL block copolymer micelles in D_2O . Limited mobility of the core forming block has been demonstrated from the reduced ϵ -caprolactone peaks in the ^1H NMR spectrum.

3.3.5. Assessing the biocompatibility of prepared block copolymers- Biocompatibility of the novel self associating block copolymers developed here was assessed by cytotoxicity study against human fibroblast cells and *in vitro* hemolysis study against rat RBCs. MePEO-*b*-PCL, MePEO-*b*-PBCL, MePEO-*b*-PCCL, MePEO-*b*-PCL₁₆-*co*-PCCL₁₀, and MePEO-*b*-PCL₂₅-*co*-PCCL₅ block copolymers demonstrated a very low degree of cytotoxicity with relative cell viability above 90% for all copolymer concentrations (ranging from 5 to 500 µg/mL) (Figure 3.8 A). Even at highest copolymer concentration of all the block copolymers, there was no significant decrease in cell viability relative to controls following 24 h incubation period. In hemolysis study, micelles prepared from the synthesized block copolymers did not show any significant degree of hemolysis of rat RBCs, while 100 % hemolysis was obtained by 1000 µg/mL of triton-X 100 (Figure 3.8 B). At highest polymer concentration (500 µg/mL) the percent hemolysis obtained for MePEO-*b*-PCL, MePEO-*b*-PBCL, MePEO-*b*-PCCL, MePEO-*b*-PCL₁₆-*co*-PCCL₁₀, and MePEO-*b*-PCL₂₅-*co*-PCCL₅ block copolymers were 2.7, 2.5, 2.4, 0.08 and 0.5 %, respectively. These results provide a preliminary indication that this copolymer is suitable for biomedical applications such as drug delivery.

A)



B)

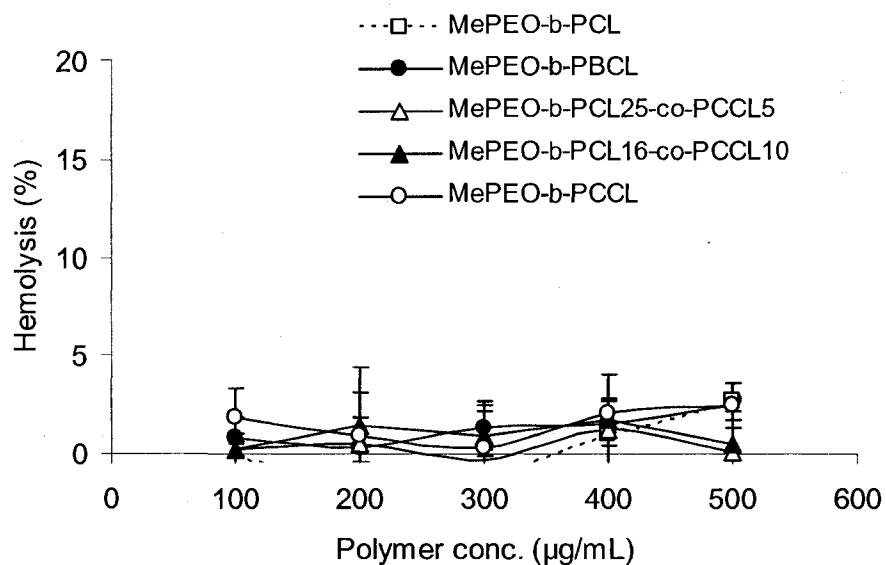


Figure 3.8- *In vitro* biocompatibility assessment of MePEO-*b*-PCL, MePEO-*b*-PBCL, MePEO-*b*-PCCL, MePEO-*b*-PCL₂₅-*co*-PCCL₅ and MePEO-*b*-PCL₁₆-*co*-PCCL₁₀ block copolymers: **A)** cytotoxicity study against human fibroblast cells; and **B)** hemolysis study against RBCs. The cell viabilities are expressed as a function of the logarithm of the copolymer concentrations. Each experiment was performed in triplicate, and results are plotted as the mean \pm SD.

3.4. Conclusion

A family of novel biodegradable MePEO-*b*-poly(ester) block copolymers having functional pendant α -benzylcarboxylate or carboxyl group attached to the core forming block was successfully synthesized and self assembled to polymeric micelles possessing different tailorable properties related to drug delivery application. Biocompatible MePEO-*b*-PCL micelles with benzylcarboxylate and carboxyl groups in the micellar core may serve as new polymeric micellar delivery systems for the chemical conjugation, optimized solubilization and controlled delivery of several therapeutic agents.

3.5. References

- [1] S. Gimenez, S. Ponsart, J. Coudane, M. Vert, *J Bioact Compat Pol* 16 (2001) 32-46.
- [2] J. Mauduit, N. Bukh, M. Vert, *Journal of Controlled Release* 23 (1993) 209-220.
- [3] L.S. Nair, C.T. Laurencin, *Progress in Polymer Science* 32 (2007) 762-798.
- [4] C.G. Pitt, M.M. Gratzl, A.R. Jeffcoat, R. Zweidinger, A. Schindler, *Journal of Pharmaceutical Sciences* 68 (1979) 1534-1538.
- [5] T. Nakanishi, S. Fukushima, K. Okamoto, M. Suzuki, Y. Matsumura, M. Yokoyama, T. Okano, Y. Sakurai, K. Kataoka, *Journal of Controlled Release* 74 (2001) 295-302.
- [6] M. Yokoyama, S. Fukushima, R. Uehara, K. Okamoto, K. Kataoka, Y. Sakurai, T. Okano, *J Control Release* 50 (1998) 79-92.
- [7] A. Lavasanifar, J. Samuel, S. Sattari, G.S. Kwon, *Pharm Res* 19 (2002) 418-422.
- [8] Y. Li, G.S. Kwon, *Pharm Res* 17 (2000) 607-611.
- [9] N. Nishiyama, Y. Kato, Y. Sugiyama, K. Kataoka, *Pharm Res* 18 (2001) 1035-1041.
- [10] M. Yokoyama, A. Satoh, Y. Sakurai, T. Okano, Y. Matsumura, T. Kakizoe, K. Kataoka, *J Control Release* 55 (1998) 219-229.
- [11] H.M. Aliabadi, D.R. Brocks, A. Lavasanifar, *Biomaterials* 26 (2005) 7251-7259.
- [12] H.M. Aliabadi, A. Mahmud, A.D. Sharifabadi, A. Lavasanifar, *J Control Release* 104 (2005) 301-311.
- [13] C. Allen, A. Eisenberg, J. Mrcic, D. Maysinger, *Drug Delivery* 7 (2000) 139-145.
- [14] C. Allen, J.N. Han, Y.S. Yu, D. Maysinger, A. Eisenberg, *Journal of Controlled Release* 63 (2000) 275-286.
- [15] C. Allen, Y.S. Yu, D. Maysinger, A. Eisenberg, *Bioconjugate Chemistry* 9 (1998) 564-572.
- [16] M.L. Forrest, C.Y. Won, A.W. Malick, G.S. Kwon, *J Control Release* 110 (2006) 370-377.
- [17] S.Y. Kim, Y.M. Lee, *Biomaterials* 22 (2001) 1697-1704.
- [18] S.Y. Kim, Y.M. Lee, H.J. Shin, J.S. Kang, *Biomaterials* 22 (2001) 2049-2056.
- [19] B. Shi, C. Fang, M.X. You, Y. Zhang, S.K. Fu, Y.Y. Pei, *Colloid Polym Sci* 283 (2005) 954-967.
- [20] G. Kwon, M. Natio, M. Yokoyama, T. Okano, Y. Sakurai, K. Kataoka, *Journal of Controlled Release* 48 (1997) 195-201.
- [21] J. Lee, E.C. Cho, K. Cho, *J Control Release* 94 (2004) 323-335.
- [22] V.P. Sant, D. Smith, J.C. Leroux, *J Control Release* 97 (2004) 301-312.
- [23] C. Batalini, L.W. Bieber, *Eclat Quim* 26 (2001) 69-76.
- [24] A. Mahmud, A. Lavasanifar, *Colloids Surf B Biointerfaces* 45 (2005) 82-89.
- [25] M.L. Yuan, Y.H. Wang, X.H. Li, C.D. Xiong, X.M. Deng, *Macromolecules* 33 (2000) 1613-1617.
- [26] Y. Kimura, K. Shirotani, H. Yamane, T. Kitao, *Macromolecules* 21 (1988) 3338-3340.
- [27] S. Ponsart, J. Coudane, M. Vert, *Biomacromolecules* 1 (2000) 275-281.
- [28] X.D. Lou, C. Detrembleur, R. Jerome, *Macromol Rapid Comm* 24 (2003) 161-172.

- [29] M. Trollsas, V.Y. Lee, D. Mecerreyes, P. Lowenhielm, M. Moller, R.D. Miller, J.L. Hedrick, *Macromolecules* 33 (2000) 4619-4627.
- [30] K. Yasugi, Y. Nagasaki, M. Kato, K. Kataoka, *J Control Release* 62 (1999) 89-100.
- [31] A. Lavasanifar, J. Samuel, G.S. Kwon, *Colloids Surf B Biointerfaces* 22 (2001) 115-126.
- [32] R. Nagarajan, K. Ganesh, *Macromolecules* 22 (1989) 4312-4325.
- [33] J. Georges, *Spectrochim Acta Rev* 13 (1990) 27-45.
- [34] Kazunori Kataoka, Glenn S. Kwon, Masayuki Yokoyama, Teruo Okano, Yasuhisa Sakurai, *Journal of Controlled Release* 24 (1993) 119-132.

Chapter 4

Development of novel polymeric micellar drug conjugates and nanocontainers with hydrolysable core structure for doxorubicin delivery

A version of this chapter has been accepted for publication: Abdullah Mahmud, Xiao-Bing Xiong, and Afsaneh Lavasanifar, *European journal of pharmaceutics and biopharmaceutics*; (2008) In press.

4.1. Introduction

Development of new dosage forms that can change the normal fate of drugs in a biological system and direct them towards their cellular or sub-cellular targets has been the focus of many pharmaceutical research efforts during the past few decades. Nanodelivery systems of appropriate stability, size, and surface properties have been designed that can avoid penetration through continuous capillary in normal tissue, escape glomerular filtration in kidneys, evade uptake by the reticuloendothelial system (RES), thus, circulate for longer periods in blood and eventually accumulate in solid tumors through enhanced permeability and retention (EPR) phenomenon. However, tumor accumulation of the carrier does not guarantee the preferential access of the incorporated drug to its targets. For efficient drug targeting, in addition to the above mentioned qualities, the carrier should be able to retain the incorporated drug during blood circulation and preferentially release it in the extracellular space or appropriate intracellular organelle in tumor. Polymeric micelles have gained a lot of interest as promising delivery systems for drug targeting as they appear to have the potential for fulfilling several of these criteria [1-3]. Polymeric micelles have the right dimension and required surface properties for tumor accumulation as a result of EPR effect. More importantly, the structure of the core and shell in polymeric micelles can be chemically manipulated to achieve the required micellar stability, drug release and cellular interaction profile for the incorporated drug. In this context, the presence of free functional groups on micelle forming block copolymers is considered an important advantage. It allows for chemical manipulation of block copolymer structure for optimized drug delivery related properties [4-10].

In the previous chapter, we reported on the successful synthesis and assembly of novel PEO-*b*-poly(ester) copolymers bearing several functional side groups on the poly(ester) chain, i.e., methoxy poly(ethylene oxide)-*block*-poly(α -benzylcarboxylate- ϵ -caprolactone) (MePEO-*b*-PBCL) and MePEO-*b*-poly(α -carboxyl- ϵ -caprolactone) (MePEO-*b*-PCCL) [11]. In this chapter, we report on the successful conjugation of doxorubicin (DOX) to the pendant carboxyl groups of MePEO-*b*-PCCL by an amide bond. This has led to the formation of novel self associating MePEO-*b*-P(CL-DOX) conjugate that bear a hydrolysable polymeric backbone (i.e., PCL) and at the same time accommodate several DOX molecules per polymer chain. Chemical conjugation of DOX to the polymeric micellar core in MePEO-*b*-P(CL-DOX) is expected to reduce the chance of premature drug release outside tumor tissue. On the other hand, since PCL backbone is prone to hydrolysis especially in acidic environment, core degradation followed by micellar dissociation and release of DOX-caprolactone (DOX-CL) derivatives may be facilitated in the acidic environment of tumor extracellular space or in the endosome/lysosomes after endocytosis of MePEO-*b*-P(CL-DOX) micelles by tumor cells. The validity of this assumption was tested in this study assessing the possibility of polymeric chain cleavage for MePEO-*b*-P(CL-DOX) in acidic medium by gel permeation chromatography (GPC). In further studies, in an effort to develop novel polymeric micellar nanocontainers for DOX delivery, the effect of manipulations in the chemical structure of the micellar core in MePEO-*b*-PCL micelles on physical encapsulation of DOX were assessed. Finally, to define the superior polymeric micellar design and structure for targeted DOX delivery, the *in vitro* release and cytotoxicity of conjugated DOX as part of MePEO-*b*-P(CL-DOX) micelles was investigated and compared to that of physically encapsulated DOX in MePEO-*b*-PCL, MePEO-*b*-PBCL, MePEO-*b*-PCCL and MePEO-*b*-P(CL-DOX) nano-containers.

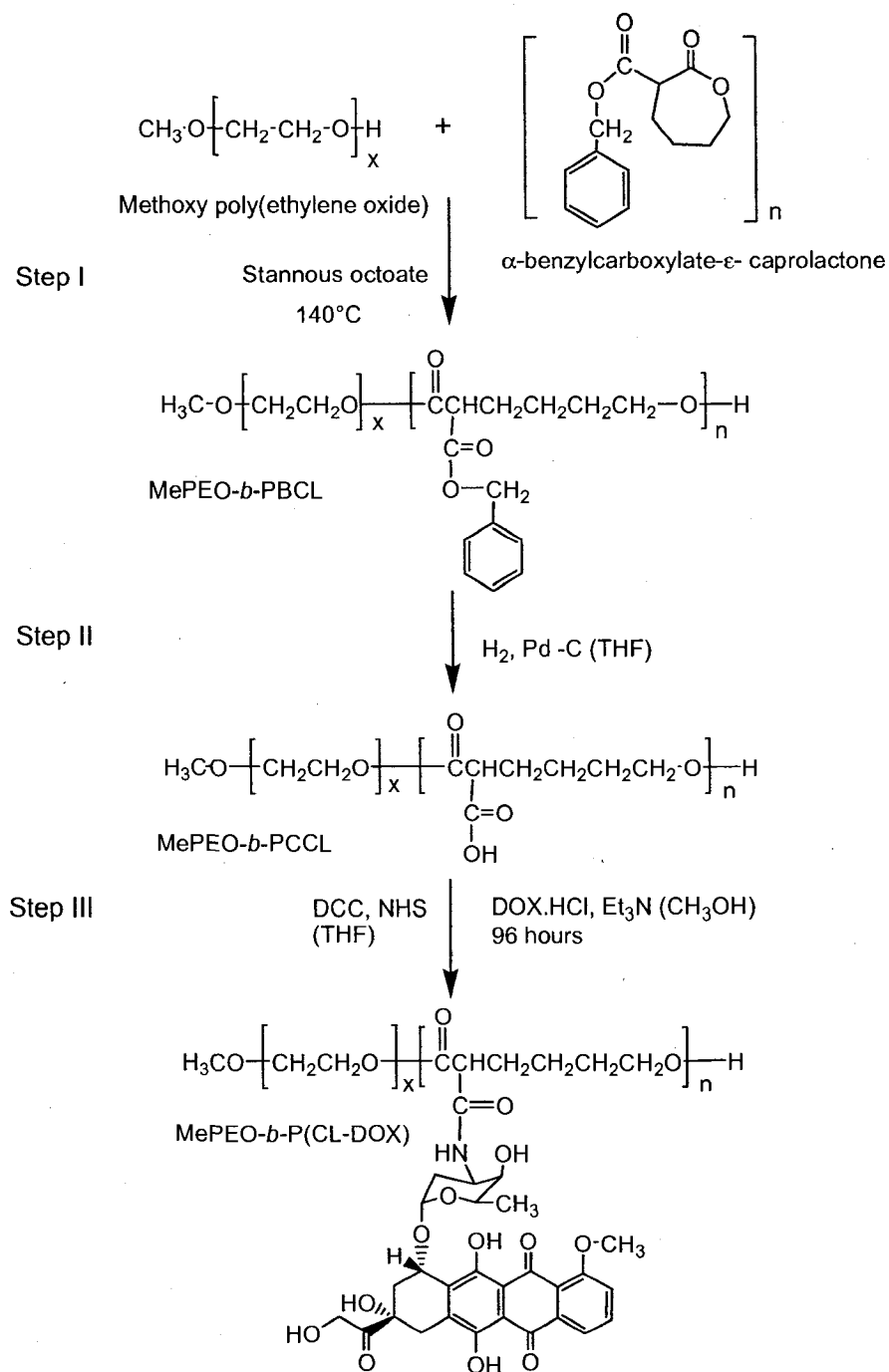
4.2. Experimental section

4.2.1. Materials- MePEO (average molecular weight of 5000 g mol^{-1}), diisopropyl amine (99%), benzyl chloroformate (tech. 95%), sodium (in Kerosin), butyl lithium (Bu-Li) in hexane (2.5 M Solution), palladium coated charcoal, N, N dicyclohexyl carbodiimide (DCC), N-hydroxy succinimide (NHS), triethylamine, and pyrene were purchased from Sigma chemicals (St. Louis, MO, USA). ϵ -caprolactone was purchased from Lancaster Synthesis, UK. DOX.HCl was purchased from Hisun Pharmaceutical Co. (Zhejiang, China). Stannous octoate was purchased from MP Biomedicals Inc, Germany. Fluorescent probe 1,3-(1,1'-dipyrenyl)propane was purchased from Molecular Probes, USA. Sephadex LH20 was purchased from Amersham Biosciences (Sweden). Cell culture media RPMI 1640, penicillin-streptomycin, fetal bovine serum, L-glutamine and HEPES buffer solution (1 M) were purchased from GIBCO, Invitrogen Corp. All other chemicals were reagent grade.

4.2.2. Synthesis of MePEO-*b*-P(CL-DOX) and its characterization- Synthesis of MePEO-*b*-P(CL-DOX) was accomplished in 3 steps: I) ring opening polymerization of functionalized caprolactone with MePEO to prepare MePEO-*b*-PBCL; II) reduction of MePEO-*b*-PBCL to MePEO-*b*-PCCL; and III) conjugation of DOX to free carboxyl groups of MePEO-*b*-PCCL (Scheme 4.1). Synthesis of functionalized monomer, i.e., α -benzyl carboxylate- ϵ -caprolactone, preparation of core functionalized block copolymers, MePEO-*b*-PBCL and MePEO-*b*-PCCL have been described in previous chapter (Chapter 3, section 3.2.2).

For the conjugation of DOX to MePEO-*b*-PCCL, NHS (17.3 mg, 0.15 mM) and DCC (31 mg, 0.15 mM) were added to a stirred solution of MePEO-*b*-PCCL (MW: 7530 g mol^{-1}) (200 mg, 0.03 mM) in anhydrous tetrahydrofuran (THF) (15 mL) under nitrogen.

The reaction mixture was stirred for 2 h at room temperature. A solution of DOX.HCl (34.8 mg 0.06 mM) and triethylamine (Et₃N) (16.8 μL, 0.12 mM) in anhydrous methanol (2 mL) was then added and the reaction continued for additional 96h. Thin layer chromatography in the presence of butan-1-ol: acetic acid: water (4:1:4) as the mobile phase was used to monitor the reaction progress. Evaporation of the reaction mixture gave a residue that was dissolved in HPLC grade methanol (10 mL). The product was purified twice using Sephadex LH 20 column and methanol as eluent to remove the unreacted DOX and any other by-product. The produced MePEO-*b*-P(CL-DOX) was lyophilized to a deep orange powder for further use.



Scheme 4.1- Synthetic scheme for the preparation of MePEO-*b*-P(CL-DOX) block copolymer

Prepared block copolymers were characterized for their number average molecular weight (M_n), weight average molecular weight (M_w) and polydispersity (M_w/M_n) by ^1H NMR and GPC. ^1H NMR was carried out by a Bruker Unity-300 spectrometer at room temperature, using deuterated dimethyl sulfoxide (DMSO-d_6) or deuterated chloroform (CDCl_3) as solvent. Gel permeation chromatography was carried out at 25°C with an HP instrument equipped with Waters Styragel HT4 column (Waters Inc., Milford, MA). The elution pattern was detected at 35°C by refractive index (PD2000, Percision Detectors, Inc.)/light scattering (Model 410, Waters Inc) detectors. THF was used as eluent at a flow rate of 1.0 mL/min . The column was calibrated with a series of standard polystyrenes of varying molecular weights (M_w : from 4750 g.mol^{-1} to 13700 g.mol^{-1}).

4.2.3. Measurement of DOX conjugated levels- Reversed phase HPLC was carried out with a $10\ \mu\text{m}$ C18-125 Å column ($3.9 \times 300\text{ mm}$, Waters) heated at $40\ ^\circ\text{C}$ using a Waters 625 LC system. Samples of $20\ \mu\text{L}$ were injected in a gradient elution using 0.05% trifluoroacetic acid aqueous solution and acetonitrile at a flow rate of 1.0 mL/min . The percentage of acetonitrile in the mobile phase was 15% at time 0, which was increased to 85% within 15 minutes at a constant rate. The detection was performed at 485 nm using a Waters 486 tunable UV/Vis absorbance detector. The level of conjugated DOX was estimated from the integration of MePEO-*b*-P(CL-DOX) related peak in HPLC and also UV/Vis spectroscopy for MePEO-*b*-P(CL-DOX) at 485 nm based on a calibration curve of free DOX under the same HPLC condition assuming an identical molar absorptivity for free DOX and polymer conjugated DOX.

4.2.4. Self assembly of block copolymers and physical encapsulation of DOX in the assembled structures- Self assembly of block copolymers was accomplished through a co-solvent evaporation method where block copolymer (10 mg) was dissolved in THF (2 mL) and added to doubly distilled water (10 mL) in a drop-wise manner under moderate stirring. After 4 h of stirring at room temperature, vacuum was applied to ensure the complete removal of organic solvent. Encapsulation of DOX in MePEO-*b*-PCL, MePEO-*b*-PBCL, MePEO-*b*-PCCL and MePEO-*b*-P(CL-DOX) micelles was carried out by an identical procedure with 1 mg of DOX and 20 μ L of triethylamine added to the polymeric THF solution at the initial step. During encapsulation, the glycosidic amino group in DOX was deprotonated in the presence of triethylamine to increase the hydrophobicity of DOX. All the resulting micellar solutions were dialyzed (Spectra Por, MW cut off 3,500 Da) against distilled water for 8 h exchanging the medium at 2 h intervals to remove un-encapsulated DOX.

4.2.5. Characterization of polymeric micelles- A change in the fluorescence excitation spectra of pyrene in the presence of varied concentrations (0.1 μ g/mL to 500 μ g/mL) of MePEO-*b*-P(CL-DOX) block copolymer was used to measure its CMC according to the method described in previous chapter (Chapter 2, section 2.2.3). The viscosity of prepared micellar core was estimated at a polymer concentration of 500 μ g/mL by measuring excimer to monomer intensity ratio (I_c/I_m) from the emission spectra of 1,3-(1,1'-dipyrenyl)propane at 373 and 480 nm, respectively, according to the method described in previous chapter (Chapter 2, section 2.2.3). Average diameters and size distribution of prepared micelles were estimated by dynamic light scattering (DLS) using Malvern Zetasizer 3000 at a polymer concentration of 10 mg/mL.

The level of entrapped DOX in polymeric micelles was determined in an aliquot of the micellar solution in water (200 μ L) diluted 5 times with DMSO using DOX absorbance at 485 nm by a UV/Vis spectrophotometer (Beckman DU 640, USA). A calibration curve was constructed using different concentrations of free DOX (1-50 μ g/mL) in an identical solvent mixture. The level of DOX loading and encapsulation efficiency were calculated from the following equations:

$$\text{DOX loading } [M(\text{DOX})/M(\text{monomer})](\%) = \frac{\text{Moles of loaded DOX}}{\text{Moles of monomer}} \times 100 \quad (\text{Eq. 4.1})$$

$$\text{DOX loading } [\text{weight} / \text{weight}](\%) = \frac{\text{amount of loaded DOX in mg}}{\text{amount of copolymer in mg}} \times 100 \quad (\text{Eq. 4.2})$$

$$\text{DOX loading } [M(\text{DOX})/M(\text{copolymer})](\%) = \frac{\text{Moles of loaded DOX}}{\text{Moles of copolymer}} \times 100 \quad (\text{Eq. 4.3})$$

$$\text{Encapsulation efficiency } (\%) = \frac{\text{amount of loaded DOX in mg}}{\text{amount of DOX added in mg}} \times 100 \quad (\text{Eq. 4.4})$$

The level of physically loaded DOX in MePEO-*b*-P(CL-DOX) was calculated by deducting the level of chemically conjugated DOX (obtained by HPLC measurement as described above) from the total DOX content.

4.2.6. Release of DOX from polymeric micelles- DOX loaded micellar solutions (15 mL) were prepared at 1 mg/mL polymer concentration from MePEO-*b*-PCL, MePEO-*b*-PBCL, MePEO-*b*-PCCL and MePEO-*b*-P(CL-DOX) block copolymers according to the above mentioned method. The micellar solutions were transferred into a dialysis bag (Mw cutoff: 3,500 Da, supplied by Spectrum Laboratories, USA). The dialysis bags were placed in 500 mL of phosphate buffer (pH 7.4) or acetate buffer (pH: 5.0) solutions. Release study was

performed at 37 °C in a Julabo SW 22 shaking water bath (Germany). At selected time intervals, 200 µL of micellar solution was withdrawn from inside the dialysis bag for UV/Vis analysis. DOX concentration was calculated based on the absorbance intensity at 485 nm as described in the previous section. An identical procedure was performed to investigate the level of DOX release from MePEO-*b*-P(CL-DOX) conjugates. For this test group, at the end of the study, a sample of the remained polymer in the dialysis bag was dialyzed against distilled water for 8 hours to remove the dissolved salt in the micellar solution. The sample was freeze dried, dissolved in THF, centrifuged and injected to the GPC system to assess the possibility of chain cleavage by hydrolysis for MePEO-*b*-P(CL-DOX) block copolymers. The condition used in GPC was identical to what described for polymer characterization.

4.2.7. Assessing the hydrolysis of poly(ester) core in MePEO-*b*-P(CL-DOX) micelles-

Micellar solution of MePEO-*b*-P(CL-DOX) in acetate buffer (pH 5.0) was prepared at a polymer concentration of 1 mg/mL. Prepared micellar solution (3 mL) was incubated in a closed vial at 37 °C in a Julabo SW 22 shaking water bath (Germany). After 72 hours, micellar solution was withdrawn from incubation and freeze dried. The freeze dried MePEO-*b*-P(CL-DOX) micelles were dissolved in THF and centrifuged at 12000 ×g to remove the salt and other insoluble ingredients. A sample (20 µL) of this solution was injected to the GPC system. The condition used in GPC was identical to what described for polymer characterization. The eluent from the GPC system was analyzed by mass spectroscopy (Waters, Micromass ZQ™ 4000 Quadrupole Mass Analyser, USA)

4.2.8. In-vitro cytotoxicity of polymeric micellar DOX nanocontainers and drug conjugate against mouse melanoma cells- The cytotoxicity of free DOX, MePEO-*b*-

P(CL-DOX) conjugates and DOX loaded MePEO-*b*-PCL, MePEO-*b*-PBCL and MePEO-*b*-P(CL-DOX) block copolymer micelles against B16F10 murine melanoma cells was investigated using 3-(4,5-dimethylthiazol-2-yl)-2,5-diphenyltetrazolium bromide (MTT) assay. The cells were grown in RPMI 1640 complete growth media supplemented with 10 % fetal bovine serum, 1% L-glutamine, 100 units/mL penicillin and 100 µg/mL streptomycin and maintained at 37 °C with 5% CO₂ in a tissue culture incubator. In the logarithmic growth phase the cells were harvested and seeded into 96-well plates at a density of 5×10^3 cells/well in 100 µL of RPMI 1640 media. After 24 h when the cells had adhered, micellar solutions and free DOX at different concentrations were incubated separately with the cells for 24 and 48 h. After this time, MTT solution (20 µL; 5mg/ml in sterile-filtered PBS) was added to each well and the plates were re-incubated for further 3 h. The yellow MTT is reduced to purple formazan in the mitochondria of living cells. The formazan crystals were dissolved in DMSO, and the absorbance was read by a Power Wave _x 340 microplate reader (Bio-Tek Instruments, Inc. USA) at 550 nm. Percentage of cell viability was plotted against logarithm of DOX concentration and used to calculate the DOX concentration required to inhibit the growth of 50% of the cell population (IC₅₀).

4.2.9. Statistical analysis- Data are reported as mean \pm standard deviation (S.D.). Differences among the mean of formulation characteristics for polymeric micelles were compared by either one-way analysis of variance (ANOVA) followed by the Student–Newman–Keuls post hoc test for multiple comparisons using Sigma stat software or Student’s unpaired t-test assuming unequal variance. Differences between means of IC₅₀ were assessed using One way ANOVA followed by *post hoc* analysis using Dunnett T3 test (SSPS for Windows v.13, Cary, NC). The level of significance was set at $\alpha = 0.05$.

4.3. Results

4.3.1. Synthesis of MePEO-*b*-P(CL-DOX) and its characterization- DOX conjugated MePEO₁₁₄-*b*-P(CL-DOX)₁₆ was synthesized by forming an amide bond between carboxyl groups of MePEO-*b*-PCCL and a primary amine group of DOX using DCC as coupling agent and NHS as catalyst (Scheme 4.1). The conjugation of the DOX molecule with block copolymer was confirmed by thin layer chromatography (TLC), where free DOX eluted with the solvent and showed a spot at R_f value of 0.68, but the polymer conjugated DOX did not elute and stayed at the baseline (Figure 4.3). Further evidence for the conjugation of DOX to MePEO-*b*-PCCL polymer was provided by the ¹H NMR spectrum of MePEO-*b*-P(CL-DOX) and free DOX (Figure 4.1B). ¹H NMR spectrum of MePEO-*b*-P(CL-DOX) in CDCl₃ (Figure 4.1 A) showed characteristic DOX peaks at δ 7.4-7.8 ppm as well as ¹H NMR spectrum in DMSO-*d*₆ revealed the characteristic DOX peaks (Figure 4.1 A) at δ(ppm): 5.6; 5.3; 3.6; 3.3; 2.25; 2.0; and 1.2. Similar peaks were also present in the ¹H NMR spectrum of free DOX (Figure 4.1 B). The dependence of ¹H NMR spectrum of DOX-polymer conjugates on the organic solvent used for ¹H NMR spectroscopy is due to a difference in the conformation of DOX-polymer conjugate in various organic solvents. In the HPLC chromatogram of MePEO-*b*-P(CL-DOX) block copolymer, peak related to free DOX was absent (Figure 4.2). The HPLC data along with the TLC results provided evidence for the efficient removal of free DOX from the MePEO-*b*-P(CL-DOX) polymer-drug conjugate after the purification process.

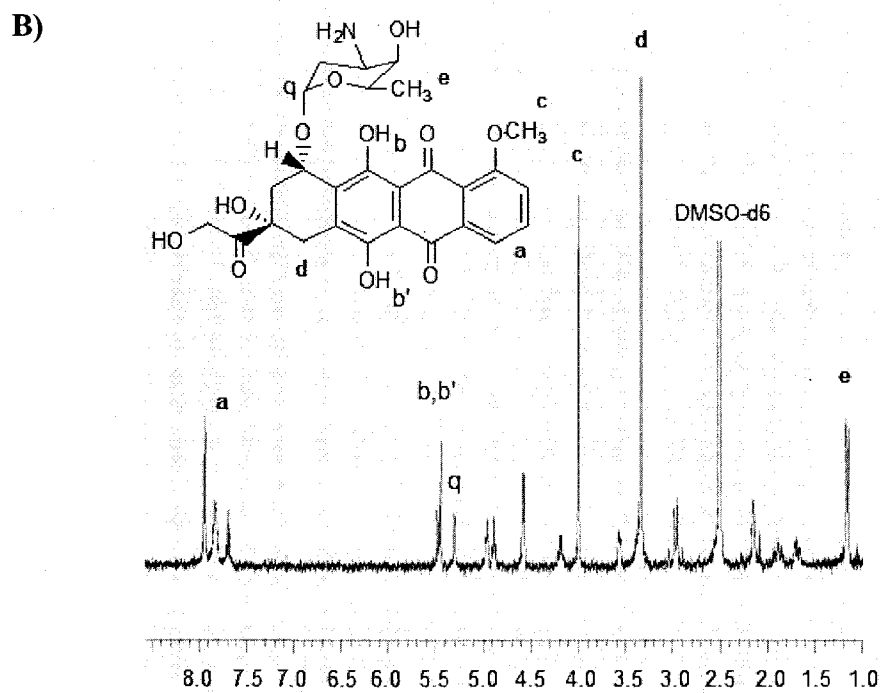
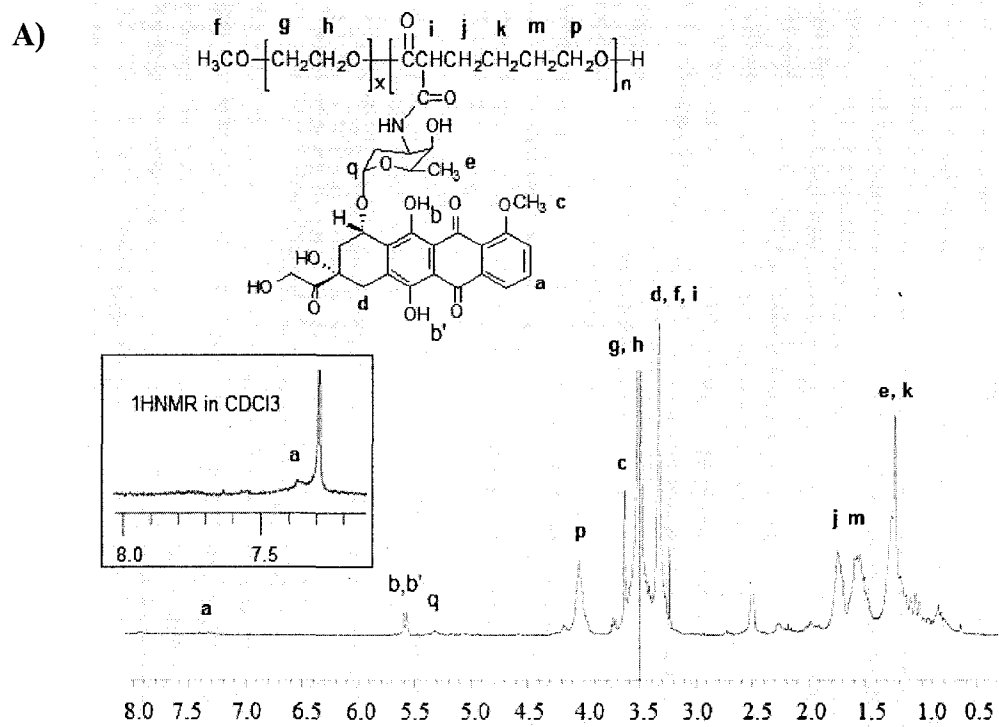


Figure 4.1- ¹H NMR spectrum and peak assignments of **A)** MePEO-*b*-P(CL-DOX) block copolymer in DMSO-*d*₆ and in CDCl₃ (Figure 4.1A, window); **B)** free DOX in DMSO-*d*₆

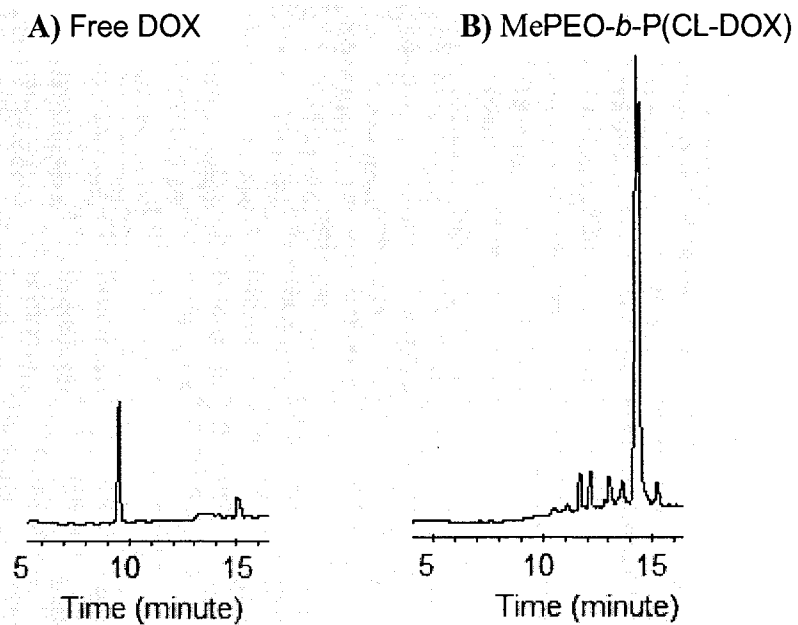


Figure 4.2- Typical HPLC chromatogram of **A)** free DOX; and **B)** MePEO-*b*-P(CL-DOX) polymer. Reversed phase chromatography was carried out with a Waters 10 μ m C18-125 Å column (3.9 \times 300 mm) in a gradient elution using 0.05% trifluoroacetic acid aqueous solution and acetonitrile.

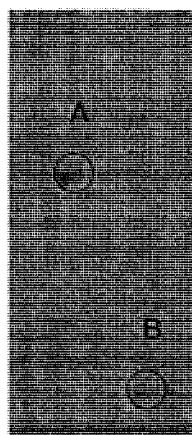


Figure 4.3- TLC chromatogram showing the spot of **A)** free DOX at R_f value of 0.68 and **B)** MePEO-*b*-P(CL-DOX) at the base line after running with butan-1-ol:acetic acid: water (4:1:4) as mobile phase.

The substitution level of DOX on the polymer backbone was 14 % (mole DOX/mole monomer) as measured by UV analysis at 485 nm, which was consistent with the DOX conjugation level, estimated from the HPLC analysis (Figure 4.2). This corresponds to 2.25 DOX molecules per MePEO₁₁₄-*b*-P(CL-DOX)₁₆ chain on average. Conjugation by DCC is known to produce low substitution of DOX on the polymeric backbone [12]. The M_n of MePEO-*b*-P(CL-DOX) obtained from ¹H NMR by comparing the peak related to methylene protons (CH₂) of PCL at δ 4.0 ppm to that for the methylene protons (CH₂-CH₂) of PEO at δ 3.5 ppm and considering the number of DOX attached to PCL chain (~2.25 for each PCL chain on average) was 8800 g.mole⁻¹. The M_n of MePEO-*b*-P(CL-DOX) block copolymer determined by GPC showed a small increase (MW=9600 g.mole⁻¹) compared to the molecular weight determined by ¹H NMR and a relatively broad molecular weight distribution (M_w/M_n = 1.47).

4.3.2. Self assembly of MePEO-*b*-P(CL-DOX) and characterization of micellar structures- Characteristics of prepared polymeric micelles is summarized in Table 4.1. The average diameter of the unloaded MePEO-*b*-PCL, MePEO-*b*-PBCL, MePEO-*b*-PCCL and MePEO-*b*-P(CL-DOX) block copolymer micelles were 40.0, 65.5, 55.3, and 81.6 nm, respectively. The broad polydispersity index (0.58) for MePEO-*b*-P(CL-DOX), indicated existence of secondary aggregation. Despite the presence of secondary association, the micellar solutions were still transparent. Secondary association of polymeric micelles has been described by several authors previously [13, 14].

Low CMC values were revealed for MePEO-*b*-PCL and MePEO-*b*-PBCL (Table 4.1), whereas MePEO-*b*-PCCL block copolymers showed lower tendency for self association reflected by higher CMC values (1.22×10^{-2} mM). DOX attachment reduced the CMC of

MePEO-*b*-PCCL by 3.5 times ($370 \times 10^{-2} \mu\text{M}$) although the polymer chain contained a considerable number of free COOH groups. A reverse relationship between the hydrophobicity of the core-forming block and CMC has been shown in many studies [15-17]. However, a decrease in the microviscosity of micelle core was observed after DOX attachment to the MePEO-*b*-PCCL, evidenced from a significantly higher I_e/I_m ratio (0.045) for MePEO-*b*-P(CL-DOX) than MePEO-*b*-PCCL micelles (0.025) ($P < 0.05$, unpaired Student's *t* test).

Table 4.1- Characteristics of empty block copolymer micelles (n=3).

Block copolymer	Average micellar size \pm SD (nm) ^a	Sec. peaks (nm)	PDI ^c	CMC ^d \pm SD (μM)	$I_e/I_m \pm$ SD ^e
MePEO ₁₁₄ - <i>b</i> -PCL ₄₂	40.0 \pm 2.0	-	0.19	$18.2 \times 10^{-2} \pm 0.01^*$	0.055 \pm .007*
MePEO ₁₁₄ - <i>b</i> -PBCL ₁₉	65.5 \pm 3.6	-	0.31	$9.8 \times 10^{-2} \pm 0.01^*$	0.028 \pm .002*
MePEO ₁₁₄ - <i>b</i> -PCCL ₁₆	55.3 \pm 4.0	-	0.15	$1220 \times 10^{-2} \pm 0.42^*$	0.025 \pm .002*
MePEO ₁₁₄ - <i>b</i> -P(CL-DOX) ₁₆	81.6 \pm 3.6	347 (60%) ^b	0.58	$370 \times 10^{-2} \pm 0.36$	0.045 \pm .030

^a Intensity mean estimated by dynamic light scattering technique.

^b Indicate the frequency of secondary peak in micellar population in percentage

^c Polydispersity index for micellar size distribution

^d Measured from the onset of a rise in the intensity ratio of peaks at 339 nm to peaks at 334 nm in the

fluorescence excitation spectra of pyrene plotted versus logarithm of polymer concentration.

^e Intensity ratio (excimer/monomer) from emission spectrum of 1,3-(1,1' dipyrenyl) propane in presence of polymeric micelle

*The data are reproduced from ref. [11, 18] for comparison.

4.3.3. Preparation of DOX loaded micelles and their characterization- The level of loaded DOX to polymer in molar ratio was found to be significantly higher for MePEO-*b*-PBCL compared to MePEO-*b*-PCL (Table 4.2). This level was significantly lower for micelles formed from MePEO-*b*-PCCL and MePEO-*b*-P(CL-DOX) block copolymers. To account for differences in the polymerization degree of hydrophobic block between block copolymers under study and demonstrate the contribution of each monomer to the drug loading efficiency in the micellar core, the mole % of loaded DOX to monomer was calculated. The loading content (mole DOX/mole monomer in core-forming block) of DOX in MePEO-*b*-PCL micelles was 2.0, which agrees well with the previously reported results [19]. Compared to MePEO-*b*-PCL, DOX loading content (mole DOX/ mole monomer in core-forming block) was increased 2.5 and 1.8 fold in MePEO-*b*-PBCL and MePEO-*b*-P(CL-DOX) micelles, respectively. The loading content of DOX (mole DOX/ mole monomer in core-forming block) in MePEO-*b*-PCCL was 2.6, slightly higher than that of MePEO-*b*-PCL ($P < 0.05$, One way ANOVA).

DOX loading did not lead to any significant change in the average size of MePEO-*b*-PCL and MePEO-*b*-PBCL micelles ($P > 0.05$, unpaired student's t test). DOX loaded MePEO-*b*-PCCL and MePEO-*b*-P(CL-DOX) nanocarriers had an average size of 120 and 125.5 nm, respectively, which was significantly higher than the size of their unloaded counterparts ($P < 0.01$, unpaired student's t test) with no sign of secondary aggregation (Table 4.2).

Table 4.2- Characteristics of DOX loaded nanocontainers (n=3).

Block copolymer Micelle	DOX loading content (%) \pm SD			Encap. efficiency (%) \pm SD	Average diameter \pm SD	PDI ^d	DOX release at 24h (%) ^e	
	DOX/ monomer (molat) ^a	DOX/ polymer (molat) ^b	DOX/ polymer (wt) ^c				pH:5.0	pH: 7.4
MePEO ₁₁₄ - <i>b</i> -PCL ₄₂	2.0 \pm 0.1	75.1 \pm 4.9	4.3 \pm 0.3	48.3 \pm 3.1	35.9 \pm 4.0	0.08	35.9 \pm 3.0	24.7 \pm 1.4
MePEO ₁₁₄ - <i>b</i> -PBCL ₁₉	5.0 \pm 0.2 [†]	83.5 \pm 1.0 [†]	5.0 \pm 0.1 [†]	54.9 \pm 1.0 [†]	63.9 \pm 2.8 [†]	0.29	20.0 \pm 1.9 [†]	13.2 \pm 1.0 [†]
MePEO ₁₁₄ - <i>b</i> -PCCL ₁₆	2.6 \pm 0.3 [†]	35.7 \pm 3.4 [†]	2.8 \pm 0.3 [†]	31.8 \pm 2.9 [†]	120 \pm 9.0 [†]	0.23	47.2 \pm 1.0 [†]	32.0 \pm 1.7 [†]
MePEO ₁₁₄ - <i>b</i> -P(CL-DOX) ₁₆	3.6 \pm 0.2 ^{††}	63.5 \pm 4.2 ^{††}	4.0 \pm 0.5 [†]	43.3 \pm 2.8 [†]	125.5 \pm 15	0.38	40.2 \pm 2.3	22.5 \pm 1.0

^a DOX loading content, calculated as moles of DOX/ moles of monomer of core forming block

^b DOX loading content, calculated as moles of DOX/ moles of copolymer

^c DOX loading content, calculated as weight of DOX/ weight of copolymer used to form micelles

^d Polydispersity index of micellar size distribution

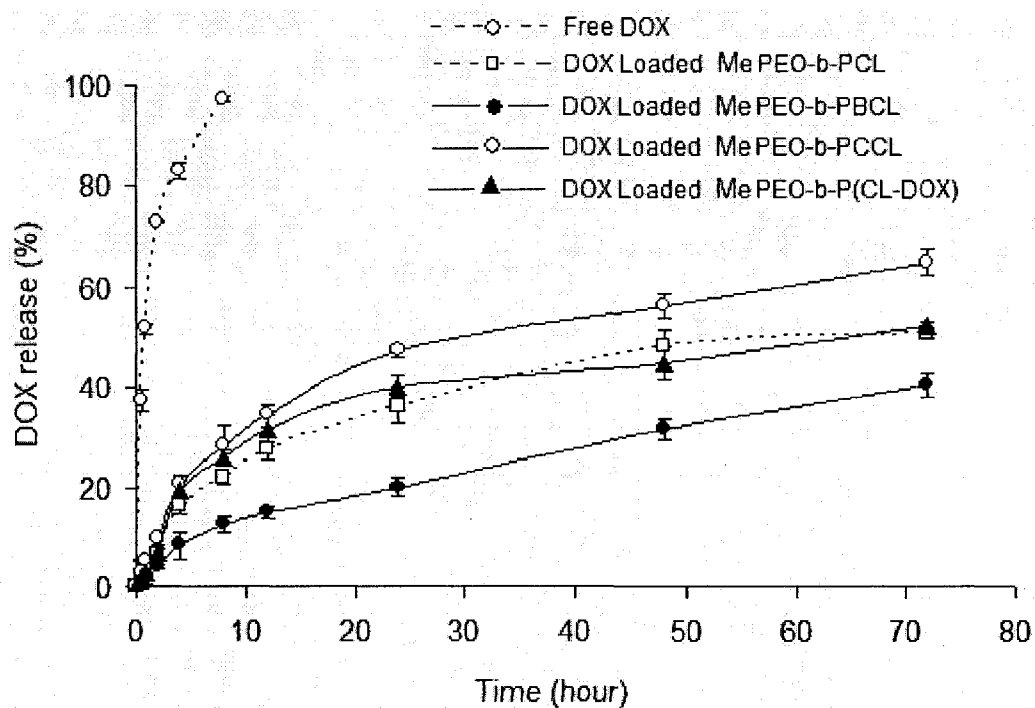
^e Release study was performed in acetate buffer (pH 5.0) and in phosphate buffer (pH 7.4)

^f The level is estimated for physically encapsulated DOX only, by subtracting the concentration of conjugated DOX from its total concentration.

[†] Significantly different from MePEO-*b*-PCL (P < 0.05)

4.3.4. Release of DOX from polymeric micelles- The release profile of DOX from micellar nano-containers and DOX-polymer conjugate was studied within 72 h; using a dialysis membrane immersed either in phosphate buffer (pH: 7.4, 0.1 M) or acetate buffer (pH: 5.0, 0.1 M) at 37 °C temperature. The concentration of copolymers was fixed at 1 mg/mL, which is much higher than their corresponding CMCs. Transfer of released DOX through dialysis membrane to buffer solution was assumed to take place rapidly, and the release of DOX from its vehicle to medium was assumed to be the rate limiting step in this process. In fact, 73% of free DOX was transferred to the release medium from the dialysis bag within 2 hours at pH 5.0 (Figure 4.4). The transfer of free DOX at pH 7.4 was slower (63% was transferred to the medium at 2h time point). The release of DOX from polymeric micelles at both pHs was strongly affected by the micellar core composition, with micelles bearing the benzyl core, i.e., MePEO-*b*-PBCL, showing the minimum rate of drug release. At pH 5, MePEO-*b*-PCL, MePEO-*b*-PBCL and MePEO-*b*-PCCL micelles released 35, 20 and 47 % of encapsulated DOX after 24 h, respectively (Table 4.2). Similar to what has been observed for free DOX, DOX release from polymeric micelles was found to be slower at pH 7.4 compared to pH 5.0, but followed the same trend between different core structures (Figure 4.4). At pH 7.4, 25, 13 and 32 % of encapsulated DOX was released from MePEO-*b*-PCL, MePEO-*b*-PBCL and MePEO-*b*-PCCL micelles after 24 h, respectively. MePEO-*b*-P(CL-DOX) micelles did not show any superiority in sustaining the release of physically loaded DOX over MePEO-*b*-PCL micelles at both pHs (Figure 4.4).

A)



B)

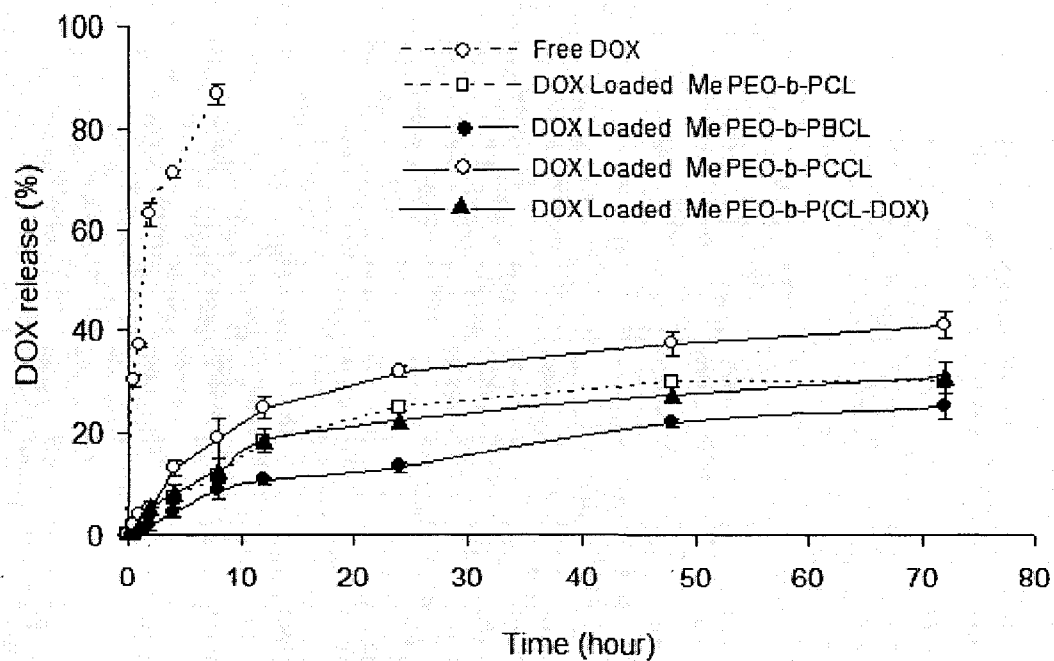


Figure 4.4- *In vitro* DOX release profile from polymeric micelles at A) pH: 5.0, and B) pH: 7.4 at 37 °C. Each point represent mean \pm SD (n=3).

No significant change in the level of DOX remained in the dialysis bag for MePEO-*b*-P(CL-DOX) conjugate was observed within the time frame of the study, reflecting the stability of the amide linkage between DOX and the polymeric backbone (data not shown). To assess the possibility of poly(ester) cleavage, a sample from the remained MePEO-*b*-P(CL-DOX) in the dialysis bag at the end of the release study was freeze-dried, dissolved in THF and injected to the GPC system. No significant change in the retention time of the polymer related peak was observed, but the polydispersity of MePEO-*b*-P(CL-DOX) at pH 5.0 was reduced from 1.47 to 1.20 after the release study pointing to a possibility for chain cleavage in the poly(ester) backbone.

4.3.5. Hydrolysis of poly(ester) core of MePEO-*b*-P(CL-DOX) micelles- GPC analysis revealed a dramatic change in the retention time of MePEO-*b*-P(CL-DOX) block copolymer from 9.6 minute to 10.3 minute after its incubation in a closed vial at pH 5.0 for 72 hours at 37 °C (Figure 4.5). Also, the generation of a new peak at 11.3 minutes which was absent in the GPC chromatogram of MePEO-*b*-P(CL-DOX) before incubation at pH 5.0 (Figure 4.5) strongly implicated the possibility for the hydrolysis of poly(ester) core at acidic pH after 72 hours. Analysis of the eluent at 11.3 minutes by mass spectroscopy revealed the presence of a peak at *m/z* of 701 (data not shown) corresponding to DOX-(6-hydroxy caproic acid), i.e., the possible product of PCL chain cleavage in MePEO-*b*-P(CL-DOX) block copolymers at pH 5.0.

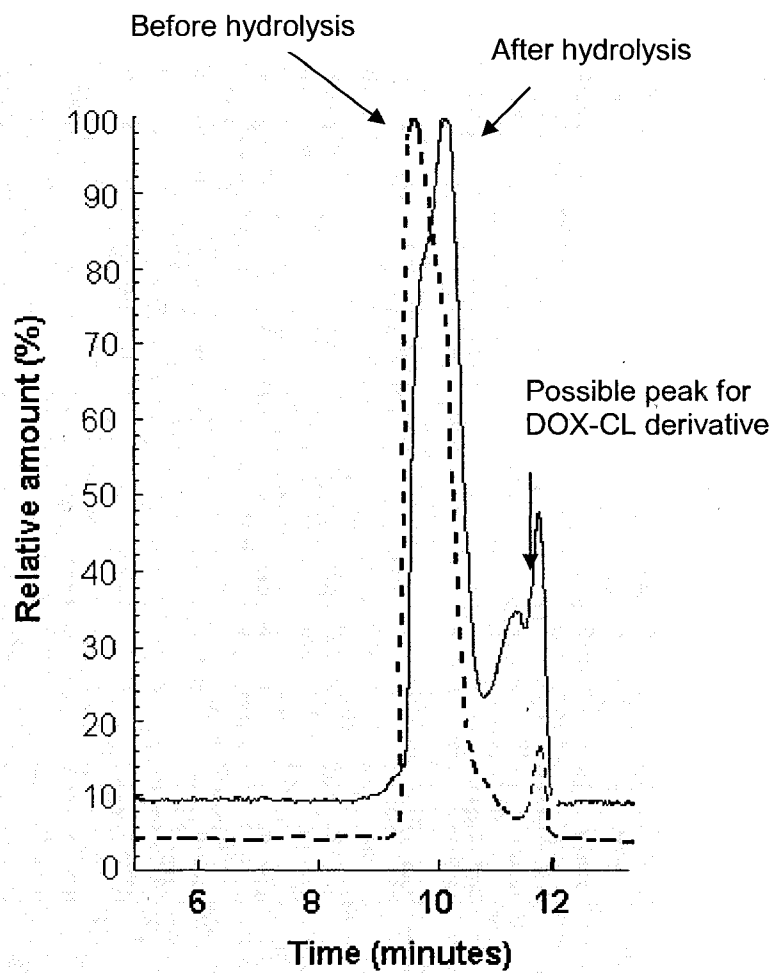
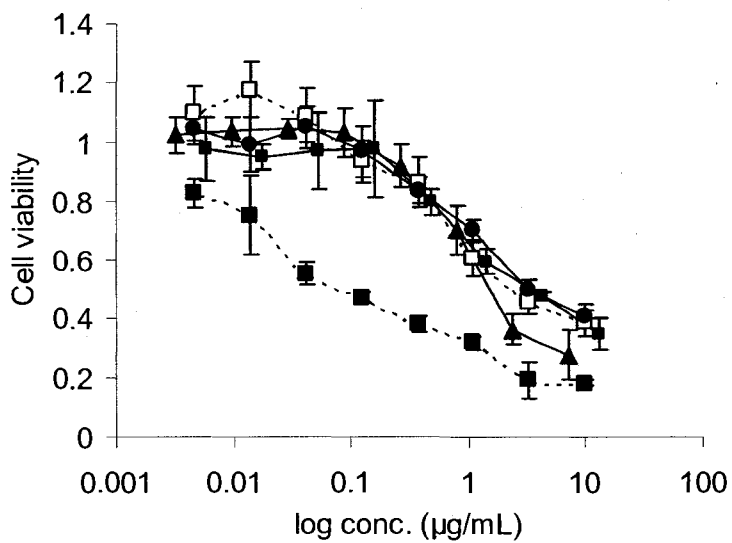


Figure 4.5- Gel permeation chromatogram of MePEO-*b*-P(CL-DOX) before and after incubation at pH 5.0 for 72 h.

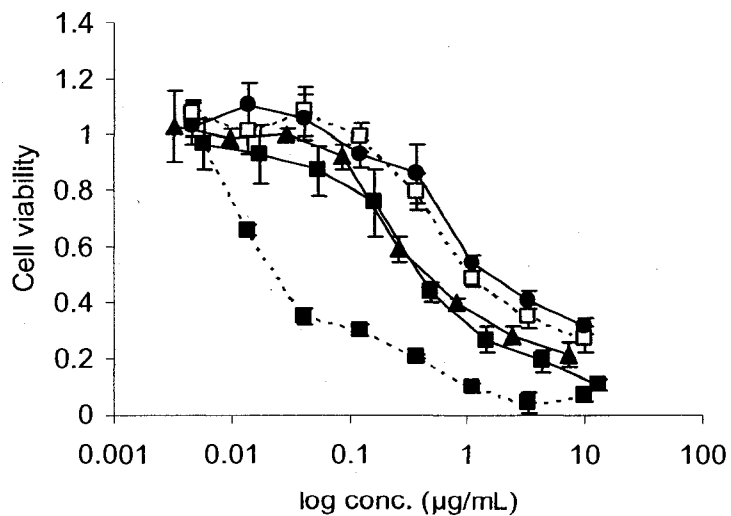
4.3.6. In vitro cytotoxicity study- The results of cytotoxicity study on free DOX, MePEO-*b*-P(CL-DOX), as well as DOX loaded MePEO-*b*-PCL, MePEO-*b*-PBCL, and MePEO-*b*-P(CL-DOX) micelles against murine melanoma B16F10 cells after 24 and 48 h incubation is shown in Figure 4.6. Overall, free DOX was shown to be more effective than the polymeric micellar formulations at both incubation times. The IC₅₀ of DOX as part of polymeric micelles was between 1.54 – 3.65 µg/mL after 24 h incubation with conjugated DOX showing the least cytotoxicity among different formulations. In comparison, the IC₅₀ of free DOX was 0.09 µg/mL after 24 h incubation (Figure 4.6 C and D). Interestingly, the IC₅₀ of conjugated DOX in MePEO-*b*-P(CL-DOX) after 48 h incubation (0.50 µg/mL) was lower than the IC₅₀ of physically encapsulated DOX in MePEO-*b*-PCL and MePEO-*b*-PBCL micelles (1.05 and 1.54 µg/mL, respectively) (P<0.01, One way ANOVA). Free DOX showed an IC₅₀ of 0.03 µg/mL after 48 h incubation with this cell line. DOX loaded in MePEO-*b*-P(CL-DOX) micelles (chemically conjugated + physically loaded) showed higher cytotoxicity (3-fold lower IC₅₀) than conjugated DOX in MePEO-*b*-P(CL-DOX) micelles at 24 h, but did not show superiority over conjugated DOX after 48 h incubation. MePEO-*b*-PBCL and MePEO-*b*-PCCL alone, did not show any sign of cytotoxicity up to 500 µg/mL concentrations in this cell line.

- Free DOX
- MePEO-b-P(CL-DOX)
- ▲— DOX loaded MePEO-b-P(CL-DOX)
- DOX loaded MePEO-b-PCL
- DOX loaded MePEO-b-PBCL

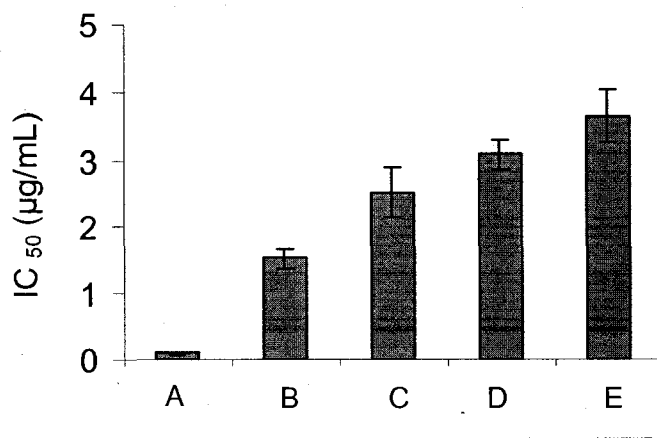
A)



B)



- C)
- A. Free DOX
 - B. DOX loaded MePEO-*b*-P(CL-DOX)
 - C. DOX loaded MePEO-*b*-PCL
 - D. DOX loaded MePEO-*b*-PBCL
 - E. MePEO-*b*-P(CL-DOX)



D)

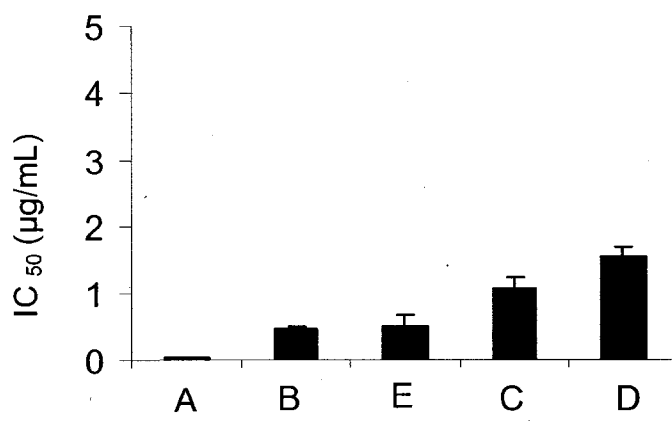


Figure 4.6- *In vitro* cytotoxicity of free and polymeric micellar DOX formulations against B16F10 mouse melanoma carcinoma cells after **A and C)** 24 h, and **B and D)** 48 h incubation. **A and B)** The cell viabilities are expressed as a function of the logarithm of the DOX concentration. Each point represent mean \pm SD (n=3). For DOX loaded in MePEO-*b*-P(CL-DOX) micelles, the concentration of total DOX in the micelle (physically encapsulated + chemically conjugated DOX) is calculated and used in the graph. **C and D)** IC₅₀ values of free DOX and DOX loaded polymeric micellar DOX formulations against B16F10 cells were calculated from the plots of *in vitro* cytotoxicity (plot A and B). Discontinuation of the line under the bars indicates the significant difference of the IC₅₀ values among different formulations ($P < 0.05$). Differences between means (n=3) of IC₅₀ were assessed using one way ANOVA followed by *post hoc* analysis using Dunnett T3 test (SSPS for Windows v.13, Cary, NC). The level of significance was set at $\alpha=0.05$.

4.4. Discussion

Conjugation of DOX to the block copolymer and further self association of the copolymers to micellar structure is expected to minimize the chance of DOX leakage from carrier during blood circulation and restrict the distribution of conjugated drug only to tissues accessible for the carrier. As a result, the conjugated DOX is expected to follow the fate of the polymeric micellar delivery system, circulate for prolonged period in blood and preferentially accumulate in solid tumor by EPR effect [20, 21]. The major concern is the excessive stability of the polymer-drug conjugate at target site which may lead to substantial reduction in the efficacy of the conjugated drug. In contrast to conjugated DOX, physically encapsulated DOX in polymeric micelles is expected to show a better efficacy as a result of more rapid DOX release. However, by the same token, the carrier may lose most of its drug content before reaching the target site in the biological system. In this paper, we report on the preparation of novel self associating McPEO-*b*-P(CL-DOX) conjugates with four distinct characteristics: a) A possibility for the incorporation of several DOX molecules per polymer chain, which can lower the required polymer dose of administration; b) thermodynamic stability induced by a great tendency for micellization due to the presence of hydrophobic PCL backbone as the core forming block; c) stabilization of DOX within the carrier through covalent conjugation to the polymer and further self association of the polymer, which will lower the chance of premature DOX release in blood circulation; d) degradability of the hydrophobic backbone, to which DOX is covalently attached, by hydrolysis that is catalyzed in acidic condition. The later property may trigger micellar dissociation and DOX release in acidic extra microenvironment or intracellular organelles of solid tumors leading to a better release and cytotoxicity profile for the conjugated DOX. Characterization studies on the prepared polymer revealed successful conjugation of DOX

to MePEO-*b*-PCCL (Figure 4.1) and absence of free DOX after polymer purification (Figure 4.2 & 4.3). DOX conjugation to MePEO-*b*-PCCL reduced the CMC of this polymer, but the CMC of MePEO-*b*-P(CL-DOX) was higher than that of MePEO-*b*-PCL (Table 4.1). DOX conjugation to MePEO-*b*-PCCL had a negative impact on the viscosity of micellar core, probably as a result of interruption in intramicellar hydrogen bonds between carboxyl groups of MePEO-*b*-PCCL within the micellar core by substituted DOX. Polymeric micellar MePEO-*b*-P(CL-DOX) that contained conjugated DOX did not show any significant release of free DOX at physiological (pH 7.4) or acidic condition (pH 5.0) using the dialysis method (data not shown).

The observation was attributed to the stability of the amide bond between caprolactone and DOX in the micellar core and was consistent with the findings of Kataoka on DOX release from PEO-*b*-P(Asp-DOX) micellar drug conjugates [22]. A decrease in the polydispersity of the MePEO-*b*-P(CL-DOX) remained in the dialysis bag after the release experiment at pH 5.0, pointed to a possibility for chain cleavage in poly(ester) backbone of P(CL-DOX) at pH 5.0. This assumption was further confirmed in a study where MePEO-*b*-P(CL-DOX) micelles were incubated at acidic pH for three days. Change in the retention time of polymer related peak and generation of an extra peak at 11.3 minutes in the GPC chromatogram of the incubated polymer strongly confirms the hydrolysis of P(CL-DOX) backbone and release of active DOX-CL derivative (Figure 4.5). Mass spectrum analysis of the fraction corresponding to the peak at 11.3 minutes lends further support to this assumption due to the presence of ion at m/z 701 showing the presence of DOX-CL derivative, i.e., DOX-(6-hydroxy caproic acid), produced after hydrolysis in the sample incubated at pH 5.0. Recently, Geng *et al* have shown PCL end hydrolysis and production of 6-hydroxy caproic acid as hydrolysed product from MePEO-*b*-PCL block copolymer worm

like micelle at pH 5.0 [23]. Degradation of aliphatic poly(ester)s occurs via random hydrolytic scission of ester bonds [24]. The degradation rate of PCL is considerably slower compared to other aliphatic polys(ester)s due to its hydrophobicity and high crystallinity [25, 26]. However, Gimenez *et al* demonstrated a dramatic increase in the hydrolytic degradation rate of PCL polymer bearing pendant COOH group compared to the parent PCL due to the increase in hydrophilicity of the polymer backbone [27]. Degradation is also accelerated by the surface area of the polymeric scaffold and acidic pH of the media [26]. Moreover, poly(ester)s may degrade faster *in vivo* than *in vitro* due to the presence of lysosomal enzyme (e.g. lysosomal esterase, cathepsin B etc.) at cellular level [26, 28, 29].

In further studies, physical encapsulation of DOX in MePEO-*b*-PCL block copolymers and its PCL modified derivatives was carried out. Physical loading of DOX did not lead to any significant change in size of MePEO-*b*-PCL and MePEO-*b*-PBCL micelles compared to unloaded micelles, which may be due to the formation of more compact core after DOX loading by enhanced interaction between DOX and micellar core. Elongation of the chain length, introduction of hydrophobic groups or changing the net charge of the polymeric core has also been utilized to increase the loading efficiency and limit the rate of release for hydrophobic drugs from polymeric micelles [30-32]. Increasing the molecular weight of PCL has shown limited benefit in terms of DOX loading efficiency [19]. Alternatively, modification of the PCL with benzyl or DOX groups was expected to increase DOX loading as a result of increased hydrophobic interaction between the micellar core and DOX. Introduction of carboxyl groups in the micellar core was also hypothesized to have a positive impact on DOX encapsulation because of the possibility for hydrogen bonding and/or electrostatic complexation between DOX and COOH in the micellar cores [11]. In effect, the mole % of loaded DOX to monomer was ranked as PBCL>P(CL-

DOX) > PCCL > PCL (Table 4.2). The π - π interaction between the aromatic rings of PBCL or conjugated DOX and physically encapsulated DOX may account for higher DOX solubilization in PBCL and P(CL-DOX) cores [33]. Whereas, formation of hydrogen bonds between the carboxyl groups of DOX and PCCL may explain the better solubilization of DOX in PCCL. An alternative possibility is the formation of electrostatic complex between the amine group of DOX and carboxyl group of PCCL as shown in previous studies for poly(acrylic acid)/DOX pairs [34, 35].

Among different micellar core structures a core of PBCL provided the most control over the rate of DOX release in both pHs. A more rapid rate of DOX release from all micellar nano-containers under study was seen in pH 5.0 compared to pH 7.4. The faster release of encapsulated DOX from PEO-*b*-poly(β -benzyl-L-aspartic acid) (PEO-*b*-PBLA) and MePEO-*b*-PCL in acidic pH has been observed in previous studies [19, 33]. The 3'-NH₂ group of DOX (pK_a~8.4) was in uncharged state by adding a base, Et₃N to enhance its loading in hydrophobic micellar core. Therefore, re-protonation of the 3'-NH₂ at acidic pH, which increases the partition of DOX from the micellar core to the aqueous environment as well as faster degradation of polyester core at acidic pH are assumed to be the reasons behind this observation. Accelerated release of DOX at acidic pH is an added advantage for its tumor targeted delivery, because it allows preferential drug release at the extracellular space of solid tumors or cellular endosomes where pH is acidic (5.0-5.5).

The cytotoxicity of different DOX formulation was performed against murine melanoma B16F10 cells. B16F10 cell line was chosen as a model metastatic cancer cells. The results of cytotoxicity study on free DOX, MePEO-*b*-P(CL-DOX), as well as DOX loaded MePEO-*b*-PCL, MePEO-*b*-PBCL, and MePEO-*b*-P(CL-DOX) micelles after 24 and 48 h incubation of physically encapsulated DOX in different polymeric micelles followed a similar

trend to what has been observed in the release study where polymeric micelles with higher level of DOX release showed higher cytotoxicity (lower IC_{50}) values at both incubation times (Figure 4.6). Accordingly, the IC_{50} of conjugated DOX was higher than physically encapsulated DOX after 24 h of incubation. However, after 48 h incubation, The IC_{50} of conjugated DOX was found to be lower than physically encapsulated DOX in MePEO-*b*-PCL and MePEO-*b*-PBCL and similar to that of DOX loaded MePEO-*b*-P(CL-DOX) micelles. The micellar DOX conjugate was also less cytotoxic than free drug, but the difference in the cytotoxicity of conjugated and free DOX decreased as the incubation time was raised. Given that the results of *in vitro* release study did not show any significant release of free DOX from the micellar polymer-DOX conjugate; the cytotoxicity of MePEO-*b*-P(CL-DOX) conjugate may be an indication for the release of active DOX derivatives from the polymer-drug conjugate due to PCL chain cleavage within 48 h of incubation and/or a direct anti growth activity for the MePEO-*b*-P(CL-DOX) conjugate in B16F10 cells. Several mechanisms have been proposed to explain the antitumor activity of DOX [36, 37] including intercalation into DNA, interaction with plasma membranes and the formation of free radicals through bioreductive activation. Although release of free DOX from conjugate is essential for the first mechanism, it may not be necessary if alternative mechanisms play a crucial role in the cytotoxicity. Cytotoxic effects for conjugated DOX as part of polyacetal-DOX conjugates [12] and PEO-*b* poly(Glutamic acid-DOX) micelles [38] against different cancer cells have also been reported.

4.5. Conclusion

Manipulation of the micellar core in MePEO-*b*-PCL micelles through introduction of benzyl and carboxyl groups, endow polymeric micelles superior DOX solubilizing capacity as well

as a better control over DOX rate of release from the colloidal carrier. Modification of the core in MePEO-*b*-PCL micelles through conjugation of DOX, on the other hand, provides viable means for the development of polymeric micellar drug conjugates that can afford efficient control over the rate of DOX release in physiological pH, core hydrolysis in acidic pH and maintained cytotoxicity in cancer cells.

4.6. Reference

- [1] H.M. Aliabadi, A. Lavasanifar, *Expert Opinion on Drug Delivery* 3 (2006) 139-162.
- [2] G. Gaucher, M.H. Dufresne, V. Sant, N. Kang, D. Maysinger, J. Leroux, *J Control Release* 109 (2005) 169-188.
- [3] A. Mahmud, X.B. Xiong, H.M. Aliabadi, A. Lavasanifar, *Journal of Drug Targeting* (2007) *In press*.
- [4] T. Nakanishi, S. Fukushima, K. Okamoto, M. Suzuki, Y. Matsumura, M. Yokoyama, T. Okano, Y. Sakurai, K. Kataoka, *Journal of Controlled Release* 74 (2001) 295-302.
- [5] A. Lavasanifar, J. Samuel, S. Sattari, G.S. Kwon, *Pharmaceutical Research* 19 (2002) 418-422.
- [6] Y. Li, G.S. Kwon, *Pharm Res* 17 (2000) 607-611.
- [7] M. Yokoyama, A. Satoh, Y. Sakurai, T. Okano, Y. Matsumura, T. Kakizoe, K. Kataoka, *J Control Release* 55 (1998) 219-229.
- [8] N. Nishiyama, M. Yokoyama, T. Aoyaga, T. Okano, Y. Sakurai, K. Kataoka, *Langmuir* 15 (1999) 377-383.
- [9] S. Katayose, K. Kataoka, *Bioconjugate Chemistry* 8 (1997) 702-707.
- [10] M. Oishi, Y. Nagasaki, K. Itaka, N. Nishiyama, K. Kataoka, *J Am Chem Soc* 127 (2005) 1624-1625.
- [11] A. Mahmud, X.B. Xiong, A. Lavasanifar, *Macromolecules* 39 (2006) 9419-9428.
- [12] R. Tomlinson, J. Heller, S. Brocchini, R. Duncan, *Bioconjugate Chemistry* 14 (2003) 1096-1106.
- [13] R.L. Xu, M.A. Winnik, F.R. Hallett, G. Riess, M.D. Croucher, *Macromolecules* 24 (1991) 87-93.
- [14] S.B. La, T. Okano, K. Kataoka, *Journal of Pharmaceutical Sciences* 85 (1996) 85-90.
- [15] G. Kwon, M. Naito, M. Yokoyama, T. Okano, Y. Sakurai, K. Kataoka, *Langmuir* 9 (1993) 945-949.
- [16] Y.I. Jeong, J.B. Cheon, S.H. Kim, J.W. Nah, Y.M. Lee, Y.K. Sung, T. Akaike, C.S. Cho, *Journal of Controlled Release* 51 (1998) 169-178.
- [17] A. Lavasanifar, J. Samuel, G.S. Kwon, *Colloids Surf B Biointerfaces* 22 (2001) 115-126.
- [18] H.M. Aliabadi, D.R. Brocks, A. Lavasanifar, *Biomaterials* 26 (2005) 7251-7259.
- [19] X. Shuai, H. Ai, N. Nasongkla, S. Kim, J. Gao, *J Control Release* 98 (2004) 415-426.
- [20] H. Maeda, *Advanced Drug Delivery Reviews* 46 (2001) 169-185.
- [21] F.M. Muggia, *Clinical Cancer Research* 5 (1999) 7-8.
- [22] M. Yokoyama, S. Fukushima, R. Uehara, K. Okamoto, K. Kataoka, Y. Sakurai, T. Okano, *J Control Release* 50 (1998) 79-92.
- [23] Y. Geng, D.E. Discher, *J Am Chem Soc* 127 (2005) 12780-12781.
- [24] C.G. Pitt, F.I. Chasalow, Y.M. Hibionada, D.M. Klimas, A. Schindler, *Journal of Applied Polymer Science* 26 (1981) 3779-3787.
- [25] C.G. Pitt, M.M. Gratzl, G.L. Kimmel, J. Surles, A. Schindler, *Biomaterials* 2 (1981) 215-220.

- [26] H.J. Sung, C. Meredith, C. Johnson, Z.S. Galis, *Biomaterials* 25 (2004) 5735-5742.
- [27] S. Gimenez, S. Ponsart, J. Coudane, M. Vert, *Journal of Bioactive and Compatible Polymers* 16 (2001) 32-46.
- [28] H. Tsuji, Y. Kidokoro, M. Mochizuki, *Macromolecular Materials and Engineering* 291 (2006) 1245-1254.
- [29] F.P. Seib, A.T. Jones, R. Duncan, *Journal of Drug Targeting* 14 (2006) 375-390.
- [30] N. Nishiyama, M. Yokoyama, T. Aoyagi, T. Okano, Y. Sakurai, K. Kataoka, *Langmuir* 15 (1999) 377-383.
- [31] X. Shuai, T. Merdan, A.K. Schaper, F. Xi, T. Kissel, *Bioconjugate Chemistry* 15 (2004) 441-448.
- [32] A. Lavasanifar, J. Samuel, S. Sattari, G.S. Kwon, *Pharm Res* 19 (2002) 418-422.
- [33] K. Kataoka, T. Matsumoto, M. Yokoyama, T. Okano, Y. Sakurai, S. Fukushima, K. Okamoto, G.S. Kwon, *J Control Release* 64 (2000) 143-153.
- [34] M.V. Kitaeva, N.S. Melik-Nubarov, F.M. Menger, A.A. Yaroslavov, *Langmuir* 20 (2004) 6575-6579.
- [35] M.V. Kitaeva, N.S. Melik-Nubarov, F.M. Menger, A.A. Yaroslavov, *Langmuir* 20 (2004) 6796-6799.
- [36] B.K. Sinha, E.G. Mimnaugh, S. Rajagopalan, C.E. Myers, *Cancer Research* 49 (1989) 3844-3848.
- [37] K. Kataoka, G.S. Kwon, M. Yokoyama, T. Okano, Y. Sakurai, *Journal of Controlled Release* 24 (1993) 119-132.
- [38] J. Vega, S. Ke, Z. Fan, S. Wallace, C. Charsangavej, C. Li, *Pharm Res* 20 (2003) 826-832.

Chapter 5

Chemical tailoring of micelle forming poly(ethylene oxide)-*b*-poly (ϵ -caprolactone) block copolymers for the solubilization and controlled delivery of STAT-3 inhibitor Cucurbitacin I

5.1. Introduction

Compatibility between solubilizate and micellar core is known to be one of the key factors in determining the effectiveness of polymeric micellar delivery systems in drug solubilization and controlled release. A polymer is a good solubilizing agent for a drug when there are favorable interactions between polymer/drug pairs. In polymeric micelles, enhanced degree of compatibility between drug and micellar core has been shown to lead to better encapsulation efficiency and lower rate of drug release from these carriers [1-5]. Through modification of the core structures in poly(ethylene oxide)-*block*-poly(L-amino acid) (PEO-*b*-PLAA) based micelles, desired stability, drug loading, and release properties have been achieved for the delivery of doxorubicin (DOX) [2, 6], amphotericin B [7], methotrexate [4], cisplatin [5] and KRN-5500 [8]. However, chemical modification is restricted in poly(ester) containing block copolymers due to the lack of proper functional groups for modification on the polymer backbone. In chapter 3 and 4, we reported on the development of a new family of methoxy poly(ethylene oxide)-*b*-poly(ϵ -caprolactone) (MePEO-*b*-PCL) block copolymers, bearing carboxyl, benzylcarboxylate and DOX as pendant groups on the poly(ester) block [9, 10]. The synthesis of these core functionalized MePEO-*b*-PCL block copolymers was made possible through functionalization of the ϵ -caprolactone monomer. Development of this synthesis strategy allows for the substitution of different moieties on the PCL block. In this chapter, we describe the attachment of cholesteryl moiety to the PCL backbone using a similar synthesis strategy (Scheme 5.1 and 5.2). Polymeric nanocarriers with cholesteryl modified core structures, i.e., MePEO-*b*-poly(α -cholesteryl carboxylate ϵ -caprolactone) (MePEO-*b*-PChCL), were expected to increase the solubilization and improve the release profile of chemically compatible drug, cucurbitacin I (CuI) from its polymeric micellar carrier (Figure 5.1).

5.2. Experimental section

5.2.1. Materials- MePEO (average molecular weight of 5000 g.mol⁻¹), diisopropyl amine (99%), cholesteryl chloroformate (tech. 95%), sodium (in kerosin), butyl lithium (Bu-Li) in hexane (2.5 M solution), and pyrene were purchased from Sigma, St. Louis, MO, USA. ϵ -Caprolactone was purchased from Lancaster Synthesis, UK. Stannous octoate was purchased from MP Biomedicals Inc, Germany. Fluorescent probe 1,3-(1,1'-dipyrenyl)propane was purchased from Molecular Probes, USA. All other chemicals were reagent grade.

5.2.2. Calculation of the compatibility between micellar core and CuI- The compatibility between drugs and micellar core was calculated by measuring the Flory–Huggins interaction parameter (χ_{sp}) as outline in Eq. 5.1.

$$\chi_{sp} = (\delta_s - \delta_p)^2 V_s / RT \quad (\text{Eq. 5.1})$$

where $(\delta_s - \delta_p)$ is the solubility difference between the drug (s) and polymer (p). V_s is the molar volume of solubilizate, R is the gas constant and T the Kelvin temperature. The solubility parameter (δ) was obtained by Hansen's approach [11], which uses partial solubility parameters to calculate the total solubility parameter as outlined in Eq. 5.2.

$$\delta = (\delta_d^2 + \delta_p^2 + \delta_h^2)^{1/2} \quad (\text{Eq. 5.2})$$

where, δ_d , δ_p , and δ_h are the partial solubility parameters indicating contributions from Van der

waals dispersion forces between atoms, dipole–dipole interactions between molecules, and propensity of hydrogen bonding between molecules, respectively. The partial solubility parameters for the drug (CuI) and polymers were calculated by group contribution method (GCM) using the following three equations:

$$\delta_d = \sum F_{di} / V \quad (\text{Eq 5.3})$$

$$\delta_p = [\sum F_{pi}^2]^{1/2} / V \quad (\text{Eq. 5.4})$$

$$\delta_h = [\sum E_{hi}]^{1/2} / V \quad (\text{Eq. 5.5})$$

where F_{di} , F_{pi} and E_{hi} refer to the specific functional group contributions: van der Waals dispersion forces (F_{di}), dipole–dipole interactions (F_{pi}), and hydrogen bonding (E_{hi}). The total molar volume (V) of CuI and core forming blocks of different polymer repeat units were obtained by the Fedors method [12]. F_{di} , F_{pi} and E_{hi} were obtained by the Hoftyzer Van Krevelen’s method [13]. We divided the molecules into small chemical groups and used their F_{di} , F_{pi} and E_{hi} values to calculate the partial and total solubility parameters of CuI and different core forming blocks of MePEO-*b*-PCL based block copolymers.

5.2.3. Synthesis of α -cholesteryl carboxylate ϵ -caprolactone monomer- Cholesteryl bearing monomer, i.e., α -cholesteryl carboxylate ϵ -caprolactone, was synthesized using similar methods to what described in chapter 3, section 3.2.2 (Scheme 5.1). Briefly, Bu-Li (24 mL) in hexane was slowly added to dry diisopropylamine (8.4 mL) in 60 mL of dry tetrahydrofuran (THF) in a three-neck round-bottomed flask at -30 °C under vigorous stirring with continuous argon supply. The solution was cooled to -78 °C. ϵ -Caprolactone (3.42 g) was dissolved in 8 mL of dry THF and added to the above-mentioned mixture slowly, followed by the addition of α -cholesteryl chloroformate (13.47 g). The temperature was allowed to rise to 0 °C, and the reaction was quenched with 5 mL of saturated ammonium chloride solution. The reaction mixture was diluted with water and extracted with ethyl acetate. The combined extracts were dried over Na_2SO_4 and evaporated. The yellowish semisolid crude mixture was purified twice over a silica gel column using hexane: ethyl acetate at 3:1 ratio as eluent. The purity of the compound was confirmed with thin-layer chromatography (TLC). The chemical structure was analyzed by ^1H NMR, IR and mass

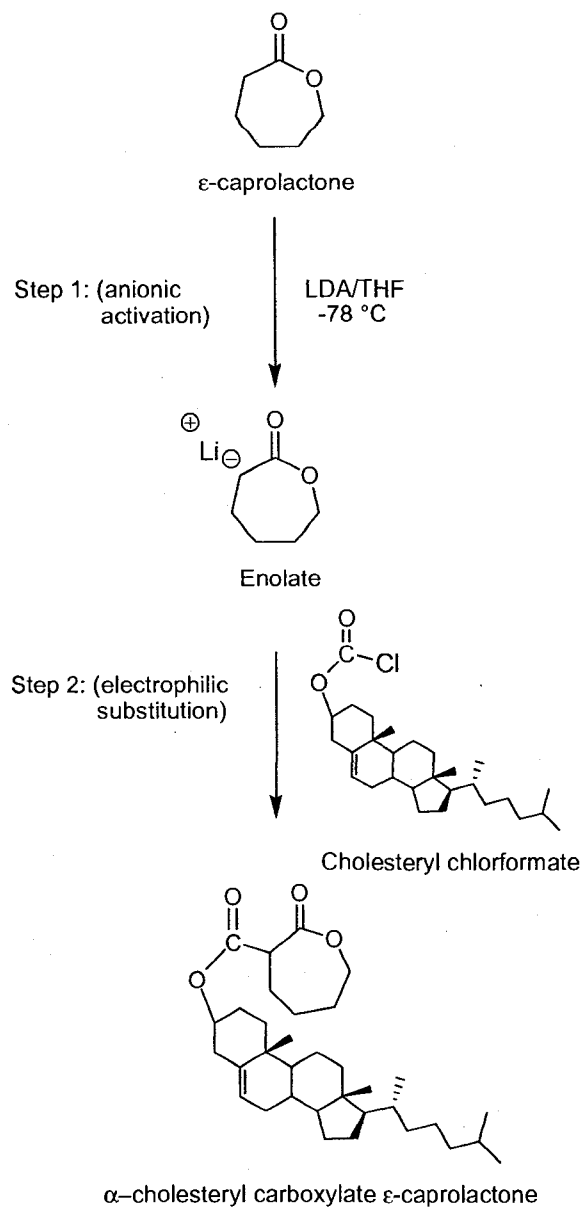
spectroscopy. Benzyl group containing monomer, i.e., α -benzylcarboxylate ϵ -caprolactone, was also synthesized according our previously reported procedure (Chapter 3, section 3.2.2).

The reaction yield was calculated using the equation outlined as Eq. 5.6.

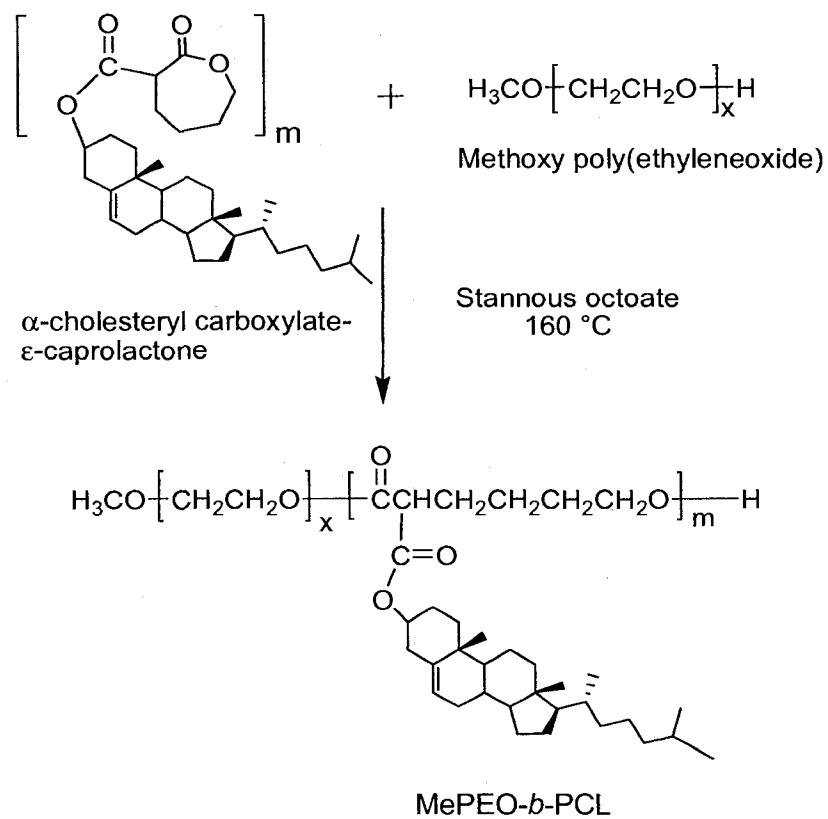
Yield (%) =

$$\frac{\text{Amount of } \alpha\text{-cholesteryl carboxylate } \epsilon\text{-caprolactone produced in the reaction}}{\text{Predicted amount of } \alpha\text{-cholesteryl carboxylate } \epsilon\text{-caprolactone to be produced in the reaction}} \times 100$$

(Eq.
5.6)



Scheme 5.1- Synthetic scheme for the preparation of α-cholesteryl carboxylate-ε- caprolactone



Scheme 5.2 - Synthetic scheme for the preparation of MePEO-*b*-PChCL block copolymers

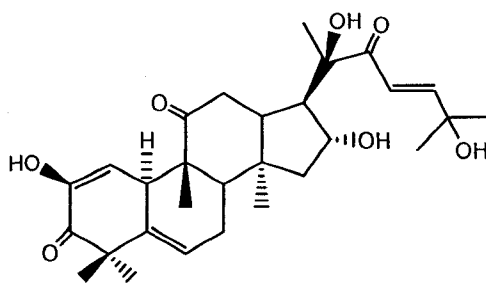


Figure 5.1- Chemical structure of Cucurbitacin I

5.2.4. Synthesis of MePEO-*b*-PChCL block copolymer- Cholesteryl group bearing block copolymer, i.e., MePEO-*b*-PChCL, was synthesized by ring opening polymerization of α -cholesteryl carboxylate ϵ -caprolactone using MePEO as initiator and stannous octoate as catalyst (Scheme 5.2) according to the procedure described previously (Chapter 3, Section 3.2.3). Briefly, MePEO (MW: 5000 g mol⁻¹) (1.5g), α -cholesteryl carboxylate- ϵ -caprolactone (3.0 g), and stannous octoate (0.002 equiv of monomer) were added to a 10 mL previously flamed ampoule, nitrogen purged and sealed under vacuum. The polymerization reaction was allowed to proceed for 4 h at 160 °C in oven. The reaction was terminated by cooling the product to room temperature.

¹H NMR spectrum of MePEO-*b*-PChCL in CDCl₃ at 300 MHz was used to assess the conversion of α -cholesteryl carboxylate ϵ -caprolactone monomer to PChCL comparing the peak intensities of methylene protons (-O-CH₂-, δ 4.28 ppm) of α -cholesteryl carboxylate- ϵ -caprolactone monomer to the intensity of the same proton of PChCL (-O-CH₂-, δ 4.10 ppm).

5.2.5. Characterization of MePEO-*b*-PChCL block copolymer- The number average molecular weight (M_n) of MePEO-*b*-PChCL was determined from ¹H NMR spectrum comparing the peak intensity of MePEO (-CH₂CH₂O-, δ 3.65 ppm) to that of PChCL (-O-CH₂-, δ 4.10 ppm), considering a 5000 g mol⁻¹ molecular weight for MePEO. The M_n and weight average molecular weight (M_w) as well as polydispersity (M_w/M_n) of the prepared block copolymers were assessed by gel permeation chromatography (GPC) according to the method described in previous chapters (Chapter 2, section 2.2.2).

5.2.6. Assembly of block copolymers and characterization of self assembled structures- Micellization was achieved by dissolving prepared block copolymers (30 mg) in THF (0.5 mL) and drop-wise addition (1 drop/15 s) of polymer solutions to doubly distilled water (3 mL) under moderate stirring at 25 °C, followed by the evaporation of THF under vacuum. Average diameter (intensity mean) and size distribution of prepared micelles were estimated by dynamic light scattering (DLS) using a Malvern Zetasizer 3000 at a polymer concentration of 2.5 mg/mL in water at 25 °C after centrifuging the micellar solution at 11,600×g for 5 min. Morphology of self assembled structures was investigated at a polymer concentration of 1 mg/mL, using a Hitachi H 700 transmission electron microscope (TEM) according to the procedure described in previous chapter (Chapter 2, section 2.2.3). Images were obtained at a magnification of × 18000 at 75 KV.

A change in the fluorescence excitation spectra of pyrene in the presence of varied concentrations of MePEO-*b*-PChCL block copolymer was used to measure its CMC according to the method described in previous chapters (Chapter 2, section 2.2.3). The viscosity of prepared micellar core was estimated by measuring excimer to monomer intensity ratio (I_c/I_m) from the emission spectra of 1,3-(1,1'-dipyrenyl)propane at 373 and 480 nm, respectively, according to the method described in previous chapter (Chapter 2, section 2.2.3).

5.2.7. Encapsulation of CuI in polymeric micelles- Encapsulation of CuI in MePEO-*b*-PCL, MePEO-*b*-poly(α -benzyl carboxylate ϵ -caprolactone) (MePEO-*b*-PBCL) and MePEO-*b*-PChCL micelles was achieved by a co-solvent evaporation method. Briefly, 15 mg of copolymer and 1.5 mg of CuI were dissolved in 0.5 mL THF. This solution was added to 3 mL of doubly distilled water in a drop-wise manner. After 4 h stirring at room temperature,

the remaining THF was removed by applying vacuum. The aqueous solution of the micellar formulation was then centrifuged at $11,600 \times g$ for 10 min to remove free cucurbitacin precipitates. The hydrodynamic diameter of CuI loaded micelles were measured by light scattering as described above.

CuI loading level and encapsulation efficiency was determined by using liquid chromatography mass spectrometry (LC-MS) [14]. To determine the level of encapsulated CuI, free CuI in the micellar solution was separated by centrifuging the micellar solution at $11,600 \times g$ for 10 min. Then 20 μL aliquot of the micellar solution (the top layer) was diluted with 980 μL of methanol to disrupt the micellar structure and release incorporated drug. Diluted micellar solution (200 μL) was added to 200 μL of internal standard (I.S) (4-hydroxy benzophenone solution in methanol, 2 $\mu\text{g}/\text{mL}$). 10 μL of this solution was injected to Waters, Micromass ZQ4000 LC-Mass spectrophotometer. For chromatographic separation a mobile phase consisting of a mixture of acetonitrile:water containing 0.2% ammonium hydroxide (40:60) was employed for 3 min. This was followed by a non-linear gradient to a final ratio of 60:40 (v/v) over 8 min at a constant flow rate of 0.2 mL/min. A calibration curve was constructed over the quantification range of 50–5,000 ng/mL of CuI solution in methanol. The ratios of CuI to I.S. peak areas were calculated and plotted versus CuI concentration. CuI loading and encapsulation efficiency were calculated by the following equations:

$$\text{CuI loading (M/M) (\%)} = \frac{\text{Moles of loaded CuI}}{\text{Moles of monomer}} \times 100 \quad (\text{Eq. 5.7})$$

$$\text{CuI loading (w/w) (\%)} = \frac{\text{amount of loaded CuI in mg}}{\text{amount of copolymer in mg}} \times 100 \quad (\text{Eq. 5.8})$$

$$\text{CuI loading (M/M)(\%)} = \frac{\text{Moles of loaded CuI}}{\text{Moles of copolymer}} \times 100 \quad (\text{Eq. 5.9})$$

$$\text{Encapsulation efficiency (\%)} = \frac{\text{amount of loaded CuI in mg}}{\text{amount of CuI added in mg}} \times 100 \quad (\text{Eq. 5.10})$$

5.2.8. Release of CuI from polymeric micelles- Release study was performed using dialysis method as described in the previous chapter (Chapter 4, section 4.2.5). Briefly, CuI loaded micellar solutions (3 mL) were prepared at 2.5 mg/mL polymer concentration from MePEO-*b*-PCL, MePEO-*b*-PBCL and MePEO-*b*-PChCL block copolymers according to the method described in section 5.2.7. As a control, free CuI solution in water was prepared at a concentration of 500 µg/mL with the aid of methanol (2% v/v). The micellar solutions were transferred into a dialysis bag (Mw cutoff: 3,500 Da, supplied by Spectrum Laboratories, USA). The dialysis bags were placed into 500 mL of doubly distilled water in a beaker. Release study was performed at 37 °C in a Julabo SW 22 shaking water bath (Germany). At selected time intervals, 20 µL of micellar solution was withdrawn from inside the dialysis bag to measure the drug concentration by LC-MS. Three parallel measurements were performed for each time point.

5.2.9. Statistical analysis- Data are reported as mean ± standard deviation (S.D.). Differences among the mean of formulation characteristics for polymeric micelles were compared by either one-way analysis of variance (ANOVA) followed by the Student–Newman–Keuls post hoc test for multiple comparisons using Sigma stat software or Student’s unpaired t-test assuming unequal variance.

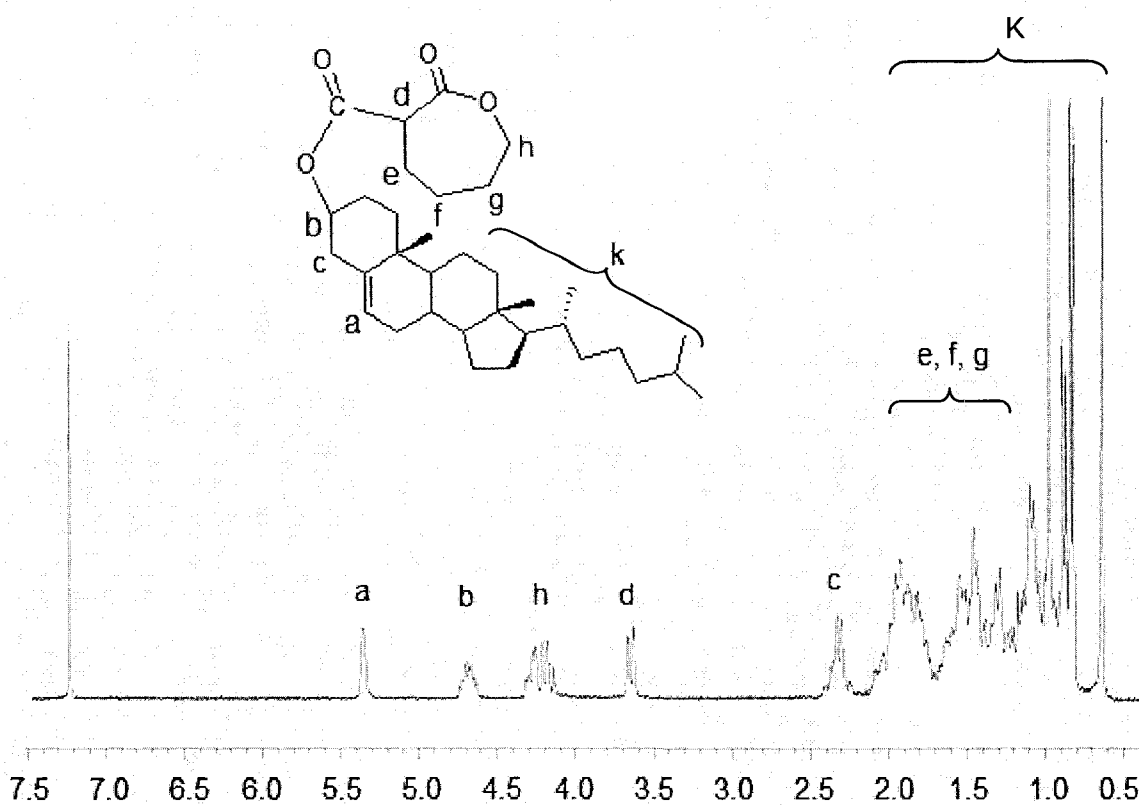
5.3. Results

5.3.1. Calculation of the compatibility between micellar core and CuI- Flory–Huggins interaction parameter as outlined in Eq. 5.1 was used as a means to predict the compatibility of CuI with different block copolymer cores. This approach has successfully been used to predict drug-polymer miscibility and solubility [15-18]. The predicted compatibility between the drug and different core structures under current study according to the interaction parameter (χ_{sp}) were in the order of PChCL>PBCL>PCL ($\chi_{sp}(\text{PCL}/\text{CuI})= 3.39$, $\chi_{sp}(\text{PBCL}/\text{CuI})= 2.08$ and $\chi_{sp}(\text{PChCL}/\text{CuI})= 0.86$). The lower the positive value of χ_{sp} (ideally equal to zero), the greater the compatibility between the solubilize and the core-forming block reflecting a favorable interaction between the hydrophobic block of copolymer and the encapsulated drug.

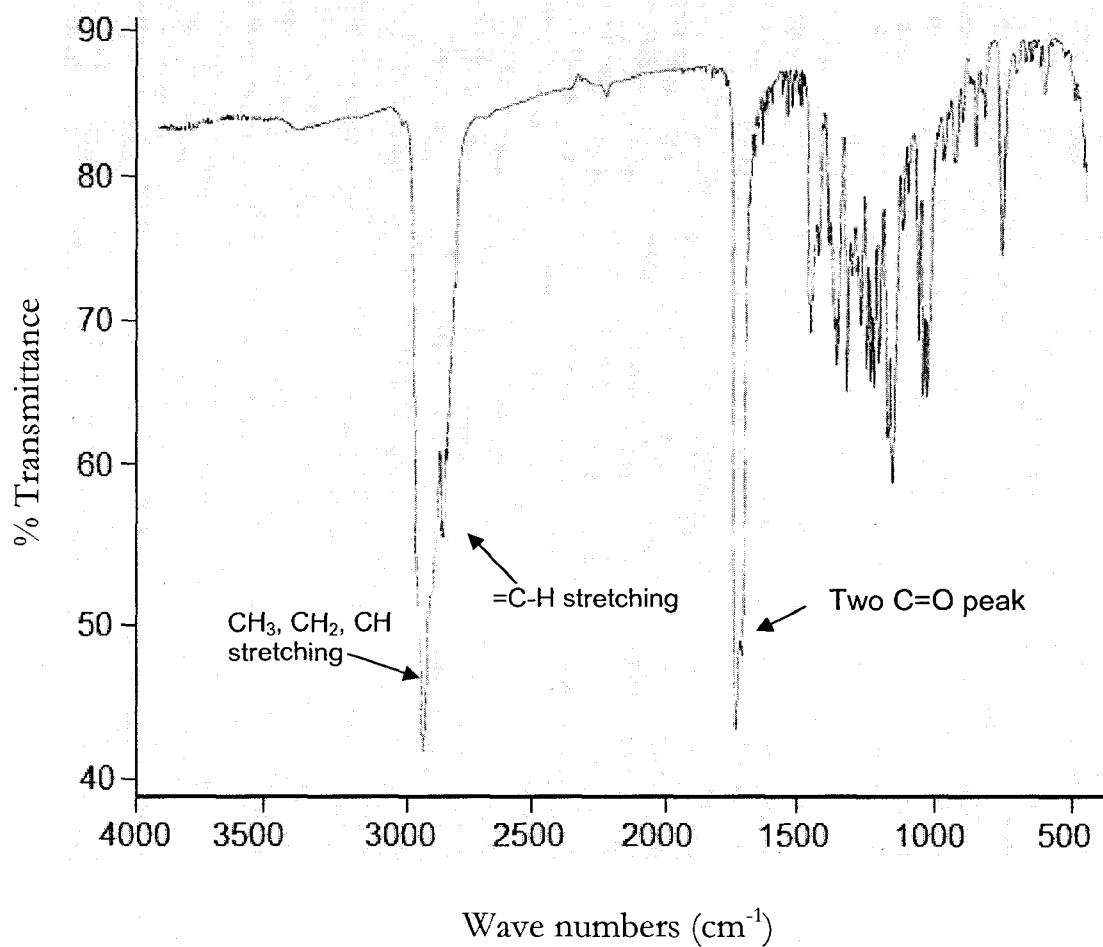
5.3.2. Preparation of MePEO-*b*-PCL block copolymers with cholesteryl side groups on the PCL block- Attachment of cholesteryl side groups to MePEO-*b*-PCL block copolymer was carried out through conjugation of cholesteryl chloroformate with ϵ -caprolactone monomer producing α -cholesteryl carboxylate- ϵ -caprolactone (Scheme 5.1) and further ring opening polymerization of synthesized monomer (Scheme 5.2). The yield of first reaction (synthesis of substituted monomer) was 65%. The structure was confirmed by combined analysis of ^1H NMR, IR, and mass spectroscopy (Figure 5.2 A-C). In 300 MHz ^1H NMR spectroscopy in CDCl_3 , corresponding proton peaks were observed at δ (ppm): 0.681 (s, 3H); 0.86-1.7 (m, 34H); 1.8-2.1 (m, 10H); 2.35 (m, 2H); 3.68 (dd, 1H); 4.25 (m, 2H); 4.73 (m, 1H) 5.38 (m, 1H) (Figure 5.2 A). The peak at δ 3.68 ppm (Figure 5.2 A) for α -cholesteryl carboxylate- ϵ -caprolactone, which corresponds to a single proton instead of two protons of ϵ -caprolactone monomer, indicates the successful substitution of the cholesteryl carboxylate

on ϵ -caprolactone monomer at the α -position. The presence of two sharp carbonyl peaks in the IR spectrum at 1725 and 1700 cm^{-1} corresponds to the carbonyl groups in lactone and cholesteryl carboxylate, respectively (Figure 5.2 B). Finally, mass spectroscopy resulted in the formation of molecular ion peak (M^+) at m/z 526.49; $M^+ + \text{Na}$ peak at m/z 549.15; $M^+ + \text{K}$ at m/z 565.09 (Figure 5.2 C).

A)



B)



C)

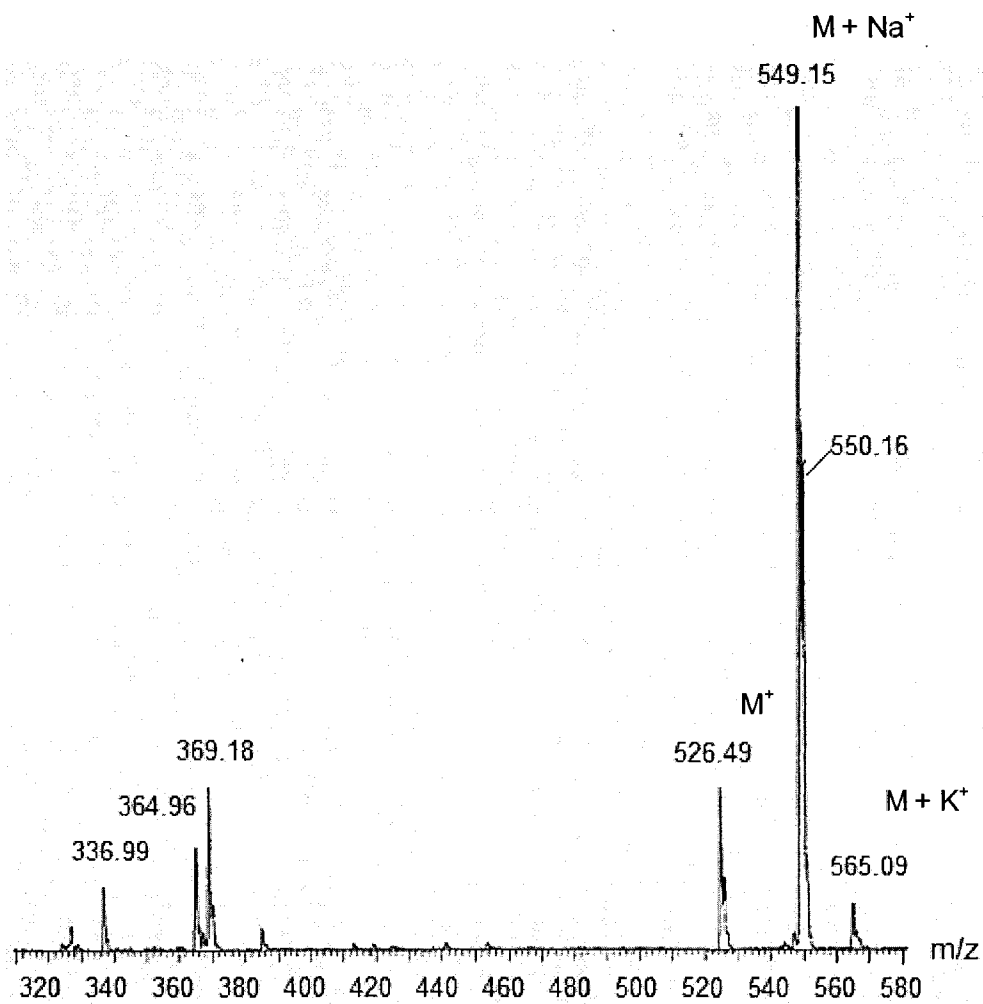


Figure 5.2- A) ¹H NMR in CDCl₃; B) IR; and C) Mass spectra of α-cholesteryl carboxylate-ε-caprolactone (substituted monomer) and peak assignments.

The composition of MePEO-*b*-PChCL block copolymer was confirmed from ^1H NMR spectrum in CDCl_3 (Figure 5.3). The percent of conversion of MePEO-*b*-PChCL block copolymer from α -cholesteryl carboxylate ϵ -caprolactone was found to be 78 %. In 300 MHz ^1H NMR spectroscopy in CDCl_3 corresponding proton peaks for the product were observed at δ (ppm): 0.68 (s, 3H); 0.84-1.7 (m, 34 H); 1.73-2.0 (m, 10 H); 2.30 (m, 1H); 3.28 (m, 1H); 3.65 (s, 4H); 4.63 (m, 1H); 5.35 (m, 1H) (Figure 5.3). The presence of characteristic peaks for cholesteryl moiety at δ 5.35 (-CH=C< proton), δ 4.63 (>CH-O- proton), and δ 0.84-1.7 ppm (other cholesteryl protons) confirm the presence of pendant cholesteryl group in the structure of block copolymer. Furthermore, the characteristic downfield shift of -OCH₂- protons (from δ 4.25 to 4.10 ppm) and O=C-CH- proton (from δ 3.75 to 3.28 ppm) of caprolactone backbone in the ^1H NMR spectra (Figure 5.2 A and 5.3) strongly indicates the ring opening polymerization of the monomer and formation of block copolymers.

The calculated molecular weight of PChCL block, determined by comparing the peak intensity of MePEO (-CH₂-CH₂-) at δ 3.65 ppm to that of PChCL (-CH₂-O-) at δ 4.10 ppm (Figure 5.3) was found to be 7400 g mol⁻¹, which was close to the molecular weight determined by GPC ($M_n=11800$) (Table 5.1). However, the calculated molecular weight from ^1H NMR indicates lower degree of polymerization (DP=14) of α -cholesteryl carboxyl ϵ -caprolactone compared to the theoretical molecular weight according to the feed ratio (M/I=18) which is consistent with the previously reported result for MePEO-*b*-PBCL (Table 5.1). The resulting copolymer showed a broad polydispersity ($M_w/M_n=1.53$) compared to the un-functionalized MePEO-*b*-PCL block copolymer ($M_w/M_n=1.04$) which may be due to the presence of trace of PChCL homopolymer.

Table 5.1- Characteristics of synthesized block copolymers

Block copolymer ^a	[M]/[I] ^b	Theoretical Mol. Wt. (g.mol ⁻¹)	M _n (g.mol ⁻¹) ^c	M _n (g.mol ⁻¹) ^d	PDI ^e
MePEO ₁₁₄ - <i>b</i> -PCL ₄₂	44	10000	9800*	11500*	1.04*
MePEO ₁₁₄ - <i>b</i> -PBCL ₁₉	21	10200	9700*	9200*	1.74*
MePEO ₁₁₄ - <i>b</i> -PChCL ₁₄	18	14500	12400	11800	1.53

^aThe number showed as subscript indicates the polymerization degree of each block determined from ¹H NMR spectroscopy.

^bMonomer/Initiator molar ratio

^cNumber average molecular weight measured by ¹H NMR.

^dNumber average molecular weight measured by GPC

^ePolydispersity index (M_w/M_n) measured by GPC

* Data are reproduced from previous chapter (Chapter 3, Table 3.1) for comparison

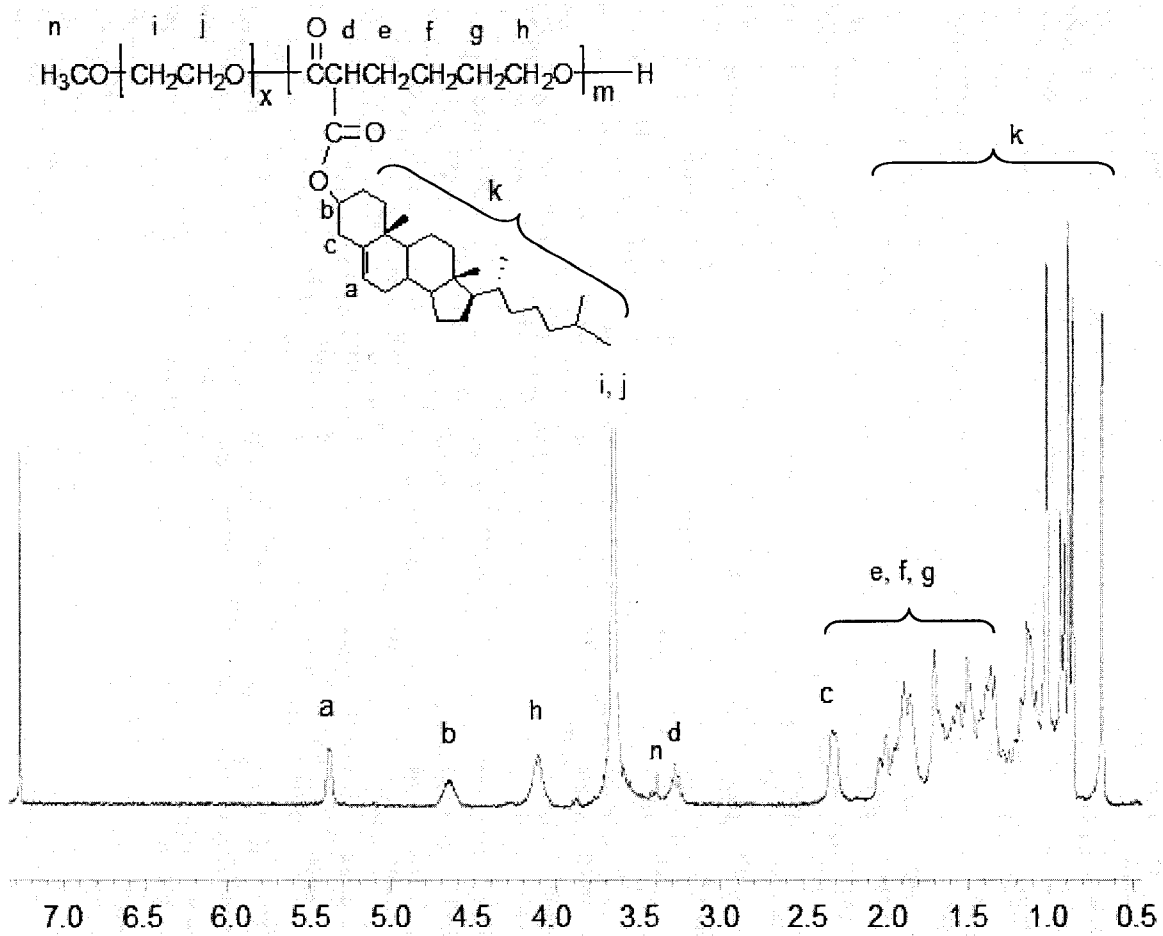


Figure 5.3- ¹H NMR spectrum and peak assignment of MePEO-*b*-PChCL block copolymer

5.3.3. Assembly of MePEO-*b*-PChCL block copolymers and characterization of self-assembled structures- The average diameter for MePEO-*b*-PChCL nanoassemblies determined by the DLS technique was 195 nm. On the other hand, micelles, formed from MePEO-*b*-PCL and MePEO-*b*-PBCL were found much smaller showing average diameters of 45 and 65.5 nm, respectively (Table 5.2). The size of polymeric nanocarriers is controlled by various factors, among which the length and nature of the core and corona-forming chains are predominant [19, 20]. The calculated polydispersity index of PEO-*b*-PChCL nanocarrier size distribution was found to be very narrow (PDI=0.08) which indicates the absence of any secondary aggregation in the nanocarrier population. The TEM picture of MePEO-*b*-PChCL nanoassemblies shows the formation of true spherical carriers having a clear boundary, and the average diameter was 75 nm (Figure 5.4) which is much smaller than the size obtained from DLS measurement.

The CMC of synthesized block copolymer determined by fluorescence probe technique as described in previous chapter (Chapter 2, section 2.2.3) was found to decrease upon attachment of cholesteryl group. Indeed, the CMC of MePEO-*b*-PChCL copolymer with a degree of polymerization (DP) of 14 in hydrophobic block was 7.5×10^{-2} μ M, which was 2.5 and 1.3 times lower than that of MePEO-*b*-PCL (ϵ -caprolactone DP=42) and MePEO-*b*-PBCL (α -benzylcarboxylate- ϵ -caprolactone DP=19) block copolymer micelles, respectively ($P < 0.05$, One way ANOVA) (Table 5.2). The lower CMC value for MePEO-*b*-PChCL clearly shows that introduction of more hydrophobic cholesteryl carboxylate makes self-association of block copolymers, thermodynamically more favorable.

The synthesized MePEO-*b*-PChCL block copolymer nanoassemblies possessed viscous cores, as evidenced by the low I_c/I_m ratios (0.23) compared to that of surfactant

micelles, which has liquid-like core. However, the I_c/I_m value of synthesized block copolymer was higher than the I_c/I_m values of MePEO-*b*-PBCL and MePEO-*b*-PCL block copolymer, which indicates lower viscosity of cholesteryl containing core compared to benzyl containing, PBCL or unfunctionalized, PCL core.

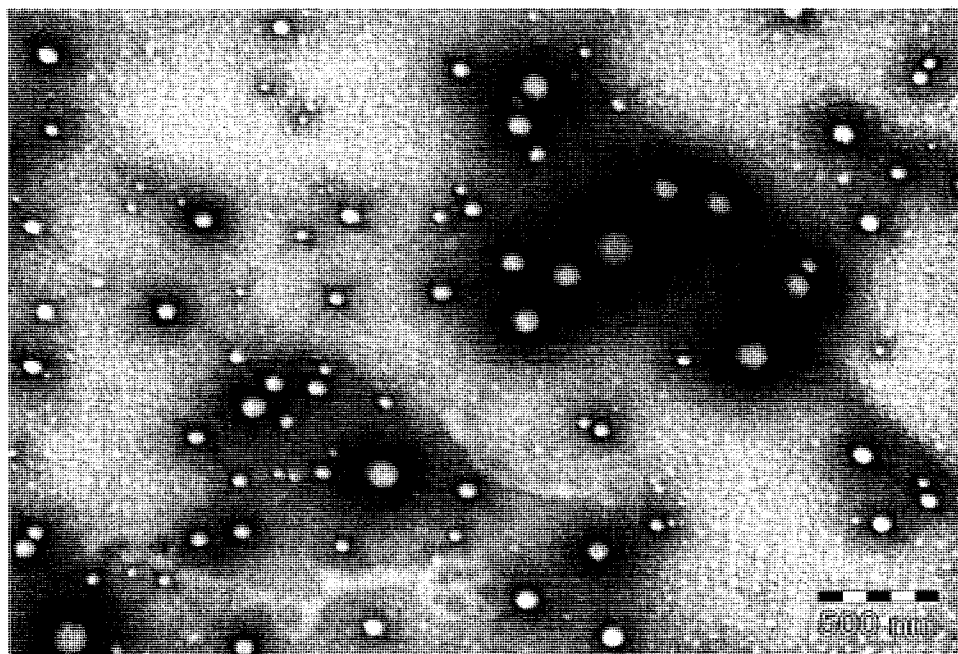


Figure 5.4- TEM picture of nanoassemblies prepared from MePEO-*b*-PChCL block copolymer (magnification 18000×6.1). The bar on the images represents 500 nm.

Table 5.2- Characteristics of empty block copolymer nanocarriers (n=3).

Block copolymer ^a	Average micellar size \pm SD (nm) ^b	PDI ^c	CMC ^d \pm SD (μ M)	I _e /I _m \pm SD ^e
MePEO ₁₁₄ - <i>b</i> -PCL ₄₂	45.0 \pm 2.0	0.20	18.2 \times 10 ⁻² \pm 0.01*	0.055 \pm .007*
MePEO ₁₁₄ - <i>b</i> -PBCL ₁₆	65.5 \pm 3.6 [†]	0.31	9.8 \times 10 ⁻² \pm 0.01 ^{††}	0.028 \pm .002 ^{††}
MePEO ₁₁₄ - <i>b</i> -PChCL ₁₄	195 \pm 7.5	0.10	7.5 \times 10 ⁻² \pm 0.01	0.23 .030

^aThe number showed as subscript indicates the polymerization degree of each block

^bIntensity mean estimated by dynamic light scattering technique.

^cPolydispersity index (PDI) of size distribution estimated by DLS technique

^dMeasured from the onset of a rise in the intensity ratio of peaks at 339 nm to peaks at 334 nm in the fluorescence excitation spectra of pyrene plotted versus logarithm of polymer concentration.

^eIntensity ratio (excimer/monomer) from emission spectrum of 1,3-(1,1' dipyrenyl) propane in presence of polymeric micelle

[†]Significantly different from MePEO-*b*-PCL and MePEO-*b*-PChCL (P < 0.05, One way ANOVA)

*The data are reproduced from previous chapter (Chapter 3, Table 3.2) for comparison

5.3.4. Encapsulation of CuI in polymeric micelles- The calculated loading level based on the drug to polymer molar percentage for PChCL, PBCL and PCL core were 203.3, 154.7, and 125.8 %, respectively (Table 5.3). To account for differences in the polymerization degree of hydrophobic block between block copolymers under study and demonstrate the contribution of each monomer to the drug loading efficiency in the micellar core, the mole % of loaded CuI to monomer was also calculated. The molar loading ratio of drug to monomer in MePEO-*b*-PCL micelles was 3.0 %, where the core was unmodified. Compared to PCL core, the molar loading content was increased 2.8 and 5-fold in MePEO-*b*-PBCL and MePEO-*b*-PChCL nanocarriers, respectively. The size of the CuI-loaded MePEO-*b*-PCL, MePEO-*b*-PBCL micelles measured by DLS technique was 50.4 and 64.5 nm, respectively, (Table 5.3). In contrast, the size of MePEO-*b*-PChCL nanocarriers was

found to be 201 nm using the same technique. No significant differences between the average diameters of unloaded and loaded carriers were observed compared for all three block copolymers under study ($P > 0.05$, unpaired student's t test).

Table 5.3- Characteristics of CuI loaded block copolymer nanocarriers (n=3).

Block copolymer nanocarriers ^a	CuI loading content (%) ± SD		Encap. efficiency (%) ± SD	Average diameter ^b ± SD	PDI ^c
	CuI/monomer (molar)	CuI/polymer (wt)			
MePEO ₁₁₄ - <i>b</i> -PCL ₄₂	3.0 ± 0.3	125.8 ± 5.0	64.7 ± 3.0	50.4 ± 5	0.21
MePEO ₁₁₄ - <i>b</i> -PBCL ₁₉	8.3 ± 0.2 [†]	154.7 ± 3.7 ^{†*}	81.6 ± 1.9 [†]	64.5 ± 4 ^{†*}	0.29
MePEO ₁₁₄ - <i>b</i> -PChCL ₁₄	15.4 ± 0.5 [†]	203.3 ± 7.0 [†]	87.2 ± 3.0 [†]	201 ± 7 [†]	0.08

^a The number showed as subscript indicates the polymerization degree of each block

^b Intensity mean estimated by dynamic light scattering technique

^c Polydispersity index (PDI) of size distribution estimated by DLS technique

[†] Significantly different from MePEO-*b*-PCL (P < 0.05, One way ANOVA)

* Significantly different from MePEO-*b*-PChCL (P < 0.05, One way ANOVA)

5.3.5. *In vitro* release of CuI from different block copolymer nanocarriers- The release profile of free CuI (solution in 2 % methanol) and polymeric nanoformulations is shown in figure 5.5. The transfer of free CuI from methanolic solution through the dialysis bag was found to be relatively rapid (>60 and 90% transfer in 1 and 4 h, respectively). On the other hand, polymeric nanocarriers were able to reduce the rate of drug transfer from the dialysis membrane to outside medium in the *in vitro* release experiment (Figure 5.5). MePEO-*b*-PCL micelles exhibited a burst release of 42 % in the first hour followed by 80% drug release within 8 h (Figure 5.5). MePEO-*b*-PBCL micelles, having benzyl group in the core, significantly reduced the burst release of CuI from the solubilizing vehicle and resulted in a significant decrease in accumulative drug release at the further time points ($P < 0.01$, One way ANOVA). This system showed an initial release of 28 % within 1 h followed by an accumulative release of 71 % within 8 h. On the other hand, nanoassemblies of MePEO-*b*-PChCL, having cholesteryl group in the core, were able to reduce the burst release at initial time points (35 % drug release at 1 h) compared to MePEO-*b*-PCL micelles ($P < 0.05$, One way ANOVA), but failed to show any superiority in reducing the rate of drug release at later time points (Figure 5.5). In fact, the release pattern of CuI from MePEO-*b*-PChCL nanoassemblies was almost identical with MePEO-*b*-PCL micelles at later time points (> 2 h).

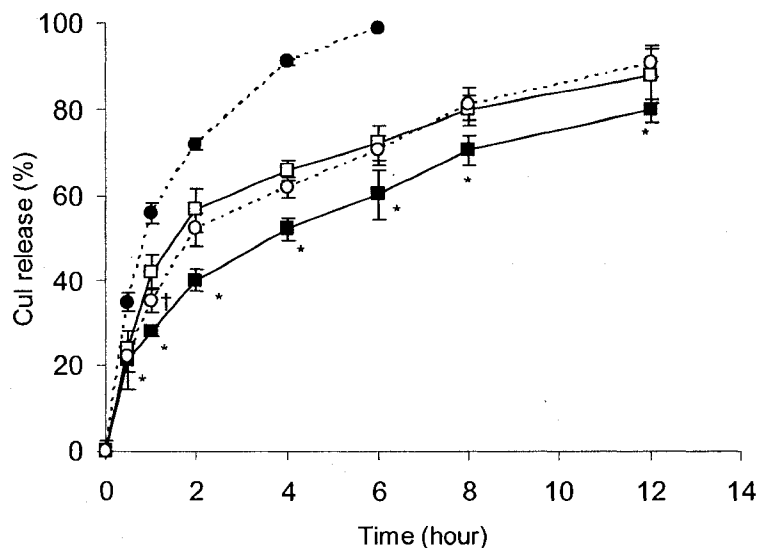
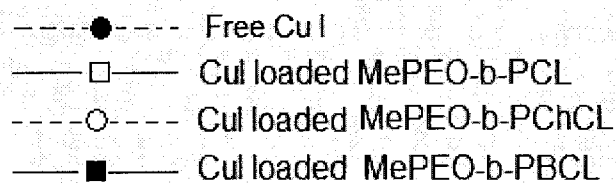


Figure 5.5- *In vitro* CuI release profile from polymeric nanocarriers at 37 °C. Each point represent mean \pm SD (n=3). * Shows significant difference in release profile from MePEO-*b*-PCL and MePEO-*b*-PChCL ($P < 0.05$, One way ANOVA). † Shows significant difference from MePEO-*b*-PCL at 1 hour ($P < 0.05$, One way ANOVA).

5.4. Discussion

Cucurbitacins are of great interest due to their selective inhibitory activity on signal transducer and activator of transcription 3 (STAT3) pathway and strong anti-proliferative function against a number of human carcinoma cell lines [21-23]. The IC_{50} values of cucurbitacins against several cancer cells are comparable with DOX, a widely used anti-cancer drug [22]. Moreover, selective STAT3 inhibitory activity of cucurbitacins makes them

excellent drug candidates for delivery to tumor microenvironment to overcome tumor-induced immunosuppression, which may eventually lead to potent anti-tumor immune responses through inhibition of STAT3 [24]. However, clinical development of this drug and its analogues has mostly been limited by their poor water solubility and non specific toxicity. A polymeric nanocarrier that can encapsulate cucurbitacins efficiently, control their rate of release and limit their distribution to non-target sites in the body may overcome both limitations. The potential of MePEO-*b*-poly(ester) block copolymers composed of PCL, PBCL and PChCL core forming block for this purpose have been assessed in this study.

Since each drug has its own unique chemical and physical properties, no delivery vehicle prepared from a particular polymer will serve as a universal carrier for all drugs. Compatibility or degree of interaction between polymer and drug affects many of the performance related characteristics of the delivery system such stability, drug-loading, and drug release kinetics. In previous studies it has been found that an increase in the degree of compatibility between the core-forming block of the copolymer and drug to be delivered results in an improvement in both drug loading, retention, and sustained release kinetics for different therapeutic agents [8, 25-27]. Therefore, in the present study, the optimization of polymeric micellar formulation of CuI has been carried out through chemical modification of the core of MePEO-*b*-PCL micelle to achieve high drug encapsulation and controlled release properties. For this purpose, ring opening polymerization of cholesteryl bearing monomer, α -cholesteryl carboxylate- ϵ -caprolactone was used to prepare MePEO-*b*-PChCL block copolymers (Scheme 5.1). It was found that unlike MePEO-*b*-PCL and MePEO-*b*-PBCL, a reaction temperature of 140 °C resulted in incomplete polymerization of α -cholesteryl carboxylate- ϵ -caprolactone. However, sufficient conversion (78 %) of α -cholesteryl carboxylate- ϵ -caprolactone to PChCL occurred at a reaction temperature of 160

°C and reaction time of 4 h. Potential degradation of polymer has been reported at higher temperature and longer reaction period due to transesterification or backbiting side reaction [28, 29]. The polymerization reactivity of α -cholesteryl carboxylate ϵ -caprolactone is lower than benzyl group bearing monomer, α -benzylcarboxylate ϵ -caprolactone (91%) discussed in previous chapter (Chapter 3, section 3.3.1). Indeed, the attachment of bulky group decreases the ring opening polymerization capacity of the cyclic ester and the effect is stronger for the larger groups attached.

Prepared block copolymers were assembled to core-shell structure by a co-solvent evaporation method and characterized for their functional properties in drug delivery. A decrease in CMC of MePEO-*b*-PChCL block copolymer indicates higher thermodynamic stability of the prepared nanocarrier, although the core forming block of the synthesized polymer had shorter hydrophobic chain length than MePEO-*b*-PCL under study. But the presence of cholesteryl moiety in MePEO-*b*-PChCL polymer had a negative impact on the viscosity of micellar core. The observation may be attributed to the bulkyness of cholesteryl moiety in MePEO-*b*-PChCL.

Among different core forming blocks, PChCL and PBCL showed better efficiency for the solubilization of CuI (Table 5.3). Based on the compatibility assessment by calculating Flory-Huggins interaction parameter (χ_{sp}) between CuI and different core structures under this study, we assume that polymeric nanocarriers with CuI compatible cores may be able to solubilize CuI effectively and control its rate of release to a larger extent. The calculated compatibility of CuI with different core forming structures under this study was in the order of PChCL > PBCL > PCL which was inversely proportional to the χ_{sp} values, confirming the better solubilization of CuI in polymeric nanocarriers having more compatible hydrophobic block structures. The results of encapsulation studies confirmed the

validity of this hypothesis where improved encapsulation of CuI in MePEO-*b*-PChCL based nano-carriers compared to MePEO-*b*-PBCL and MePEO-*b*-PCL micelles was observed.

The *in vitro* release studies clearly illustrate that polymeric micelle based CuI formulation can release the drug in a sustained manner (Figure 5.5). The results suggest that the release of CuI from polymeric micelles can be controlled, by varying the structure of core (Figure 5.5). In general, MePEO-*b*-PBCL micelles having benzyl group in the core was found to be more efficient in sustaining the rate of release for CuI, *in vitro*, the rate of drug release from MePEO-*b*-PBCL was rapid at the initial time point (<1 h), but it became more gradual at longer time. Surprisingly, MePEO-*b*-PChCL, containing cholesteryl core failed to show superiority in sustaining the drug release compared to PCL core. Less viscous core of PChCL compared to PCL and PBCL may be a possible reason for the rapid release of CuI from MePEO-*b*-PChCL nanocarriers.

5.5. Conclusion

Chemical tailoring of the MePEO-*b*-PCL micellar core through substitution of cholesteryl moieties enhanced the solubilization of poorly water soluble and cholesterol-compatible drug CuI in polymeric micelles. The *in vitro* rate of CuI release from polymeric nanocarriers was not affected by cholesteryl substitution, however. The most control over the rate of CuI release was achieved by polymeric micelles bearing benzyl groups in their core-structure.

5.6. References

- [1] A. Lavasanifar, J. Samuel, S. Sattari, G.S. Kwon, *Pharmaceutical Research* 19 (2002) 418-422.
- [2] T. Nakanishi, S. Fukushima, K. Okamoto, M. Suzuki, Y. Matsumura, M. Yokoyama, T. Okano, Y. Sakurai, K. Kataoka, *Journal of Controlled Release* 74 (2001) 295-302.
- [3] M. Yokoyama, S. Fukushima, R. Uehara, K. Okamoto, K. Kataoka, Y. Sakurai, T. Okano, *Journal of Controlled Release* 50 (1998) 79-92.
- [4] Y. Li, G.S. Kwon, *Pharm Res* 17 (2000) 607-611.
- [5] N. Nishiyama, Y. Kato, Y. Sugiyama, K. Kataoka, *Pharm Res* 18 (2001) 1035-1041.
- [6] M. Yokoyama, S. Fukushima, R. Uehara, K. Okamoto, K. Kataoka, Y. Sakurai, T. Okano, *J Control Release* 50 (1998) 79-92.
- [7] A. Lavasanifar, J. Samuel, S. Sattari, G.S. Kwon, *Pharm Res* 19 (2002) 418-422.
- [8] M. Yokoyama, A. Satoh, Y. Sakurai, T. Okano, Y. Matsumura, T. Kakizoe, K. Kataoka, *J Control Release* 55 (1998) 219-229.
- [9] A. Mahmud, X.B. Xiong, A. Lavasanifar, *Macromolecules* 39 (2006) 9419-9428.
- [10] A. Mahmud, X.B. Xiong, A. Lavasanifar, *European Journal of Pharmaceutics & Biopharmaceutics* (2008) *accepted for publication*.
- [11] C.M. Hansen, *J Paint Technol* 39 (1967) 104-117.
- [12] R.F. Fedors, *Polymer Engineering and Science* 14 (1974) 147-154.
- [13] D.V. Krevelen, Cohesive properties and solubility., in: D.V. Krevelen (Ed.), *Properties of polymer: Their correlation with chemical structure; Their numerical estimation and prediction from additive group contributions*, Elsevier Scientific Pub. Co., 3rd Ed. New York, 1990, pp. 189-224.
- [14] O. Molavi, A. Shayeganpour, V. Somayaji, S. Hamdy, D.R. Brocks, A. Lavasanifar, G.S. Kwon, J. Samuel, *Journal of Pharmacy and Pharmaceutical Sciences* 9 (2006) 158-164.
- [15] P.J. Marsac, S.L. Shamblin, L.S. Taylor, *Pharm Res* 23 (2006) 2417-2426.
- [16] J. Liu, Y. Xiao, C. Allen, *J Pharm Sci* 93 (2004) 132-143.
- [17] A. Forster, J. Hempenstall, I. Tucker, T. Rades, *Drug Development and Industrial Pharmacy* 27 (2001) 549-560.
- [18] D.J. Greenhalgh, A.C. Williams, P. Timmins, P. York, *J Pharm Sci* 88 (1999) 1182-1190.
- [19] S. Jain, F.S. Bates, *Science* 300 (2003) 460-464.
- [20] L.F. Zhang, A. Eisenberg, *Journal of the American Chemical Society* 118 (1996) 3168-3181.
- [21] M.A. Blaskovich, J. Sun, A. Cantor, J. Turkson, R. Jove, S.M. Sebti, *Cancer Res* 63 (2003) 1270-1279.
- [22] B. Jayaprakasam, N.P. Seeram, M.G. Nair, *Cancer Lett* 189 (2003) 11-16.
- [23] J. Sun, M.A. Blaskovich, R. Jove, S.K. Livingston, D. Coppola, S.M. Sebti, *Oncogene* 24 (2005) 3236-3245.
- [24] H. Yu, M. Kortylewski, D. Pardoll, *Nat Rev Immunol* 7 (2007) 41-51.
- [25] J. Lee, E.C. Cho, K. Cho, *J Control Release* 94 (2004) 323-335.
- [26] J. Liu, F. Zeng, C. Allen, *Journal of Controlled Release* 103 (2005) 481-497.

- [27] M.L. Adams, D.R. Andes, G.S. Kwon, *Biomacromolecules* 4 (2003) 750-757.
- [28] A. Beletsi, L. Leontiadis, P. Klepetsanis, D.S. Ithakissios, K. Avgoustakis, *Int J Pharm* 182 (1999) 187-197.
- [29] R.T. Liggins, H.M. Burt, *Adv Drug Deliv Rev* 54 (2002) 191-202.

Chapter 6

**The effect of block copolymer structure on the internalization of polymeric micelles
by human breast cancer cells**

A version of this chapter has been published: Abdullah Mahmud and Afsaneh Lavasanifar,
Colloids and Surfaces B: Biointerfaces, 45:82-89 (2005).

6.1. Introduction

The alteration of the core structures in methoxy poly(ethylene oxide)-*block*-poly(ϵ -caprolactone) (MePEO-*b*-PCL) based micelles and assessing the effects of such alterations on the relevant properties of polymeric micelles in drug delivery such as micellar size, morphology, thermodynamic and kinetic stability have been conducted in the previous chapters. The result of such studies have led to the development of optimal polymeric micellar carriers that can incorporate therapeutic agents through physical or chemical means efficiently, provide controlled release and demonstrated cytotoxic activity to cancer cells. The results of studies by our group and others indicate controlling the rate of drug release from polymeric micelles may jeopardize the efficacy of the incorporated drug. We have seen reduced cytotoxicity from physically encapsulated or chemically conjugated doxorubicin (DOX) in B16F10 murine melanoma cells compared to free DOX. Cytotoxicity of cucurbitacin I was also seen to decrease as a result of its incorporation to polymeric micelles [1].

Little is known on the effect of variations in the core/shell structure on the biological fate of polymeric micelles at the target site and its interaction with target cells. Understanding of the effect of chemical manipulations on the extent and mechanism of micellar uptake by target cells is essential in the design and development of nano-engineered polymeric micelles for drug or gene delivery to subcellular targets. Few studies have assessed the rate and extent of polymeric micellar uptake by different cells and provided insight on the subcellular distribution of polymeric micelles [2-4]. Uptake of MePEO-*b*-PCL micelles by mouse embryonal carcinoma cells, rat adrenal pheochromocytoma cells (PC12 cells) and mixed neuron-glia cultures have been investigated by Maysinger *et al* [5-8]. The same group has reported on the preferential subcellular distribution of PEO-*b*-PCL micelles in the

cytoplasm and several cytoplasmic organelles of PC12 cells [9]. In the present study, the effect of block copolymer structure in micelles of MePEO-*b*-PCL on their extent, rate and mechanism of micellar internalization by human breast cancer cells was evaluated to define optimal core/shell architectures that can achieve either intra or extracellular modes of drug delivery. The aim of this chapter was to find out whether manipulation in the structure of core/shell forming blocks through changes in their molecular weight can be used to enhance the internalization of polymeric micelles by target cells. Enhanced polymeric micelle-cell interactions may compensate for a delay in the release of incorporated drug leading to better in vivo efficacy for the encapsulated drug.

6.2. Experimental section

6.2.1. Synthesis, characterization and self assembly of block copolymers- MePEO-*b*-PCL block copolymers of different core and shell forming block lengths were synthesized by ring opening polymerization of ϵ -caprolactone using MePEO as initiator and stannous octoate as catalyst according to the method described in previous chapters (Chapter 2, section 2.2.2). The synthesized polymers were characterized by ^1H NMR and Gel permeation chromatography (GPC) for their average molecular weight and polydispersity according to the method described in Chapter 2, section 2.2.2.

6.2.2. Assembly of MePEO-*b*-PCL block copolymers and characterization of self-assembled structures- Micellization was achieved by dissolving MePEO-*b*-PCL block copolymer (30 mg) in acetone (0.5 mL) and drop-wise addition (~ 1 drop/15 sec) of polymer solution to doubly distilled water (3 mL) under moderate stirring at 25°C, followed by evaporation of acetone under vacuum. Average diameter and size distribution of prepared

micelles were estimated by dynamic light scattering (DLS) using Malvern Zeta-sizer 3000 at a polymer concentration of 10 mg/mL. Critical micelle concentration (CMC) of block copolymers were determined following changes in the fluorescence excitation spectra of pyrene in the presence of varied concentrations of block copolymers as described in previous chapters (Chapter 2, section 2.2.3).

6.2.3. Preparation and characterization of fluorescent dye loaded MePEO-*b*-PCL

micelles- Physical entrapment of hydrophobic fluorescent probe, DiI, was used to prepare fluorescent dye loaded polymeric micelles. DiI (10 $\mu\text{g/mL}$) and copolymer (10 mg/mL) were dissolved in acetone (0.5 mL). This solution was added to 3 mL of water in a drop-wise manner and remaining of the organic solvent was removed by evaporation under vacuum. The micellar solution was then centrifuged at $11600 \times g$ for 5 minutes, to remove DiI precipitates. The hydrodynamic diameter of DiI loaded MePEO-*b*-PCL micelles was measured by DLS as described in section 6.2.2. An aliquot of the micellar solution was diluted with an equal volume of dimethyl sulfoxide (DMSO) and used to quantify the level of encapsulated DiI by UV-Visible spectroscopy at 550 nm (Beckman coulter DU 530, USA).

The stability of DiI physical incorporation in polymeric micelles was assessed measuring the *in vitro* rate of DiI release from polymeric micelles using lipid vesicles as the receiver phase. Multilamellar vesicle liposome (MLVs) with total lipid content of 15 mM were prepared in phosphate buffer solution (PBS) by the lipid film method using 1,2-Distearoyl-sn-glycero-3-phosphocholine (DSPC) and cholesterol in the molar ratio of 3:1. Free probe and micelles labeled with probe (at a DiI level of 10 $\mu\text{g/mL}$) were incubated with liposomes (2 mM) at 37°C for different time intervals up to 24 h. One sample was taken at

each time point and centrifuged at $11600 \times g$ for 10 min to separate the lipid pellet. An aliquot of supernatant was diluted with the same volume of methanol and the level of DiI in the supernatant was determined from its absorbance at 550 nm. For time zero, block copolymer micelles loaded with DiI and free DiI were incubated with PBS. Lipid pellets were also dissolved in methanol and assayed for the amount of transferred DiI by UV/visible spectroscopy. Each experiment was conducted in triplicate. The percentage of released DiI was calculated and plotted versus time.

6.2.4. Cellular uptake studies- MCF-7 human adenocarcinoma breast cancer cell line was a generous gift from the laboratory of Dr. Susan Bates, National Cancer Institute. Cells were grown in RPMI 1640 complete growth medium supplemented with 10 % fetal bovine serum, 1% L-glutamine, and 100 units/mL penicillin and 100 $\mu\text{g}/\text{mL}$ streptomycin in a 75 cm^2 culture flask and maintained at 37°C with 5% CO_2 in a tissue culture incubator (5% CO_2 incubator, Isotemp model 546, Forma scientific). Cells were then seeded into 12-well plates at a density of 2×10^5 cells/well containing 1.5 mL of media on sterile round glass cover slip. Following a 24-h incubation period, aliquots of free and encapsulated DiI in PEO-*b*-PCL micelles (75 μL) were incubated with MCF-7 cells for 6 and 12 h. Free DiI was dissolved in PBS with the aid of DMSO (< 1 %). The final DiI and polymer concentration in each well was 0.5 $\mu\text{g}/\text{mL}$ and 0.5 mg/mL , respectively. Samples having free and encapsulated DiI without cells, and cells incubated with the medium were used as negative controls. Following the incubation period the medium was removed and the cover slips containing the cells were washed with cold PBS three times and transferred to a new 12 well plate. Trypsin EDTA (0.05% trypsin with EDTA.4Na), 400 μL , was added to each well and incubated for 5 minutes at 37°C. The cell suspension from each well was transferred to 96

well plate and exposed to 1% triton X-100 to lyse the cells. Fluorescence emission intensity of DiI at 550 nm (fluorescence concentration analyzer, Baxter, USA) provided means for the measurement of internalized DiI levels. DiI cellular accumulation was normalized with respect to total cellular protein content which was quantified by Lowry method using bovine serum albumin (BSA) as standard. Briefly, 125 μ L of reagent A (1 mL of 1% CuSO_4 + 1 mL of 2% NaK tartarate + 20 mL of 10% Na_2CO_3 anhydrous in 0.5 M NaOH) was added to empty clean test tubes containing either 125 μ L of the standard or the samples. After 10 minutes, 375 μ L of reagent B (1/10 diluted solution of Folin-Phenol reagent) was added to each tube under continuous vortex. Samples were left in the water bath at 50°C for 10 minutes. The assay was carried out using El 312e microplate Bio-Kinetics reader from Biotek instrument. Percent uptake was calculated using the following equation.

$$\text{Uptake (\%)} = \frac{\text{Normalized level of internalized DiI}}{\text{Level of DiI added to each well}} \quad (\text{Eq. 6.1})$$

To investigate the mechanism of cellular uptake, MCF-7 cells grown in 12 well plates were incubated with the micellar formulations at 4°C, or were treated with either chlorpromazine (8 $\mu\text{g}/\text{mL}$)[10, 11] or cytochalasin B (5 $\mu\text{g}/\text{mL}$)[12, 13] for 30 minutes prior to the addition of polymeric micelles. Following 6 h incubation of MCF-7 cells with polymeric micelles at mentioned condition, the media was removed. Cells were then treated as described previously and used to measure the level of internalized free and encapsulated DiI at reduced temperature or in the presence of uptake inhibitors.

6.2.5. Confocal microscopy studies- MCF-7 cancer cells were seeded into 8-well glass chamber slide (Lab-Tek, USA) containing RPMI complete growth media (2×10^5 cells per well). Following 30 minutes incubation at 37 °C in a 5% CO_2 atmosphere with a 95% relative

humidity, 30 μL aliquots of DiI labeled MePEO-*b*-PCL micelles were added to each well and incubated with cells for 4 h at 37 and 4°C. The final DiI and polymer concentrations were 0.6 $\mu\text{g}/\text{mL}$ and 0.6 mg/mL respectively. The media was removed and the cells were washed 3 times with ice cold PBS and incubated with 100 μL of 0.0005% Concavallin A- Alexa fluor 488 conjugates in PBS for 2 min to label the cell membranes, then fixed with 100 μL of 4% paraformaldehyde in PBS for 10 min. After the final wash, slides were prepared with a solution of 2.5% 1,4-Diazabicyclo [2.2.2.] octane.

6.2.6. Statistical analysis- Data are reported as mean \pm standard deviation. (S.D.). Differences among the mean of formulation characteristics and cellular internalization assessment of polymeric micelles were compared by Student's unpaired t-test assuming unequal variance.

6.3. Results

6.3.1. Synthesis, characterization and micellization of MePEO-*b*-PCL block copolymers- Synthesis of MePEO-*b*-PCL block copolymers through ring opening polymerization of ϵ -caprolactone by MePEO in the presence of stannous octoate as catalyst has been reported in chapter 2. In this study, three different molecular weights of MePEO (2000, 5000 and 13000 $\text{g}\cdot\text{mol}^{-1}$) were used and the feed ratio of monomer (ϵ -caprolactone) to initiator (MePEO) was changed to prepare MePEO-*b*-PCL block copolymer of five different structures. A nomenclature of 2000-5000, 5000-5000, 5000-13000, 5000-24000 and 13000-5000 in which the left number corresponds to the theoretical molecular weight of the shell forming block (MePEO) and the right number corresponds to the molecular weight of the core forming block (PCL), is used throughout this chapter to distinguish between prepared

MePEO-*b*-PCL block copolymers. The characteristics (average molecular weights, polydispersity and calculated hydrophilic/lipophilic balance (HLB)) of synthesized copolymers are described in Table 6.1.

Micellization of MePEO-*b*-PCL block copolymers were achieved through a co-solvent evaporation method using acetone as the organic co-solvent. DLS technique revealed an average diameter of 33 to 100 nm for MePEO-*b*-PCL micelles of different block size prepared by this method (Table 6.2).

6.3.2. Preparation and characterization of DiI loaded MePEO-*b*-PCL micelles-

Physical encapsulation of hydrophobic fluorescent probe, DiI, was shown to be an efficient method for labeling of MePEO-*b*-PCL micelles owing to high levels of DiI entrapment and limited dye leakage from the micellar carrier. DiI was encapsulated into micelles of MePEO-*b*-PCL through an identical method to the self-assembly process reaching encapsulation efficiencies of ≥ 80 percent in all polymeric micellar formulations (Table 6.2).

Table 6.1- Characteristics of the prepared PEO-*b*-PCL block copolymers.

MePEO M wt. (g.mol ⁻¹)	PCL M wt. (g.mol ⁻¹) ^a	MePEO- <i>b</i> -PCL M _n ^b	MePEO- <i>b</i> -PCL M _n ^c	MePEO- <i>b</i> -PCL PDI ^d (M _w /M _n)	HLB ^e
2000	5000	6800	12000	1.035	5.71
5000	5000	9900	11007	1.035	10.0
13000	5000	17200	NA	NA	14.5
5000	13000	17318	23008	1.063	5.55
5000	24000	27800	30035	1.065	3.45

^a Theoretical molecular weight

^b Number average molecular weight (M_n) determined by ¹H NMR

^c Number average molecular weight determined by GPC

^d Polydispersity index (weight average molecular weight/number average molecular weight (M_w/M_n)) measured by GPC

^e Hydrophilic lipophilic balance (HLB) determined by Griffin equation [14]

The capability of the PCL core in retaining the hydrophobic fluorescent probe within the micellar structure and stability of the labeled micelles during the time course of the cell uptake studies was assessed following the *in vitro* transfer of DiI from the polymeric micellar carrier to lipid vesicles. The phospholipids layer of the lipid vesicles is expected to maintain sink condition for the release of hydrophobic molecules from their vehicles. The results of our study showed a rapid rate of transfer for free DiI to lipid vesicles (Figure 6.1). Within 2 h, 70 % of unencapsulated DiI partitioned to the liposomes. The level of free probe transfer from micellar carrier to lipid vesicles approached 95 % in 8 h. In contrast, MePEO-*b*-PCL micelles retained their DiI content. After 24 h incubation with lipid vesicles, < 20 % of the encapsulated DiI has been released from MePEO-*b*-PCL micelles of different core/shell structure. At 6 and 12 h time points (time frame of the cell uptake studies) 3-6 % and 8-12 % of the encapsulated probe was released from the polymeric micellar carrier, respectively. The difference in the extent of DiI release from polymeric micelles having different MePEO/PCL block lengths at 6 and 12 h time points was not significant ($P > 0.05$, unpaired student's t test).

6.3.3. The effect of block copolymer structure on the extent, rate and mechanism of MePEO-*b*-PCL micellar uptake by MCF-7 cells- The rate and extent of cell uptake for free hydrophobic fluorescent probe DiI and MePEO-*b*-PCL micelles has been quantified by incubating MCF-7 cells with free or DiI-loaded polymeric micelles at polymer concentrations above their CMC. Cells were then separated from free or DiI-loaded polymeric micelles in the supernatant and the fluorescent intensity of DiI in the separated, washed and lysed cells was measured (Figure 6.2).

Table 6.2- Characteristics of the prepared MePEO-*b*-PCL block copolymer micelles

MePEO- <i>b</i> -PCL	CMC \pm SD (μ M)	Micellar size \pm SD (nm) ^b		Dil : Polymer molar ratio (M/M)	Encapsulation efficiency (%)
		Empty micelles	Dil-loaded micelles		
2000-5000	$14.3 \times 10^{-2} \pm 0.01$	33 ± 2.5	40 ± 1.5	0.0063	84
5000-5000	$18.2 \times 10^{-2} \pm 0.01^a$	40 ± 2.0	50 ± 2.0	0.0086	80
13000-5000	NA	90 ± 9.0	110 ± 7.0	0.0153	80
5000-13000	$4.30 \times 10^{-2} \pm 0.01^a$	80 ± 2.0	87 ± 3.0	0.0175	90
5000-24000	$1.80 \times 10^{-2} \pm 0.01^a$	92 ± 3.1	105 ± 4.3	0.0270	90

^a CMC values are reported from previous chapter (Chapter 2, Table 2.2).

^b Intensity mean measured by DLS technique

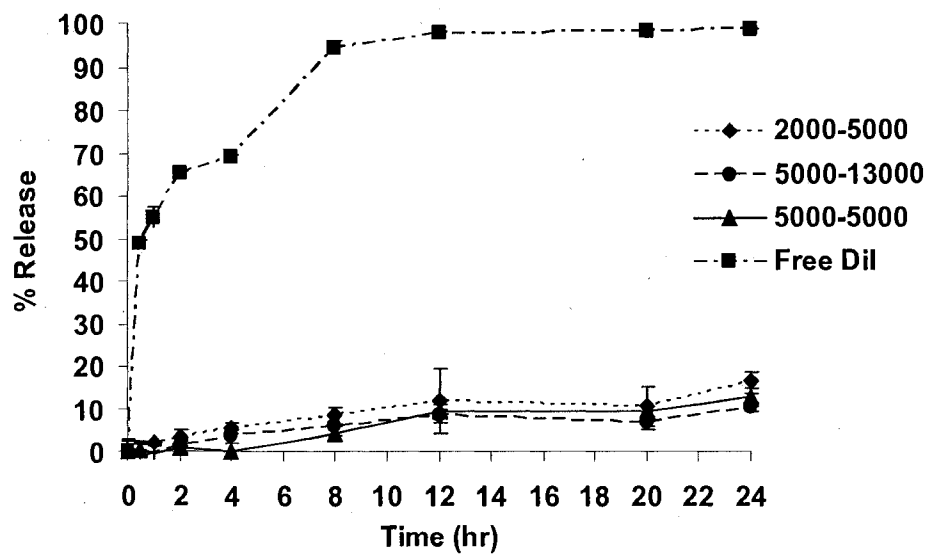


Figure 6.1- Release of free and encapsulated fluorescent probe, DiI, to lipid vesicles. Each point represents the mean of three samples \pm S.D.

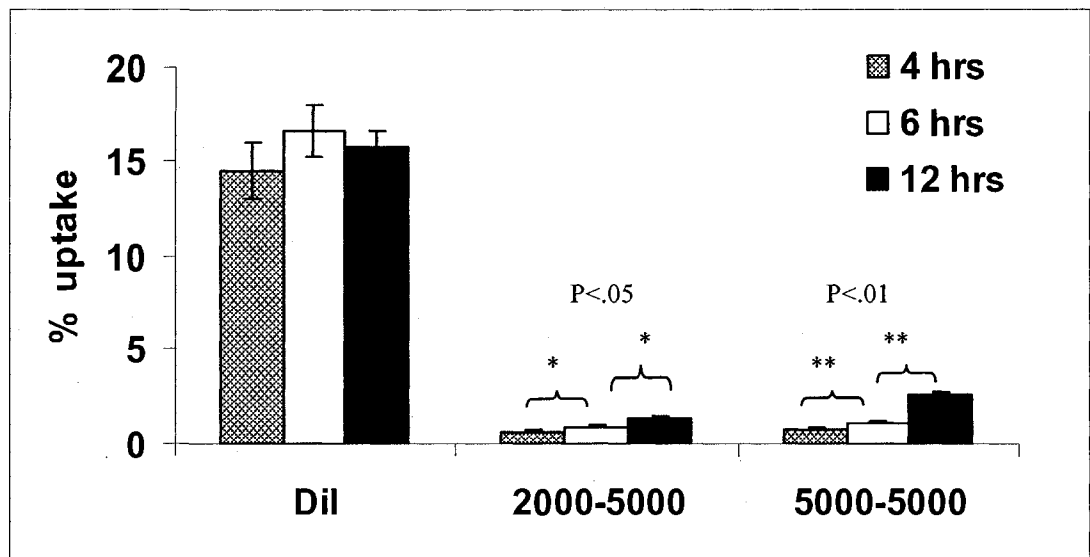
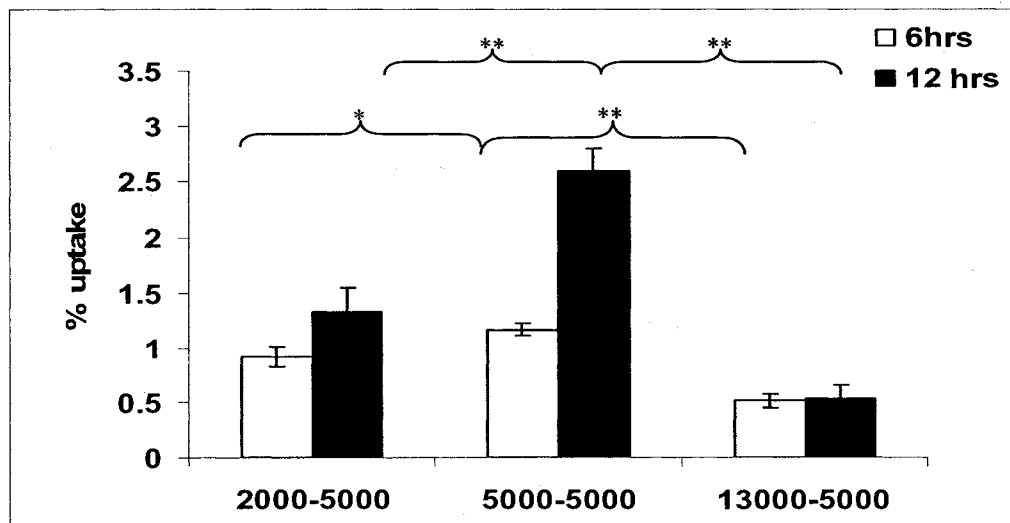


Figure 6.2- Comparative uptake of free and MePEO-*b*-PCL block copolymer micelle loaded DiI by MCF-7 human breast cancer cells after 6 and 12 h incubation. Each bar represents the mean of three samples \pm S.D.

In the next step, uptake of the block copolymer micelles of 5 different chain lengths by MCF-7 cells was assessed after 6 and 12 h of incubation (Figure 6.3). Incubation at reduced temperature (4°C) and preincubation of cells with inhibitors of macropinocytosis and clathrin mediated endocytosis was used to assess the mechanism of cell uptake for polymeric micelles of different core/shell structure (Figure 6.4). Internalization of the free and encapsulated probe into MCF-7 cells was confirmed by confocal microscopy (Figure 6.5). Free DiI appears to enter cells much faster and to a greater extent than micelle incorporated DiI (16 % uptake for free DiI versus 0.5-3 % uptake for encapsulated DiI in different MePEO-*b*-PCL micelles after 12 h of incubation) reflecting a difference in the mechanism of cellular uptake for free and encapsulated probe (Figure 6.2). Similar results were seen in confocal micrograph where internalization of free DiI and DiI encapsulated in 5000-5000 MePEO-*b*-PCL micelles by MCF cells were evaluated after 4 h of incubation at 37 °C (Figure 6.5 B & 6 C). The effect of variations in the molecular weight of the shell and core forming blocks on the extent of micellar cell uptake is shown in Figure 6.3A and B, respectively. After 12 h incubation, the order in the extent of cellular uptake for MePEO-*b*-PCL micelles of different structure from lowest to highest is 13000-5000 < 2000-5000 < 5000-24000 < 5000-5000 < 5000-13000. As illustrated in Figure 6.3 A, with similar PCL chain lengths, an increase in the molecular weight of MePEO from 2000 to 5000 g.mol⁻¹ increased the cellular uptake of polymeric micelles by almost 2 fold after 12 h incubation (P < 0.01, unpaired student t test). Further increase in the molecular weight of the shell forming block to 13000 g.mol⁻¹ decreased the cellular internalization of polymeric micelles by 2.1 and 4.5 folds after 6 and 12 h of incubation, respectively (P < 0.01, unpaired student t test).

A)



B)

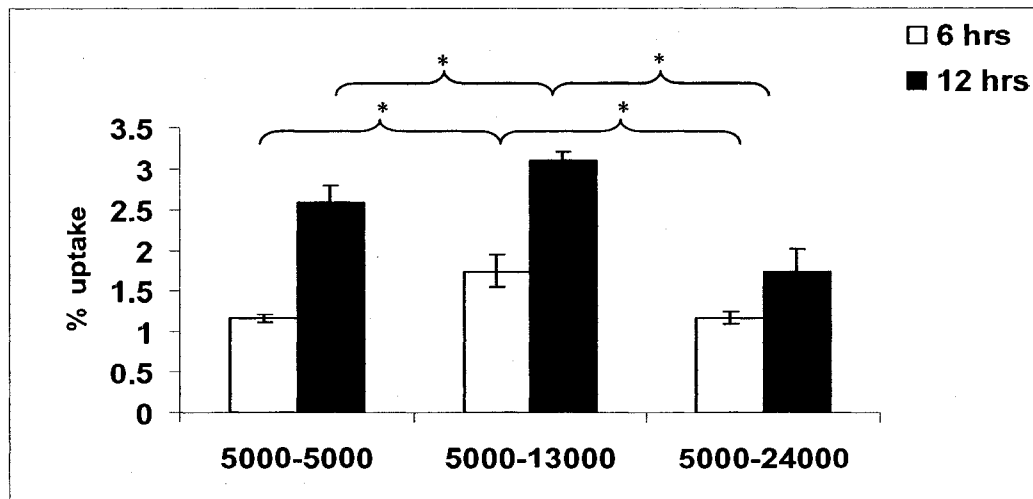


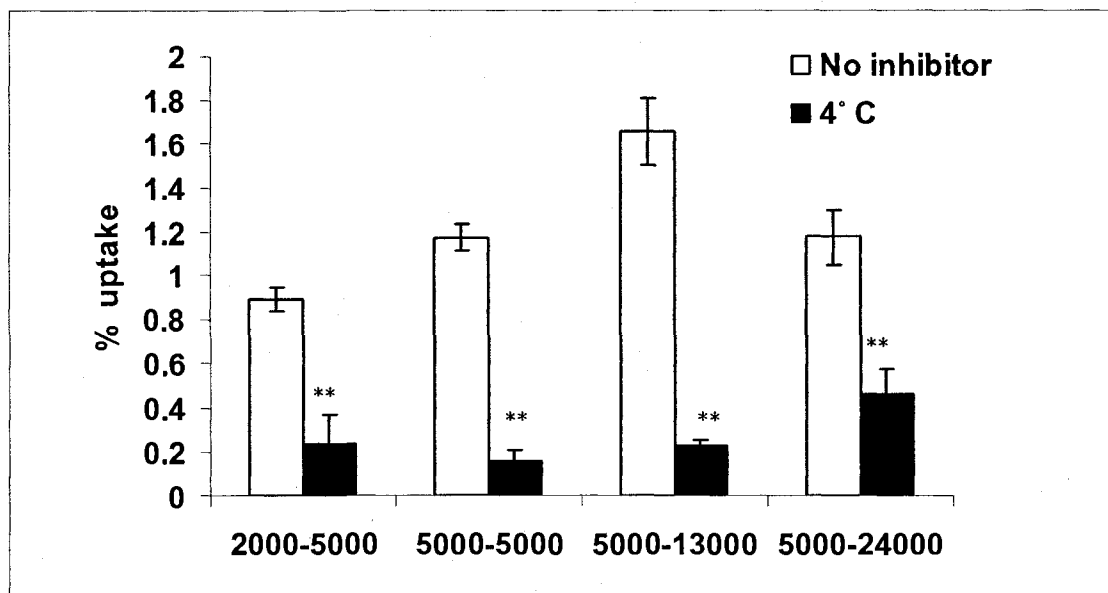
Figure 6.3- The effect of A) McPEO and B) PCL molecular weights on the uptake of McPEO-*b*-PCL micelles by MCF-7 cells. Each bar represents the mean of three experiments \pm S.D. (Symbols of * and ** correspond to a significance of difference at $P < 0.05$ and $P < 0.01$, respectively)

The internalization of MePEO-*b*-PCL block copolymer micelles was also investigated for block copolymers of different PCL block chain length (Figure 6.3 B). For polymeric micelles with an identical MePEO molecular weight of 5000 g.mol⁻¹, an increase in PCL chain length from 5000 to 13000 g.mol⁻¹ increased the micellar uptake by 1.5 and 1.2 folds after 6 and 12 h of incubation, respectively (P< 0.05, unpaired student t test) When the molecular weight of PCL was raised further from 13000 to 24000 g.mol⁻¹, cellular uptake was reduced by 1.8 fold after 12 h of incubation (P< 0.05, unpaired student t test).

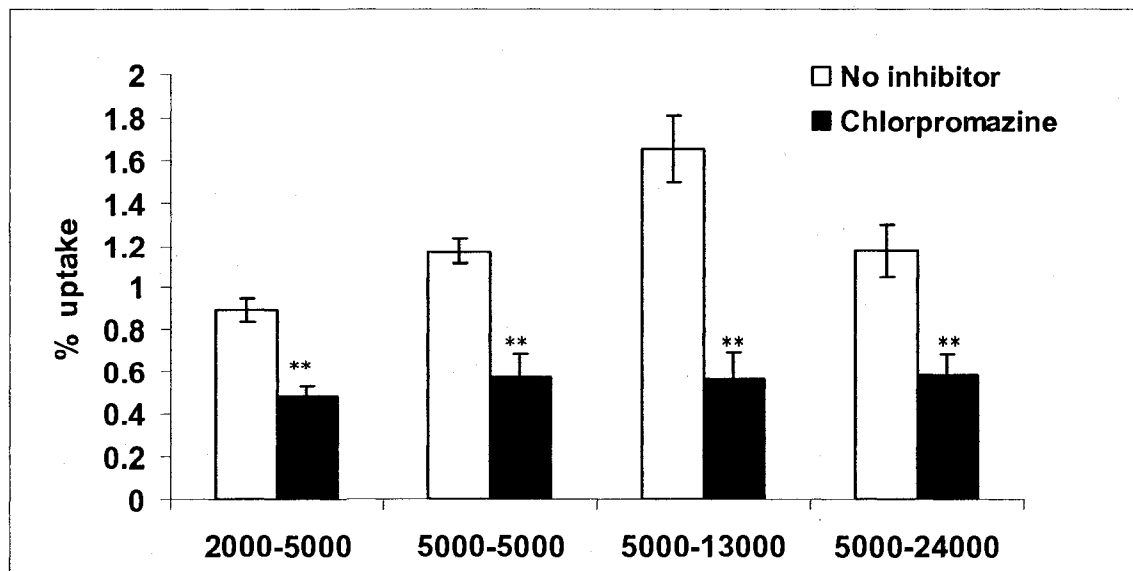
A decrease in temperature from 37° to 4°C markedly reduced the extent of polymeric micellar association with MCF-7 cells (P<0.01, unpaired t test). A similar trend has been observed in confocal micrographs (Figure 6.5 C & E). After 6 h incubation at a reduced temperature, cellular uptake of 2000-5000, 5000-5000, 5000-13000 and 5000-24000 MePEO-*b*-PCL micelles was reduced by 3.8, 7.5, 7.3 and 2.5 fold, respectively (Figure 6.4 A). Cellular uptake of free DiI was not affected by temperature, on the other hand (Data not shown).

Pretreatment of the MCF-7 cells with chlorpromazine at 8 µg/mL inhibited the cellular uptake of MePEO-*b*-PCL micelles irrespective of the shell/core structure. A 1.8, 2, 3 and 2 fold reduction in uptake was observed for 2000-5000, 5000-5000, 5000-13000 and 5000-24000 MePEO-*b*-PCL micelles in chlorpromazine treated cells, respectively (Figure 6.4 B). Pretreatment of cells with cytochalasin B at 5 µg/mL caused 2.5 and 4 fold decrease of uptake for 5000-5000 and 5000-13000 MePEO-*b*-PCL micelles, respectively (Figure 6.4 C). The uptake of 2000-5000 and 5000-24000 MePEO-*b*-PCL micelles by MCF-7 cells was not affected by pre-incubation of the cells with cytochalasin B, however (P>0.05, unpaired t test).

A)



B)



C)

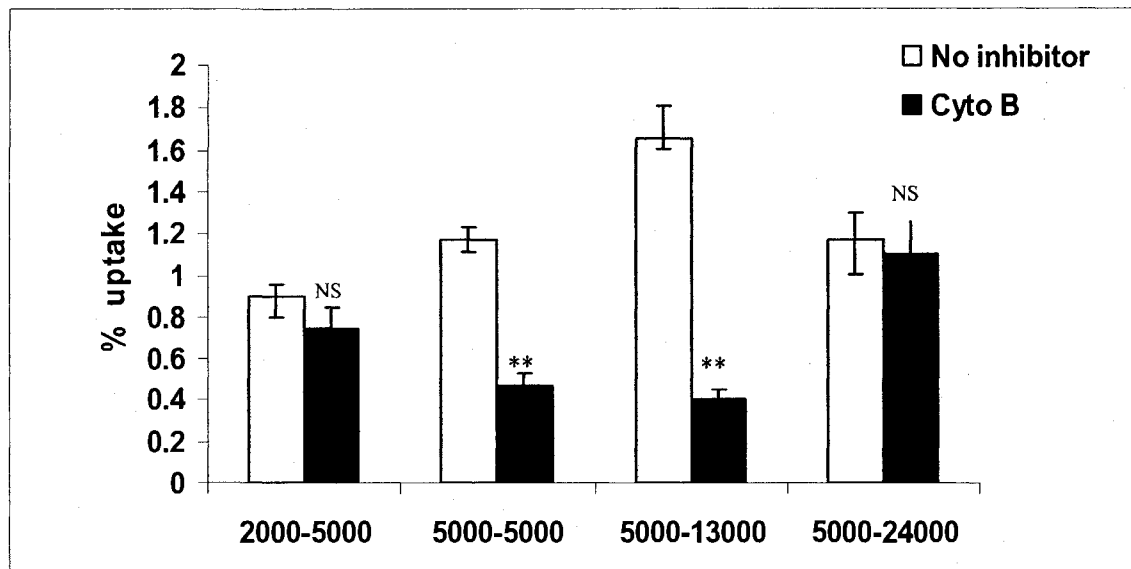
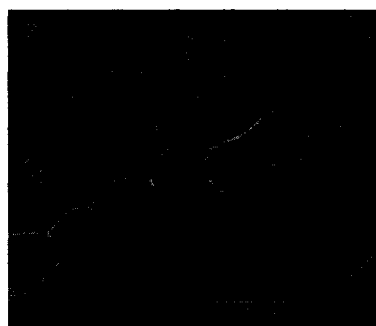


Figure 6.4- The effect of **A)** reduced temperature (incubation at 4°C); **B)** pretreatment with chlorpromazine and **C)** pretreatment with cytochalasin B on the internalization of MePEO-*b*-PCL micelles by MCF-7 cells. Uptake was quantified by fluorescence concentration analyzer after 6 h incubation. Each bar represents the mean of three samples \pm S.D. (Symbols of * and ** correspond to a significance of difference between normal uptake and inhibitor treated groups at $P < 0.05$, $P < 0.01$, respectively. NS corresponds to no significance in difference at $P > 0.05$)



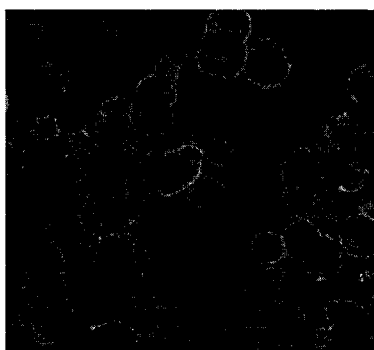
(A)



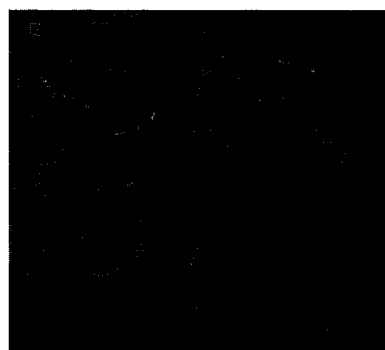
(B)



(C)



(D)



(E)

Figure 6.5- Confocal microscopy images of MCF-7 cells incubated in different conditions: **A)** MCF-7 cells stained with Con-A Alexa fluor 488 conjugate; **B)** MCF-7 cells incubated with free DiI at 37°C; **C)** MCF-7 cells incubated with DiI labeled 5000-5000 MePEO-*b*-PCL micelles at 37°C; **D)** MCF-7 cells incubated with free DiI at 4°C; **E)** MCF-7 cells incubated with 5000-5000 DiI labeled MePEO-*b*-PCL micelles at 4°C.

6.4. Discussion

Recent advances in synthetic chemistry have provided the opportunity to engineer the core/shell structure in polymeric micelles to develop tumor targeted nanodelivery system based on the physicochemical properties of the incorporated drug and characteristic features of tumor pathophysiology [15-18]. For instance, several attempts in the development of polymeric micellar drug delivery systems has shown chemical conjugation of drug-compatible moieties to the core-forming block can be used to improve encapsulation or control the rate of drug release [19, 20], while an increase in the length or density of the PEO block can be applied to reduce elimination of the micellar carrier by phagocytic cells and increase the biological half life of the micellar carrier leading to better tumor accumulation [21, 22]. Interaction of DiI loaded MePEO-*b*-PCL micelles of varied composition with MCF-7 human breast cancer cells has been investigated in this study to see whether chemical manipulation of the core/shell structures can be used to improve the access of therapeutic agent to either cell membrane or intracellular sites of drug action in polymeric micellar drug delivery. In the current study, MCF-7 human breast cancer cell line was chosen as a well characterized solid tumor model to assess the interaction of polymeric micelles at cellular level.

Measurement of the DiI fluorescent intensity in treated cells in the current study allowed quantification of cellular uptake in different treatment groups. The results demonstrated a reduction in the extent and rate of hydrophobic probe delivery to MCF-7 cells by MePEO-*b*-PCL micelles pointing to an extracellular mode of delivery for hydrophobic drugs by polymeric micelles (Figure 6.2) [23]. Similar trend has been reported by Maysinger *et al* when internalization of free and MePEO-*b*-PCL encapsulated DiI by neural cells has been investigated using fluorescence microscopy techniques [24].

The results of present study also demonstrated the extent and kinetics of micellar internalization by model target cells to be dependent on the molecular weight of the shell and core forming blocks (Figure 6.3). With equivalent PCL molecular weights (5000 g.mol⁻¹), polymeric micelles having 5000 g.mol⁻¹ of PEO showed a significantly higher uptake by cancer cells than those with 2000 and 13000 g.mol⁻¹ of PEO. In other words, a deviation from a PEO molecular weight of 5000 g.mol⁻¹ decreased the internalization of micellar carrier by cancer cells. With an identical PEO molecular weight (MePEO of 5000 g.mol⁻¹), polymeric micelles having 13000 g.mol⁻¹ of PCL showed a significantly higher uptake by cancer cells than those with 5000 or 24000 g.mol⁻¹ of PCL. However, the influence of core forming block length on micellar internalization by cancer cells was found not to be as marked as the effect of PEO molecular weight.

The presence of a hydrophilic polymeric brush on the surface of colloidal carriers induces steric repulsive forces and stabilizes the carrier's interface. This has shown to prevent the adsorption of opsonins to the carrier surface and further phagocytosis of colloidal carriers by human monocytes [25]. The extent of protection from uptake by monocytes is known to enhance as the molecular weight and density of the hydrophilic block on the colloidal carrier is raised [21, 25-27]. The effect of core forming block on the internalization of colloidal carriers by different cells have not been fully explored, however. Investigations by Gref *et al* making comparisons between nanoparticles consists of MePEO-*b*-PCL, MePEO-*b*-poly(Lactic acid) (MePEO-*b*-PLA) and MePEO-*b*-poly(Lactide-co-glycolide) (MePEO-*b*-PLGA) has shown the nature of the hydrophobic block to influence the extent and type of protein adsorption on nanocarrier [27].

Extensive hydration of a thick PEO shell (MePEO of 13000 g.mol⁻¹) on the surface of polymeric micelles may inhibit the adhesion of the delivery system to the cell surface

preventing its uptake by cancer cells. An increase in size of the hydrophobic block (from 5000 to 13,000 g. mol⁻¹ for PCL), on the other hand, may lead to an incomplete protection by the micellar shell against cell adhesion and further uptake of the colloidal carrier by target cells.

Further studies investigated the mechanisms involved in the internalization of MePEO-*b*-PCL micelles having various core/shell forming block chain lengths by cancer cells (Figure 6.4 & 6.5). Reduced micellar uptake after their incubation with cancer cells at 4 °C is an indication for the involvement of energy dependent mechanisms. This is consistent with the findings of Allen *et al* for the uptake of 2000-2300 MePEO-*b*-PCL micelles by PC12 cells [5].

The reduced uptake of MePEO-*b*-PCL micelles having different PEO/PCL block lengths after chlorpromazine treatment shows clathrin mediated mechanism of endocytosis involved in the uptake of polymeric micelles to be independent of the micellar structure. Chlorpromazine is an inhibitor of clathrin-dependent receptor-mediated endocytosis which involves the formation of “coated pits” on the plasma membrane formed by the assembly of cytosolic coat protein, i.e., clathrin with the membrane associated adaptor proteins[28, 29]. Chlorpromazine prevents the recruitment of adaptor protein to clathrin and further assembly of the coated pit to the cell surface [30, 31].

Inhibition of micellar cell uptake by cytochalasin B, on the other hand, was found to be dependent on the block copolymer structure. Pretreatment of cells with cytochalasin B inhibited the internalization of 5000-5000 and 5000-13000 MePEO-*b*-PCL micelles pointing to the possible involvement of macropinocytosis for the internalization of these structures by cancer cells. Cytochalasin B restricts the actin polymerization surrounding the endocytic vesicle by disrupting microfilament bundles that initiates membrane ruffling in

macropinocytosis [28, 32-34]. Cellular internalization of both 2000-5000 and 5000-24000 MePEO-*b*-PCL micelles was not affected by cytochalasin B treatment, although these micellar structures were found to be very different in size (average diameter of 40 nm for 2000-5000 versus 105 nm for 5000-24000 polymeric micelles) (Table 6.2). This observation points to the importance of core/shell structure (rather than the carrier size) in defining the mechanism of cellular uptake for colloidal carriers. Finally, the lower uptake of 2000-5000 and 5000-24000 MePEO-*b*-PCL micelles by cancer cells might have been originated from a difference in the mechanism of cell uptake for these specific structures. The reason behind this difference is not clear and requires further investigations.

6.5. Conclusion

The molecular weights of the core and shell forming blocks in polymeric micelles appear to influence the extent, rate and mechanism of micellar internalization by cancer cells. As a result, chemical manipulation of the core/shell structure may be used to design polymeric micellar carriers that can achieve intra or extra cellular modes of drug delivery and provide better access to either cell membrane or intracellular organelles.

6.6. References

- [1] O. Molavi, Z. Ma, A. Mahmud, A. Alshamsan, J. Samuel, R. Lai, G.S. Kwon, A. Lavasanifar, *Int J Pharm* 347 (2008) 118-127.
- [2] Y.S. Nam, H.S. Kang, J.Y. Park, T.G. Park, S.H. Han, I.S. Chang, *Biomaterials* 24 (2003) 2053-2059.
- [3] V.I. Slepnev, L.E. Kuznetsova, A.N. Gubin, E.V. Batrakova, V. Alakhov, A.V. Kabanov, *Biochem Int* 26 (1992) 587-595.
- [4] H.S. Yoo, T.G. Park, *J Control Release* 70 (2001) 63-70.
- [5] C. Allen, Y. Yu, A. Eisenberg, D. Maysinger, *Biochim Biophys Acta* 1421 (1999) 32-38.
- [6] L. Luo, J. Tam, D. Maysinger, A. Eisenberg, *Bioconjug Chem* 13 (2002) 1259-1265.
- [7] D. Maysinger, J. Lovric, A. Eisenberg, R. Savic, *Eur J Pharm Biopharm* 65 (2007) 270-281.
- [8] R. Savic, T. Azzam, A. Eisenberg, D. Maysinger, *Langmuir* 22 (2006) 3570-3578.
- [9] R. Savic, L. Luo, A. Eisenberg, D. Maysinger, *Science* 300 (2003) 615-618.
- [10] V. Puri, R. Watanabe, R.D. Singh, M. Dominguez, J.C. Brown, C.L. Wheatley, D.L. Marks, R.E. Pagano, *J Cell Biol* 154 (2001) 535-547.
- [11] R.D. Singh, V. Puri, J.T. Valiyaveetil, D.L. Marks, R. Bittman, R.E. Pagano, *Mol Biol Cell* 14 (2003) 3254-3265.
- [12] A.H. Band, S.D. Chitamber, A. Bhattacharya, G.P. Talwar, *Int J Lepr Other Mycobact Dis* 54 (1986) 294-299.
- [13] M. Ghoneum, I. Grewal, J. Brown, R. Osborne, H. Elembabi, G. Gill, *Acta Histochem* 105 (2003) 127-133.
- [14] J. Zastre, J. Jackson, M. Bajwa, R. Liggins, F. Iqbal, H. Burt, *Eur J Pharm Biopharm* 54 (2002) 299-309.
- [15] A. Lavasanifar, J. Samuel, G.S. Kwon, *Advanced Drug Delivery Reviews* 54 (2002) 169-190.
- [16] K. Kataoka, A. Harada, Y. Nagasaki, *Adv Drug Deliv Rev* 47 (2001) 113-131.
- [17] G.S. Kwon, K. Kataoka, *Advanced Drug Delivery Reviews* 16 (1995) 295-309.
- [18] T. Nakanishi, S. Fukushima, K. Okamoto, M. Suzuki, Y. Matsumura, M. Yokoyama, T. Okano, Y. Sakurai, K. Kataoka, *Journal of Controlled Release* 74 (2001) 295-302.
- [19] A. Lavasanifar, J. Samuel, G.S. Kwon, *J Control Release* 79 (2002) 165-172.
- [20] T. Nakanishi, S. Fukushima, K. Okamoto, M. Suzuki, Y. Matsumura, M. Yokoyama, T. Okano, Y. Sakurai, K. Kataoka, *J Control Release* 74 (2001) 295-302.
- [21] V.C. Mosqueira, P. Legrand, J.L. Morgat, M. Vert, E. Mysiakine, R. Gref, J.P. Devissaguet, G. Barratt, *Pharm Res* 18 (2001) 1411-1419.
- [22] G. Kwon, S. Suwa, M. Yokoyama, T. Okano, Y. Sakurai, K. Kataoka, *Journal of Controlled Release* 29 (1994) 17-23.
- [23] R. Duncan, *Nat Rev Drug Discov* 2 (2003) 347-360.
- [24] D. Maysinger, O. Berezovska, R. Savic, P.L. Soo, A. Eisenberg, *Biochim Biophys Acta* 1539 (2001) 205-217.

- [25] J.C. Leroux, P. Gravel, L. Balant, B. Volet, B.M. Anner, E. Allemann, E. Doelker, R. Gurny, *J Biomed Mater Res* 28 (1994) 471-481.
- [26] V.C. Mosqueira, P. Legrand, A. Gulik, O. Bourdon, R. Gref, D. Labarre, G. Barratt, *Biomaterials* 22 (2001) 2967-2979.
- [27] R. Gref, M. Luck, P. Quellec, M. Marchand, E. Dellacherie, S. Harnisch, T. Blunk, R.H. Muller, *Colloids Surf B Biointerfaces* 18 (2000) 301-313.
- [28] S.D. Conner, S.L. Schmid, *Nature* 422 (2003) 37-44.
- [29] F.M. Brodsky, C.Y. Chen, C. Knuehl, M.C. Towler, D.E. Wakeham, *Annu Rev Cell Dev Biol* 17 (2001) 517-568.
- [30] L.H. Wang, K.G. Rothberg, R.G. Anderson, *J Cell Biol* 123 (1993) 1107-1117.
- [31] C. Lamaze, S.L. Schmid, *Curr Opin Cell Biol* 7 (1995) 573-580.
- [32] S.G. Axline, E.P. Reaven, *J Cell Biol* 62 (1974) 647-659.
- [33] J. Heuser, *Cell Biol Int Rep* 13 (1989) 1063-1076.
- [34] S.B. Sieczkarski, G.R. Whittaker, *J Gen Virol* 83 (2002) 1535-1545.

Chapter 7

General Discussion and Conclusions

7.1. General discussion

Polymeric micelles self-assembled from amphiphilic block copolymers are of increasing interest in drug delivery [1-6]. Among different micelle forming block copolymers developed to date, those with poly(ethylene oxide) (PEO), as the shell forming block, and poly(ester)s or poly (L-amino acid)s (PLAAs), as the core-forming block, are in the front line of drug development. The placement is owed to the excellent biocompatibility of PEO and potential biodegradability of poly(ester)s and PLAAs which makes them safe for human administration. The primary advantage poly(ethylene oxide)-*block*-poly(L-amino acid) (PEO-*b*-PLAA) block copolymers over PEO-*b*-poly(ester) is the chemical flexibility of the PLAA structure that makes nanoengineering of the carrier a feasible approach. The presence of free functional side groups on the PLAA block provides sites for the attachment of drugs, drug compatible moieties or charged therapeutics such as DNA. Moreover, a systemic alteration in the structure of the core-forming block has been used to enhance drug loading and achieve efficient control over drug release. On the other hand, chemical modification or engineering on the poly(ester)s was limited due to the lack of functional group in their structures.

The aim of this study was to develop novel micelle-forming methoxy poly(ethylene oxide)-*b*-poly(ester) (MePEO-*b*-poly(ester)) block copolymers, e.g., MePEO-*b*-poly(ϵ -caprolactone) (MePEO-*b*-PCL), bearing multiple functional side groups on the PCL block and investigate the potential application of developed polymers for chemical conjugation, physical encapsulation and delivery of model anticancer drugs. In the preliminary studies, attachment of functional group, benzyl carboxylate to the MePEO-*b*-PCL block copolymer was pursued by anionic activation of PCL block with non-nucleophilic strong base lithium diisopropylamine (LDA) and further electrophilic substitution with benzyl chloroformate.

This approach resulted in a decrease in molar masses of substituted polymer, possibly due to the intra-molecular or intermolecular transesterification reaction. In order to minimize the side reaction, instead of attaching functional group directly to the polymer chain, we decided to prepare functional group bearing monomer. In the second approach, functional group bearing monomer, α -benzylcarboxylate- ϵ -caprolactone was synthesized by anionic activation of ϵ -caprolactone (Chapter 3). The synthesis of MePEO-*b*-PCL block copolymer by ring opening polymerization of ϵ -caprolactone initiated with MePEO using stannous octoate as catalyst was optimized for the reaction time, temperature and catalyst concentration (Chapter 2, Figure 2.2). [7-9]. Ring opening polymerization of lactones has been conducted at different temperatures, various reaction time lengths and catalyst concentration [7, 10, 11]. Optimum reaction condition and catalyst concentration in the ring opening polymerization of lactones is extremely important to achieve a controlled architecture of poly(ester) with high yield, however. [12-14]. Functional group bearing monomers were used in ring opening polymerization with MePEO as initiator and stannous octoate as catalyst to prepare MePEO-*b*-poly(α -benzylcarboxylate ϵ -caprolactone) (MePEO-*b*-PBCL) containing pendant benzyl groups (Chapter 3) and MePEO-*b*-poly(α -cholesteryl carboxylate ϵ -caprolactone) (MePEO-*b*-PChCL) containing cholesteryl side groups on the poly(ester) block (Chapter 5). Further catalytic debenzylation of MePEO-*b*-PBCL produced MePEO-*b*-poly(α -carboxyl ϵ -caprolactone) (MePEO-*b*-PCCL) block copolymer containing carboxylic group in the poly(ester) block (Chapter 3).

Self-assembly of MePEO-*b*-PCL based block copolymers to core shell architecture were performed by co-solvent evaporation method. The self assembled structures were characterized for their morphology and size by transmission electron microscopy (TEM) [15, 16], hydrated diameter by dynamic light scattering (DLS) and their critical micelle

concentration (CMC) and core viscosity by fluorescent probe techniques [17, 18]. The effect of core modifications on the properties of MePEO-*b*-PCL micelles was assessed in chapter 2 and 3. Structure-property relationships were built with regard to the effect of pendant benzyl and carboxylic groups as well as their degree of substitution on the PCL back bone on micellar properties such as size, CMC and core viscosity. The CMC of MePEO-*b*-PCL based micelles was found to decrease by either elongating the PCL block or substitution of more hydrophobic groups (benzylcarboxylate) on PCL chain. Substitution of benzylcarboxylate groups was found more effective in reducing the CMC compared to elongating the PCL chain (Chapter 3, Table 3.2). On the other hand, substitution of PCL block with carboxylic group in MePEO-*b*-PCCL exhibited a drastic increase in CMC indicating less thermodynamic stability of carboxylic group bearing micelles (Chapter 3, Table 3.2). Decrease in the substitution level of carboxylic group in PCL block or attachment of more hydrophobic DOX exhibited significant decrease in CMC of MePEO-*b*-PCL block copolymer (Chapter 4, table 4.1). A reverse relationship between the hydrophobicity of the core-forming block and CMC has been shown in many studies [17-19]. The core of the benzyl and carboxylic group containing micelles was found to be more viscous than unfunctionalized MePEO-*b*-PCL micelles (Chapter 3, Table 3.2). A high substitution of PCL backbone with carboxylic group noticeably increased the microviscosity of the core. Polymeric micelles with rigid core were expected to resist dissociation and lower the rate of drug diffusion, which may lead to sustained drug release.

A model anticancer drug, DOX was conjugated to the pendant carboxyl groups of MePEO-*b*-PCCL by an amide bond (Chapter 4). This has led to the formation of novel self associating MePEO-*b*-P(CL-DOX) conjugates that bear a hydrolysable poly(ester) backbone (i.e., PCL) and at the same time accommodate several DOX molecules per polymer chain.

The percent of DOX substitution to the carboxyl group of PCL block was only 14%. Attachment of DOX to the carboxyl bearing polymer decreased the CMC drastically due to the more hydrophobic nature of the core forming block for MePEO-*b*-P(CL-DOX) compared to MePEO-*b*-PCCL micelles. The core viscosity of the DOX conjugated block copolymer was found to decrease with the attachment of DOX molecule which was possibly due to the disruption of H-bonding between COOH groups. Micelle forming DOX conjugate was expected to reduce the chance of premature drug release in blood circulation while facilitating the release of DOX or DOX-caprolactone (DOX-CL) derivatives in the acidic environment of the endosome/lysosomes after internalized by tumor cells.

In further studies, MePEO-*b*-PCL block copolymers with benzyl (i.e, MePEO-*b*-PBCL), carboxylic (i.e., MePEO-*b*-PCCL) or DOX side groups (MePEO-*b*-P(CL-DOX)) were used to prepare DOX encapsulated micellar nanocontainers. Prepared polymeric micellar DOX conjugates or micellar nano-containers were evaluated for the level of DOX loading, where maximum DOX loading was achieved with MePEO-*b*-PBCL micelles (Chapter 4, Table 4.2)

The assessment of *in vitro* drug release from polymeric micelles is usually carried out by dialysis, size exclusion chromatography or by using lipid recipient phase to separate the released drug from micelle encapsulated drugs [19-23]. Use of biomimetic recipient phase has also been studied to assess the release of hydrophobic drugs [24]. However, due to the amphiphilic nature of DOX dialysis against buffer was found most effective method to separate the released DOX from encapsulated drug and has been used previously [7, 25]. DOX release from micellar nanocontainer was studied against buffer at pH, 5 and 7.4 for 72 hours. Both free DOX and micelle loaded DOX was released faster at pH 5.0 compared to pH 7.4 which is advantageous for preferential drug release at tumor acidic pH (5.0-5.5)

Among different polymeric micellar nano-containers, a core of PBCL demonstrated highest drug loading as well as provided the maximum control over the rate of DOX release (Chapter 4, Table 4.2, Figure 4.4). Enhanced compatibility between PBCL core and DOX due to hydrophobic interaction was assumed as the reason for this superiority. Micelle forming DOX conjugate, MePEO-*b*-P(CL-DOX) did not show any signs of DOX release during that time period.

The cytotoxicity of the micellar nanocontainer and DOX conjugate was assessed by MTT assay in murine melanoma B16F10 cells [26]. Free DOX demonstrated higher cytotoxicity than micellar DOX. The cytotoxicity of micellar nanocontainer followed the similar trend what has been observed in the release study (Chapter 4, Table 4.2 and Figure 4.6). The cytotoxicity of micelle forming DOX conjugate increased with time and surpassed that of physically encapsulated DOX as time elapsed although it didn't show any signs of DOX release *in vitro* within 72 hours. We assume that active DOX-caprolactone (DOX-CL) derivative released from the conjugate after 48 hours due to the hydrolysis of PCL backbone caused the observed cytotoxicity of MePEO-*b*-P(CL-DOX). Our hypothesis of poly(ester) backbone cleavage was further confirmed from the evidence of MePEO-*b*-P(CL-DOX) hydrolysis at acidic pH and production of DOX- ϵ caprolactone derivative i.e., DOX-(6 hydroxy caproic acid) by GPC and mass spectroscopy analysis (Chapter 4, Figure 4.5). The hydrolysis of poly(ester) backbone is expected to be more efficient *in vivo* compared to *in vitro* condition [27]. Since, various enzymes (e.g. lysosomal esterase, cathepsin B etc.) may facilitate the polymer degradation at cellular level [28, 29].

Polymeric micelles with engineered core have been shown to solubilize and sustain the release of many poorly water soluble drugs efficiently due to enhanced compatibility between core and solubilize [20, 30-32]. Toward this goal, Flory-Huggins interaction

parameter (χ_{sp}) was used to predict the compatibility of CuI with different block copolymer cores. The highest compatibility was achieved with the core containing pendant cholesteryl group on PCL which is termed as PChCL. The order of compatibility of CuI with different core forming block under the study was PChCL>PBCL>PCL. Development of the synthesis strategy of functional group bearing ϵ -caprolactone, allows for the substitution of different reactive groups on the core forming block of MePEO-*b*-PCL. Therefore, we engineered the PCL block by attaching compatible cholesteryl moiety to ϵ -caprolactone monomer and further ring opening polymerization of the functionalized monomer using MePEO as initiator and stannous octoate as catalyst (Chapter 5). The polymerization reactivity of functional group bearing monomer was found to be reduced compared to the unfunctionalized ϵ -caprolactone, possibly, due to the steric hindrance of the bulky group against ring opening polymerization (Chapter 3 and 5).

Engineered polymeric micellar formulations were able to solubilize CuI efficiently exhibiting the highest loading level with cholesteryl bearing polymer, MePEO-*b*-PChCL (Chapter 5, Table 5.3). However, benzyl core containing MePEO-*b*-PBCL was found more efficient than PEO-*b*-PChCL in controlling the release of CuI from polymeric nanocarriers (Chapter 5, Figure 5.5). Interestingly, the highest compatible core structure based on the Flory-Huggins interaction parameter, MePEO-*b*-PChCL micellar carrier failed to show superiority over MePEO-*b*-PCL block copolymer micelles although it exhibited 5 times higher CuI loading (molar ratio) compared to MePEO-*b*-PCL micelles (Chapter 5, Table 5.3). We assumed that the low viscosity of PChCL core was responsible for the faster CuI release from MePEO-*b*-PChCL micelles.

Attachment of a functional group to the α -position of ϵ -caprolactone monomer results in the generation of a chiral centre at the carbon attached to the functional group. Chiral centre in the functionalized monomer produces two stereo isomers, D and L α -benzylcarboxylate ϵ -caprolactone although the compound was identified as a single spot in TLC plate which was used as single molecule in the further work. However, the monomers of functionalized MePEO-*b*-PCL block copolymers may be oriented in an alternate fashion along the polymer backbone resulting in syndiotactic polymers. PCL is an isotactic polymer which makes it semicrystalline in nature. Modification of the tacticity of the core forming block may modify the kinetic stability, biodegradation or drug solubilization and release properties of MePEO-*b*-PCL micelles. This issue was not addressed in the current study and needs further investigations.

Encapsulation of drugs in polymeric micelles seem to reduce their cytotoxic effects possibly because of a slower interaction of the micellar encapsulated drug with target cells compared to free drug [33-35]. In chapter 6, we investigated the effect of PEO/PCL molecular weights on the rate, extent and mechanism of uptake of MePEO-*b*-PCL micelles by human breast cancer cells. This study was conducted to find out whether changes in the hydrophilic lipophilic balance (HLB) of the block copolymers may be used to optimize the cellular uptake of polymeric micelles. Fluorescent probe DiI loaded MePEO-*b*-PCL micelles were used to investigate the extent of micellar uptake by MCF-7 cancer cells. Cellular internalization of polymeric micelles was confirmed by laser scanning microscopy. A decrease in temperature from 37 °C to 4 °C, known to be an effective noninvasive means of inhibiting endocytosis, was found to inhibit the uptake of MePEO-*b*-PCL block copolymer micelles strongly [36]. Further inhibition of uptake by pretreatment of MCF-7 cells with chlorpromazine and cytochalasin B points the possible involvement of clathrin mediated

endocytosis or macropinocytosis in the internalization process of MePEO-*b*-PCL block copolymer micelles.

We further investigated the effect of core/shell structure on the cellular internalization process of MePEO-*b*-PCL micelles. No linear relationship between the molecular weight of PEO or PCL block or the HLB of block copolymers and micellar internalization by cancer cells was found (Chapter 6, Figure 6.3). Maximum uptake was achieved by 5000-13000 followed by 5000-5000 MePEO-*b*-PCL micelles. The 2000-5000 and 5000-24000 micelles showed minimum cellular uptake. In the uptake of 5000-13000 and 5000-5000 micelles both mechanisms of clathrin mediated endocytosis and macropinocytosis were shown to be involved, while the uptake of 2000-5000 and 5000-24000 PEO-*b*-PCL nanodelivery systems was shown to proceed only by clathrin mediated endocytosis. This finding may explain the lower level of cellular uptake for the latter two systems.

7.2. Conclusions

A family of novel micelle forming MePEO-*b*-poly(ester) block copolymers with functional groups on the poly(ester) block was successfully synthesized and characterized. MePEO-*b*-poly(ester) block copolymers with reactive side groups were shown to be able to self assemble into spherical nanoscopic core-shell structure with tailorable micellar properties for drug delivery. MePEO-*b*-poly(ester) block copolymer with reactive side groups possess high potential for the preparation of micelle forming drug conjugates with a hydrolysable core structure and nanocontainers for the solubilization and controlled delivery of various therapeutic agents. Finally, internalization of MePEO-*b*-poly(ester) micelles by cancer cells was shown an energy dependant process, which may be optimized by manipulation of the core/shell structure for the efficient delivery of therapeutic agents.

7.3. Future perspective

In this study, we explored MePEO-*b*-poly(ester) block copolymer bearing functional group on the poly(ester) block that can be covalently attached to model anticancer drugs. The developed micelle forming drug conjugate can accommodate a large number of drug molecule and expected to prevent the premature drug release in blood circulation. However, in *in-vitro* cytotoxicity study, the micelle forming drug conjugate demonstrated decreased cytotoxicity compared to free drug. The intracellular uptake of micelle forming poly(ester) drug conjugate may be enhanced by surface modification with a cancer cells specific ligand. Several cancer cell specific ligands, i.e., monoclonal antibodies [37] folate, peptides [38], sugars [39] have been used for targeted drug delivery. In addition, due to the presence of functional group on the poly(ester) block drug can be attached via stimulus (endosomal pH, enzyme or glutathione) responsive linker that might result in site specific triggered drug release.

Synthesis of MePEO-*b*-PChCL block copolymer was performed by bulk polymerization method. For an optimum degree of polymerization we had to perform the polymerization at 160 °C in presence of stannous octoate as catalyst which resulted in a yield of 78% of synthesized polymer. However, ring opening polymerization of lactones at higher temperature increase the potential for degradation of the polymer [12]. Furthermore, ester interchange and depolymerization reactions are known to occur at temperatures above 140 °C [40]. Therefore, it is important to develop a synthetic method for MePEO-*b*-PChCL block copolymer in solution at low temperature or by changing the catalyst to achieve block copolymer of controlled architecture with high yield.

Attachment of a functional group to the α -position of ϵ -caprolactone monomer results in the generation of a chiral centre at the carbon attached to the functional group.

Chiral centre in the functionalized monomer produces two stereo isomers, D and L α -benzylcarboxylate ϵ -caprolactone. Identification and purification of these two isomers and further polymerization and characterization may be performed in further work. The polymers prepared from purified D or L isomer of the monomer may be able to make the poly(ester) backbone more flexible which might be able to engineer the micellar properties more efficiently.

Although MePEO-*b*-PChCL demonstrated a high loading level of CuI, it failed to show superiority in sustaining the release over MePEO-*b*-PCL block copolymer which points the necessity of modification of the delivery system. An alternative method of developing a formulation of CuI is to conjugate CuI covalently to the pendant carboxylic groups of MePEO-*b*-PCCL by an ester bond which might be able to enhance the loading as well as control the release of CuI in an efficient manner.

Physical stability of colloidal carrier is a major concern since the colloidal nanocarriers have a tendency to aggregate on standing for longer period of time. In the current study, MePEO-*b*-PCL based core functionalized block copolymer micelles were used for loading and controlled delivery of two different chemotherapeutic agents; DOX and CuI. However, the physical *in vitro* stability of drug loaded polymeric micelles was not assessed. A long term kinetic study of MePEO-*b*-PCL micelles of different core structure may be conducted at different time points using DLS techniques or GPC analysis to assess the physical stability of prepared micelles.

The functionalized MePEO-*b*-PCL block copolymer containing benzyl carboxylate, carboxylic, or cholesteryl moiety in their core may be used to load other potential drugs such as paclitaxel, Cucurbitacin B, β estradiol, amphotericin B, cyclosporin A, PSC 833, or any

drugs that are suffering from limited water solubility and potential nonspecific toxicity. Also, PCL core may be engineered to make the core chemically compatible for a particular drug.

From a broader perspective, a better understanding on the engineering of the core/shell effect on the biodistribution and micellar properties may lead to the design of polymeric micelles with preferential accumulation in specific organs for a passive targeting such as liver or intestinal delivery. MePEO-*b*-poly(ester) block copolymer with carboxylic group on the poly(ester) block may be suitable for intestinal targeting of peptides or other drugs sensitive to gastric enzymes that prevent the drug from degradation by gastric enzyme but destabilize the micelles at intestinal basic pH where the carboxylic group will ionize.

Thermoreversible hydrogels based on synthetic block copolymers has gained increasing attention recently due to its potential biomedical applications in *in situ* forming systems, including controlled drug delivery, cell encapsulation and tissue repair [41-44]. PCL as a hydrophobic block possesses a high potential in this direction due to its hydrophobicity and biodegradability [45]. Functionalization of the PCL backbone may result more precise control over the temperature range of gel-sol phase transition by tailoring the polymer composition, which might be very useful for application in injectable drug delivery systems.

7.4. References

- [1] S.Y. Lin, Y. Kawashima, *Pharmaceutica acta Helvetiae* 60 (1985) 339-344.
- [2] H.M. Aliabadi, D.R. Brocks, A. Lavasanifar, *Biomaterials* 26 (2005) 7251-7259.
- [3] H.M. Burt, X. Zhang, P. Toleikis, L. Embree, W.L. Hunter, *Colloids and Surfaces. B, Biointerfaces* 16 (1999) 161-171.
- [4] A. Lavasanifar, Thesis, Faculty of Pharmacy and Pharmaceutical Sciences, University of Alberta (2001).
- [5] M. Yokoyama, M. Miyauchi, N. Yamada, T. Okanao, Y. Sakurai, K. Kataoka, S. Inoue, *Journal of Controlled Release* 11 (1990) 269-278.
- [6] G.S. Kwon, *Crit Rev Ther Drug Carrier Syst* 15 (1998) 481-512.
- [7] X. Shuai, H. Ai, N. Nasongkla, S. Kim, J. Gao, *J Control Release* 98 (2004) 415-426.
- [8] C. Allen, Y. Yu, A. Eisenberg, D. Maysinger, *Biochimica et Biophysica Acta - Biomembranes* 1421 (1999) 32-38.
- [9] S.M. Li, H. Garreau, B. Pauvert, J. McGrath, A. Toniolo, M. Vert, *Biomacromolecules* 3 (2002) 525-530.
- [10] M. Yuan, Y. Wang, X. Li, C. Xiong, X. Deng, *Macromolecules* 33 (2000) 1613-1617.
- [11] Z. Zhu, C. Xong, L. Zhang, X. Deng, *Journal of Polymer Science: Part A: Polymer Chemistry* 35 (1997) 709-714.
- [12] R.T. Liggins, H.M. Burt, *Adv Drug Deliv Rev* 54 (2002) 191-202.
- [13] A.C. Albertsson, I.K. Varma, *Aliphatic polyesters: Synthesis, properties and applications, Degradable Aliphatic Polyesters*, vol. 157, 2002, pp. 1-40.
- [14] A.C. Albertsson, I.K. Varma, *Biomacromolecules* 4 (2003) 1466-1486.
- [15] L.F. Zhang, A. Eisenberg, *Macromolecules* 29 (1996) 8805-8815.
- [16] L.F. Zhang, A. Eisenberg, *Polymers for Advanced Technologies* 9 (1998) 677-699.
- [17] A. Lavasanifar, J. Samuel, G.S. Kwon, *Colloids Surf B Biointerfaces* 22 (2001) 115-126.
- [18] G. Kwon, M. Naito, M. Yokoyama, T. Okano, Y. Sakurai, K. Kataoka, *Langmuir* 9 (1993) 945-949.
- [19] Y.I. Jeong, J.B. Cheon, S.H. Kim, J.W. Nah, Y.M. Lee, Y.K. Sung, T. Akaike, C.S. Cho, *J Control Release* 51 (1998) 169-178.
- [20] A. Lavasanifar, J. Samuel, G.S. Kwon, *J Control Release* 79 (2002) 165-172.
- [21] Y. Li, G.S. Kwon, *Pharm Res* 17 (2000) 607-611.
- [22] S.B. La, T. Okano, K. Kataoka, *Journal of Pharmaceutical Sciences* 85 (1996) 85-90.
- [23] S.Y. Kim, I.L.G. Shin, Y.M. Lee, C.S. Cho, Y.K. Sung, *Journal of Controlled Release* 51 (1998) 13-22.
- [24] H.M. Aliabadi, A. Mahmud, A.D. Sharifabadi, A. Lavasanifar, *J Control Release* 104 (2005) 301-311.
- [25] K. Kataoka, T. Matsumoto, M. Yokoyama, T. Okano, Y. Sakurai, S. Fukushima, K. Okamoto, G.S. Kwon, *J Control Release* 64 (2000) 143-153.
- [26] M.B. Hansen, S.E. Nielsen, K. Berg, *Journal of Immunological Methods* 119 (1989) 203-210.

- [27] H.J. Sung, C. Meredith, C. Johnson, Z.S. Galis, *Biomaterials* 25 (2004) 5735-5742.
- [28] H. Tsuji, Y. Kidokoro, M. Mochizuki, *Macromolecular Materials and Engineering* 291 (2006) 1245-1254.
- [29] F.P. Seib, A.T. Jones, R. Duncan, *Journal of Drug Targeting* 14 (2006) 375-390.
- [30] M. Yokoyama, A. Satoh, Y. Sakurai, T. Okano, Y. Matsumura, T. Kakizoe, K. Kataoka, *J Control Release* 55 (1998) 219-229.
- [31] J. Lee, E.C. Cho, K. Cho, *J Control Release* 94 (2004) 323-335.
- [32] J. Liu, F. Zeng, C. Allen, *Journal of Controlled Release* 103 (2005) 481-497.
- [33] M. Yokoyama, T. Okano, Y. Sakurai, S. Suwa, K. Kataoka, *Journal of Controlled Release* 39 (1996) 351-356.
- [34] Y. Bae, N. Nishiyama, S. Fukushima, H. Koyama, M. Yasuhiro, K. Kataoka, *Bioconjug Chem* 16 (2005) 122-130.
- [35] Y. Bae, S. Fukushima, A. Harada, K. Kataoka, *Angew Chem Int Ed Engl* 42 (2003) 4640-4643.
- [36] R.M. Steinman, I.S. Mellman, W.A. Muller, Z.A. Cohn, *The Journal of cell biology* 96 (1983) 1-27.
- [37] V.P. Torchilin, *Cell Mol Life Sci* 61 (2004) 2549-2559.
- [38] X.B. Xiong, A. Mahmud, H. Uludag, A. Lavasanifar, *Biomacromolecules* (2007).
- [39] Y. Nagasaki, K. Yasugi, Y. Yamamoto, A. Harada, K. Kataoka, *Abstracts of Papers of the American Chemical Society* 221 (2001) U434-U434.
- [40] Y.M. A. Schindler, Y.M. Hinionada, C.G. Pitt, *J. Polym. Sci., Polym. Chem. Ed.* 20 (1982) 319-326.
- [41] T. Kissel, Y.X. Li, F. Unger, *Advanced Drug Delivery Reviews* 54 (2002) 99-134.
- [42] B. Jeong, Y.H. Bae, D.S. Lee, S.W. Kim, *Nature* 388 (1997) 860-862.
- [43] B. Jeong, Y.H. Bae, S.W. Kim, *Colloids and Surfaces B-Biointerfaces* 16 (1999) 185-193.
- [44] B. Jeong, Y.H. Bae, S.W. Kim, *Macromolecules* 32 (1999) 7064-7069.
- [45] J.W. Lee, F. Hua, D.S. Lee, *Journal of Controlled Release* 73 (2001) 315-327.